Aeolian sands and sandstones

Richard Patrick Steele

AEOLIAN SANDS AND SANDSTONES

by

RICHARD PATRICK STEELE, B.Sc.

Collingwood College

A thesis submitted to the University of Durham
for the degree of Doctor of Philosophy

Department of Geological Sciences
December 1981

VOLUME II OF II

VOLUME II: CONTENTS

DIAGRAMS, PHOTOGRAPHS, TABLES AND ENCLOSURES

Page

Page

Page

IN THE END WALLET:

ENCLOSURE 1

Cullercoats shore section, Yellow Sands

Tynemouth Priory shore section, Yellow Sands

ENCLOSURE 2

Ferryhill railway cutting, Yellow Sands

North Hylton section, Yellow Sands

ENCLOSURE 3

McCall's Quarry, Houghton-le-Spring, Yellow Sands

ENCLOSURE 4

Hetton Downs Quarry, Yellow Sands

ENCLOSURE 5

Sherburn Hill Sand Pit, west face, Yellow Sands

ENCLOSURE 6

Sherburn Hill Sand Pit, north and east faces, Yellow Sands

ENCLOSURE 7

Bowburn Quarry, Yellow Sands

ENCLOSURE 8

Quarrington Hill Quarry, Yellow Sands

ENCLOSURE 9

A442 Worfe Bridge section, Bridgnorth Sandstone

A442 Worfe Mouth sectoon, Bridgnorth Sandstone

Bridgnorth Golf Club car park section, Brid Sandstone

High Rock, Bridgnorth, Bridgnorth Sandstone

CHAPTER ONE

MODERN ERGS

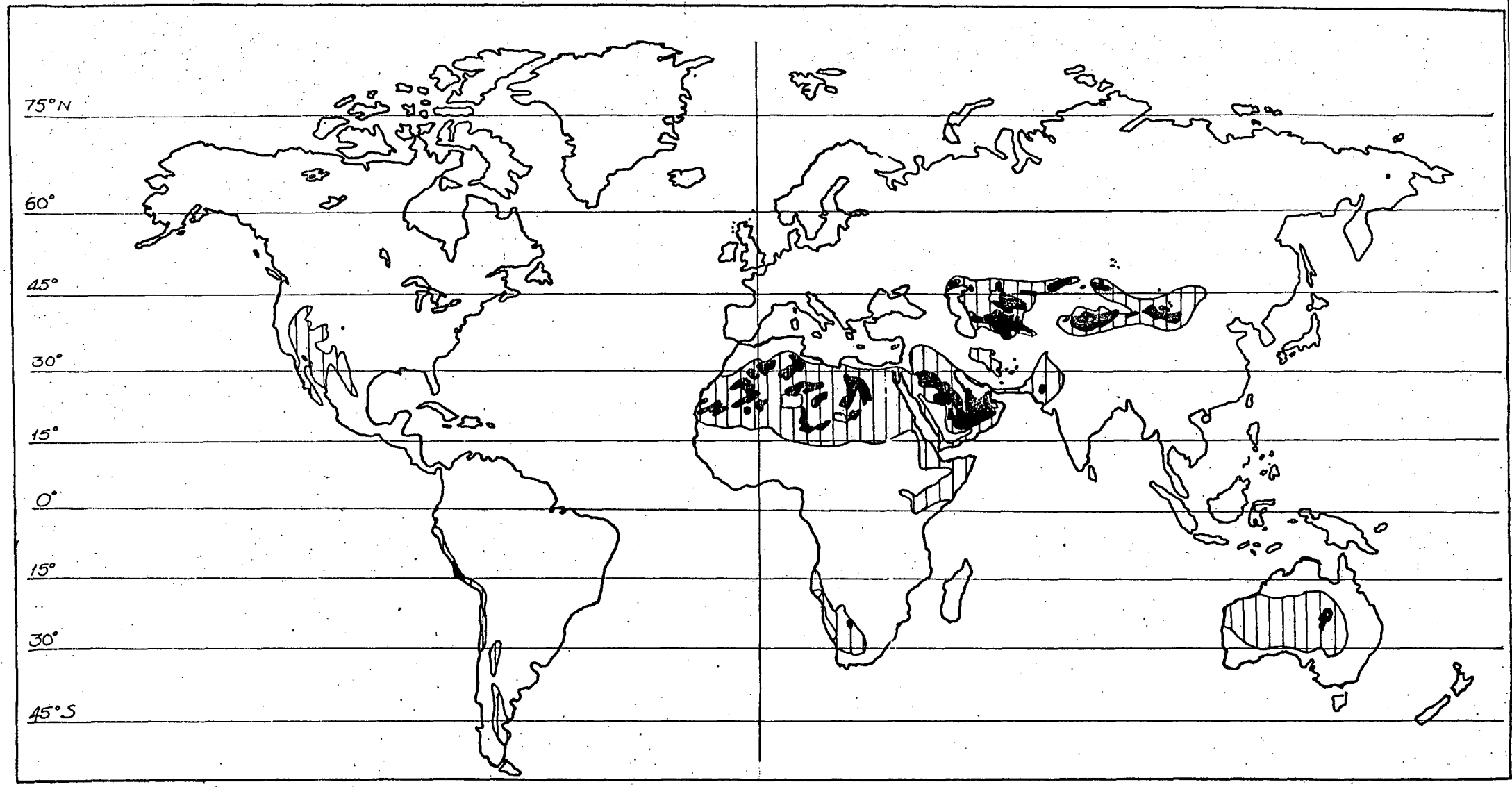

FIG.1.1 Vertical hatching marks areas designated as desert by Koppen's classification. Active ergs are shaded black. Information from The Times Atlas of The World and Cooke and Warren (1973).

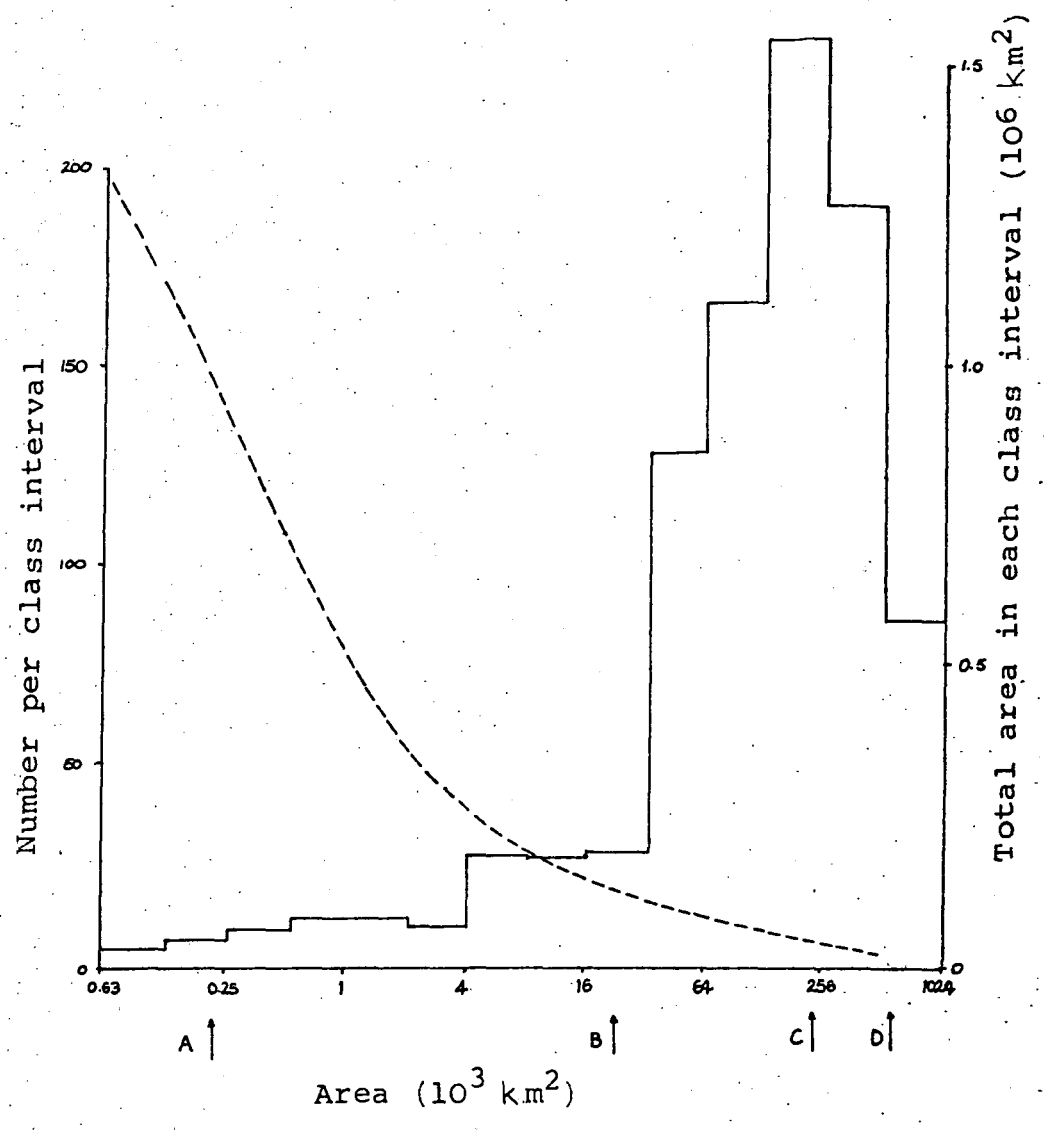

FIG. 1.2 Area v. frequency curve (dashed) of the world's ergs. The histogram shows the total area in each class interval and demonstrates that the vast majority of presently active aeolian sand is contained in a few very large ergs. From Wilson (1973).

For comparison, A = the outcrop area of the Dumfries basin,

B = Late Permian area of the Irish Sea - Cheshire basin,

C = present area of the U.K.,

D = area of the southern North Sea sedimentary basin during the Early Permian.

FIG.1.3 Illustrating subsidence, sand-drift and the development of ergs.

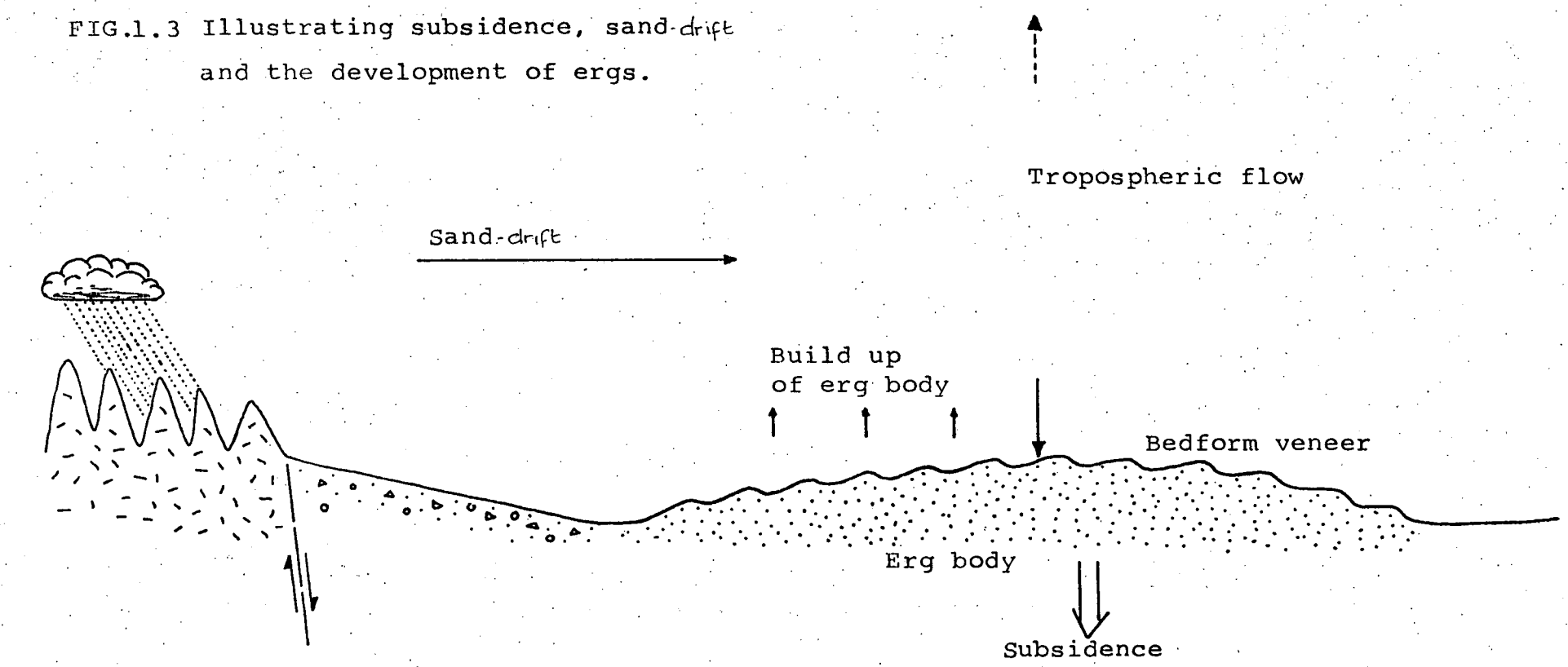

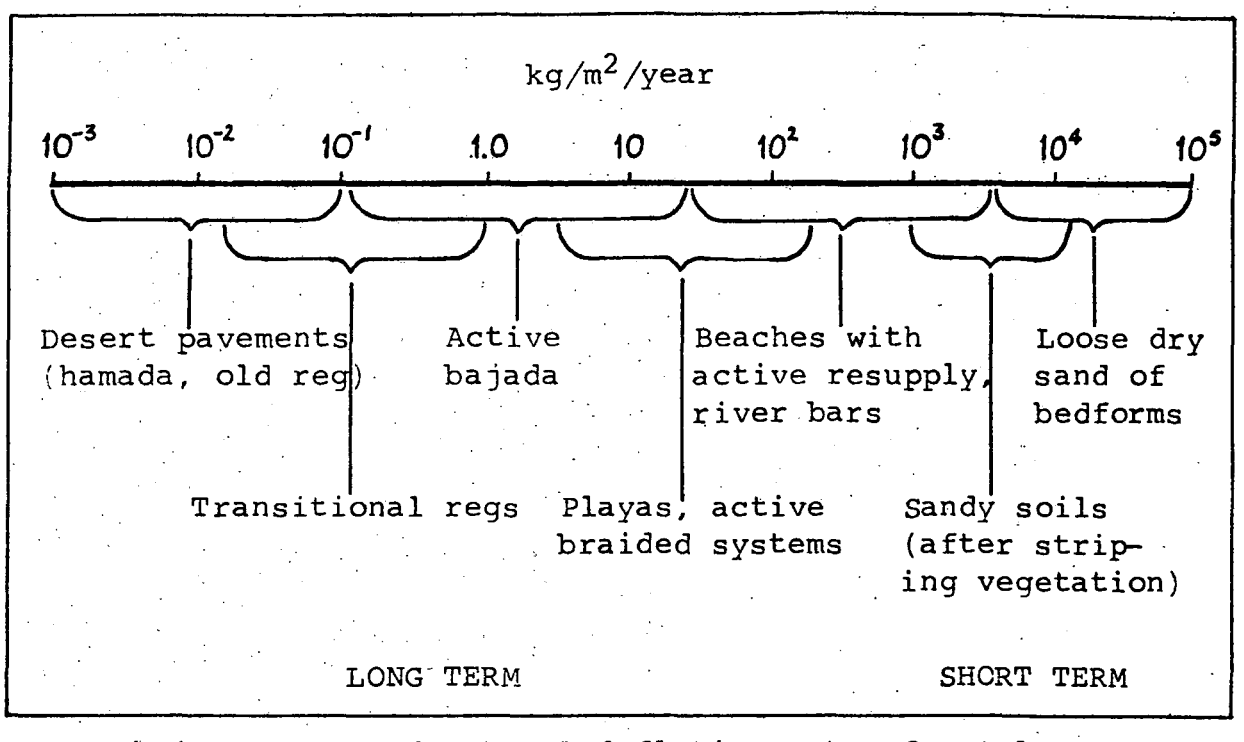

FIG.1.4a Ranges of natural deflation rates for 0.1 - 0.5mm sand. From Wilson (1971).

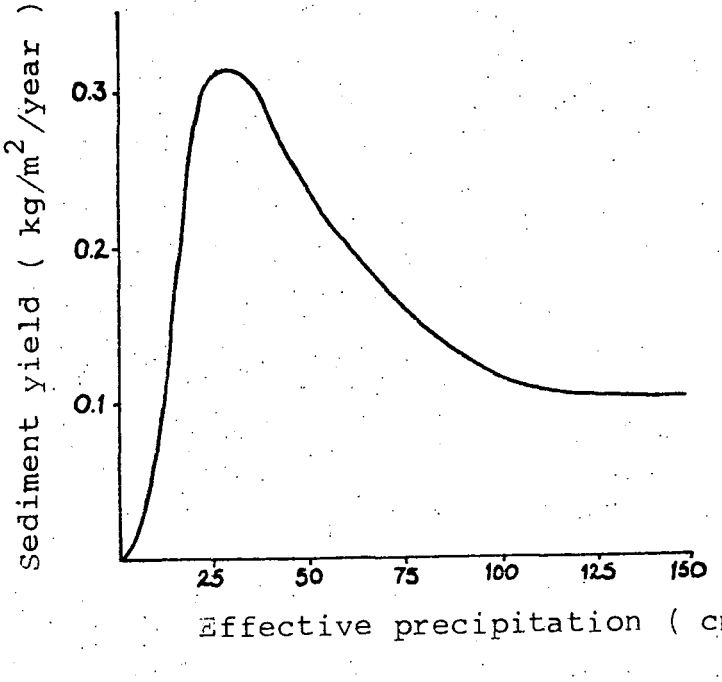

FIG.1.4b

Sediment yield v. effective annual precipitation for U.S. drainage basins. From Langbein & Schumm (1958). Tail-off above 25cm due to the effect of vegetation, that below due to lack of rainfall.

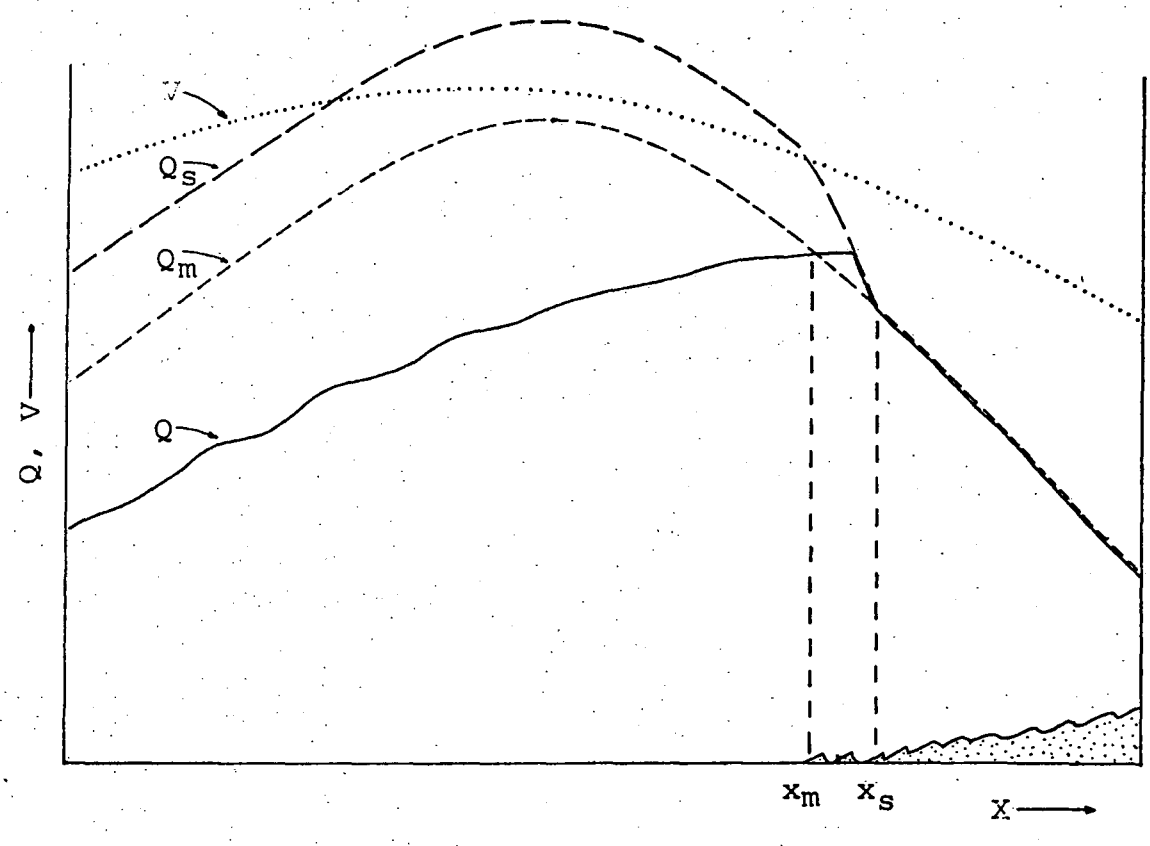

FIG.1.5a Showing the development of an erg with complete sand cover and climbing bedforms. Bedforms must climb where $x > x_s$ because $\frac{dQ}{dx}$ is negative. Note also that as sand cover increases Q_s is depressed on to Q_m.

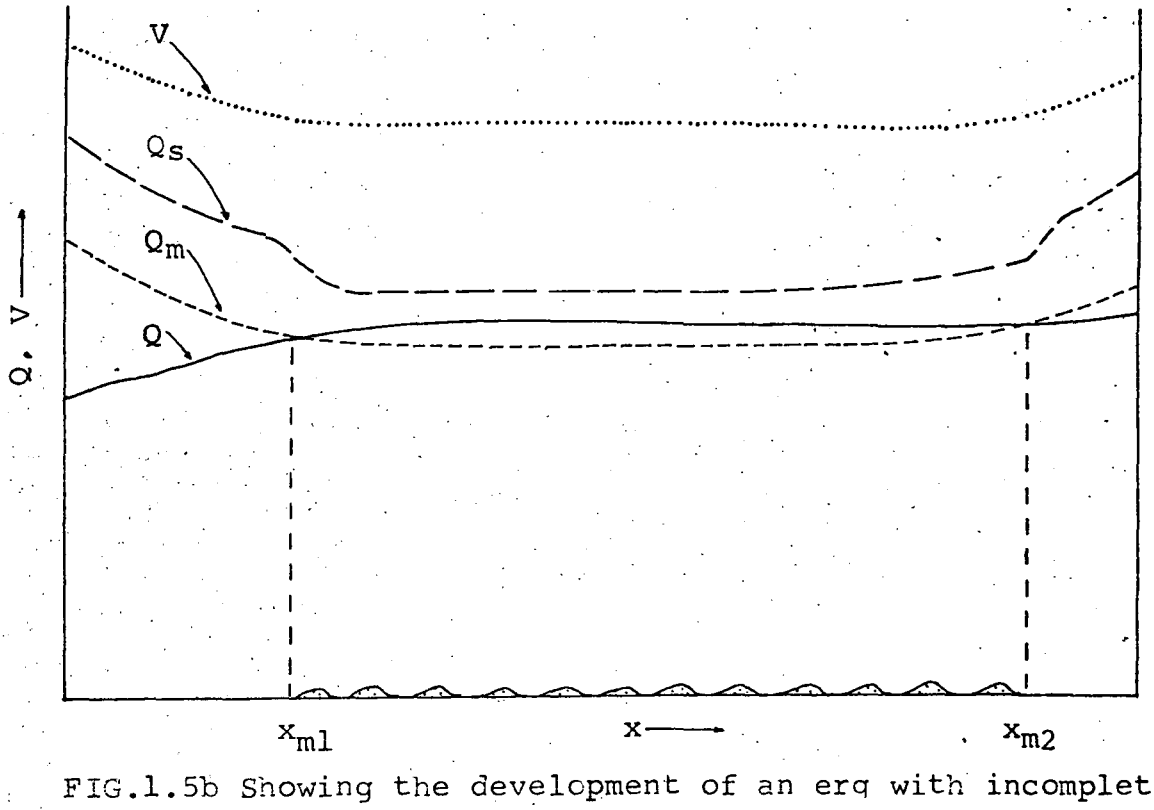

FIG.1.5b Showing the development of an erg with incomplete sand cover. With bedform cover incomplete Q_s is reduced but remains greater than Q_m. Thus the erg is more efficient at transmitting sand than one with complete cover.

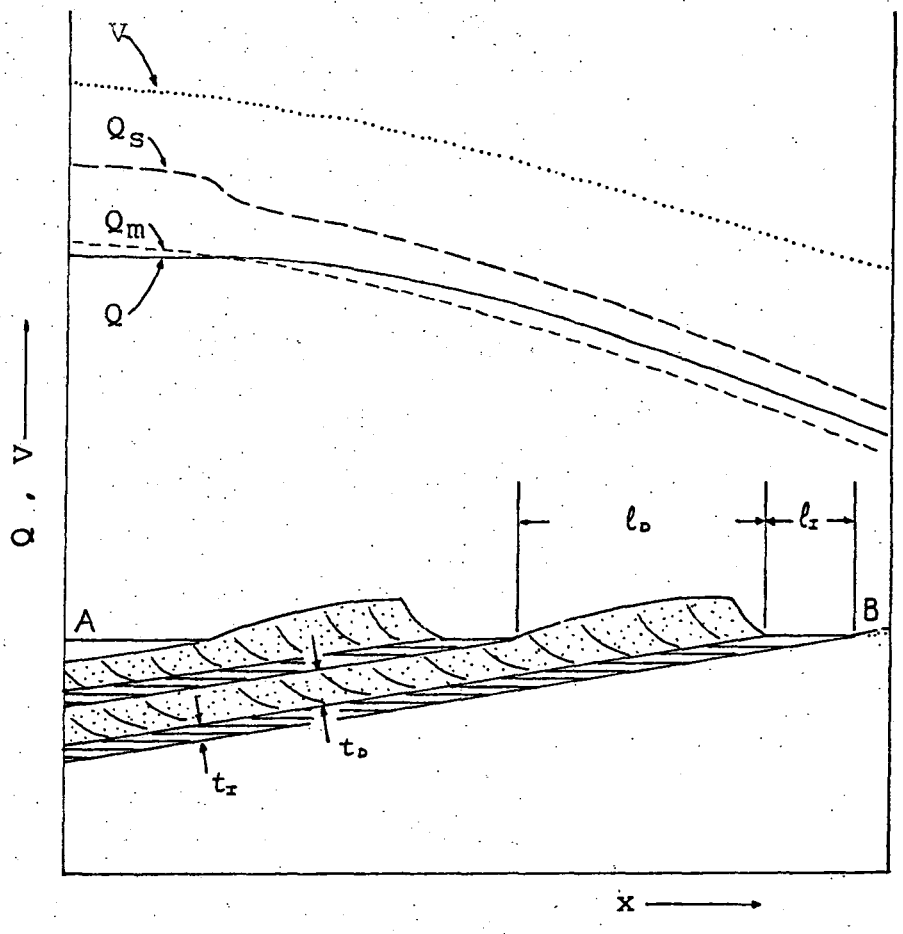

FIG. 1.5c Showing the development of an aggrading erg with incomplete sand cover by the erg model of Wilson (1971b) as modified in Chapter 1. Horizontal ruling represents interbedform deposits; stippling represents large bedform deposits. Where the sand drift is declining and exceeds the metasaturated but is less than the saturated sand-drift ($Q_s > Q > Q_m$), an erg with incomplete sand cover will form and aggrade as shown. Further explanation in text. Symbols as in figs.1.5a, 1.5b.

FIG.1.6

1. TECTONICALLY STABLE, INLAND

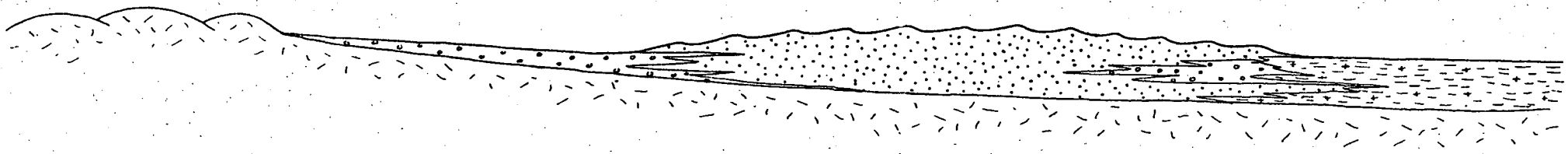

Subdued relief, sand sourced from large areas at low rates.

Alluvial fans, braided systems, ephemeral streams, wide reg & piedmont plains.

Potentially large ergs, blanket form.

Braided or meandering rivers & deltas emptying into a saline lake or ephemeral lake, playa or sabkha with no surface drainage

2. TECTONICALLY STABLE, COASTAL

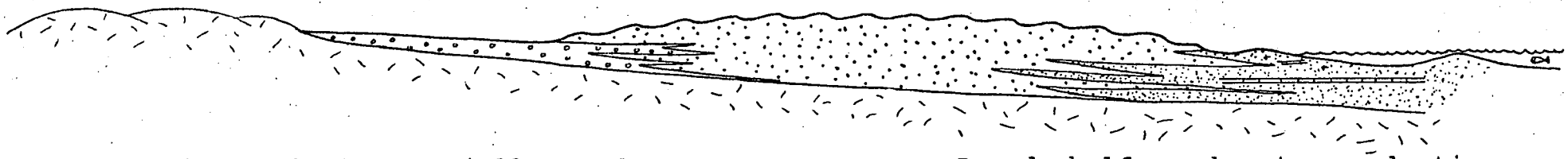

Facies on land essentially as above.

Broad shelf, carbonate or clastic shore, sediment supply likely to be low except with an offshore wind or near major river mouths and deltas. Coastal sabkhas and salinas.

Facies pattern stable, changing long term with evolution of landscape, climate & transgression or regression.

FIG. 1.7

3 & 4. TECTONICALLY ACTIVE

High relief, high rates of sand supply.

Thick, coarse fans, braided systems, ephemeral streams, limited reg plains.

Laterally limited erg. Potentially large sand supply allowing considerable thickness.

Inland:
Fringing fan & highland or longitudinal drainage of any type & persistence, or lake, sabkha or playa.

Coastal:
Narrow shelf, probably clastic shoreline with all that implies, plus salt flats, coastal sabkhas, deltas, etc, etc.

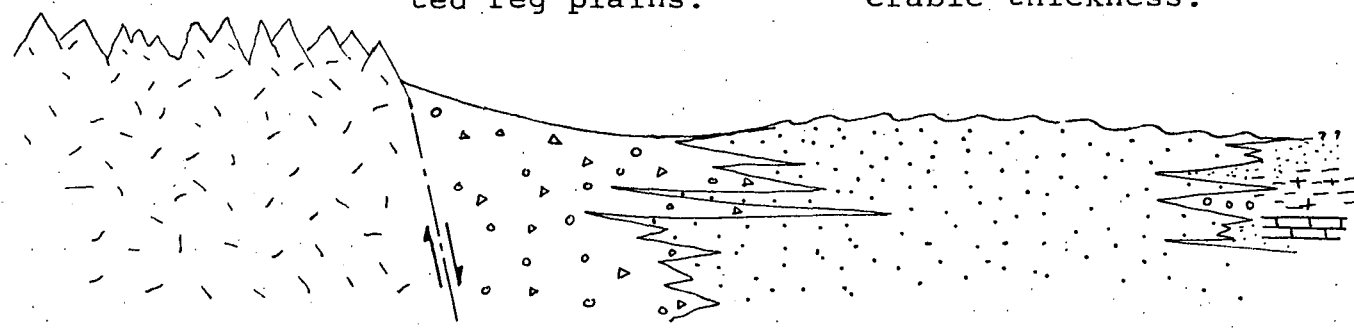

Overall facies pattern suceptible to fickle & active tectonics (especially coastal situations).

CHAPTER TWO

THE WIND, BEDFORMS AND CROSS-BEDDING

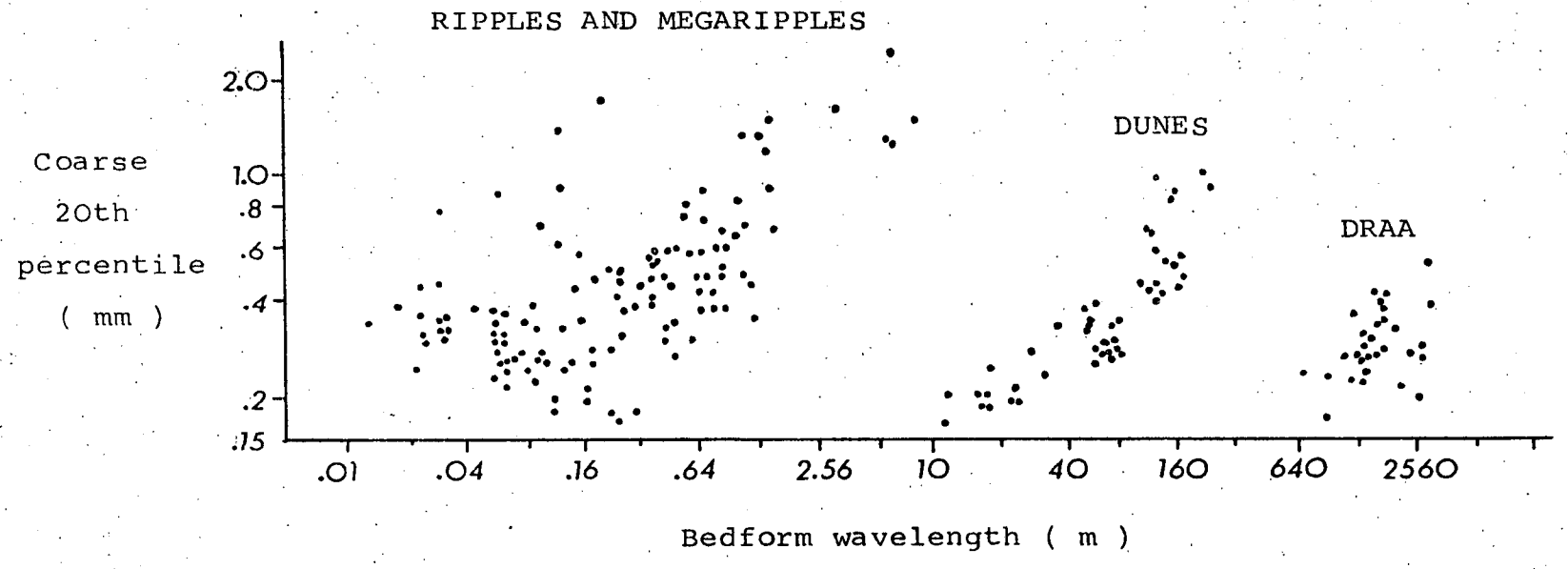

FIG. 2.1. Bedform wavelength v coarse 20th percentile. Shows three orders of bedform with wavelength tending to increase with grain size. After Ellwood et al. (1975).

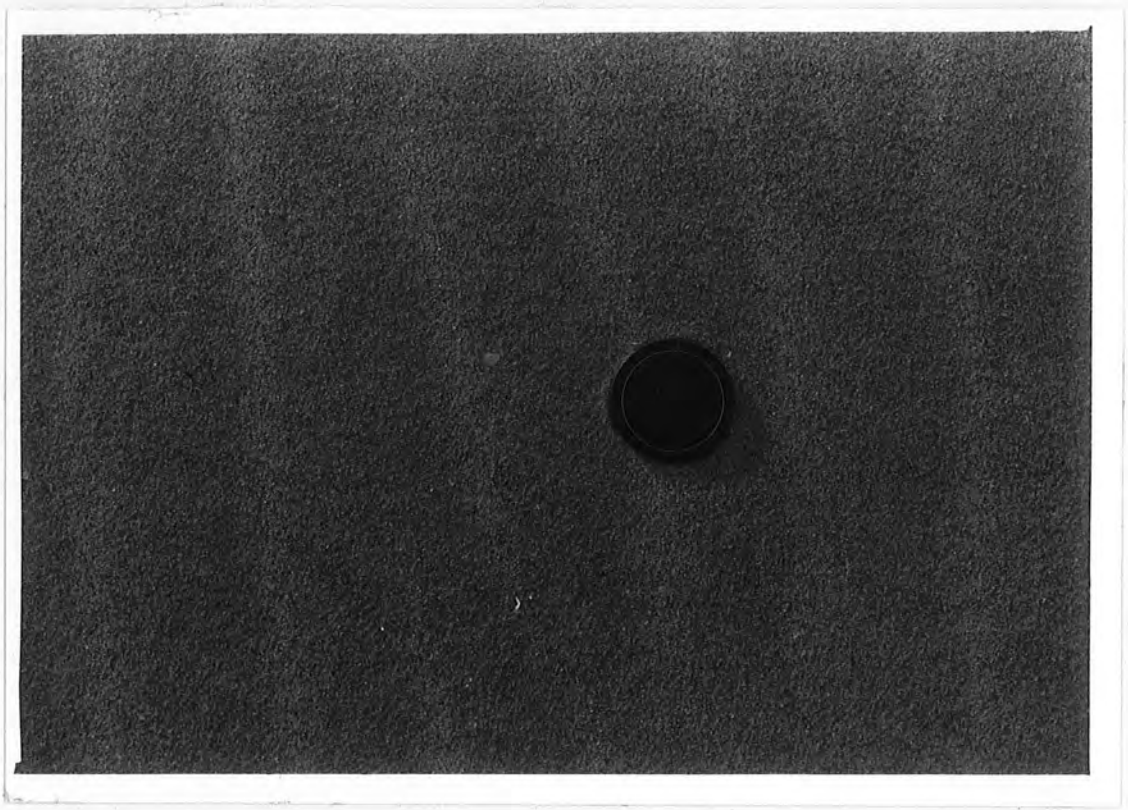

FIG. 2.2 Wind ripples on the beach at Bamburgh, Northumberland. Note low amplitude and straight crests. Wind from right to left. Diameter of lens cap = 50mm.

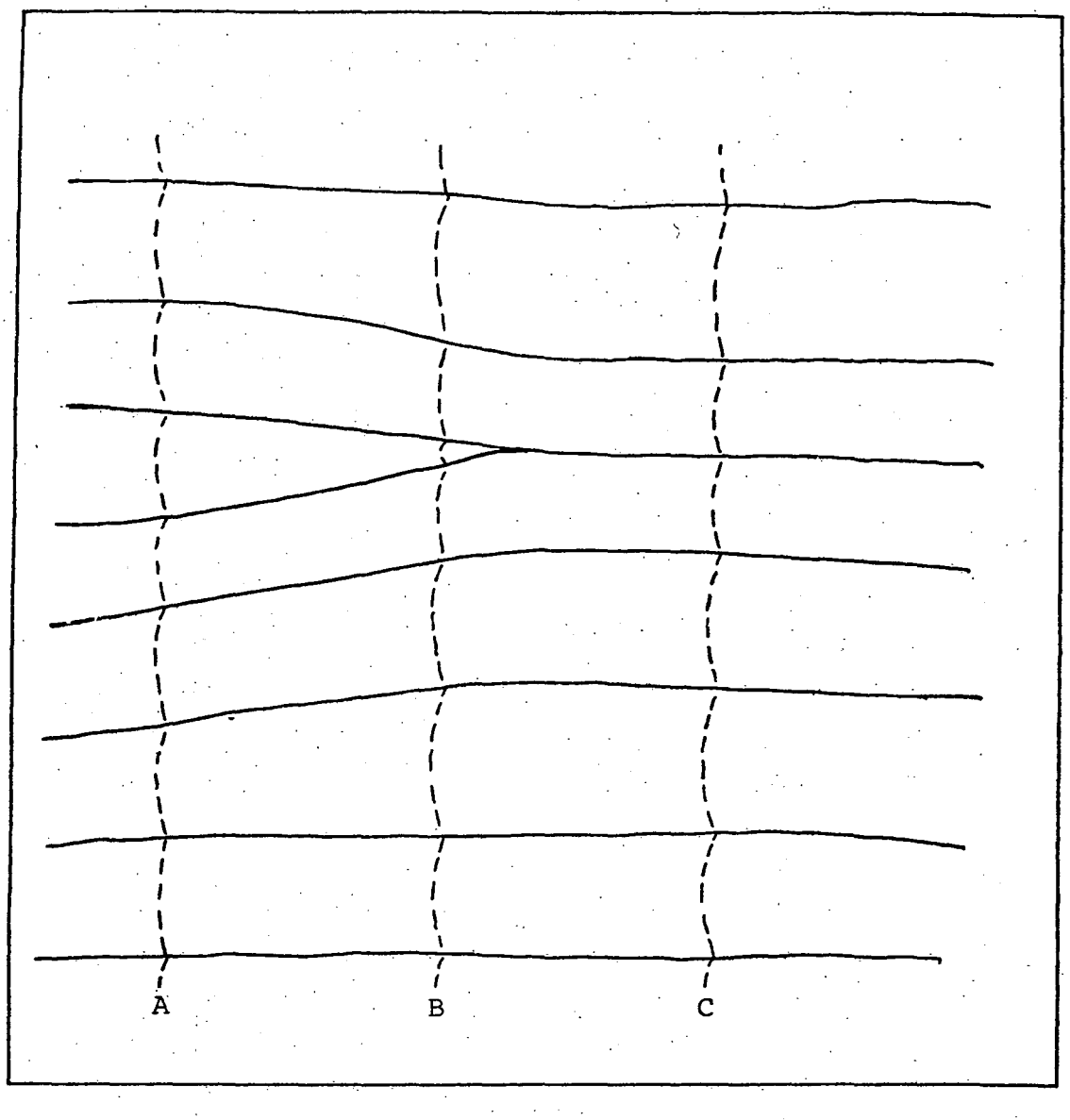

FIG.2.3 Heavy lines mark the crestlines of a typical arrangement of wind ripples. A, B and C mark the paths of 3 grains saltating across the area. According to the ballistic theory for the origin of wind ripples, each jump in saltation should correspond to one ripple wavelength. Note how the grains are therefore forced to take different length jumps at different times and places, despite the constancy of the overall flow conditions. This situation cannot be explained by the ballistic mechanism. After Folk (1977a).

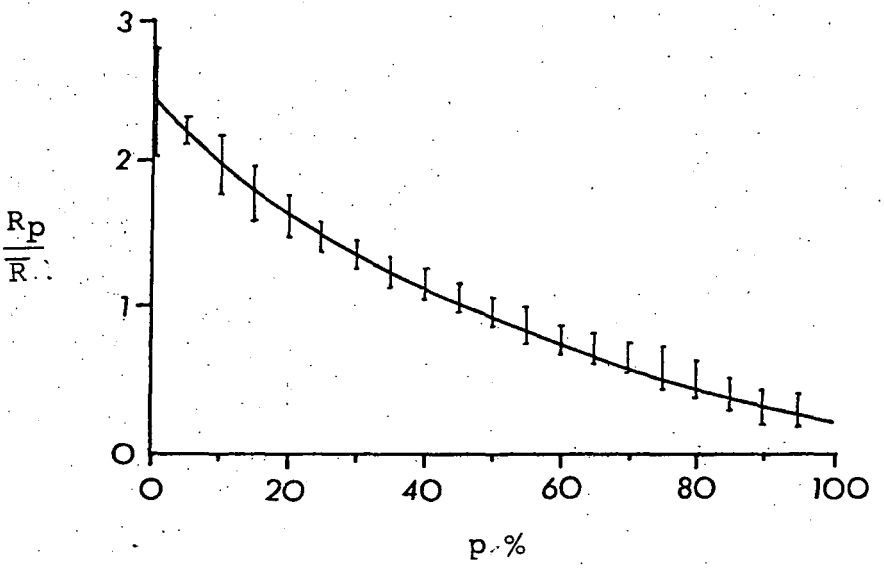

FIG 2.4 $R_p/\overline{R}$ v p where R_p = coefficient of rebound attained by p% of the grains and R = mean rebound. Vertical bars show range of results obtained. After Ellwood et al. (1975).

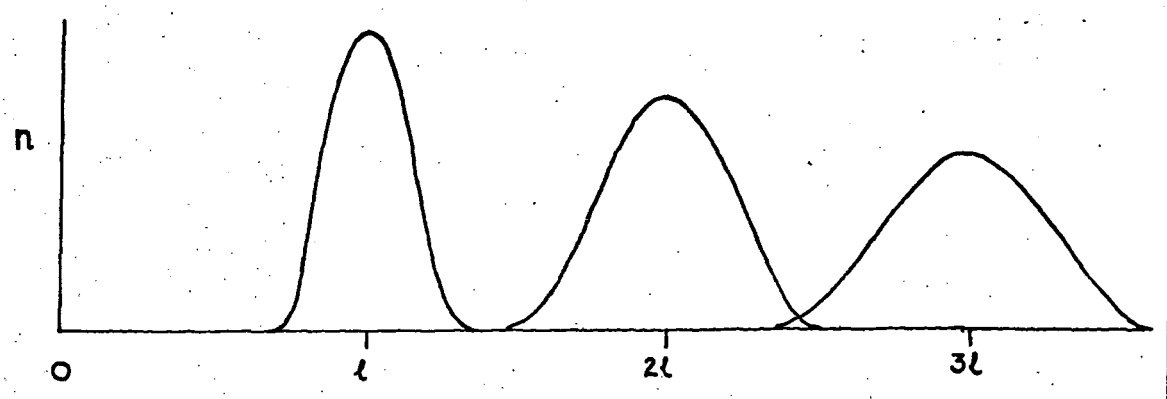

FIG. 2.5 The number of saltating grains landing at points on the surface downwind of a point source at O assuming a characteristic path length ℓ with a finite standard deviation.

FIG2.6 BEDFORM TYPES (after Wilson, 1970)

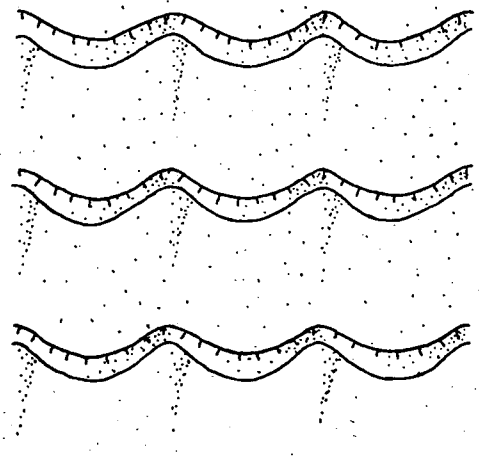

Direction of net sand drift in all examples

(all slipfaces hachured)

(A) Gridiron: longitudinal elements in phase

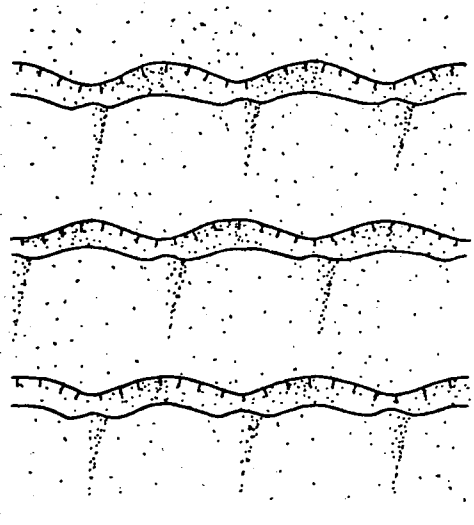

(B) Fishscale: longitudinal elements out of phase

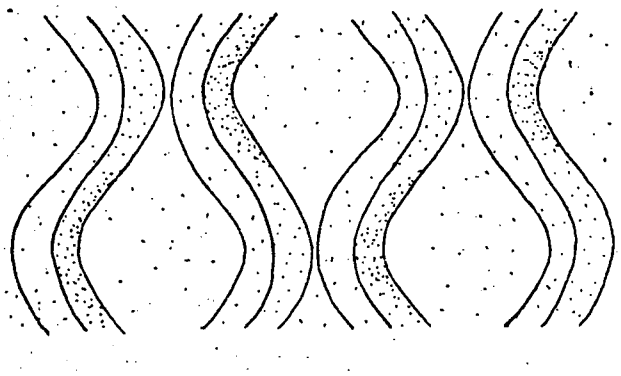

(C) Braided: transverse elements out of phase

FIG 2.6 (contd.)

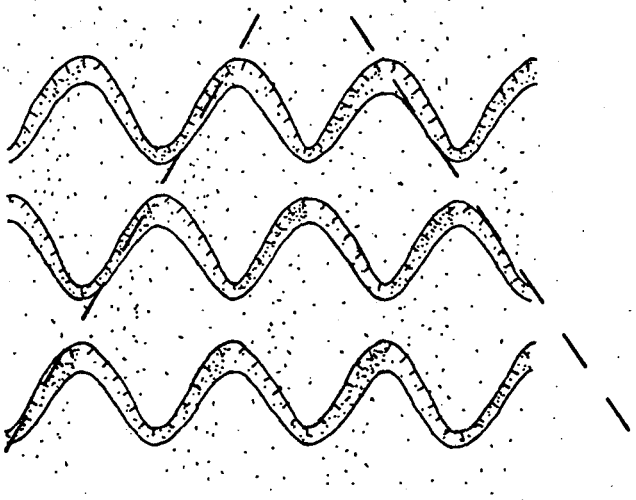

(D) Fishscale pattern tending to a two trend rhomboidal network.

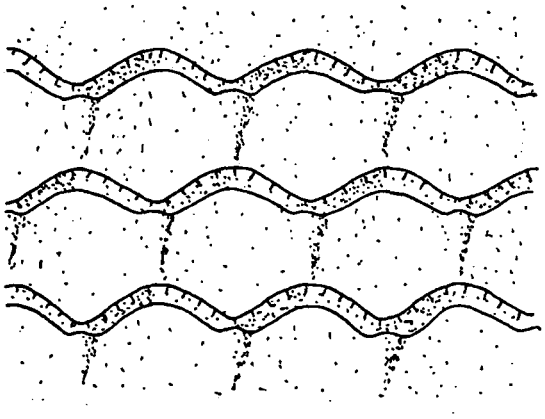

(E) Fishscale pattern tending to a hexagonal network.

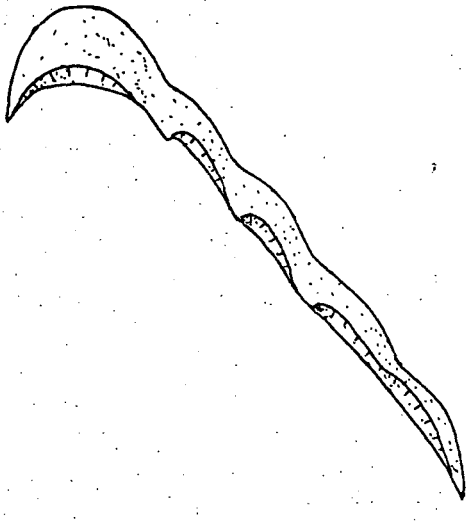

(F) Oblique elements on a barchan.

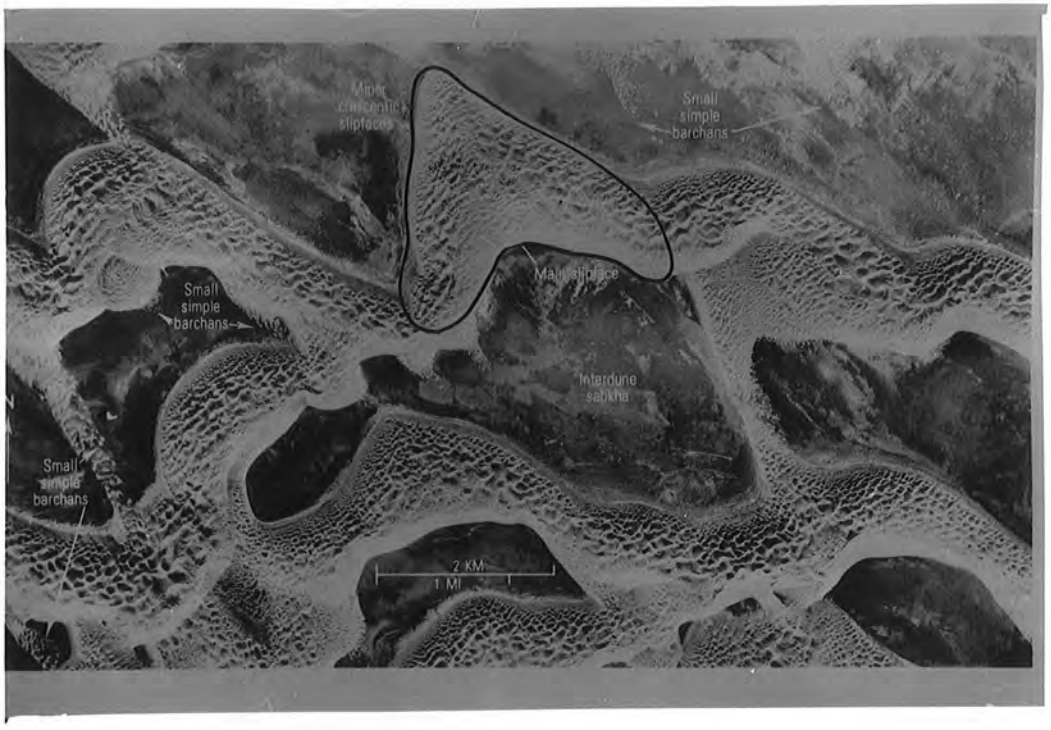

FIG. 2.7 Fairly straight-crested transverse dunes on sinuous transverse slipfaced draa with planar interdraa ares. Forward-pointing (linguoid) parts of the draa tend to be partly slipfaceless. Note the size of the bedforms and the irregularity of the pattern. Location approx. 23° N, 54° E, eastern Rub' al Khali, Saudi Arabia. Reproduced from McKee (1979a, fig.174A). Annotation is McKee's.

FIG 2.8

(A)

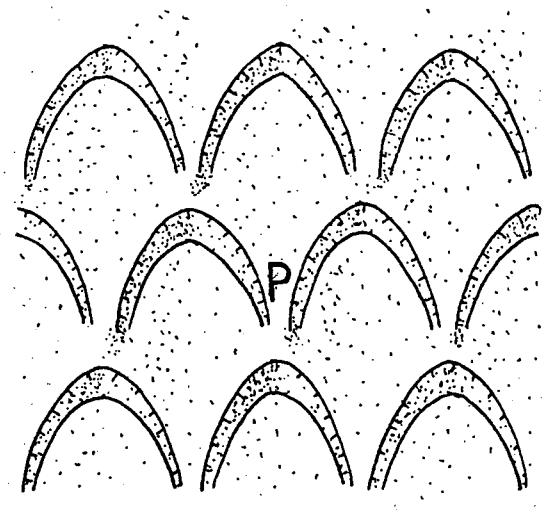

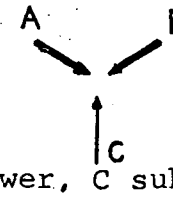

Wind regime with A & B equal in sand carrying power, C subordinate. Fishscale network, probably of slipfaceless draa or with reversal lips on dunes if C is effective. As C→0 draa develop slipfaces, dunes lose reversal lips. If A & B are not equal the pattern will lose symmetry correspondingly and one trend will become dominant. If points such as P are nodes and become emphasized the pattern may take on a stellate form.

(B)

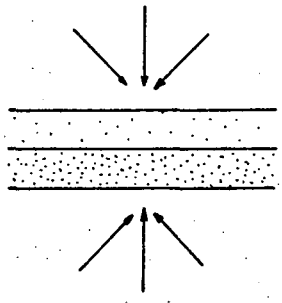

If a ridge is stable when it is either transverse or oblique to the wind a single symmetrical body can accommodate 180° of wind direction as illustrated.

(C)

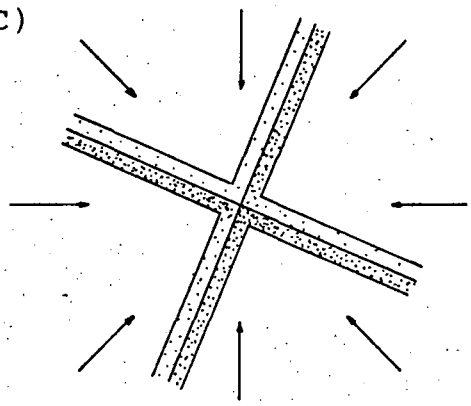

Expressing the same point in a different way, if two winds differing in direction by 45° or less share ridges, the 8-mode wind regime illustrated in (C) is the most complicated possible and is accommodated by just two symmetrical ridge trends.

(D)

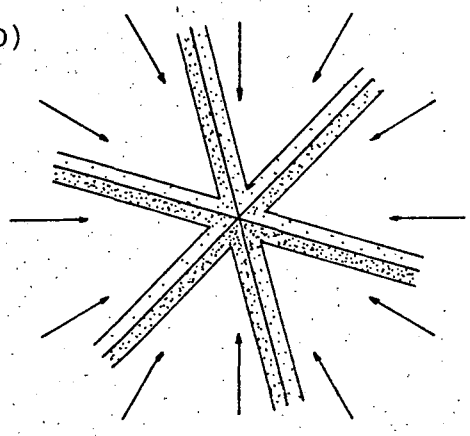

If winds need only differ by 30° in direction to develop separate ridges, a 12-mode wind regime is the most complicated possible and is accommodated by 3 symmetrical ridge trends.

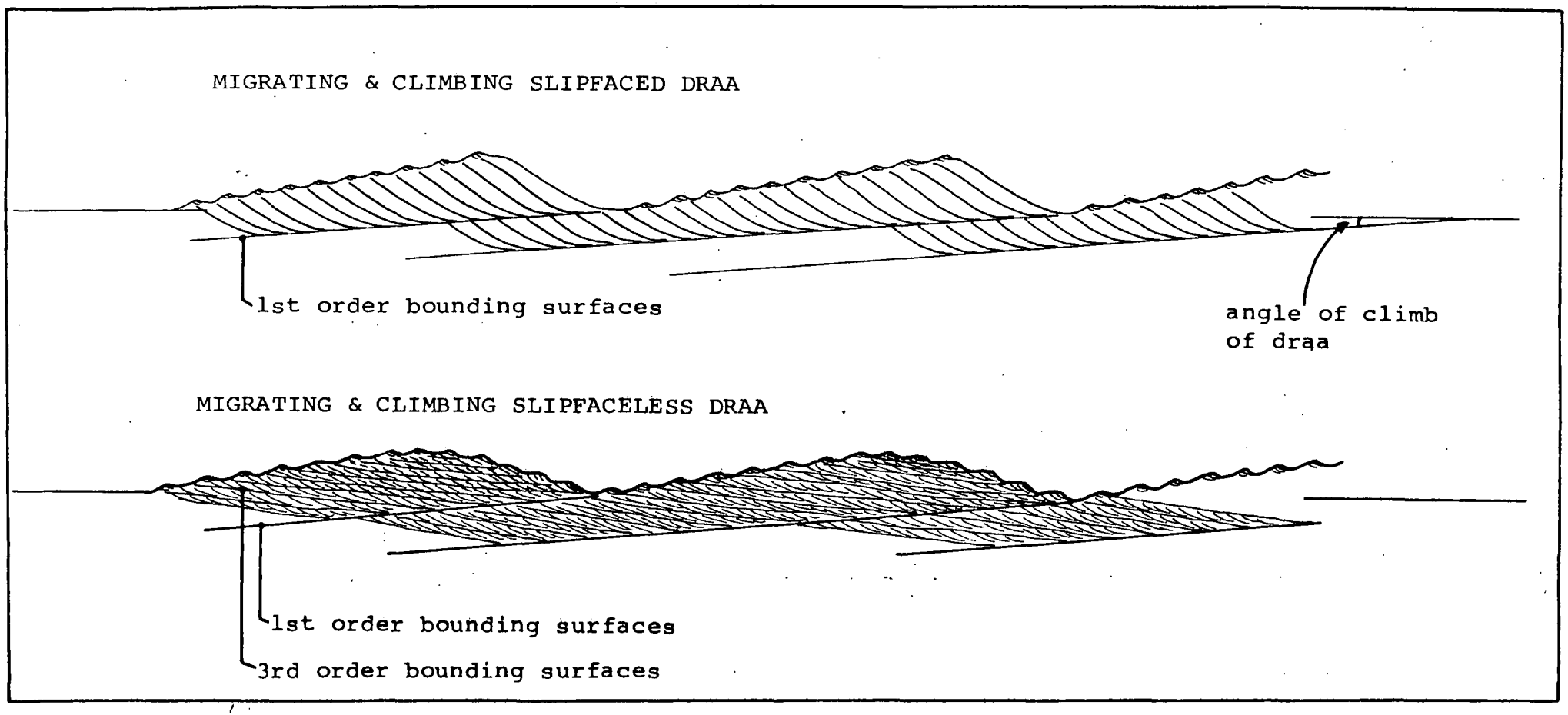

FIG. 2.9 Sections parallel to sand drift of systematically behaving slipfaced and slipfaceless draa.

FIG. 2.10 Factors governing 1st order set thickness

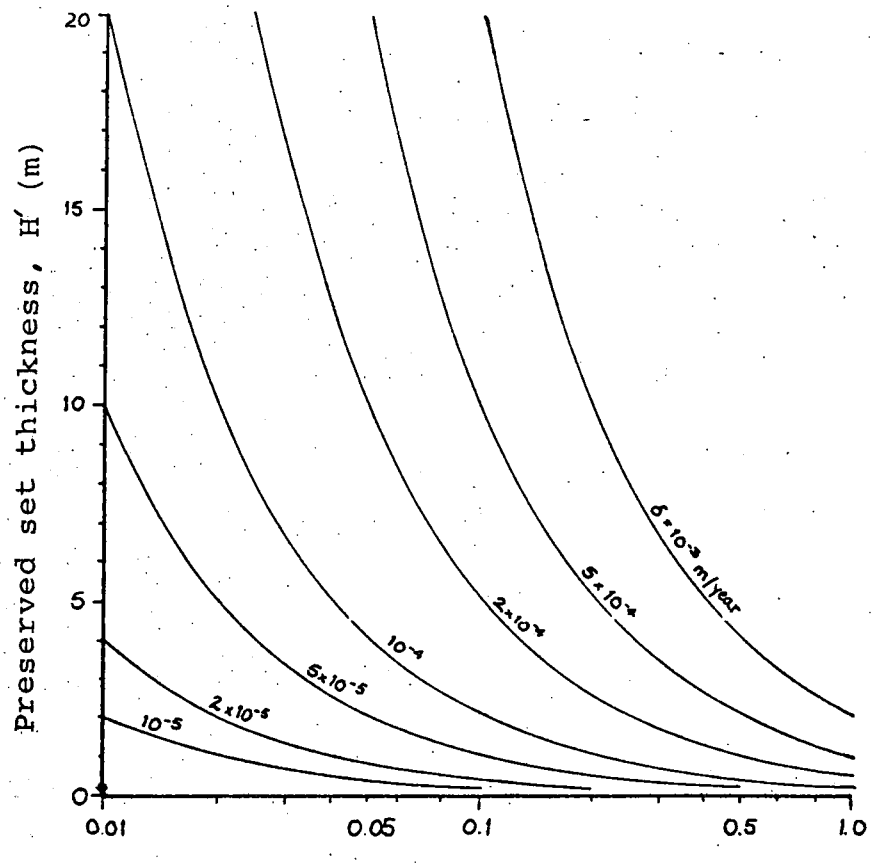

Draa migration rate, $\dot{D}$ (m/year).

(λ_D = 2000m for graph)

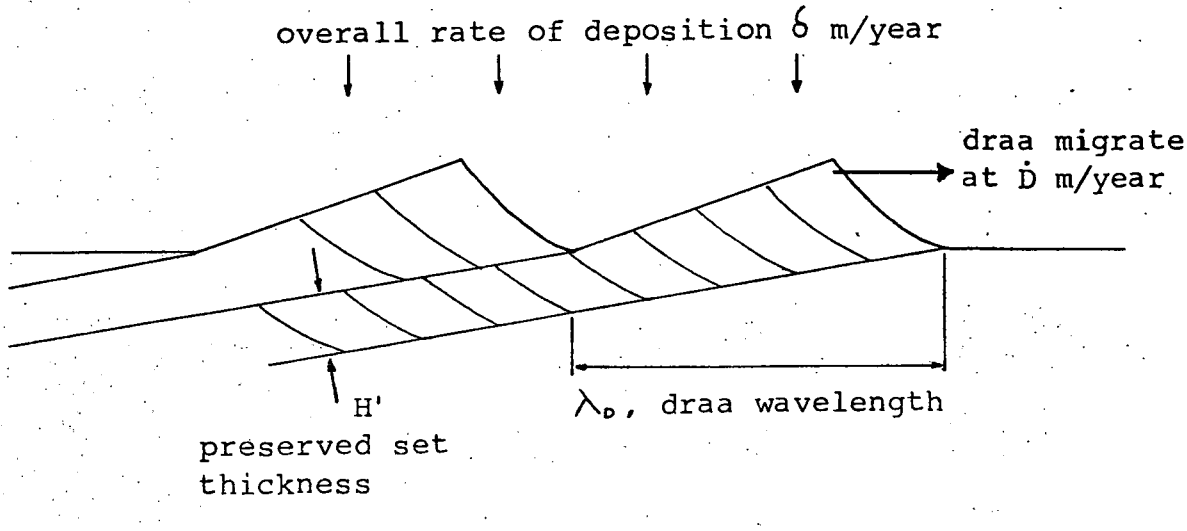

Preserved set thickness given by $H' = \frac{\lambda_D \times \delta}{\dot{D}}$ m.

Note that with a constant sand-drift rate, if the draa wavelength & height are halved, the migration rate will double & the preserved set thickness reduced by a factor of four.

FIG. 2.11 Factors governing 3rd order set thickness

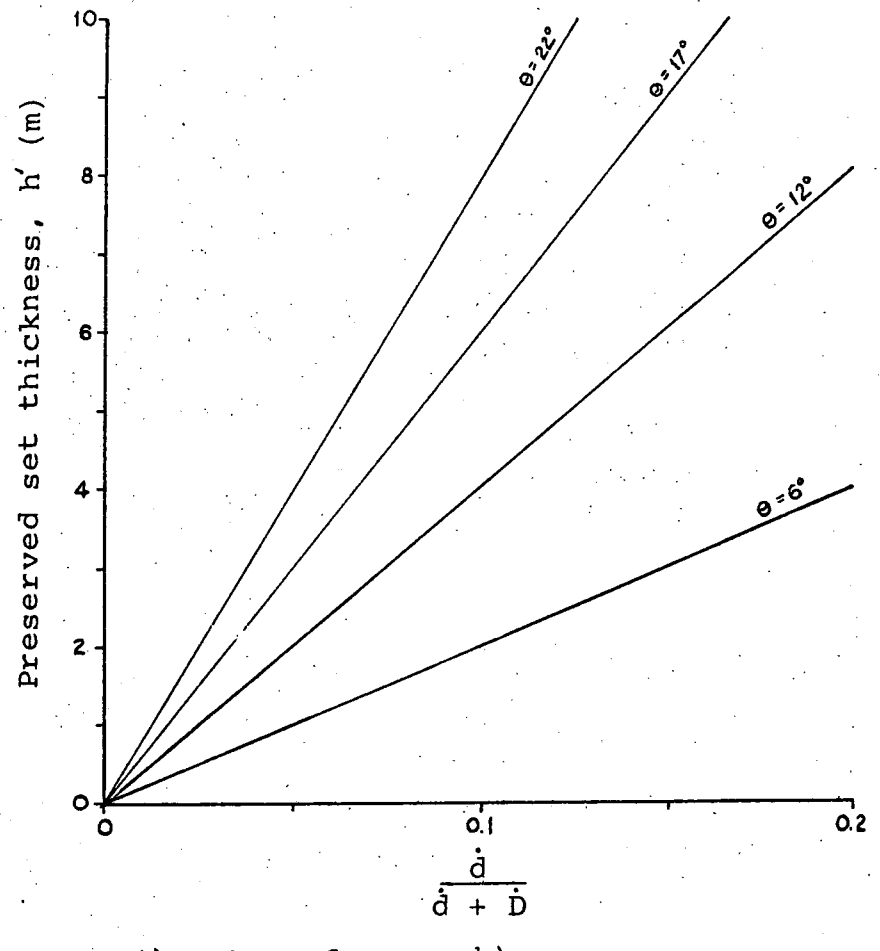

(λ_d= 200m for graph)

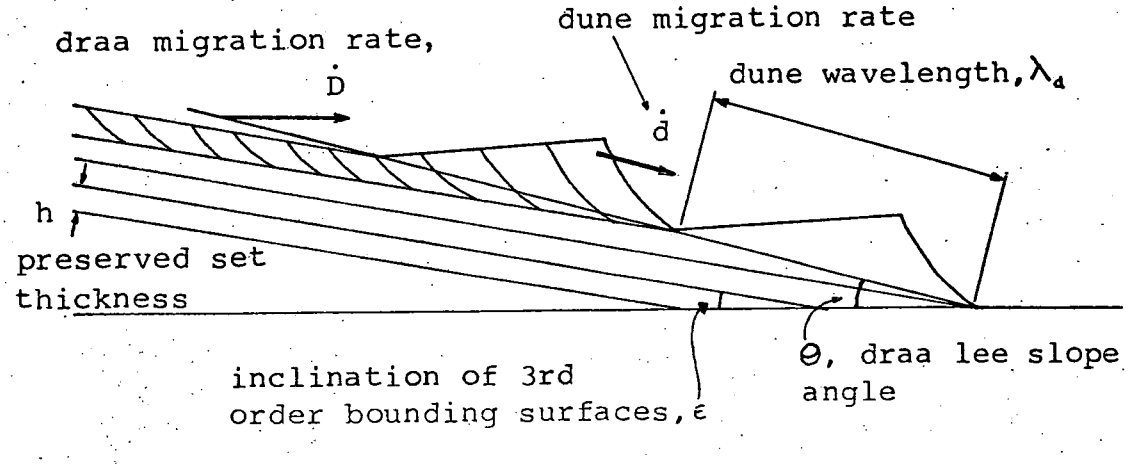

Angle of climb of dunes relative to draa lee slope $= \theta - \epsilon$

Preserved third order set thickness is given by

$h = \frac{\dot{D}}{\dot{d}} \lambda_d \sin\epsilon \simeq \frac{\dot{D}}{\dot{d} + \dot{D}} \lambda_d \sin\theta$, the approximation being good (within 1%) for natural examples.

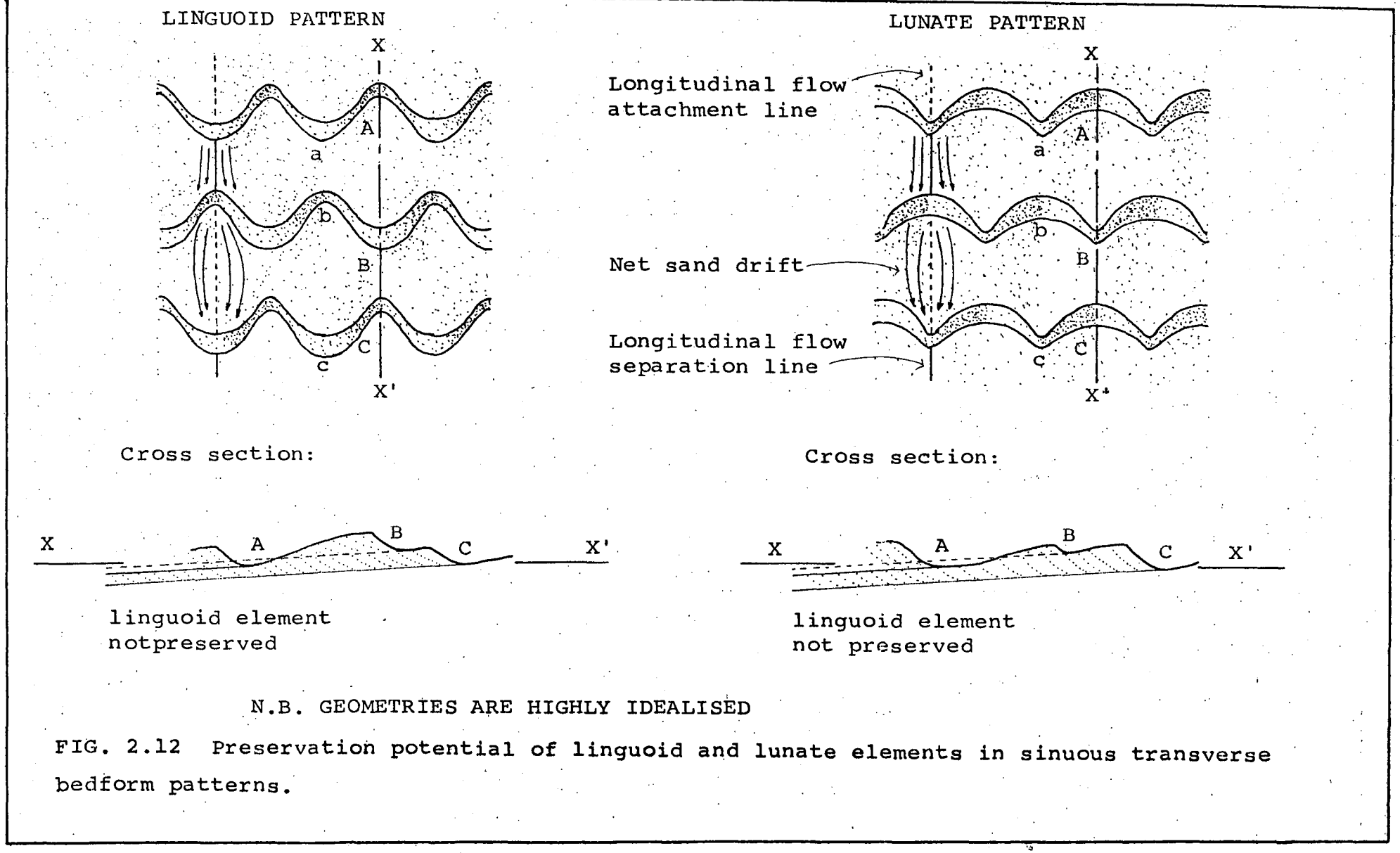

N.B. GEOMETRIES ARE HIGHLY IDEALISED

FIG. 2.12 Preservation potential of linguoid and lunate elements in sinuous transverse bedform patterns.

FIG. 2.13

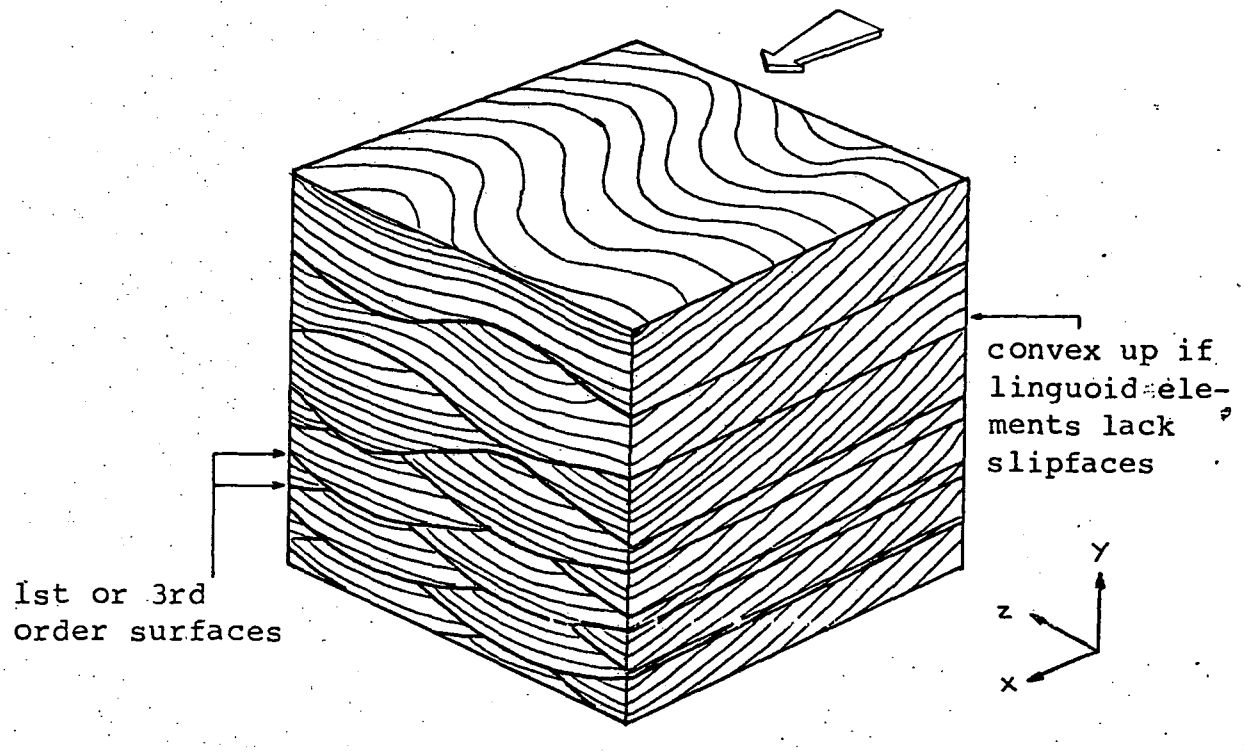

Cross-bedding pattern for one order of sinuous transverse bedform behaving entirely systematically. Angle of bedform climb decreases down the diagram, though the rate of climb represented by sets at the base of the diagram is probably greater than natural examples by a factor of at least two. If the bedforms represented are draa, side of cube = 500 to 2000m; if dunes, side of cube = 50 to 200m.

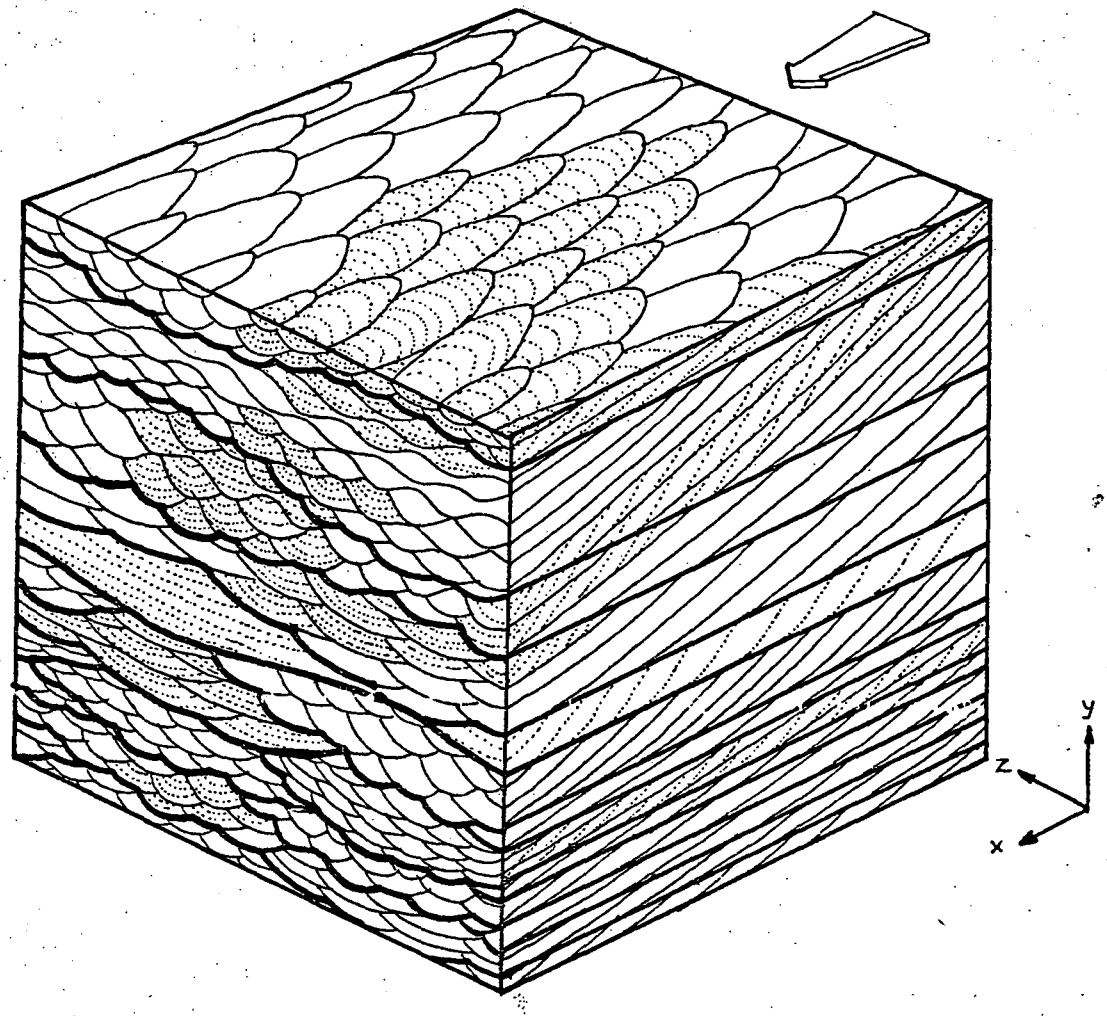

FIG. 2.14 Cross-bedding pattern for two superimposed orders of bedform, both sinuous transverse and behaving systematically. Angle of first order bedform climb decreases down the diagram. The scale of the diagram is not uniform - to facilitate representation there is some vertical exagerration. Bedform sinuosities are varied across the diagram for illustrative purposes. Note the similarity of 1st and 3rd order surfaces in the yz section.

KEY:

——— = 1st order bounding surfaces

——— = 3rd order bounding surfaces

= cross-laminae

FIG. 2.15 Longitudinal and transverse vertical sections of a selection of modification surfaces.

(A) Crest rounding by vortices induced upstream

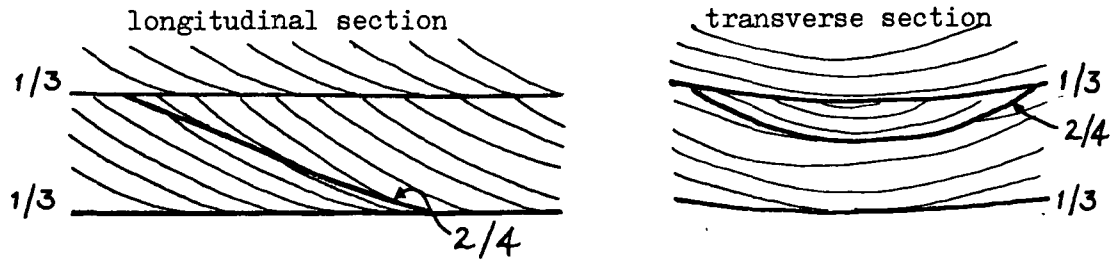

(B) Increase in crest height caused by change in flow pattern

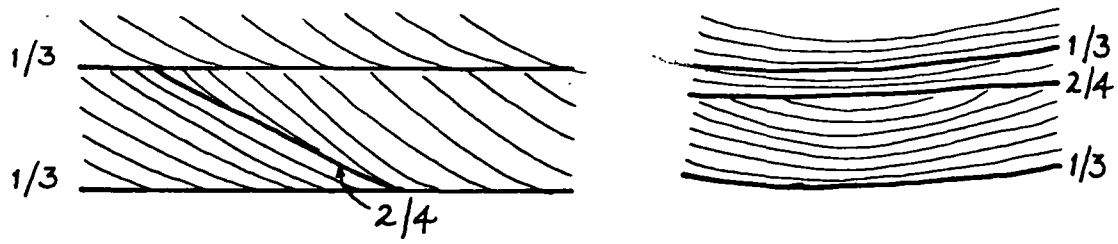

(C) Wind reversal

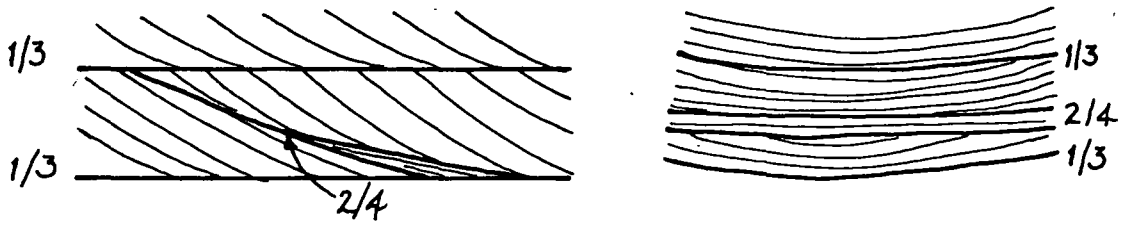

(D) Change from a slipfaceless to slipfaced draa

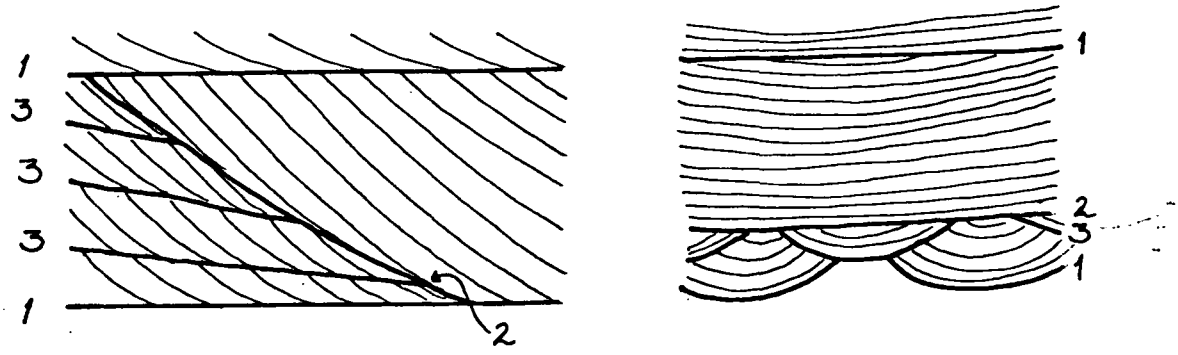

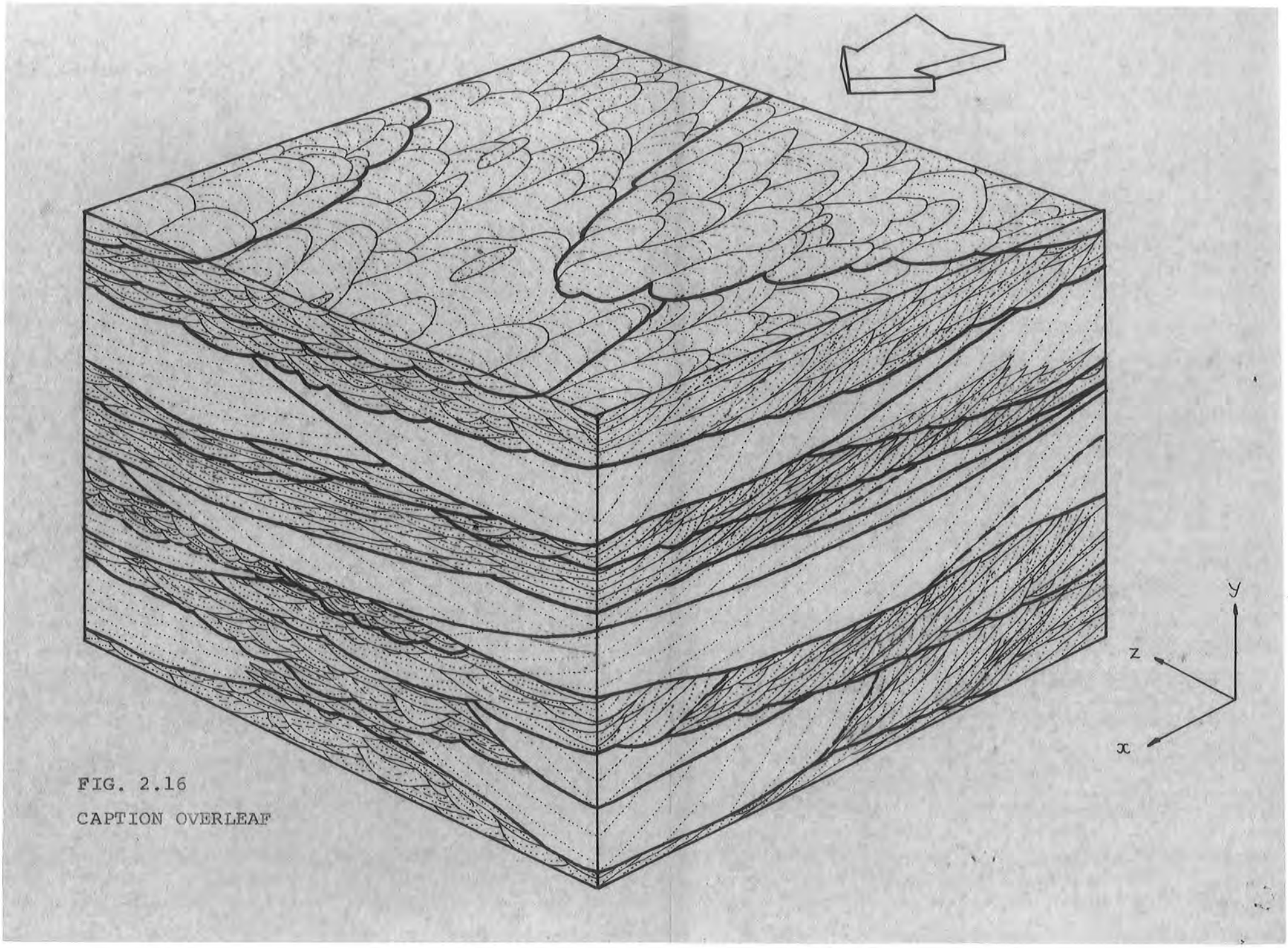

FIG. 2.16

CAPTION OVERLEAF

FIG. 2.16 Cross-bedding pattern envisaged for two superimposed orders of bedform with partly random behaviour. The bedform sinuosities and the state of the draa leesides are varied across the diagram to illustrate the possible scope of these features. Such frequent alternations are not to be expected within individual formations. Net sand drift is in the positive x direction, as indicated by the large arrow. Note the difficulty of distinguishing the various orders of bounding surface, especially in the xz and yz planes.

KEY

——— = 1st order bounding surfaces

——— = 2nd order bounding surfaces

——— = 3rd order bounding surfaces

- - - - - - = selected 4th order bounding surfaces

..... = selected cross-laminae

FIG 2.17 BEDFORM SHAPES AND POTENTIAL PALAEOCURRENT AZIMUTHS

(A)

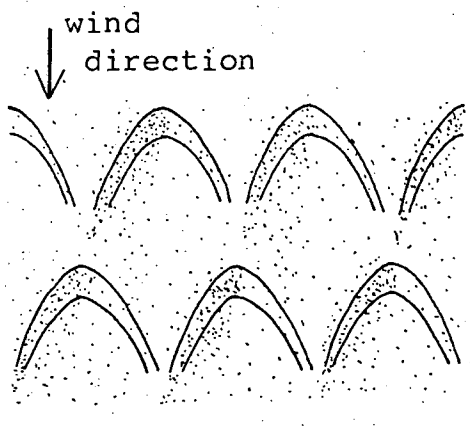

Lunate fishscale pattern. After Wilson (1970).

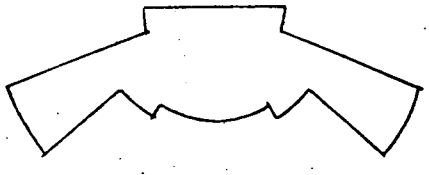

Potential palaeocurrent azimuths deduced from slip-face orientations.

(B)

Oblique pattern. After Wilson (1970). (This pattern could probably exist as an oblique trend without the SE'ly wind.)

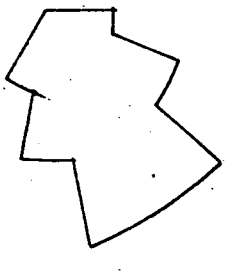

Potential palaeocurrent azimuths deduced from slip-face orientations.

(C)

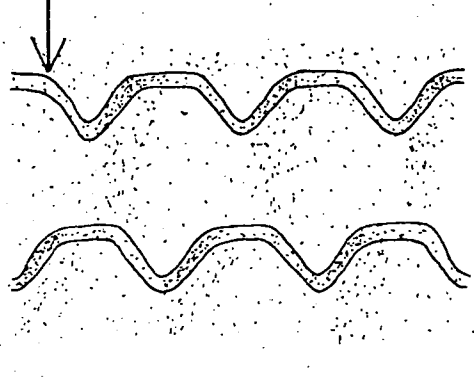

Lunate pattern.

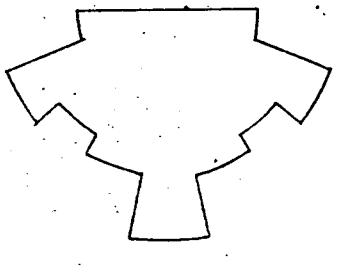

Potential palaeocurrent azimuths deduced from slip-face orientations.

CHAPTER THREE

THE LAMINATION AND GRAIN CHARACTERISTICS OF AEOLIAN SANDS

FIG. 3.1 Wind-ripple lamination in the Yellow Sands at Bowburn Quarry (see Ch.5). Note the thinness and parallelism of the laminae and their alternating grain size. Lens cap is 50mm in diameter.

FIG. 3.2 Sandflow lamination in the Yellow Sands at Sherburn Hill sand pit (see Ch.5). Note the homogeneity of the laminae, their evenness and the very thin finer-grained bounding laminae. The thicker bounding laminae may be accumulations of grainfall or wind-ripple lamination.

FIG. 3.3 Sand-sheet lamination at the base of the Yellow Sands, North Hylton (see Ch.5). The lamination is fine but slightly uneven, with wisps and lenses of coarse sand. Trowel (0.29m long) rests on the surface of the Carboniferous.

CHAPTER FOUR

THE LOWER PERMIAN SETTING IN BRITAIN

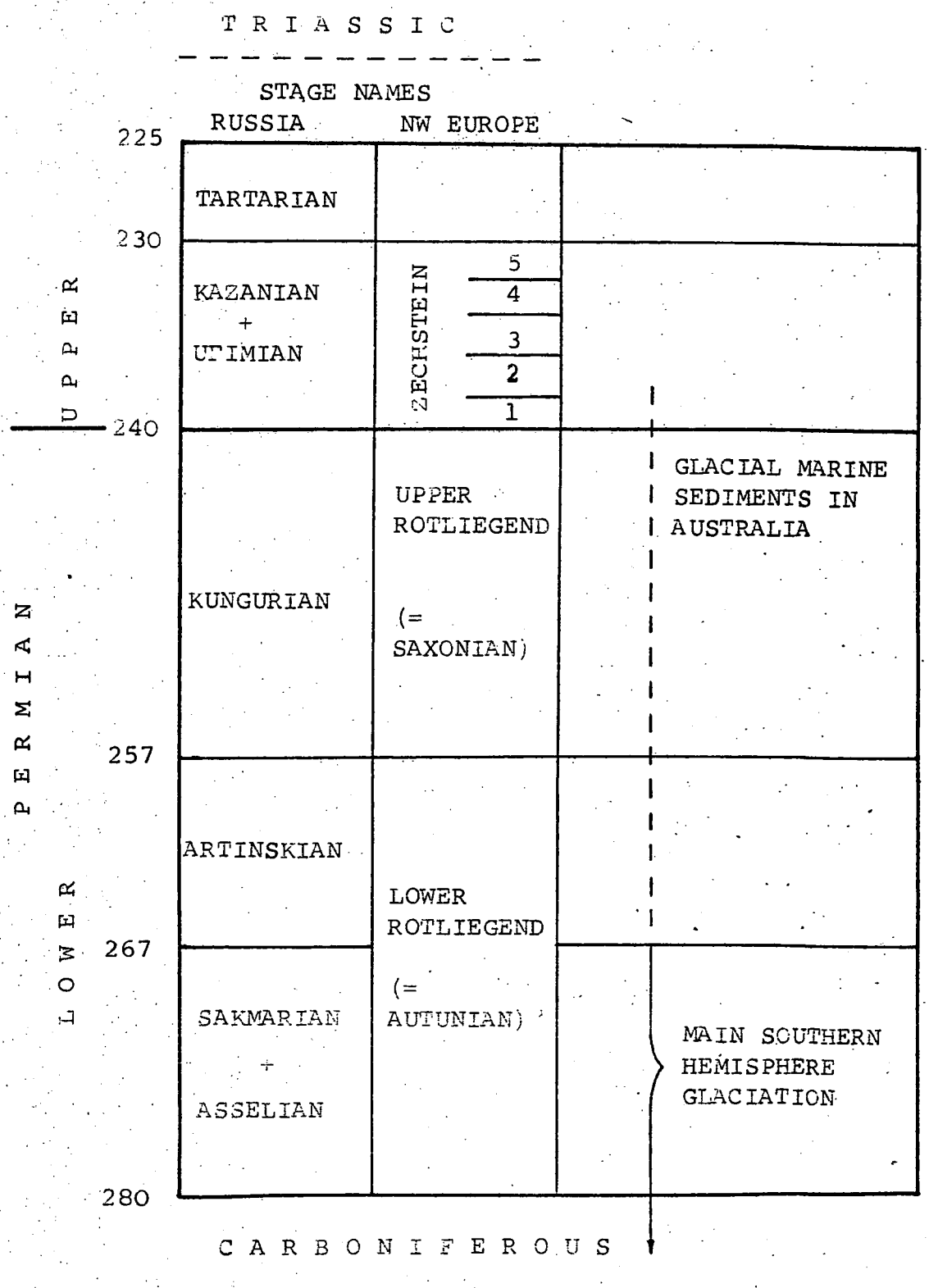

FIG.4.1 Permian stage names and time scale.

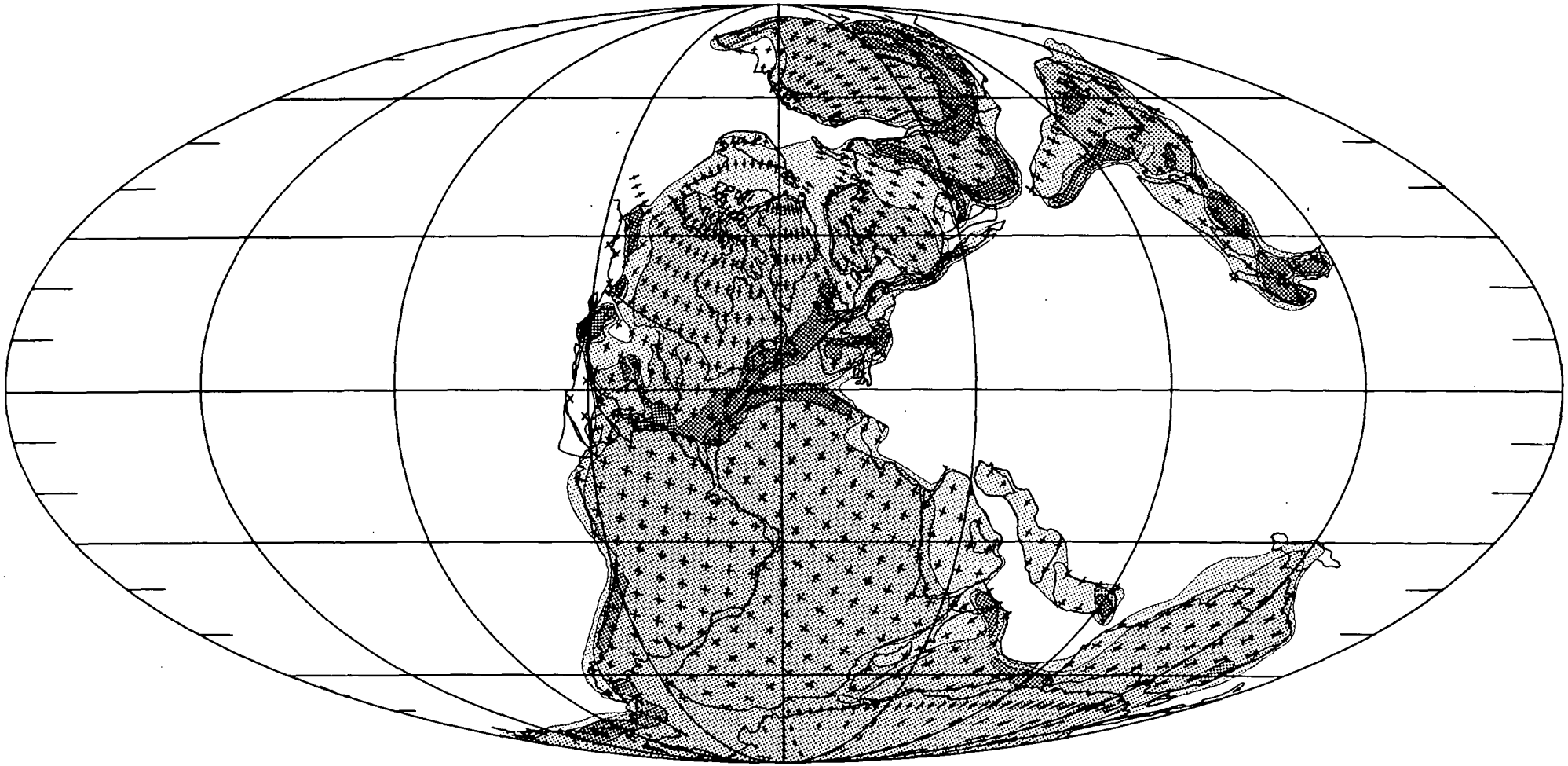

FIG. 4.2 Late Permian continent reconstruction of Scotese et al (1979). Dark stipple = mountains, medium stipple = other land, light stipple = shelf seas, blank = deep ocean. UK is at 20° N, 15° E.

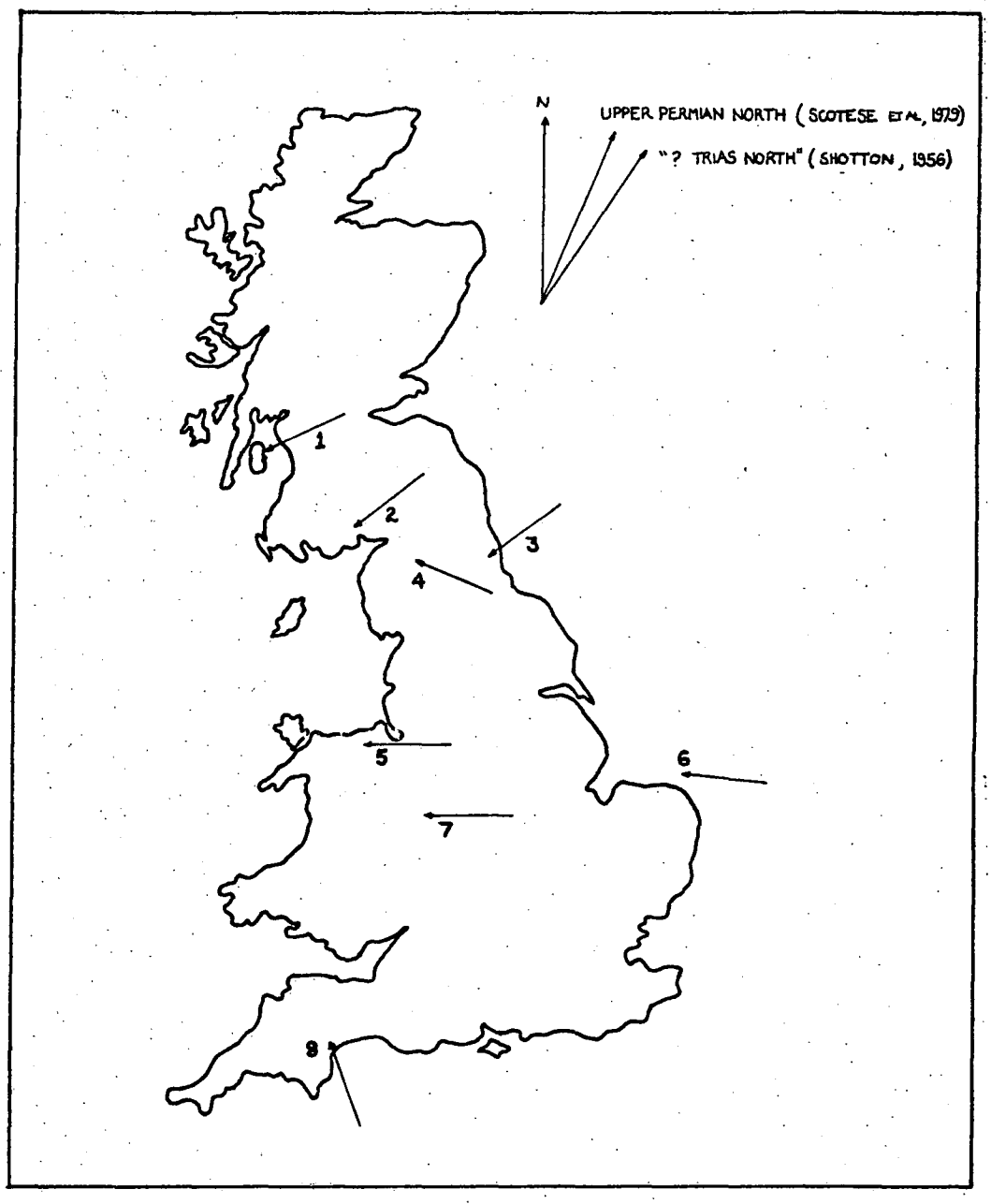

FIG. 4.3 Palaeowind directions from British Lower Permian aeolian sandstones.

1 = Corrie Sandstone, Arran, from Piper (1970)

2 = Locharbriggs Sandstone, from Brookfield (1979)

3 = Yellow Sands resultant, this thesis

4 = Penrith Sandstone, from Waugh (1970)

5 = Vale of Clwyd, from Shotton (1956)

6 = Rotliegendes gas wells, from Glennie (1972)

7 = Bridgnorth Sandstone, from Shotton (1956)

8 = Dawlish Sandstone, from Laming (1969)

CHAPTER FIVE

THE YELLOW SANDS - INTRODUCTION AND SEDIMENTARY STRUCTURES

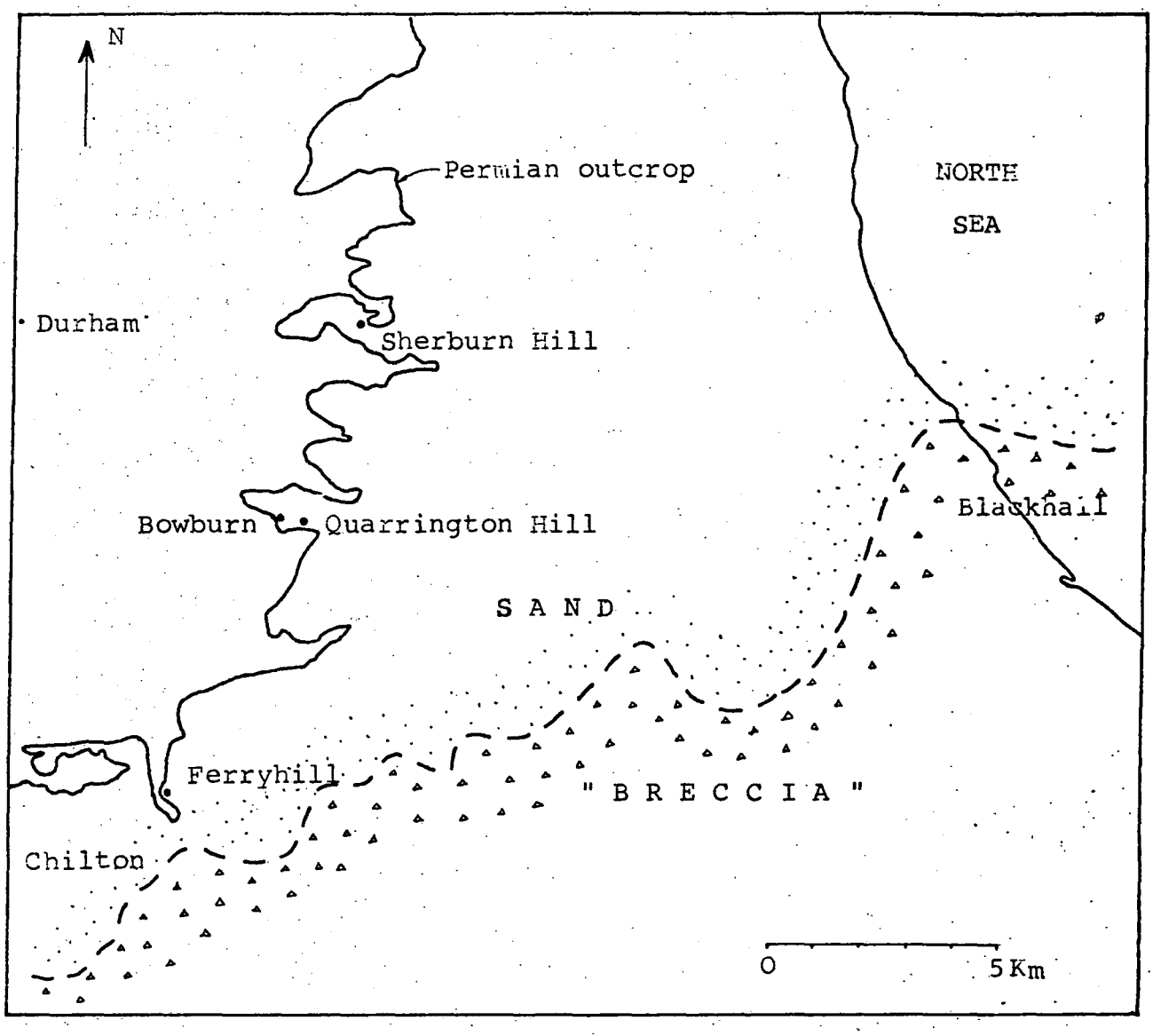

FIG. 5.1 Approximate boundary between the sand and "breccia" facies of the Basal Permian in County Durham. After Smith and Francis (1967, Pl. XV).

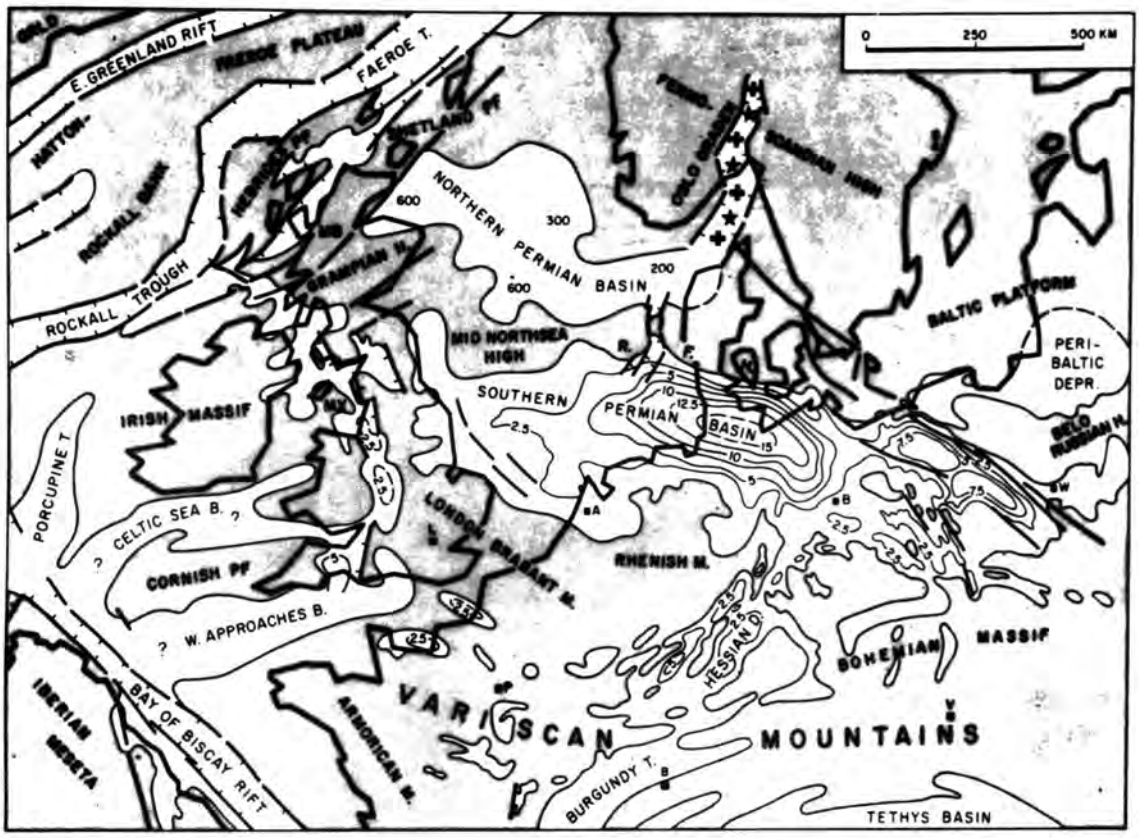

FIG. 5.2a Isopachytes of Rotliegendes sediments.

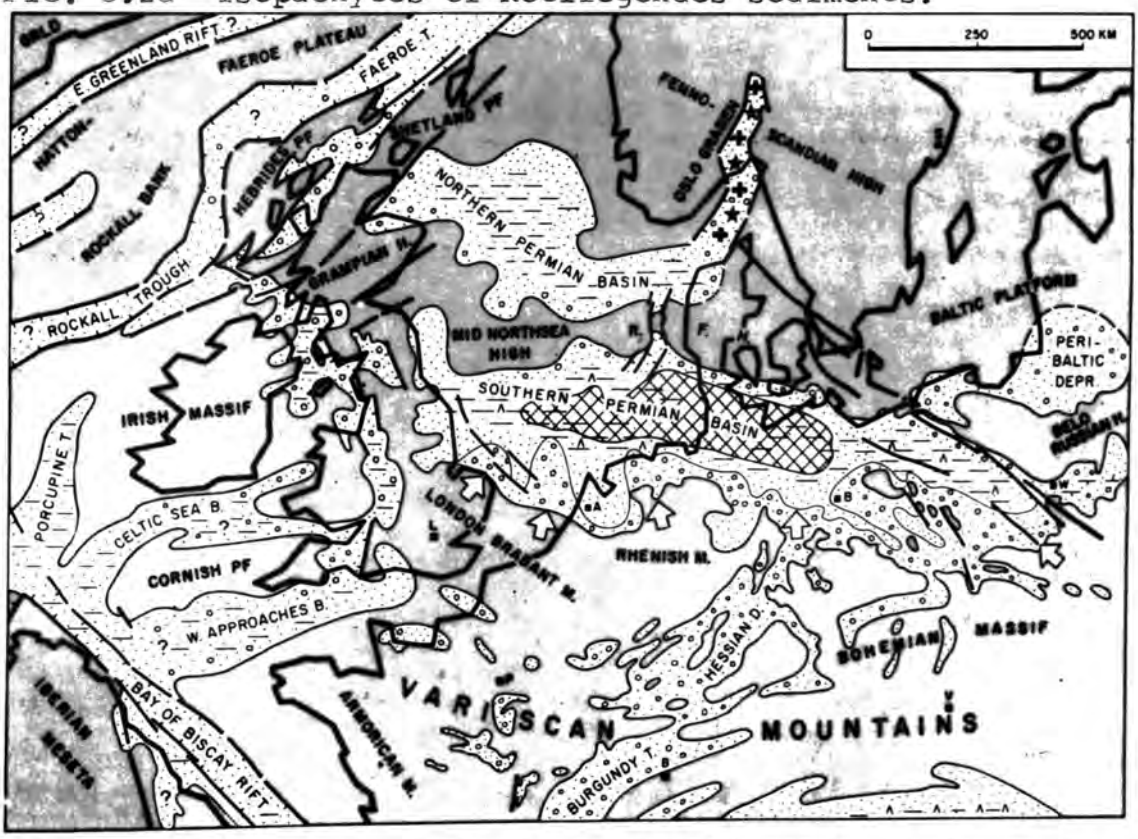

FIG. 5.2b Palaeogeography of the Rotliegendes. Both maps on this page from Ziegler (1981).

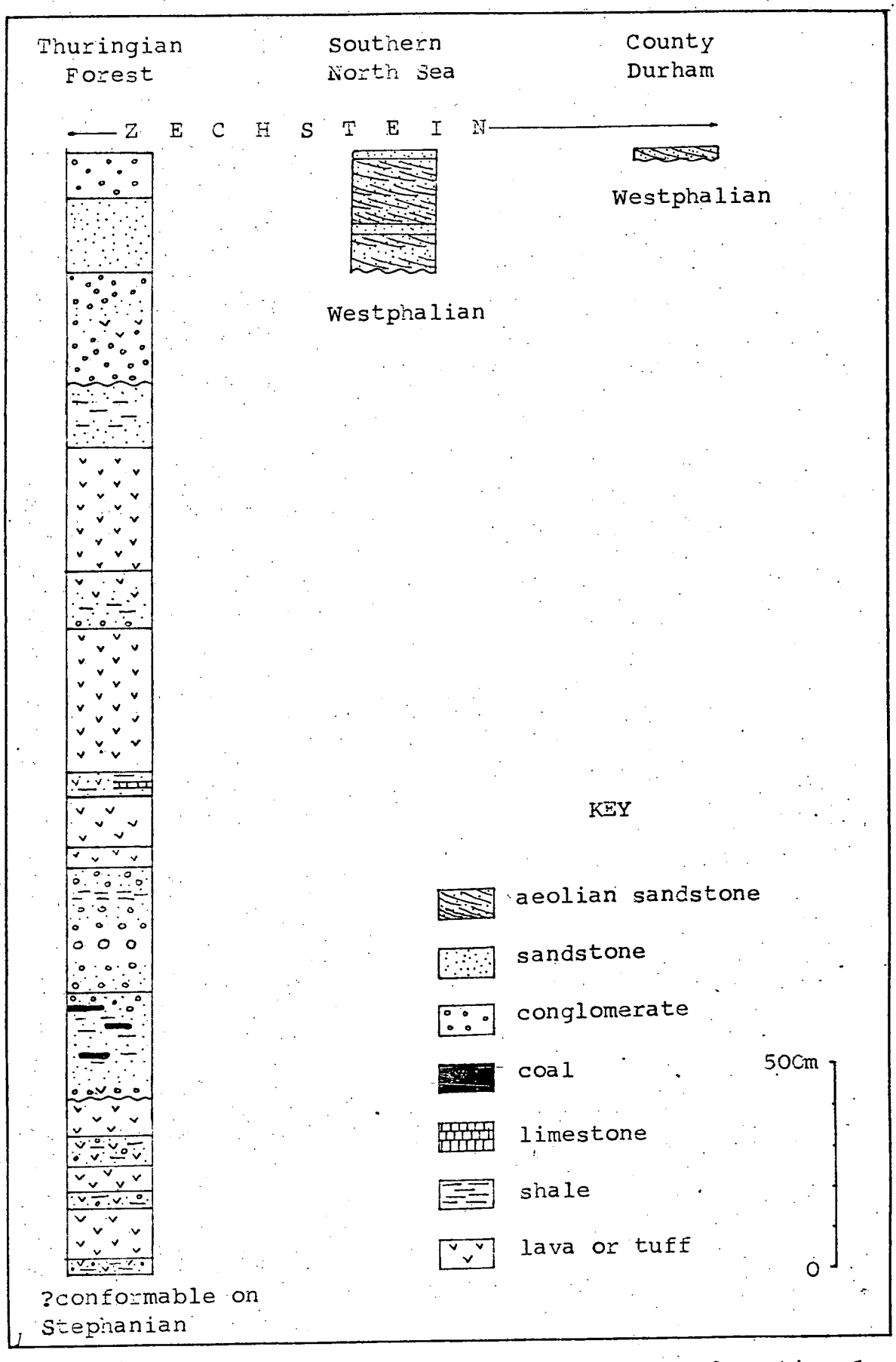

FIG.5.3 Comparative Rotliegendes sequences. Information from Falke (1972b, p.63) & Glennie (1972). The Thuringian Forest is at the southwestern extremity of East Germany.

THE SUBSURFACE DISTRIBUTION OF THE YELLOW SANDS

FIG 5.4

CROSS-BEDDING DIP AZIMUTH MODES AND RESULTANT ; NOTE THE CORRESPONDENCE OF THE RESULTANT AND THE DRAA ORIENTATION.

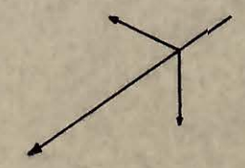

WHITLEY BAY

30 FATHOM DYKE

10+ CULLERCOATS

570

TYNEMOUTH

TYNEMOUTH PRIORY

RIVER TYNE

NEWCASTLE - UPON - TYNE

GATESHEAD

N O R T H S E A

$\bar{t}$ = 33 m

$\bar{t}$ = 3m

$\bar{t}$ = 21 m

$\bar{t}$ = 4m

$\bar{t}$ = 28m

$\bar{t}$ = 5m

$\bar{t}$ = 24 m

$\bar{t}$ = 4m

$\bar{t}$ = 26 m

$\bar{t}$ = 1 m

$\bar{t}$ = 19m

560

SUNDERLAND

NORTH HYLTON

CLAXHEUGH

550

McCALL'S QUARRY

RIVER WEAR

SEAHAM

HETTON DOWNS QUARRY

HIGH MOORSLEY

ELEMORE HALL SCHOOL

DURHAM

SHERBURN HILL SAND PIT

PETERLEE

540

BOWBURN QUARRY

QUARRINGTON HILL QUARRY

CASSOP VALE

BUTTERKNOWLE FAULT

$\bar{t}$ = 16m

FERRYHILL RAILWAY CUTTING

HARTLEPOOL

530

430

440

450

KEY

$\bar{t}$ = AVERAGE THICKNESS OF SAND IN EACH RIDGE OR CORRIDOR

0 SCALE 5 Km

EXPOSURES

LINE OF PERMIAN OUTCROP WITH YELLOW SANDS AT BASE

27 RECORDS OF YELLOW SANDS THICKNESS IN METRES

FAULTS

DRAA INTERPRETED DRAA OUTLINES (HACHURE POINTS TOWARDS SAND BODY)

N W E S

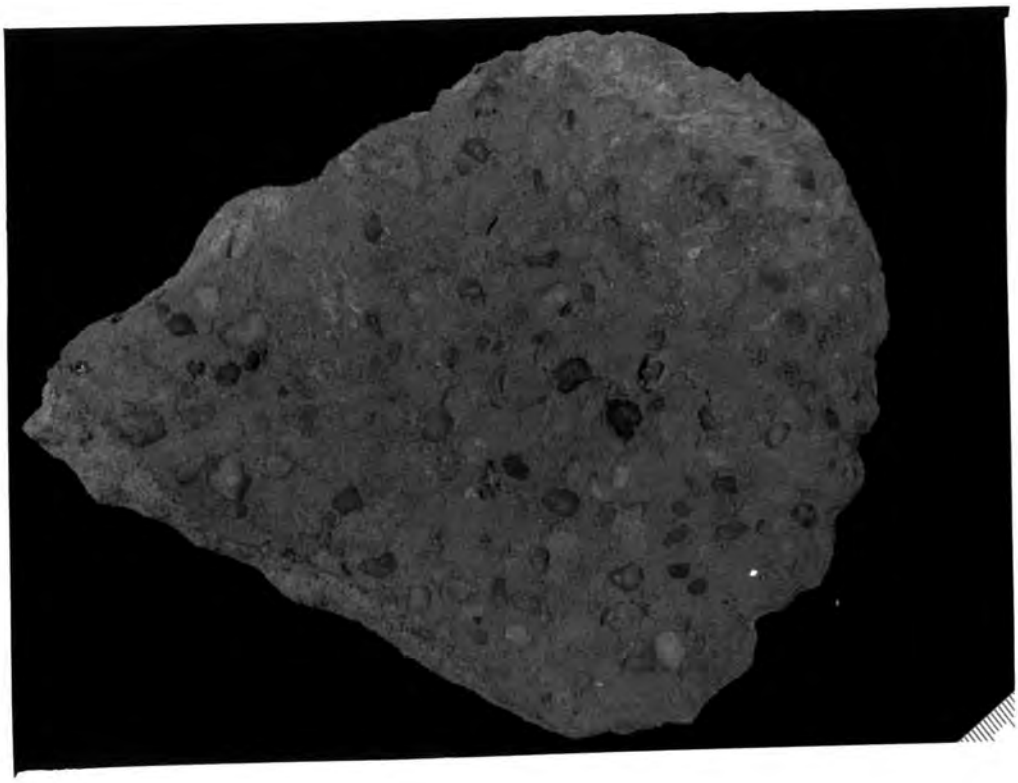

FIG. 5.5 Specimen of the pebbly layer at 33,1 in the Cullercoats section (Encl. 1). Fine pebbles of quartz evenly spread in the fine sand. Scale (mm) at bottom right.

FIG. 5.6 The base of the Yellow Sands at Tynemouth, with Westphalian sandstones and shales below. The unconformity (dotted) is offset by a small fault. The Westphalian rocks are variously coloured red, yellow and grey. Hammer (arrowed) for scale.

FIG. 5.7 The unconformable contact of the Yellow Sands and Westphalian sandstones at North Hylton (Encl. 2). The hammer (0.36m long) rests on yellow and red Carboniferous sandstones. The Yellow Sands above the unconformity show a sand-sheet lamination as far as the end of the hammer handle, with wind-ripple lamination above.

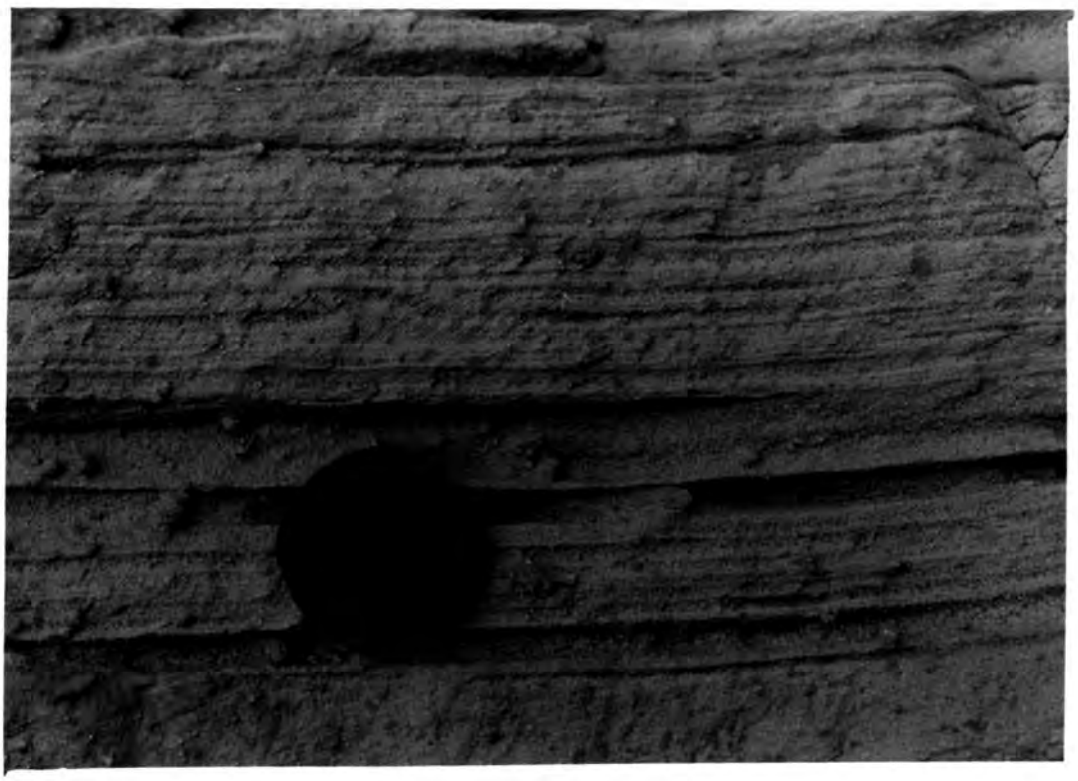

FIG. 5.8 The only example of surface deformation seen in the Yellow Sands (just above lens cap). Dip of cross bedding is ~30° to the left. Lamination is thin sandflow with wind ripples. The deformation consists of a small overthrust directed downdip. Lens cap is 50mm in diameter. McCall's Quarry, 40,7 on Enclosure 3.

FIG. 5.9 The top of the Yellow Sands at McCall's Quarry between 150 and 180m on Enclosure 3. Shows the pavement excavated on the top surface and the slope on the top. Author for scale.

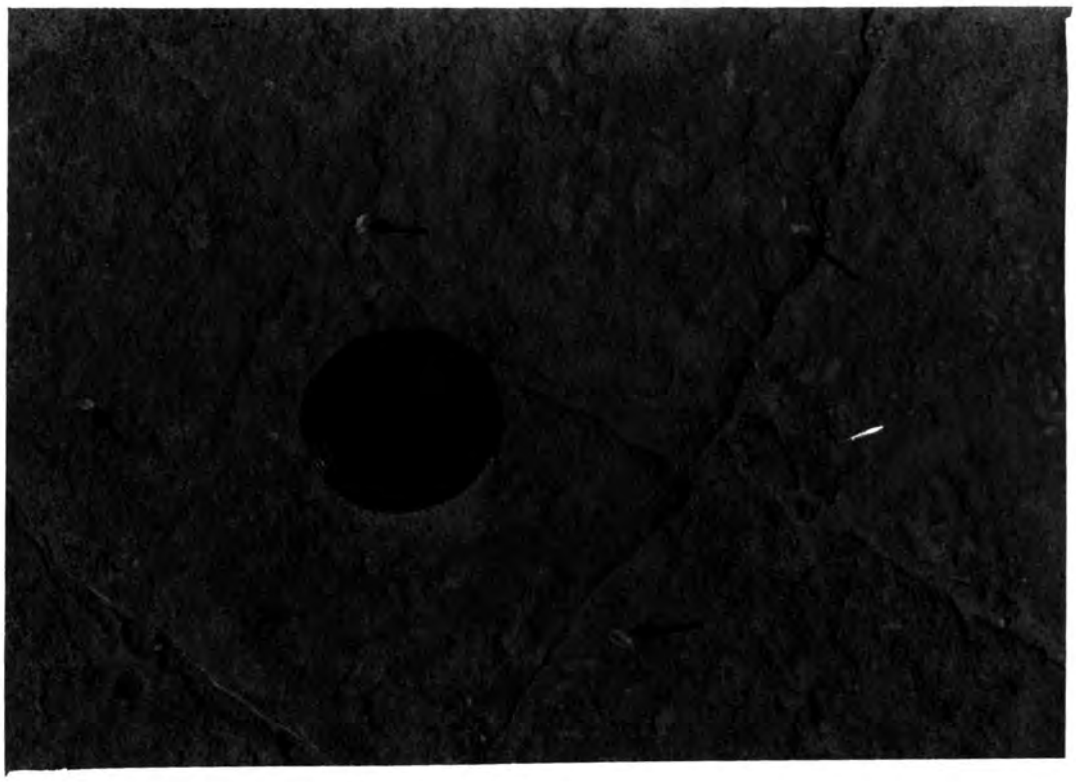

FIG. 5.10 Photograph of the pavement on top of the Yellow Sands at McCall's Quarry. Shows several specimens of Lingula crederi (arrowed). Lens cap diameter = 50mm.

FIG. 5.11 Details as above except that the fossils are believed to be casts of Permophorus costatus.

FIG. 5.12 The north face of Hetton Downs Quarry, in 1971. Far more structure was visible then than now, though cross bedding cannot be detected in the upper part of the face. From a transparency kindly loaned by Dr. D.B.Smith.

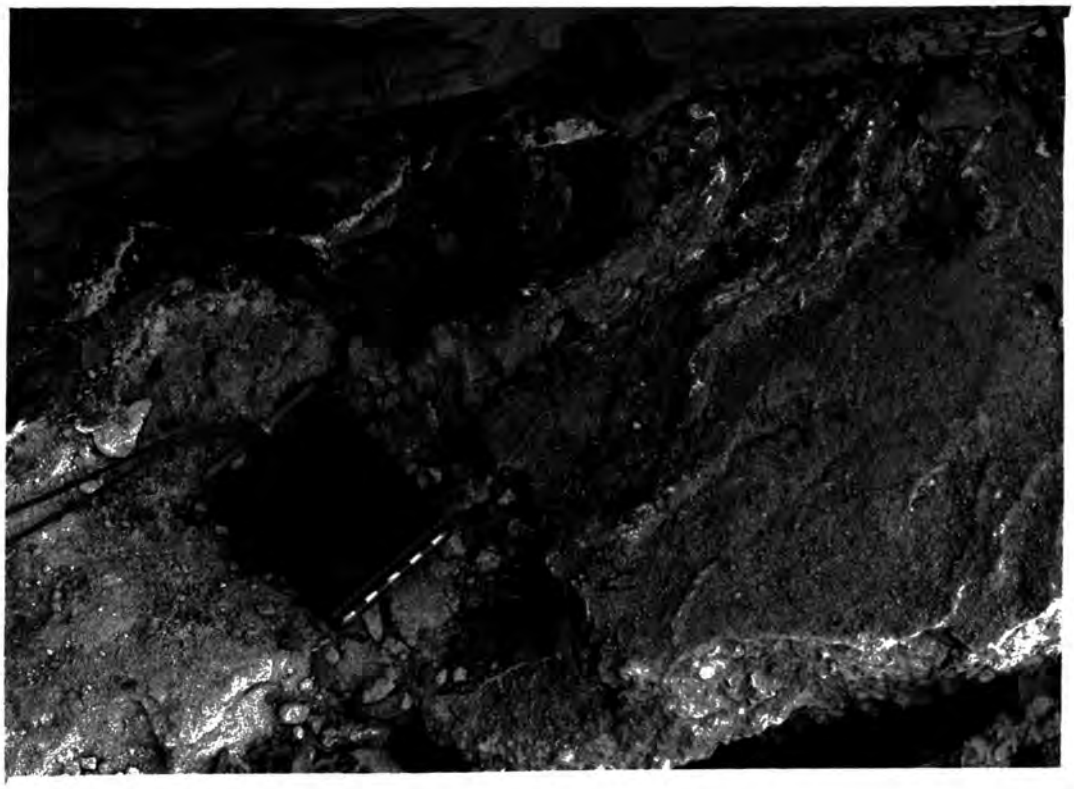

FIG. 5.13 The top surface of the Yellow Sands, with overlying Marl Slate, at the extreme W end of the N face of Hetton Downs Quarry. Shows anastomosing cylindrical ridges which protrude into the Marl Slate. Bedding plane dips 10-15° to the left. Compass is 100 x 65mm.

FIG. 5.14 View of the west face of Sherburn Hill Sand Pit. The top of the face corresponds closely to the top of the Yellow Sands. Distance from the top of the face to the floor of the quarry ~30m.

FIG. 5.15 View of Crime Rigg Quarry from the road-side at NZ349418. Main face is ~25m high. The sky-line in the centre is the crest of the west face of Sherburn Hill sand pit.

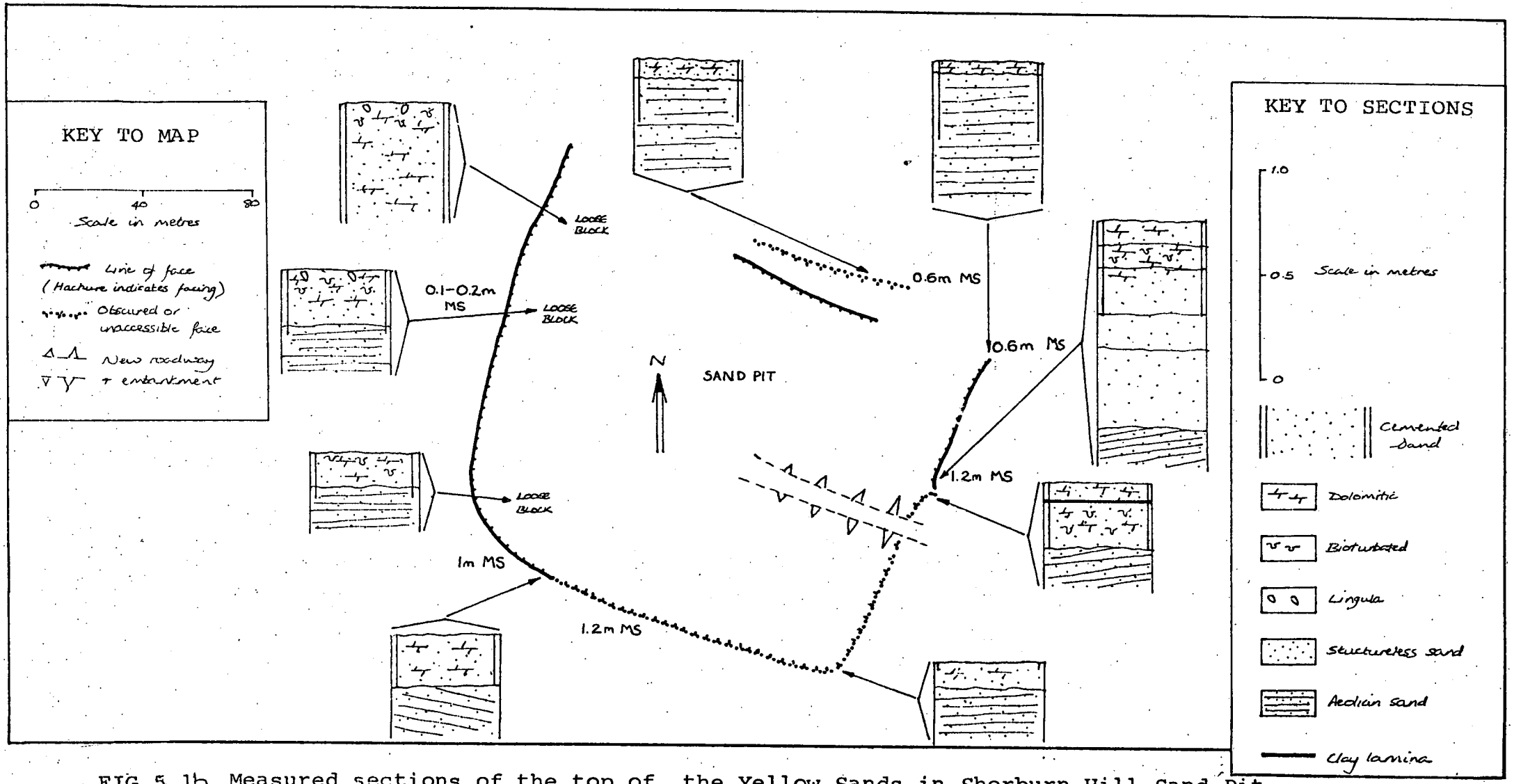

FIG.5.1b Measured sections of the top of the Yellow Sands in Sherburn Hill Sand Pit.

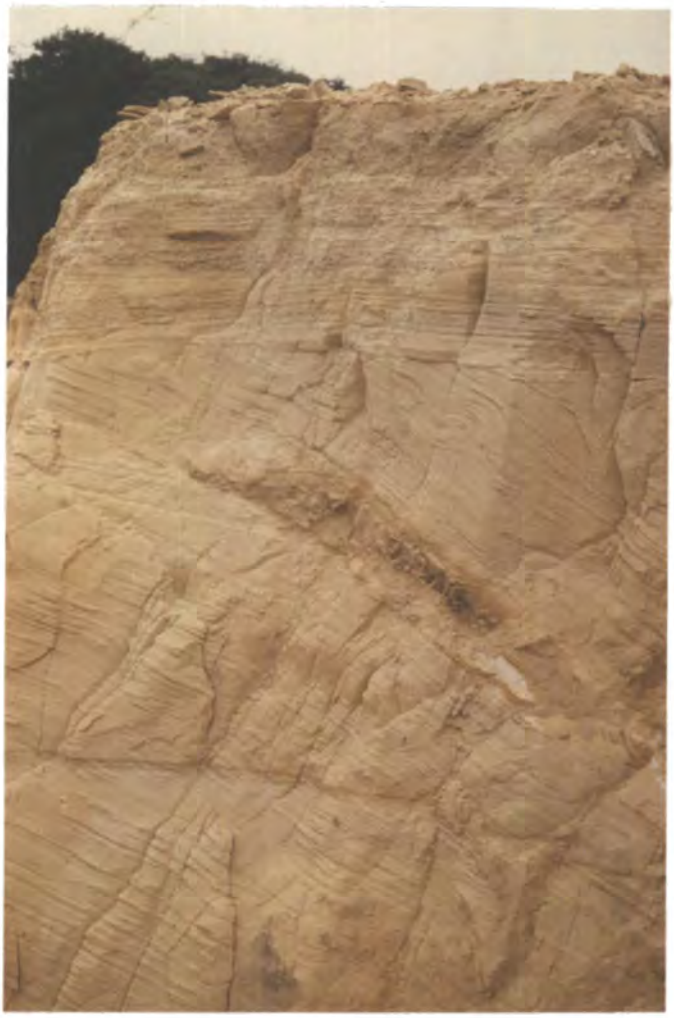

FIG. 5.17 Gentle deformation at the top of the W face of Sherburn Hill Sand Pit (68,32 on Encl. 5). The top of the face corresponds to the top of the Yellow Sands. It is underlain by ~2m of flat-lying wind-ripple laminated sand. The surface visible is oriented approximately E-W, being the wall of a gully in the main (N-S) face.

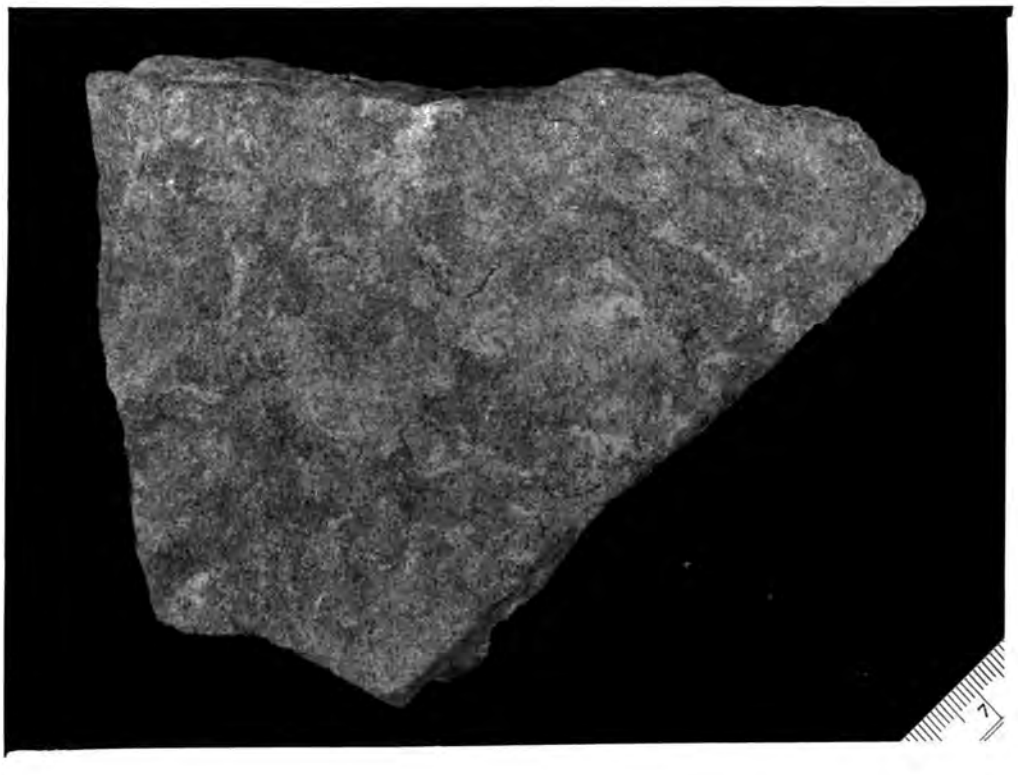

FIG. 5.18 Lower surface of a specimen 50mm thick of the top surface of the Yellow Sands from a loose block below Sherburn Hill W face. Shows mottling due to bioturbation. Lighter areas contain a high proportion of dolomite silt. Scale (mm) at lower right.

FIG. 5.19 The northern end of Bowburn Quarry, showing Yellow Sands, Marl Slate and Lower Magnesian Limestone. Note the flat top of the Yellow Sands. The Yellow Sands face is 70m long by 8m high at maximum. Further excavations took place before Enclosure 7 was drawn.

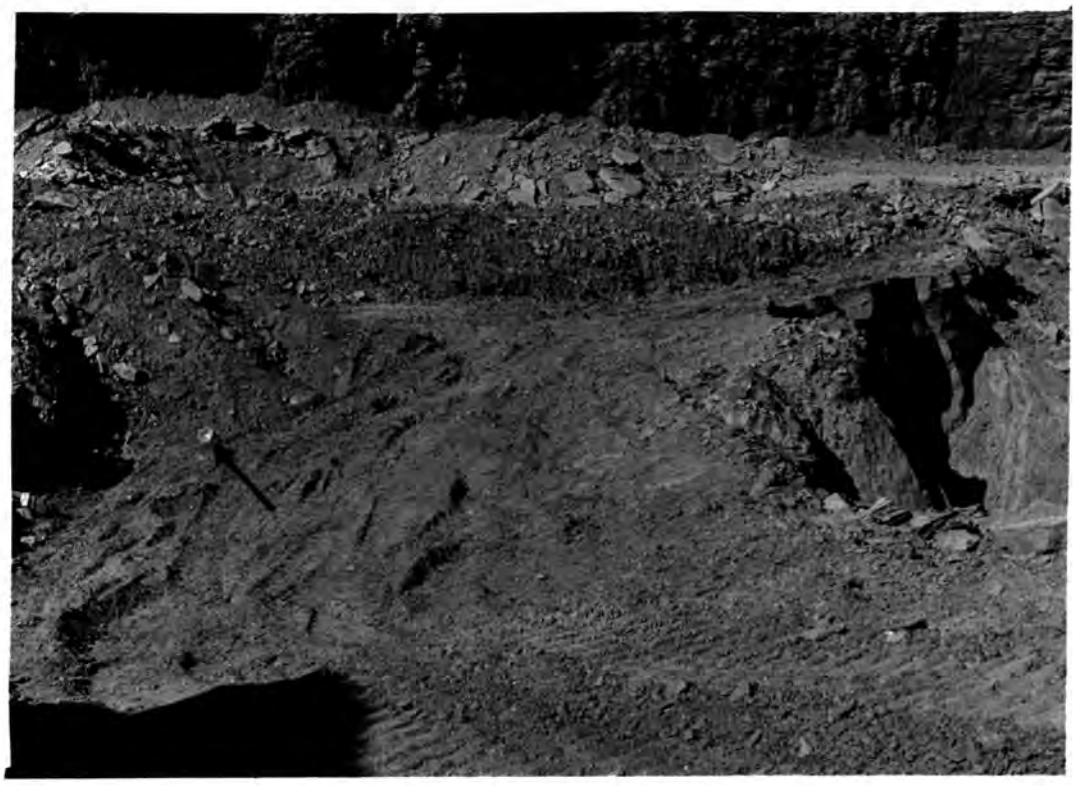

FIG. 5.20 The north-western corner of Bowburn Quarry, Yellow Sands visible at right. The trackway lies along the top surface of the Sands and parallels the slope (to the NW) of that surface. Inverted hard hat (arrowed) and vehicle tracks give scale.

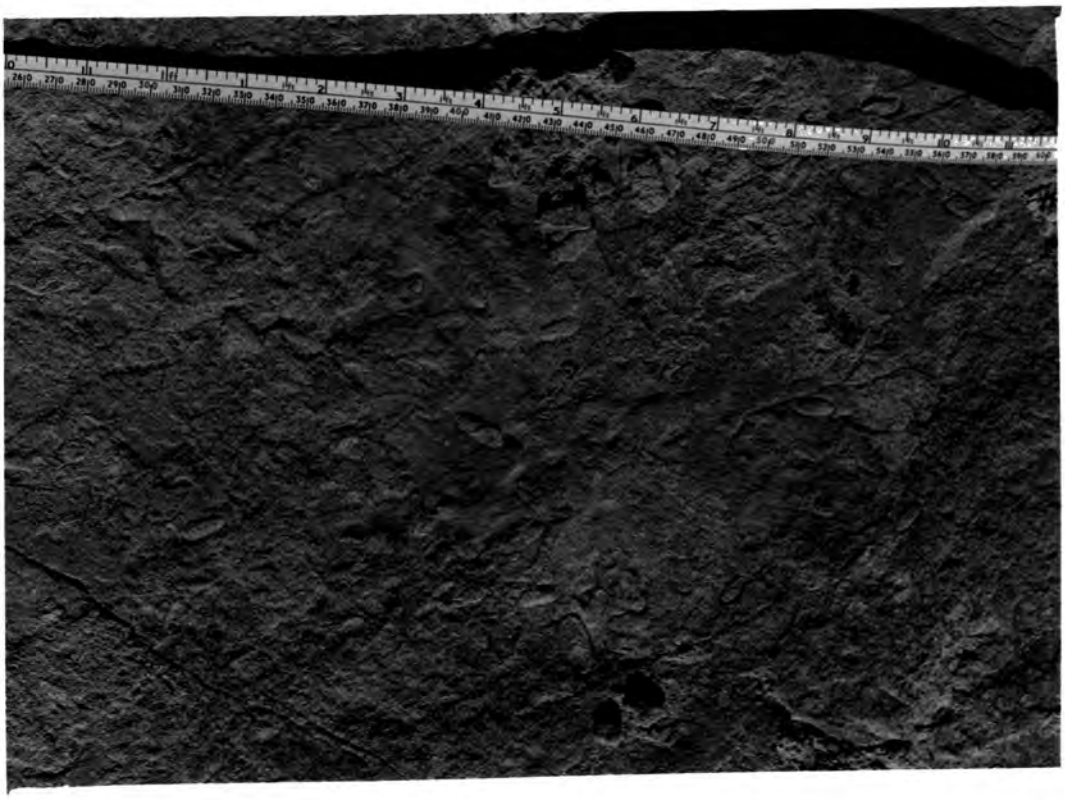

FIG. 5.21 Moulds believed to be of Permophorus costatus on the top surface of the Yellow Sands. Loose block, NW end of Bowburn Quarry.

FIG. 5.22 Deformation in Bowburn Quarry (112,11 on Encl. 7). The Marl Slate lies just above the top of the photograph, which covers an area roughly 1.5 x 2.0m.

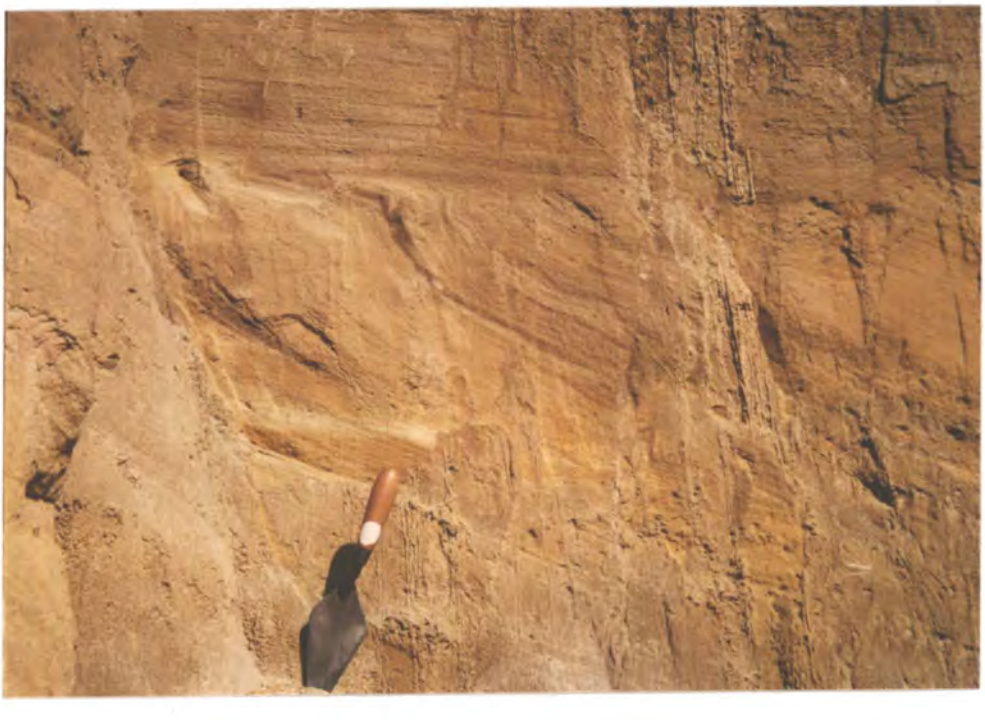

FIG. 5.23 Deformation in Bowburn Quarry at 222,11 on Enclosure 7. The deformation appears to have sheared against the overlying planar-bedded zone, which shows sand-sheet lamination. Lamination of deformed sand is a mixture of sandflow and wind-ripple types.

FIG.5.24 Loose block in the NW face of Bowburn Quarry. Top of block is top of Yellow Sands. 30-40mm of structureless sand overlies wind-ripple laminae deformed at the left hand end of the block. Length of trowel blade visible is 0.14m.

FIG.5.25 Part of the main face of Bowburn Quarry, around 150-170m on Enclosure 7. The top of the face corresponds to the top of the formation. The photograph shows a transverse cut through a trough-shaped set. Both the normal yellow colour and the lenses of red sand are visible. Author for scale.

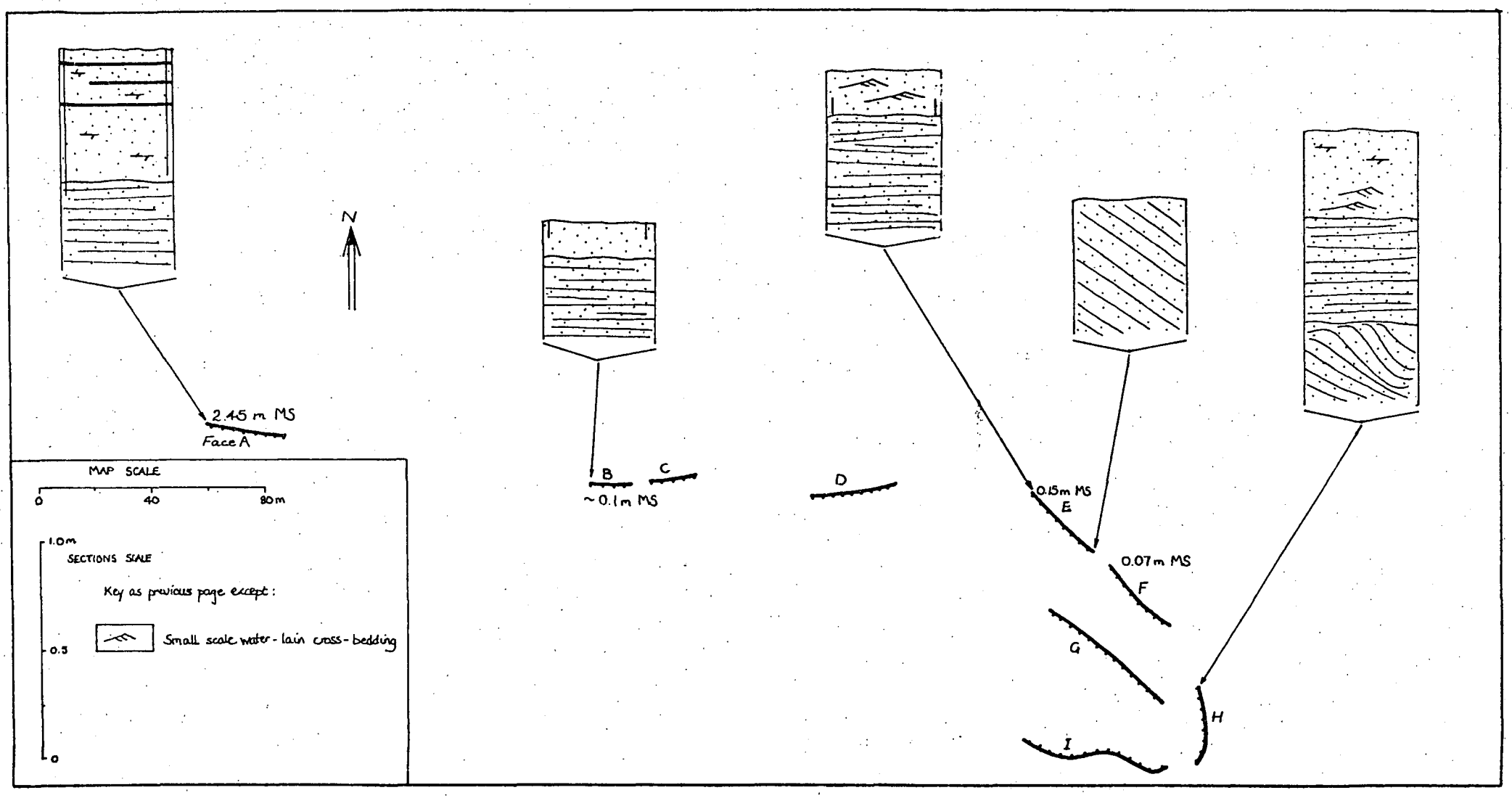

FIG.5.26 Measured sections of the top of the Yellow Sands in Quarrington Hill Quarry.

FIG. 5.27 The top of the Yellow Sands above face H at Quarrington Hill Quarry. The chisel end of the hammer-head is level with the base of the Marl Slate, which is mostly obscured by talus. Below this is ~0.2m of sand showing a poorly defined ?aqueous small-scale cross lamination, directed roughly southwards. This rests on wind-ripple laminated sand of the planar-bedded zone. Hammer-head is 0.14m long.

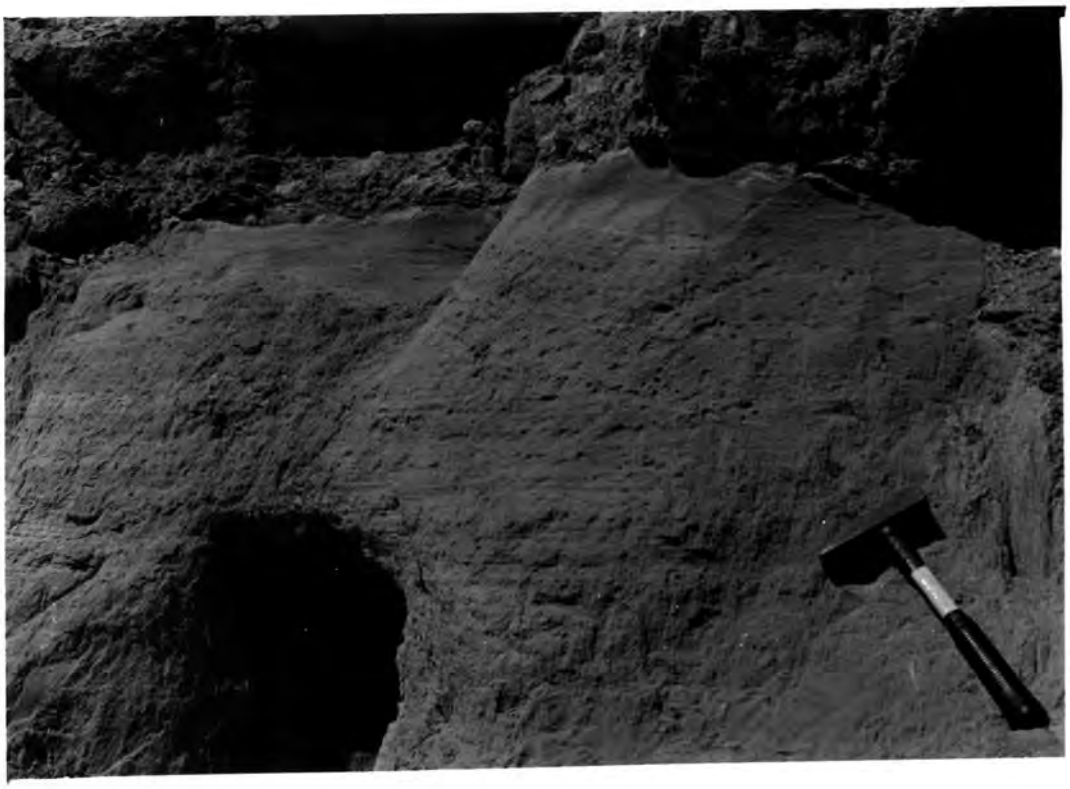

FIG. 5.28 Lower Magnesian Limestone (top) resting on very thin Marl Slate above planar-bedded and cross-bedded aeolian Yellow Sands. East end of face E at Quarrington Hill Quarry. Hammer is 0.36m long.

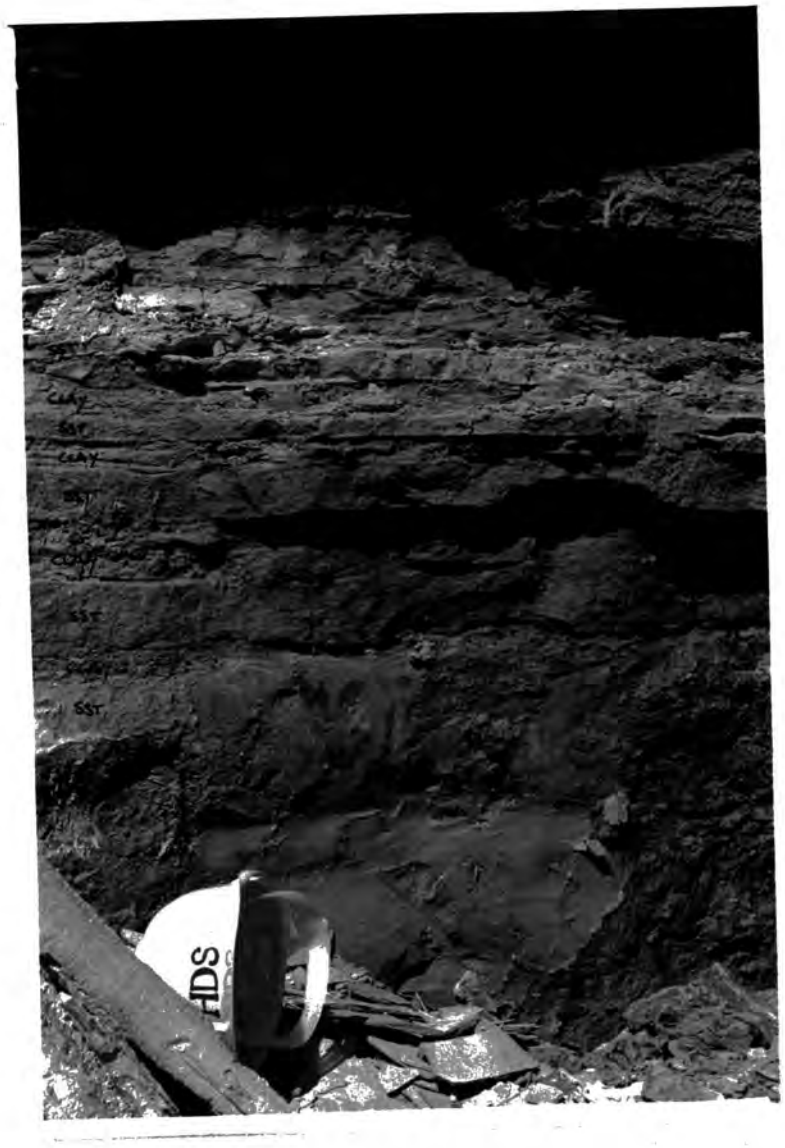

FIG. 5.29 Interbedding of sandstone and clayey Marl Slate, west end of face A, Quarrington Hill Quarry. Yellow Sands are continuous but structureless in the lower part of the picture. The sandstones visible within the Marl Slate are flat-topped and based, and also apparently structureless.

FIG. 5.30 Contorted Yellow Sands at 116,6 in Ferryhill railway cutting. This is the largest magnitude distortion exposed in the formation. Hammer is 0.36m long.

FIG. 5.31 The High Moorsley exposure (NZ 334457). Shows Marl Slate resting on a slightly irregular surface of cemented and structureless Yellow Sands. The dotted line drawn across the rock marks the boundary between structureless and wind-ripple laminated sand. 0.63m of tape is visible.

FIG. 5.32 The underside of a specimen taken from the boundary between structureless and laminated sand at High Moorsley. Shows a well-defined, inclined burrow, walled by dolomitic sand, protruding into laminated sand. Scale (mm) at lower right.

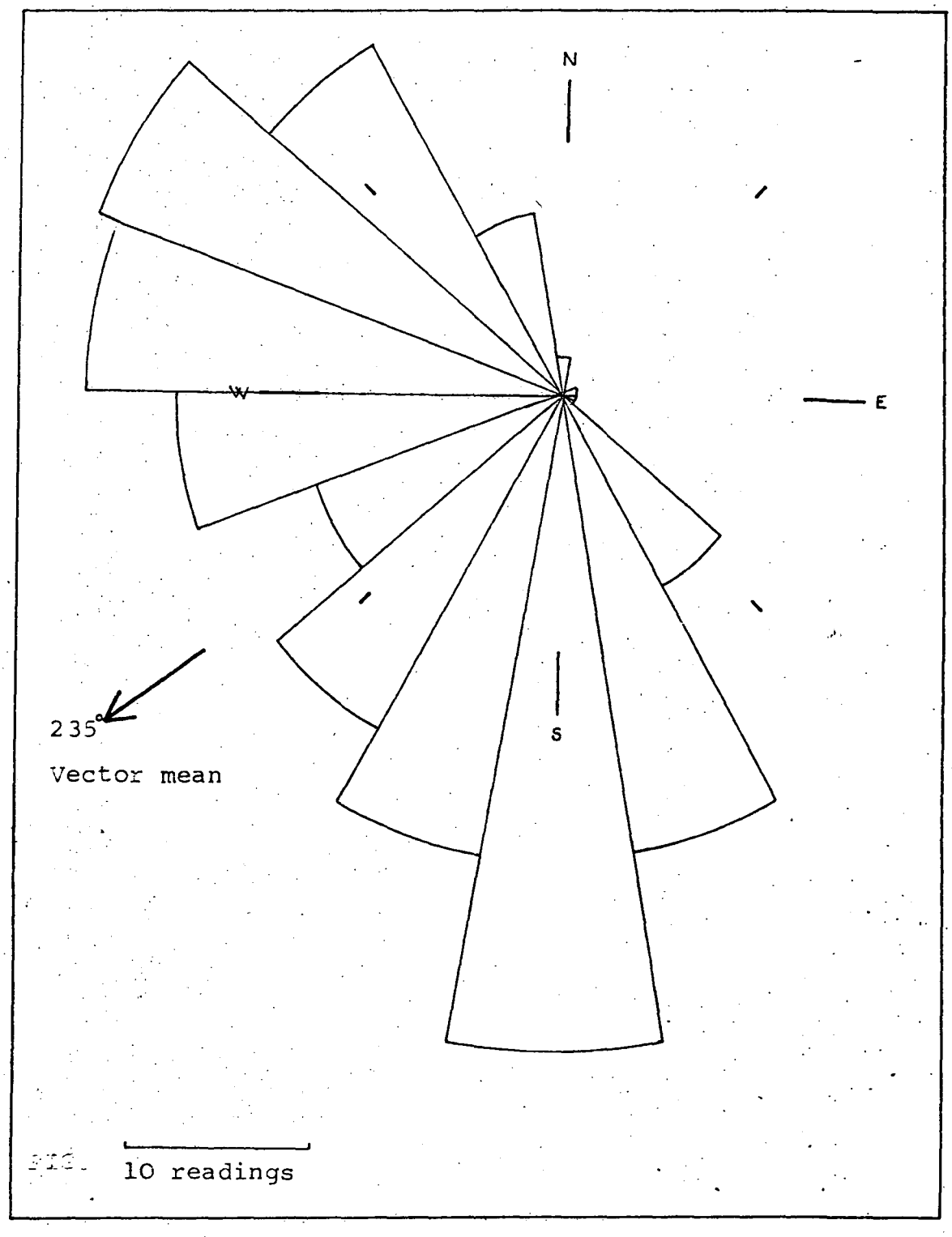

FIG.5.33 Rose diagram of cross-bedding azimuths for the Yellow Sands. Composite of all exposures (239 measurements).

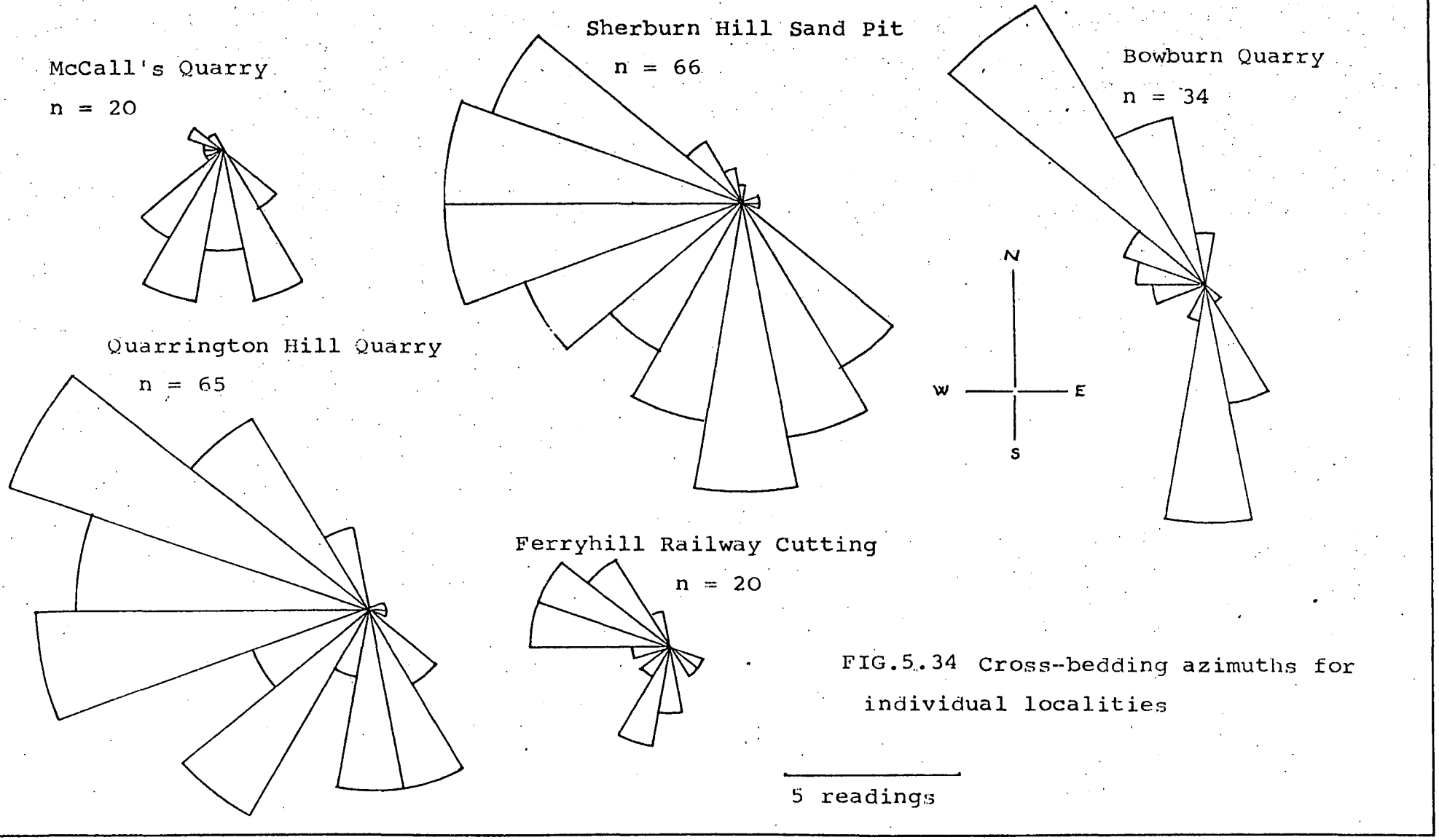

FIG.5.34 Cross-bedding azimuths for individual localities

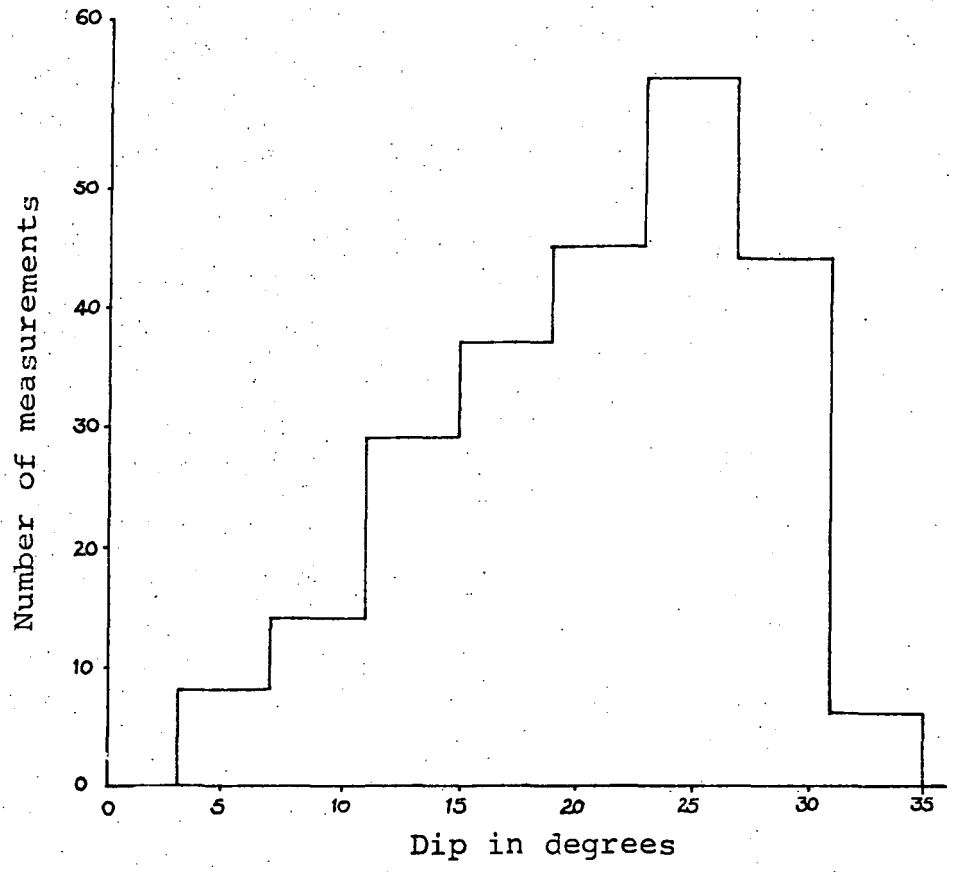

FIG.5.35 Histogram showing frequency of magnitude of dip.
(n = 242)

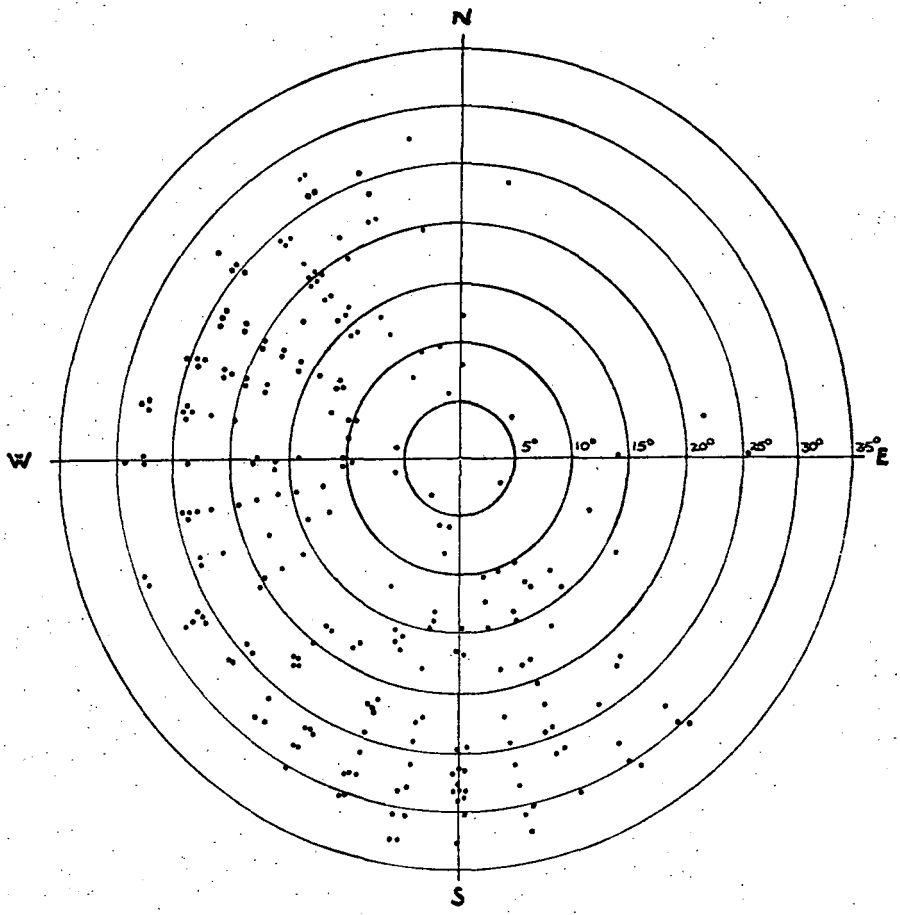

FIG.5.36 Cross-bedding dips plotted by azimuth and magnitude.

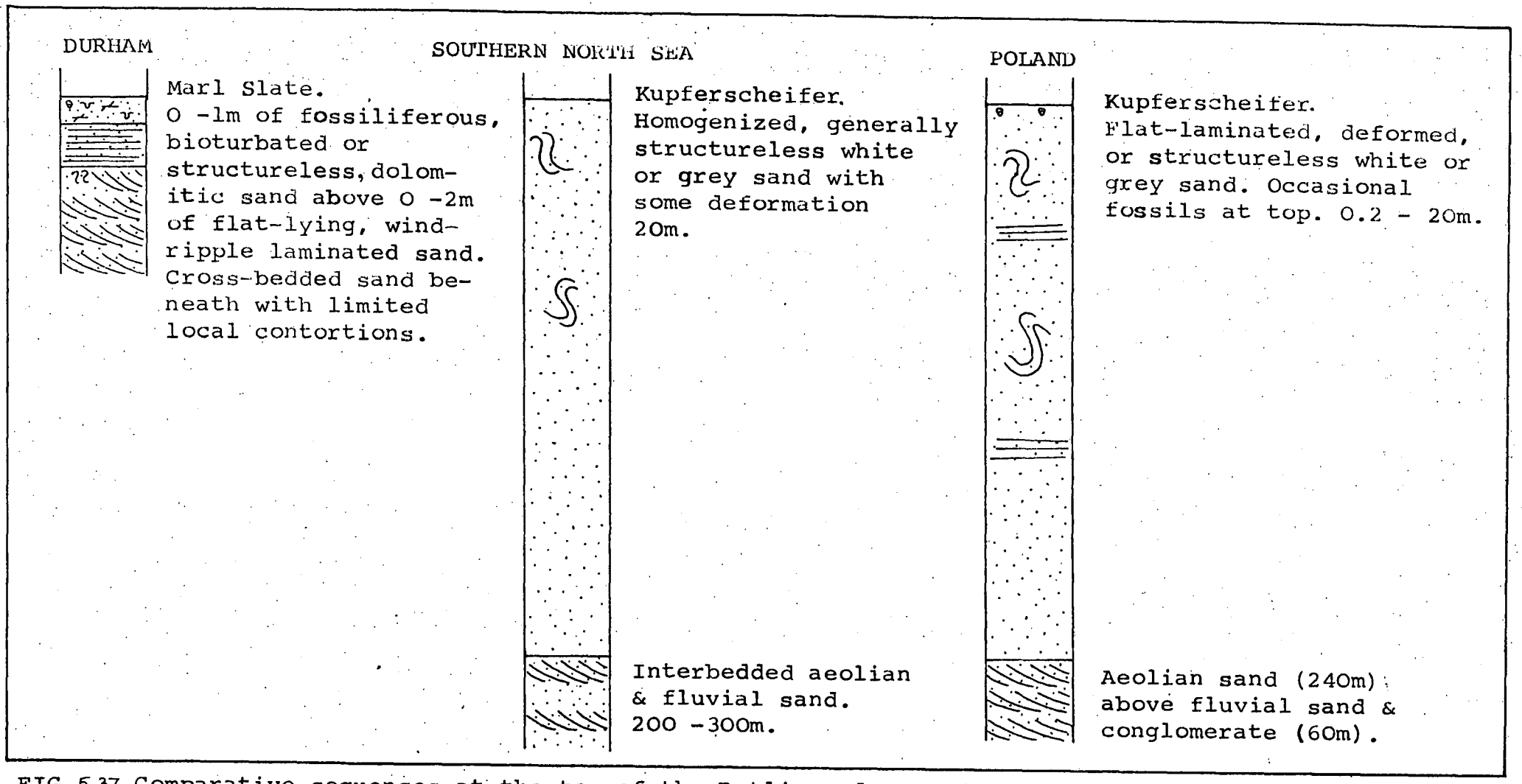

FIG.5.37 Comparative sequences at the top of the Rotliegendes. Information from Nemec & Porebski (1977) and Glennie (1972).

CHAPTER SIX

THE DEPOSITION OF THE YELLOW SANDS

FIG. 6.1

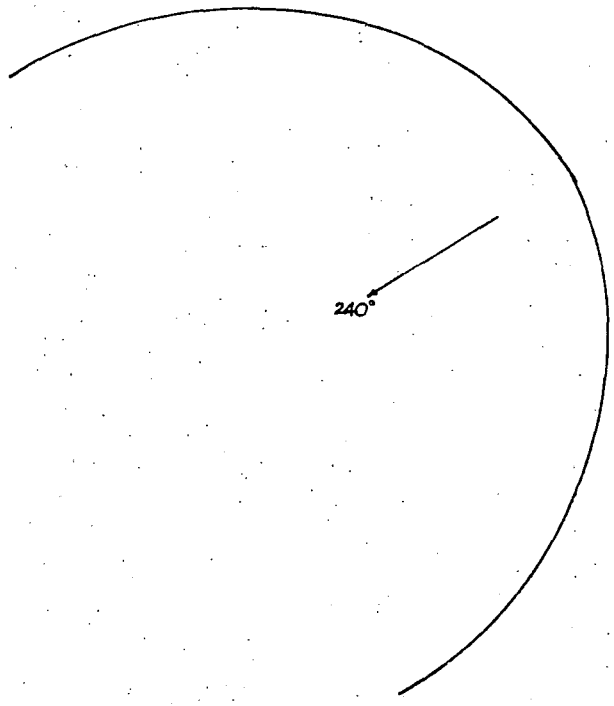

Reconstructed shape of the preserved leeside of a Yellow Sands dune assuming the presence of only 1 dune set. This pattern encompasses 98% of the data but assumes perfectly deterministic bedform behaviour and uniform shape.

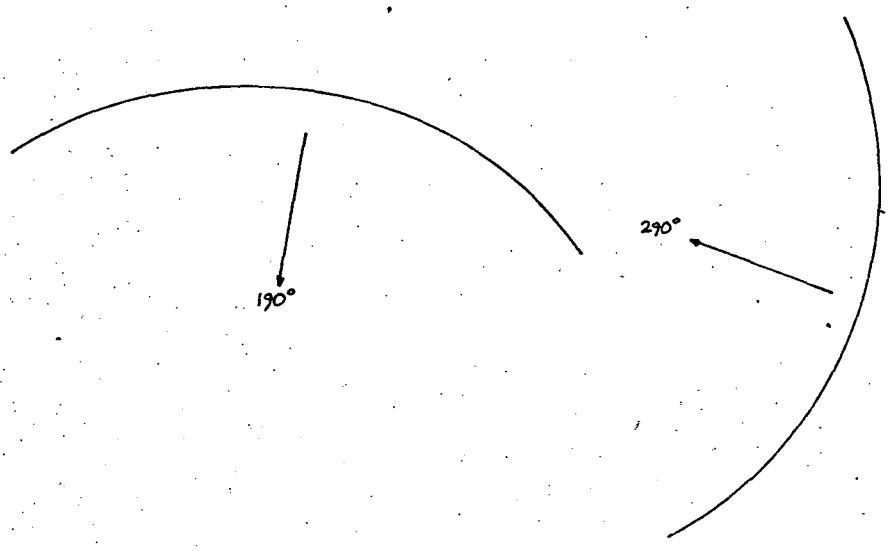

Reconstructed shape of the preserved leeside of Yellow Sands dunes assuming the presence of two dune sets. Other comments as above.

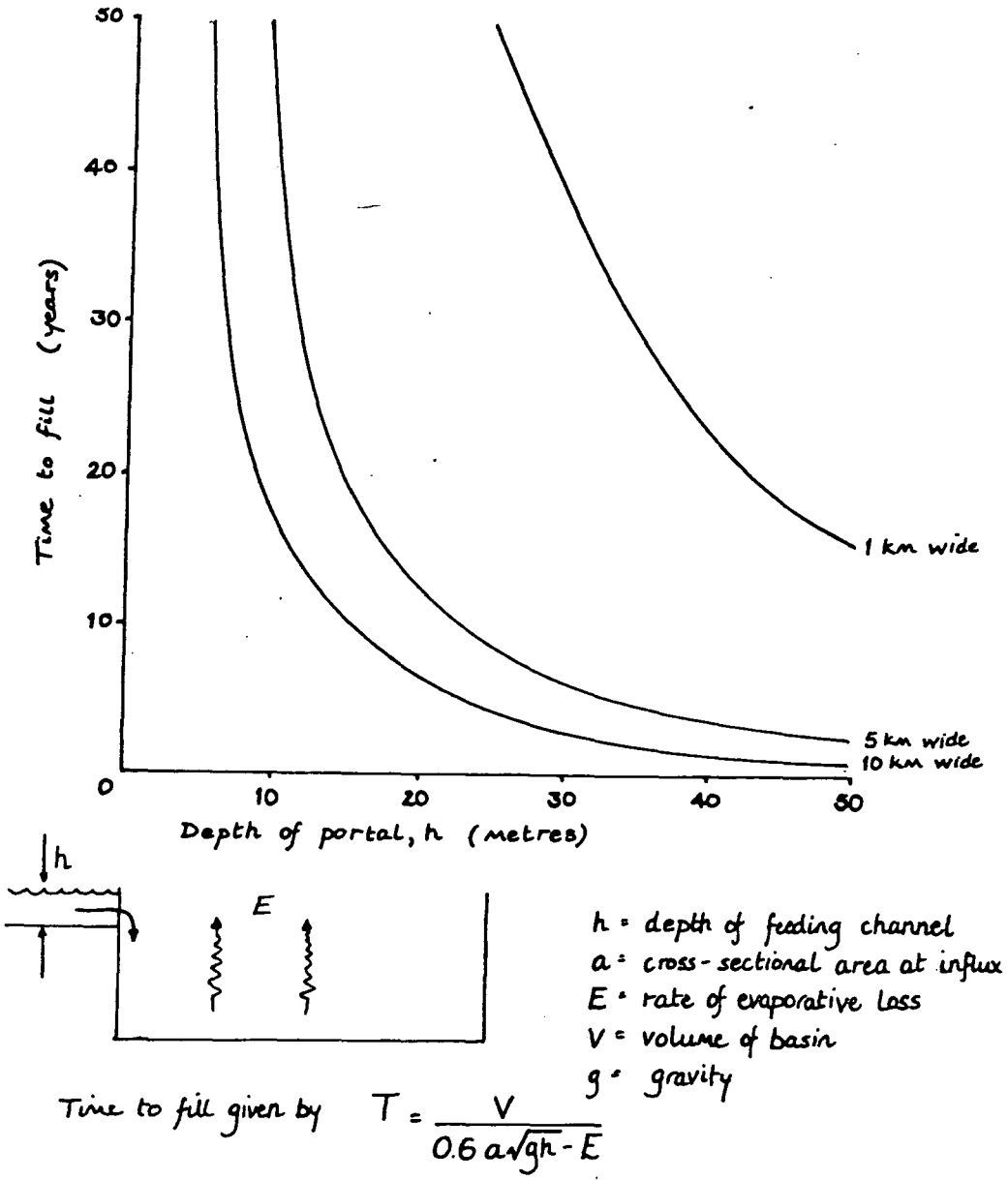

FIG. 6.2 Duration of Zechstein transgression v. portal characteristics. (For influx from a vertical waterfall).
Depth of portal plotted along abscissa, different curves drawn for various widths. Volume of basin gauged from Ziegler (1981) at 10^6 km^2. Mean depth guessed at 300m. Rate of evaporative loss set at 2000 km^3/year, taking the figure given by Hsu et al.(1973) for the Messinian flooding of the Mediterranean and adding some.

DEVELOPMENT OF THE DRAA

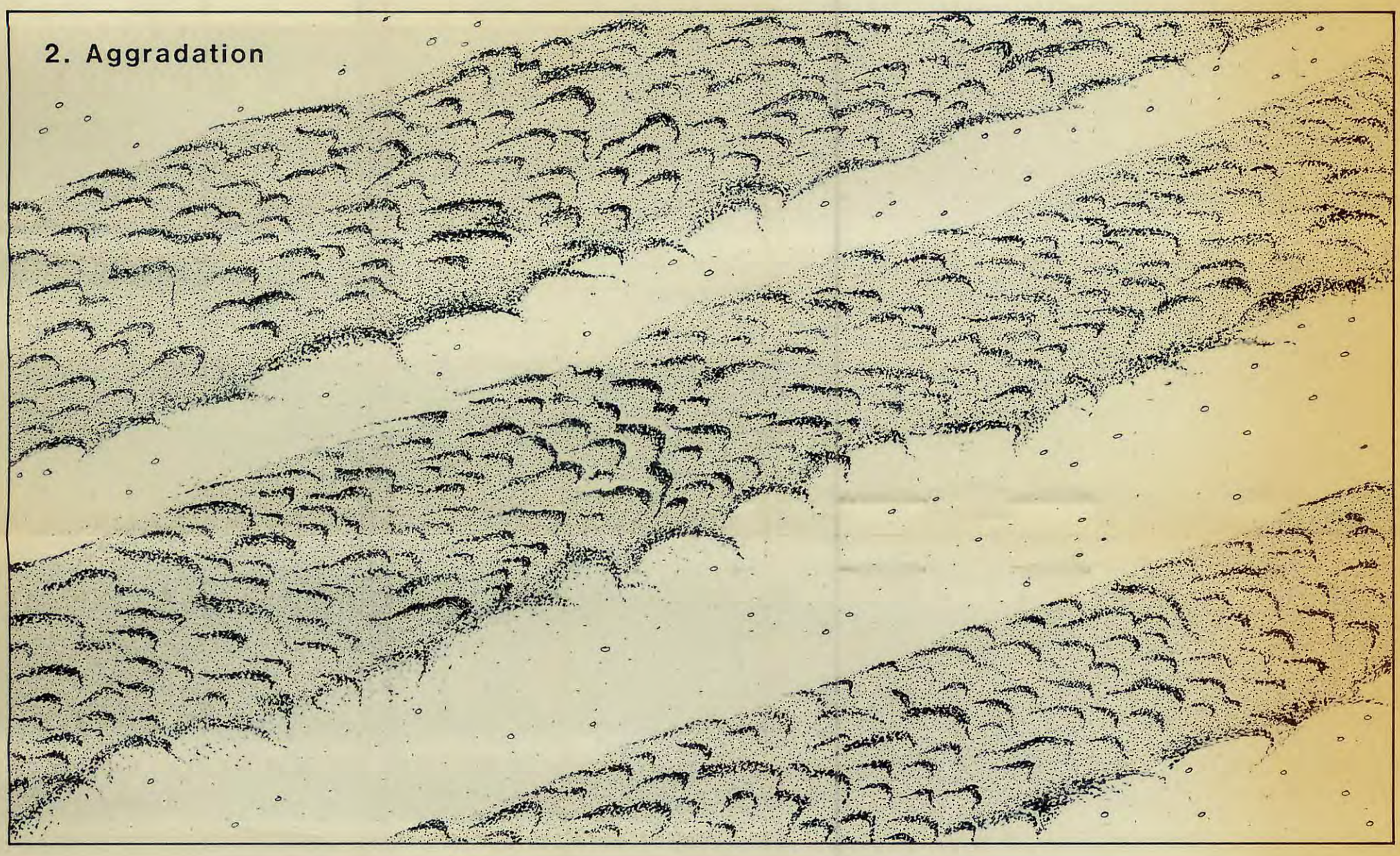

N.B. Scale of dunes relative to draa is exaggerated for clarity.

Fig. 6.3 (Opposite)

Reconstructions of the Yellow Sands bedforms

INITIATION: Sand sheets accumulate and isolated barchans migrate across a pebbly or rocky desert floor. Sand deposited by the sheets and barchans forms the nuclei of longitudinal draa.

AGGRADATION: The draa grow vertically and laterally by the accumulation of sand from climbing sinuous transverse dunes migrating along their length.

STABILITY: As the draa reach equilibrium, the population of dunes is reduced by the spread of gently rolling sand-sheets. Vertical growth of the draa effectively ceases.

(Diagram drawn by Sue Freeman, Exploration Division Drawing Office, BP, London.)

CHAPTER SEVEN

THE LAMINATION, GRAIN CHARACTERISTICS AND PETROLOGY OF THE YELLOW SANDS

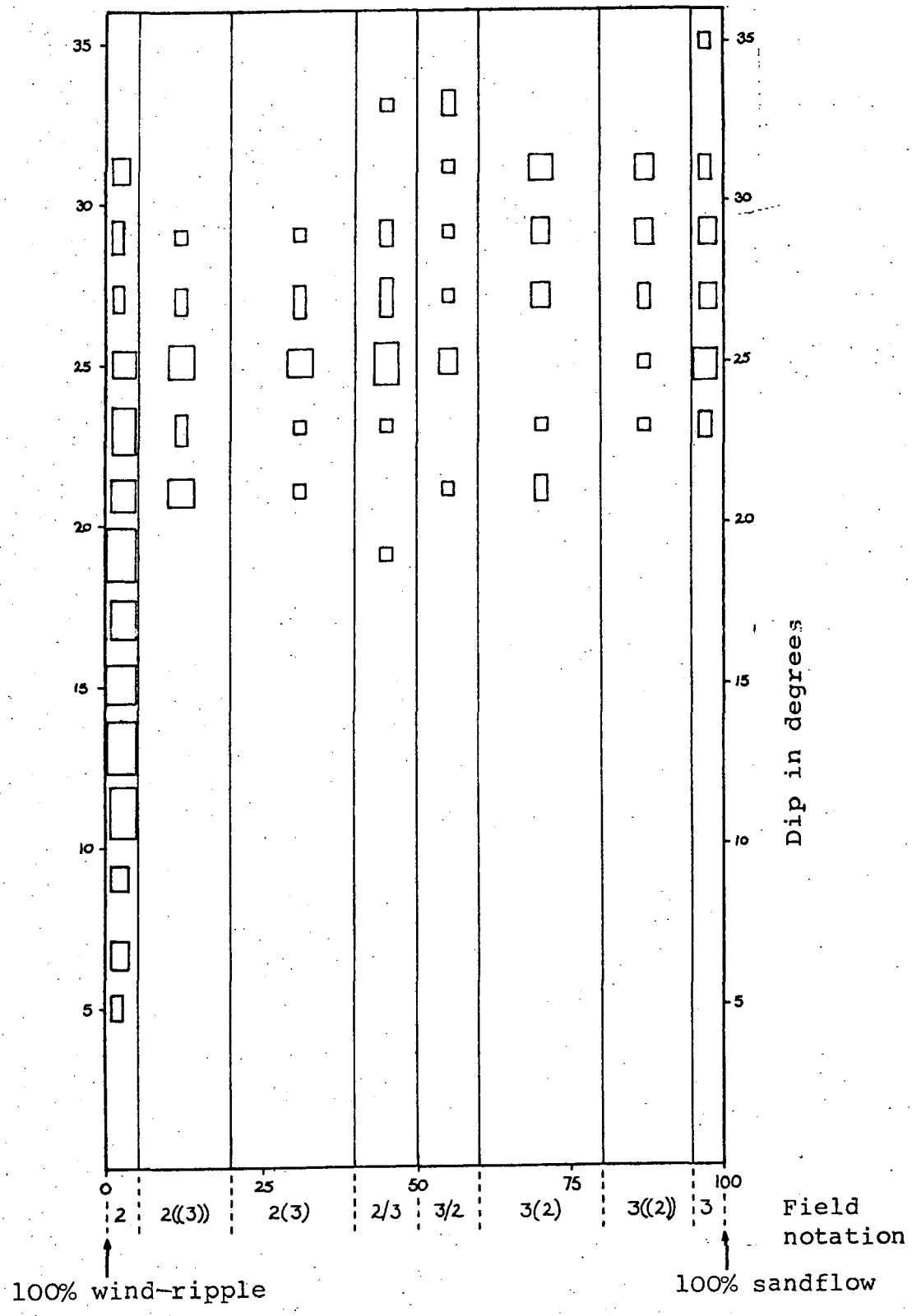

FIG.7.1 Lamination type v. dip of cross-bedding in the Yellow Sands. Size of rectangles denotes number of measurements. (n = 157)

2 = wind-ripple lamination

3 = sandflow lamination

□ = 1 measurement

YELLOW SANDS GRAIN SIZE DATA TABLE 7.1

Abbreviations used:

Bbn = Bowburn Quarry
Ccts = Cullercoats shore section
F = Ferryhill railway cutting
HD = Hetton Downs Quarry
HD' = the old pit at Hetton Downs
McC = McCall's Quarry
QH,G = face G at Quarrington Hill Quarry
QH,D = face D at Quarrington Hill Quarry
ShH,N = north face of Sherburn Hill Sand Pit
ShH,W = west face of Sherburn Hill Sand Pit

Lamination types:

1 = sand-sheet
2 = wind-ripple
3 = sandflow
S = apparently structureless

Dip azimuths are measured in degrees clockwise from true north.

Statistical Measures:

M = graphic mean size in phi units
s = inclusive graphic standard deviation in phi units
Sk = inclusive graphic skewness
K = graphic kurtosis (all after Folk, 1974)

"Section ref" indicates the grid reference of the sample locality on the quarry face diagrams.

An asterisk (*) denotes samples sieved at half ø intervals.

Summary of statistics:

TABLE 7.1 (contd)

Sand-sheet samples (n = 3)

$\overline{M}$ = 1.92ø, $\overline{s}$ = 1.24ø, $\overline{Sk}$ = -0.01, $\overline{K}$ = 0.62

Sandflow samples (n = 18)

$\overline{M}$ = 1.56 ± 0.66ø, $\overline{s}$ = 0.48 ± 0.11ø, $\overline{Sk}$ = 0.23 ± 0.36

$\overline{K}$ = 1.31 ± 0.45

Wind-ripple samples (n = 21)

$\overline{M}$ = 1.90 ± 0.26ø, $\overline{s}$ = 0.81 ± 0.21ø, $\overline{Sk}$ = 0.13 ± 0.16

$\overline{K}$ = 0.88 ± 0.13

Structureless samples (n = 4)

$\overline{M}$ = 2.17ø, $\overline{s}$ = 0.51ø, $\overline{Sk}$ = 0.04, $\overline{K}$ = 1.05

Weighted by lamination, averages for the whole formation are:

M = 1.80ø, s = 0.74ø, Sk = 0.16, K = 1.01

Specimen no.	Locality	Section ref	Lam type & dip	M	s	Sk	K
19/10-2(30)	ShH,W	08,05	1, flat	2.06ø	1.19ø	-0.22	0.60
23//4-6(31)	ShH,N		1, flat	1.89	1.29	0.01	0.63
23//4-7(35)	ShH,N		1, flat	1.81	1.25	0.18	0.63
10/11-3(5)	Bbn	52,06	3, 26/320	0.23	0.43	0.32	2.07
10/11-4(6)	Bbn	52,07	3, 26/320	1.85	0.46	0.07	1.20
18/6-1(17)	Bbn	170,05	3	0.53	0.65	0.53	1.29
18/10-3(18)	ShH,W	166,18	3, 22/250	1.23	0.41	0.05	0.89
14/9-1(24)	ShH,W	181,27	3, 24/270	2.44	0.42	0.25	0.94
23//4-5(26)	ShH,W	82,15	3, 22/330	1.50	0.37	0.00	1.12
14/9-2(37)	ShH,W	180,28	3, 24/260	1.22	0.44	0.06	0.90
15/10-2(39)	Bbn	40,07	3	0.51	0.50	0.49	2.27
11/12-A*	Ccts	28,07	3	0.70	0.41	0.40	1.83
11/12-H*	HD		3	1.80	0.29	0.12	1.36
11/12-C*	HD		3	1.88	0.51	-0.02	1.18
29/10-2(12)	HD		3	1.33	0.39	0.45	2.00
23//4-1(2)	ShH,W	50,18	3, 32/170	2.07	0.70	-0.22	1.01
23//4-3(3)	ShH,W	92,15	3, 24/300	2.17	0.66	0.34	1.01
23//4-2(4)	ShH,W	76,18	3	2.26	0.50	0.02	0.95

TABLE 7.1 (contd)

Specimen no.	Locality	Section ref	Lam type & dip	M	s	Sk	K
06/5-5(9)	QH,G		3	2.12ø	0.54ø	-0.05	0.90
29/10-4(23)	HD	174,08	3, 22/290	1.63	0.35	0.24	2.09
5/11-7(25)	HD'		3, 26/240	2.29	0.56	-0.07	0.98
19/10-3(38)	ShH,W	13,02	3, 20/320	1.68	0.52	1.49	1.54
23//4-4(1)	ShH,W	112,15	2, 26/210	1.75	0.99	0.16	0.72
13/10-6(8)	HD	33,07	2, 14/270	1.53	0.88	0.02	0.84
5/11-1(11)	HD	245,12	2, 26/230	2.26	0.70	0.01	0.93
13/10-7(14)	HD	94,03	2, 10/280	1.92	0.64	0.29	1.17
12/10-4(15)	F	115,05	2, 16/200	1.84	0.90	0.61	0.69
23/7-2(16)	McC	105,15	2, 28/210	1.97	0.96	-0.05	0.85
21/7-2(20)	QH,D		2, 18/290	1.75	1.20	0.22	0.69
13/10-8(21)	HD	178,03	2, flat	1.64	1.01	-0.04	0.97
29/10-1(22)	HD	94,03	2, 10/280	2.06	0.57	0.15	0.96
29/10-3(27)	HD	174,08	2, 18/250	2.10	0.63	0.17	0.81
12/10-2(28)	F	03,03	2, 20/290	2.29	0.56	0.06	0.75
18/10-2(29)	ShH,W	170,28	2, 18/270	2.42	0.53	0.08	0.88
18/10-1(36)	ShH,W	172,21	2, 16/200	1.77	0.89	0.15	0.78
11/12-B*	HD		2	1.48	0.88	0.02	0.94

TABLE 7.1 (contd)

Specimen no.	Locality	Section ref	Lam type & dip	M	s	Sk	K
HLH2*	HD		2	1.61ø	1.20ø	0.26	0.87
11/12-D*	HD		2	1.61	0.86	-0.14	0.84
11/12-E*	HD		2	1.88	0.59	0.06	1.00
11/12-F*	HD		2	1.95	0.63	0.13	1.08
11/12-G*	HD		2	2.07	0.56	0.25	1.05
5/11-2(13)	HD'		2	1.78	0.59	0.13	0.98
13/10-3(19)	HD	04,14	S	2.31	0.44ø	0.06	0.97
13/10-5(33)	HD	08,12	S	2.49	0.45	-0.04	1.04
14/9-3(34)	ShH,W	182,29	S	1.81	0.63	0.09	1.19
5/11-4(32)*	HD'		S, ?reworked	1.95	0.52	0.06	0.99
4/7-6(10)	SE475068 nr Leeds		2	2.09	0.93	0.25	0.76

TABLE 7.1 (contd)

FIG 7.2a

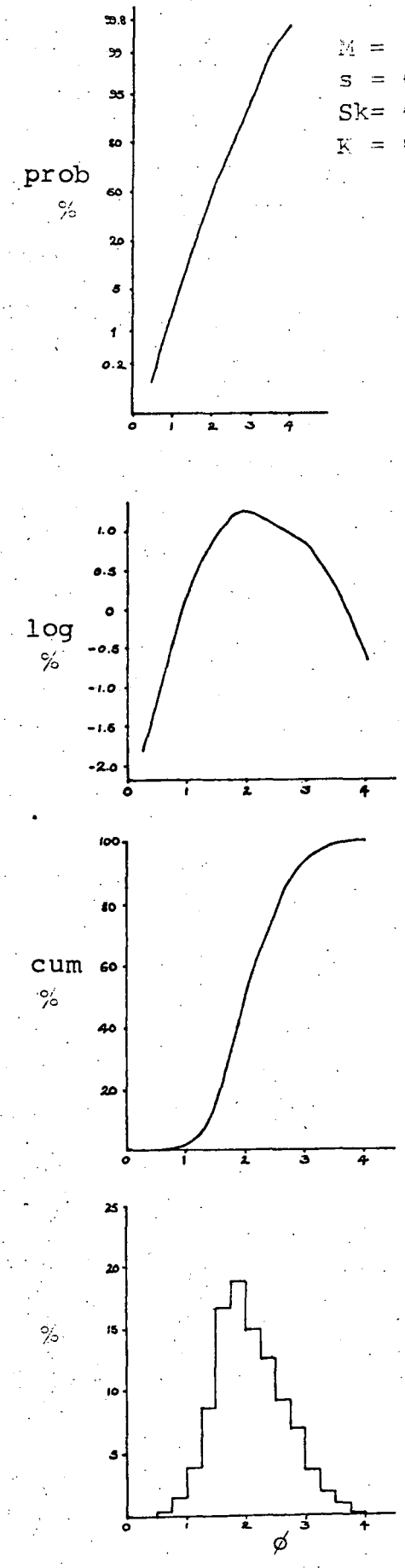

FIG 7.2b

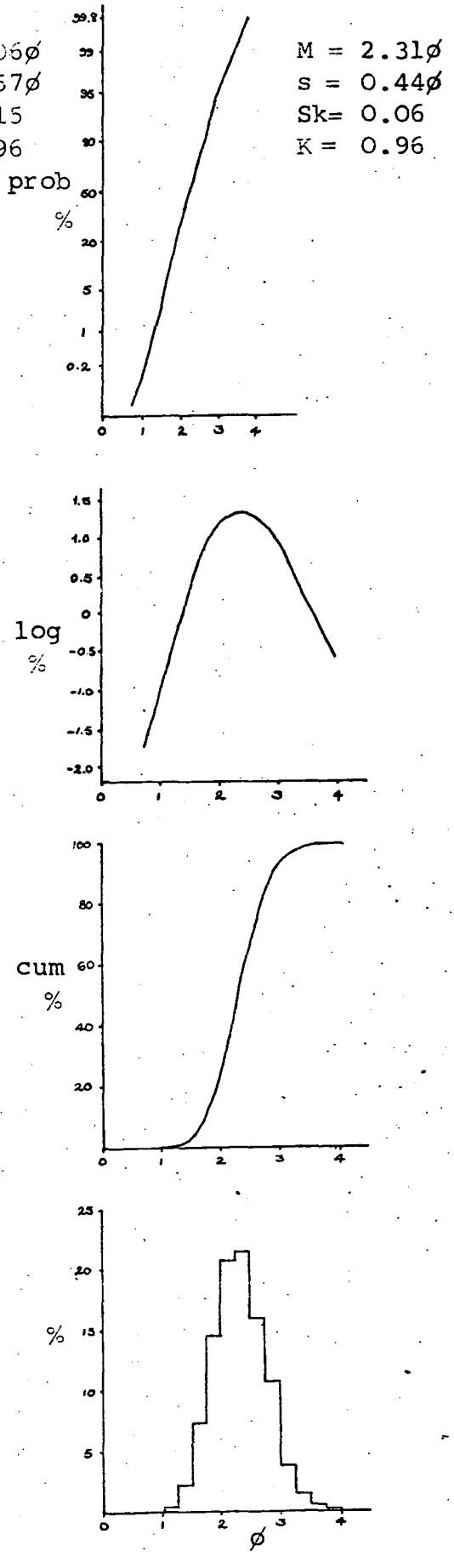

Lamination: Wind-ripple

Locality: Hetton Downs (94,03)

Structureless

Hetton Downs (04,14)

FIG 7.3a

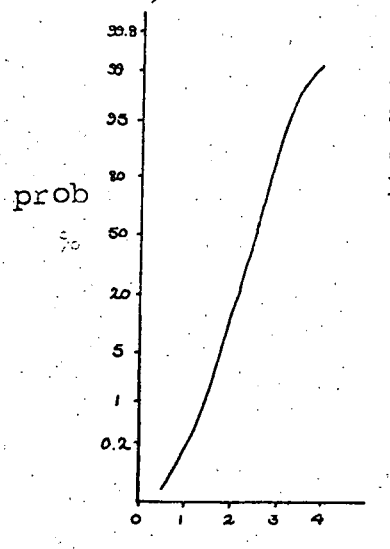

M = 2.49ø
s = 0.45ø
Sk=-0.04
K = 1.04

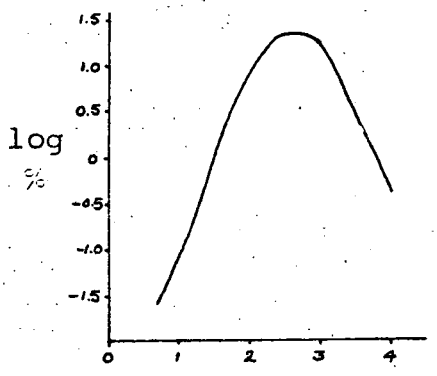

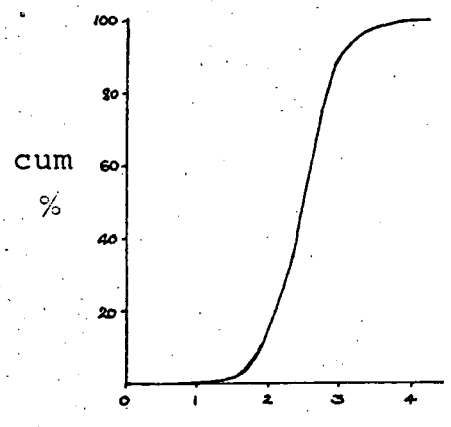

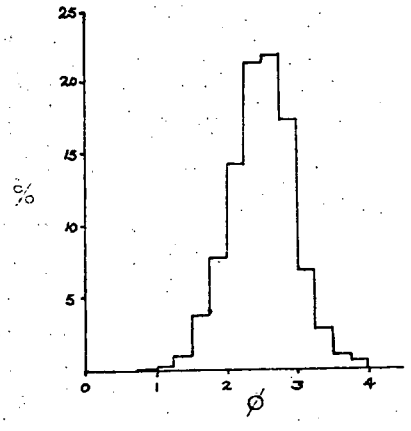

FIG 7.3b

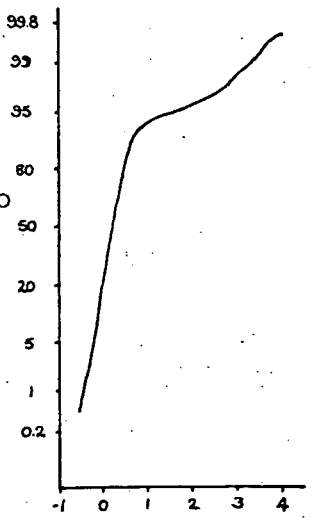

M = 0.23ø
s = 0.43ø
Sk= 0.32
K = 2.07

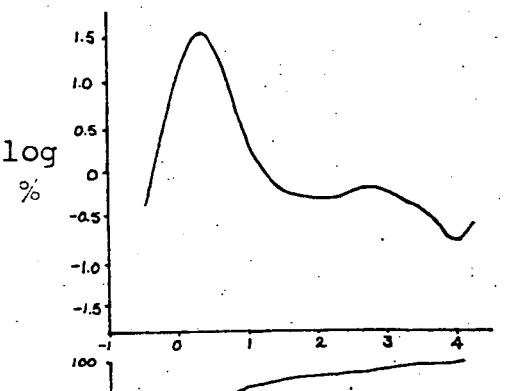

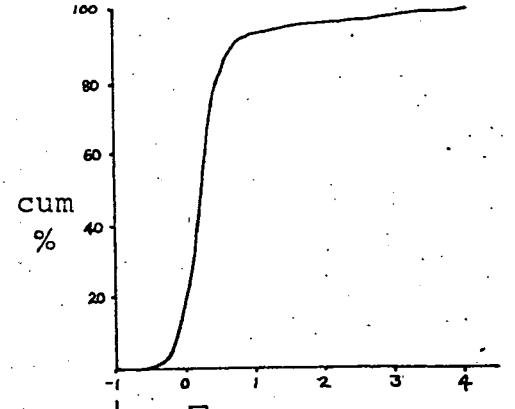

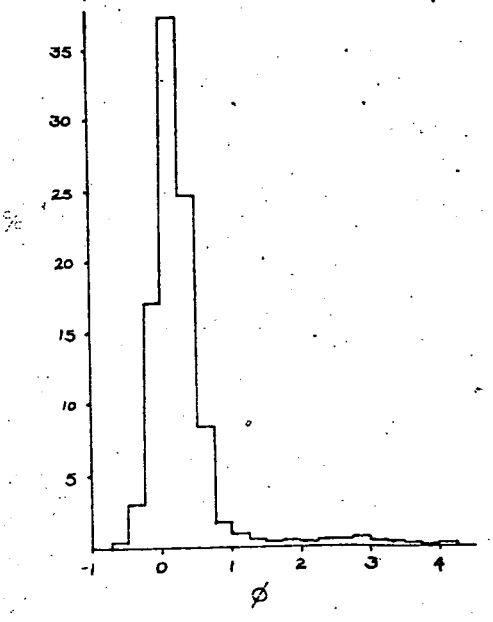

Lamination. Structureless — Sandflow

Locality: Hetton Downs (08,12) — Bowburn (52,06)

FIG. 7.4a

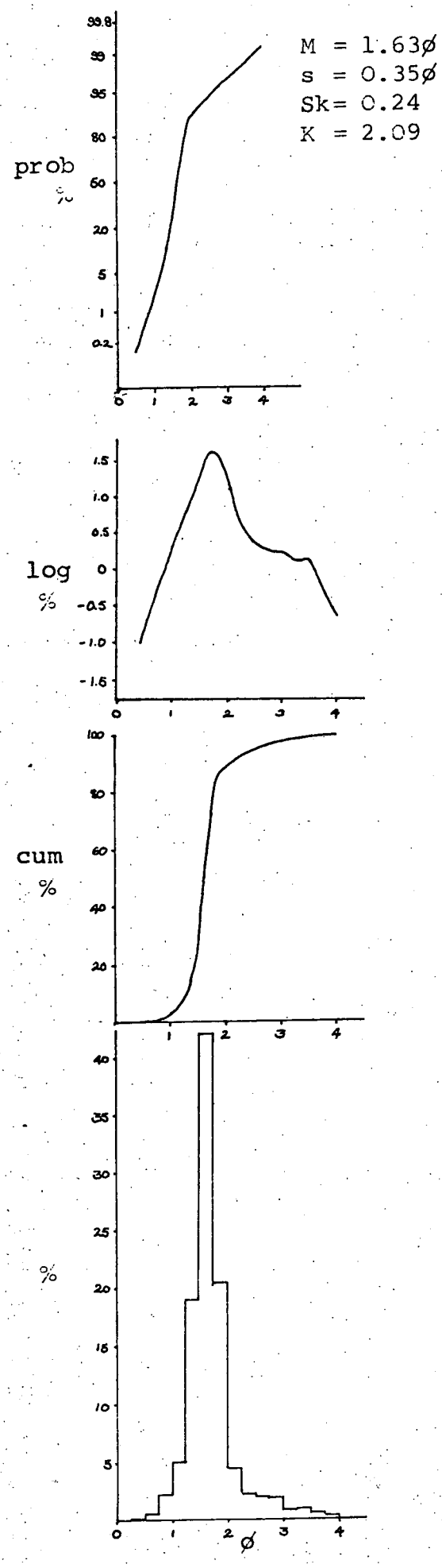

FIG.7.4b

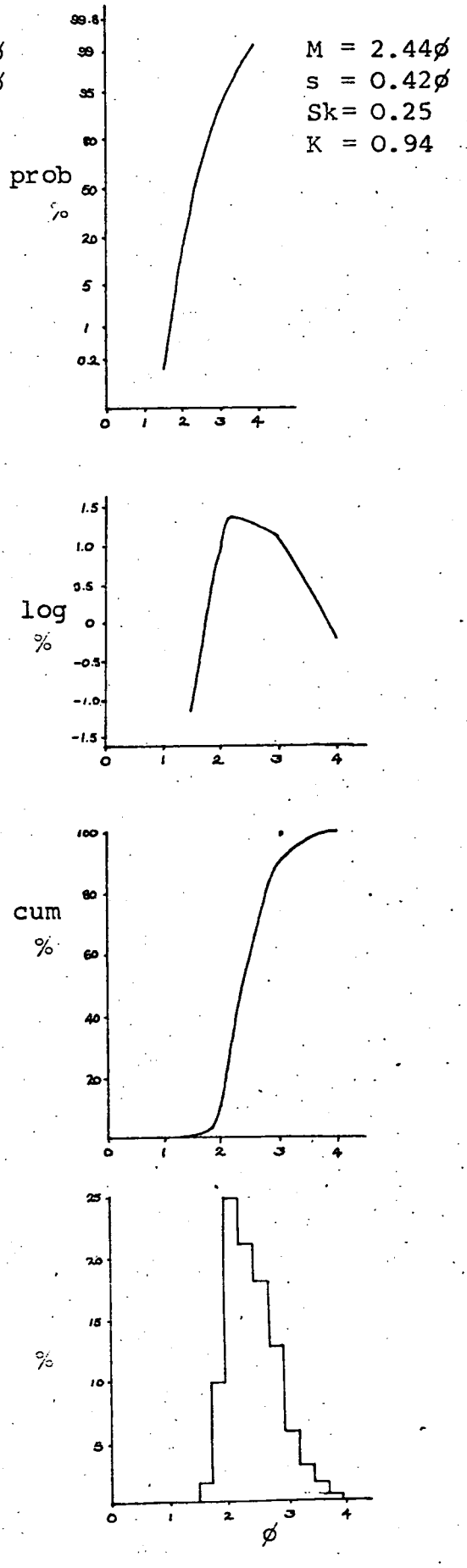

Lamination: Sandflow

Locality: Hetton Downs (174,08)

Sandflow

Sherburn Hill W face

FIG. 7.5a

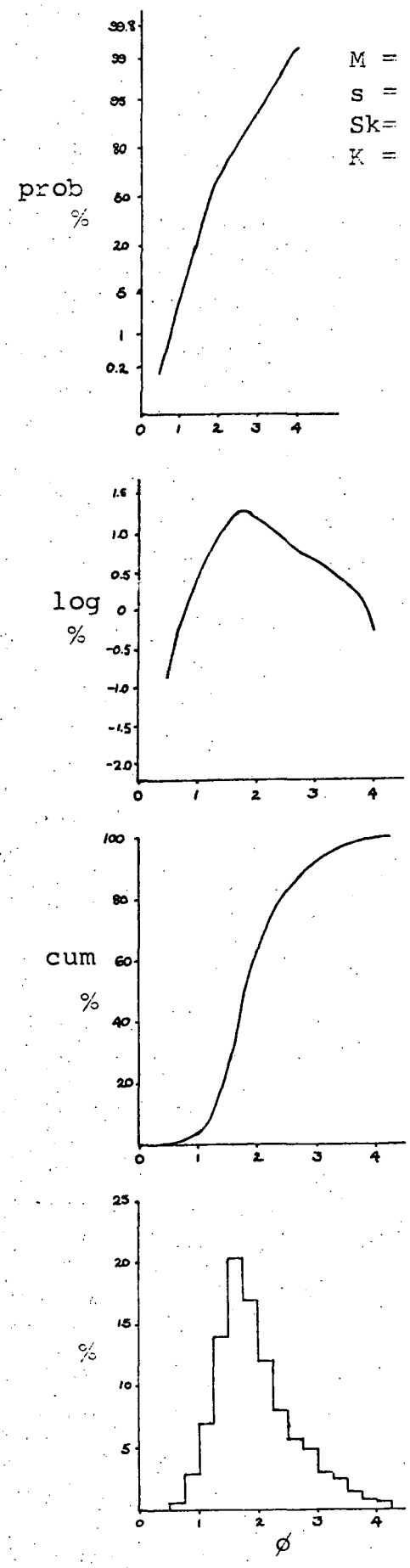

FIG. 7.5b

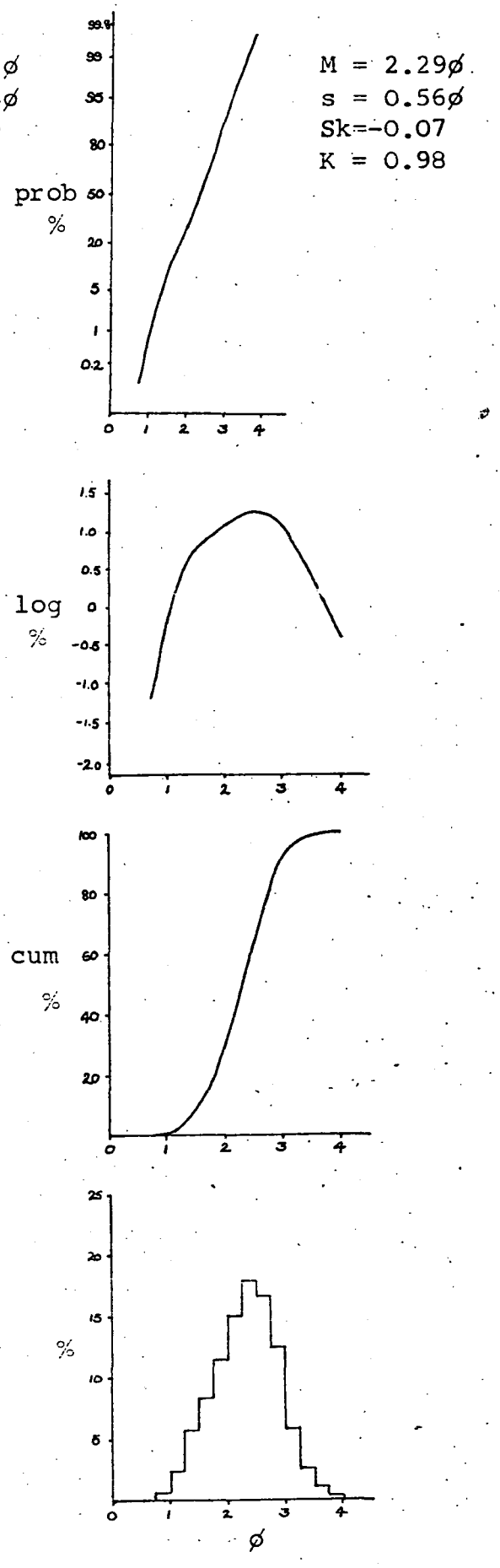

Lamination:	Wind-ripple	Sandflow
Locality:	Hetton Downs (94,03)	Hetton Downs

FIG. 7.6a

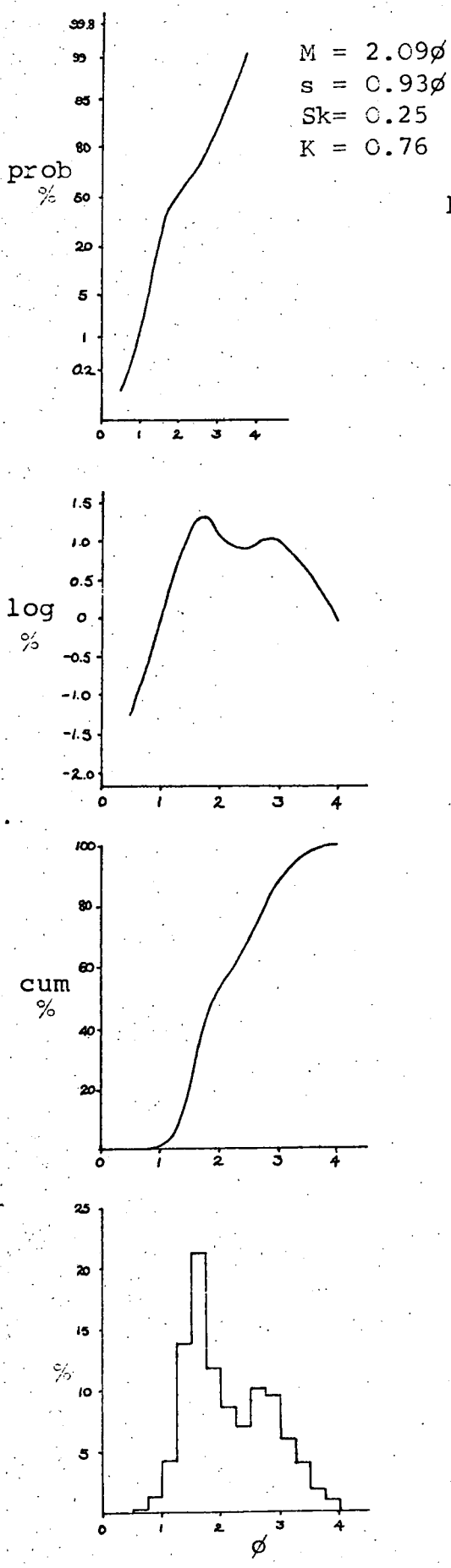

FIG. 7.6b

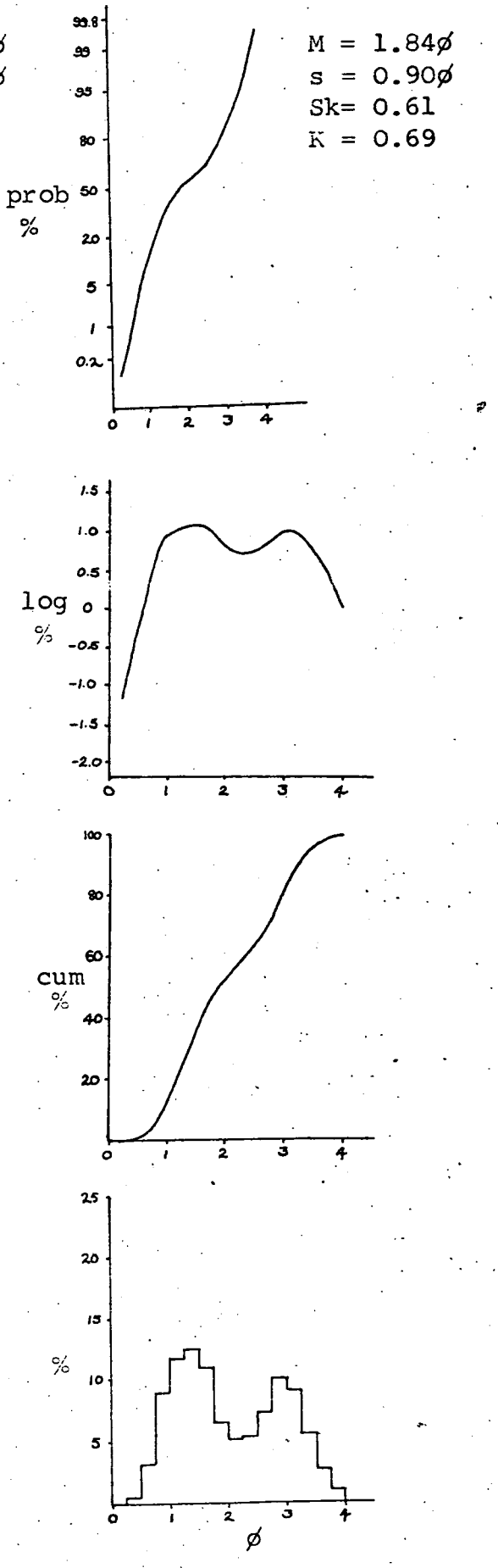

Lamination: Wind-ripple

Locality: nr. Leeds

Wind-ripple

Ferryhill (115,05)

FIG. 7.7a

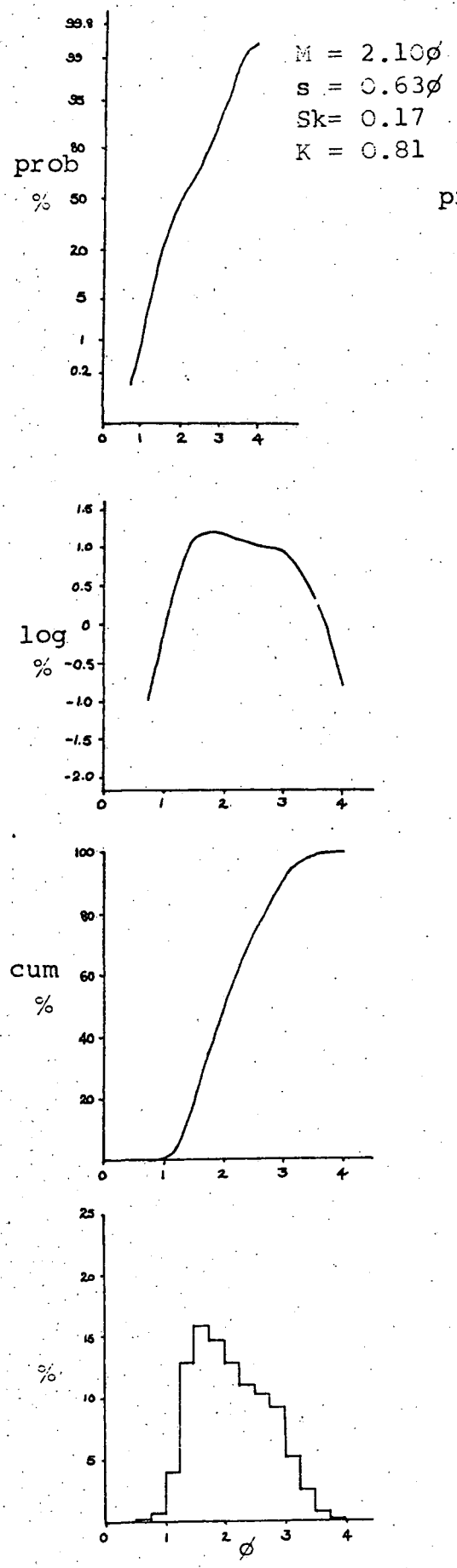

FIG. 7.7b

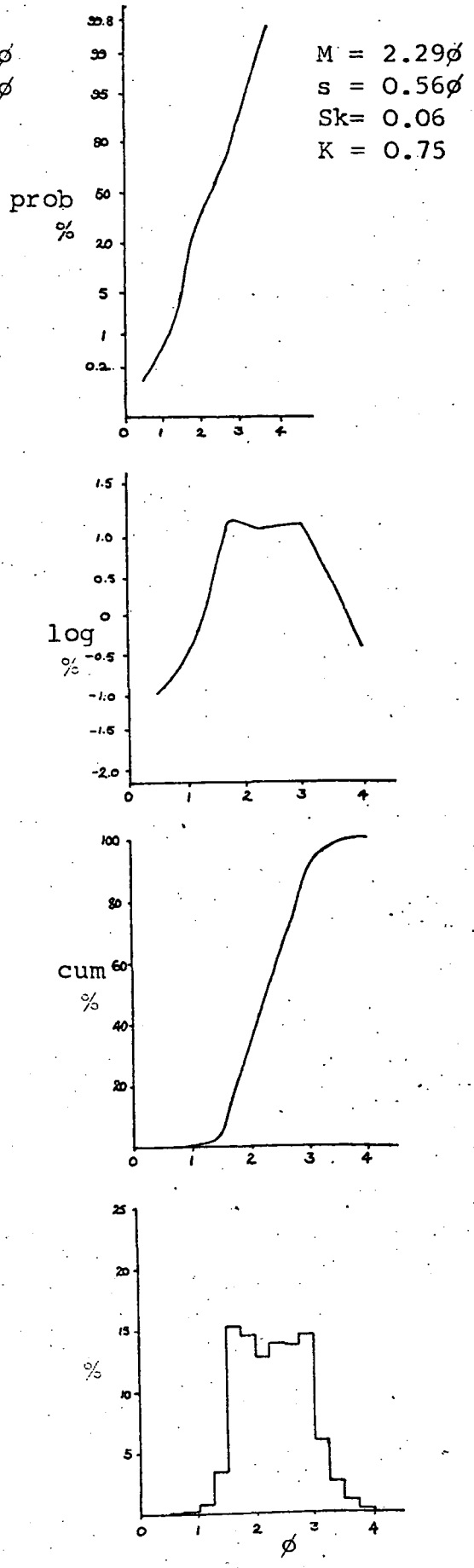

Lamination; Wind-ripple

Locality: Hetton Downs (174,08)

Wind-ripple

Ferryhill (03,03)

FIG. 7.8a

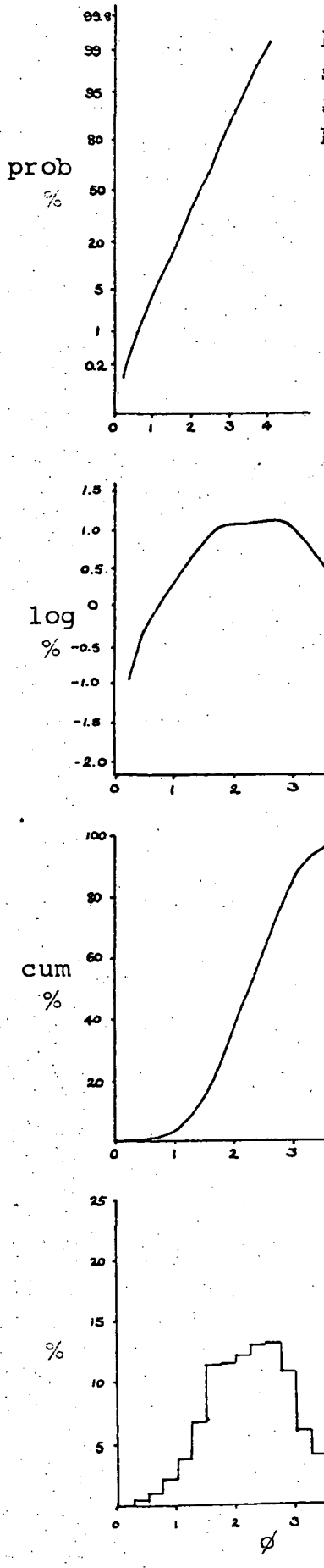

FIG. 7.8b

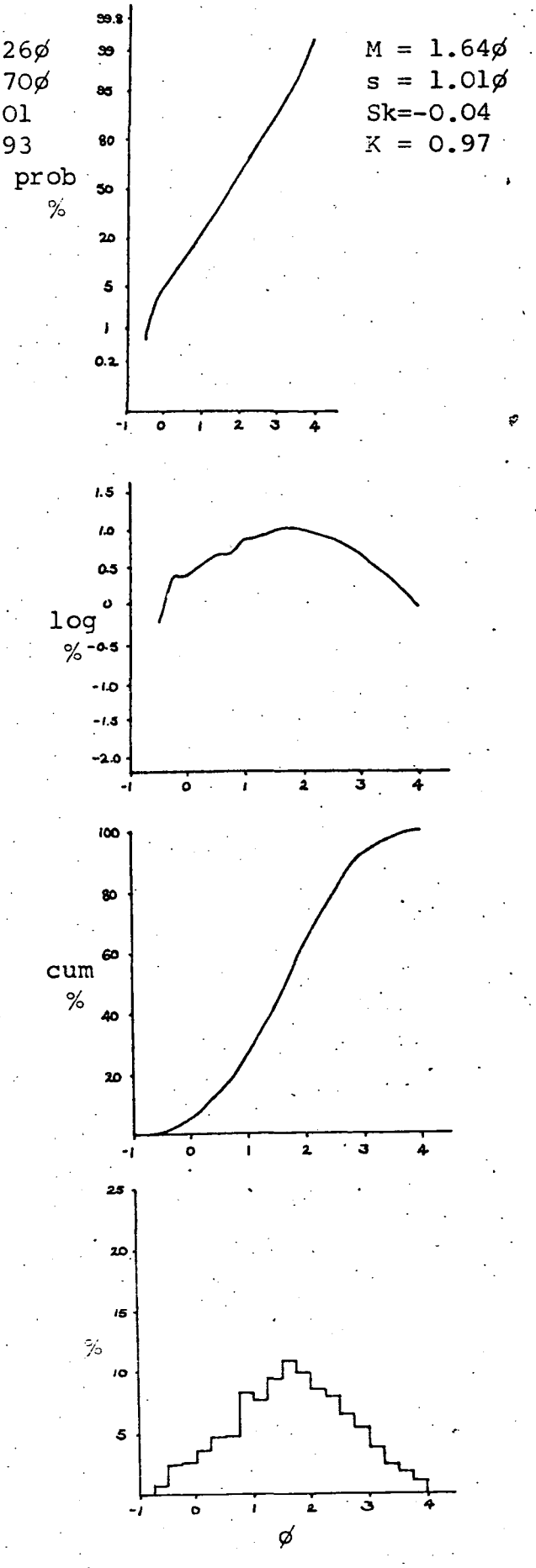

Lamination: Wind-ripple

Locality: Hetton Downs (245,12)

Wind-ripple

Hetton Downs (178,03)

FIG.7.9a

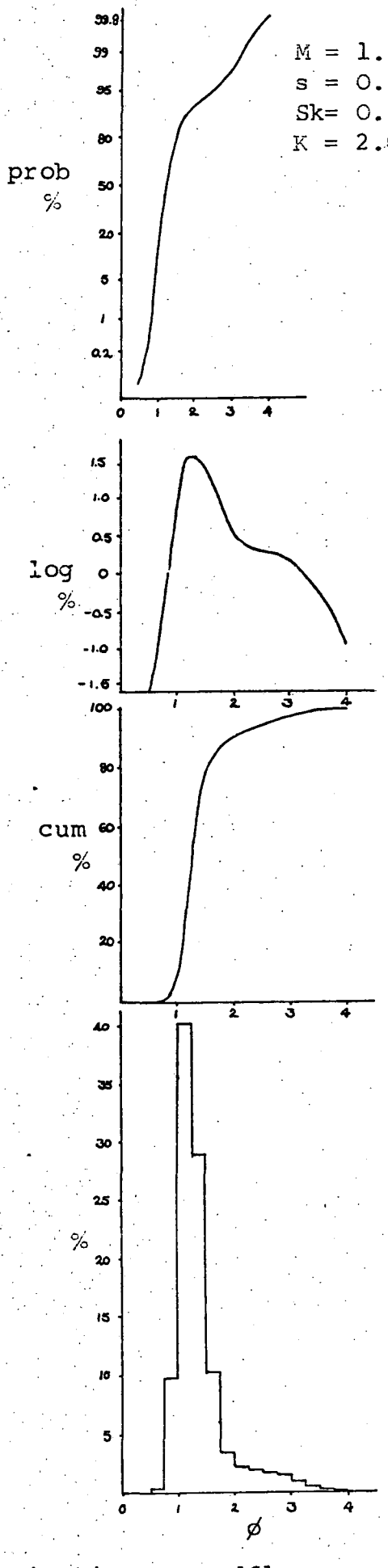

Lamination: Sandflow

Locality: Hetton Downs

FIG.7.9b

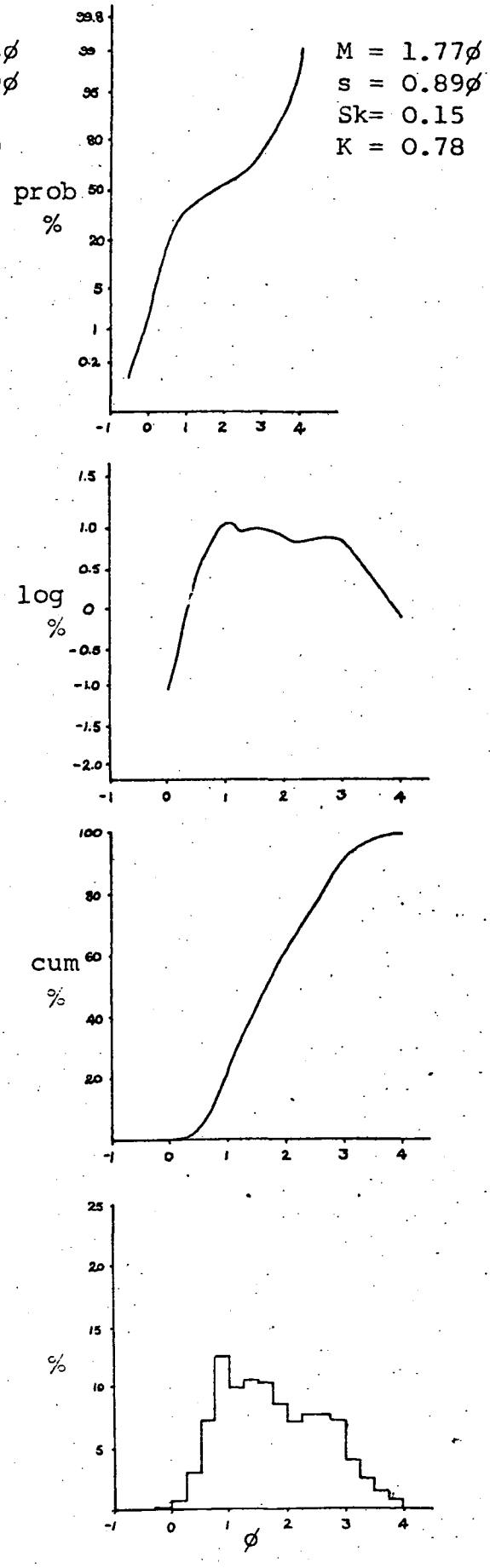

Wind-ripple

Sherburn Hill W face (122,21)

FIG. 7.10a

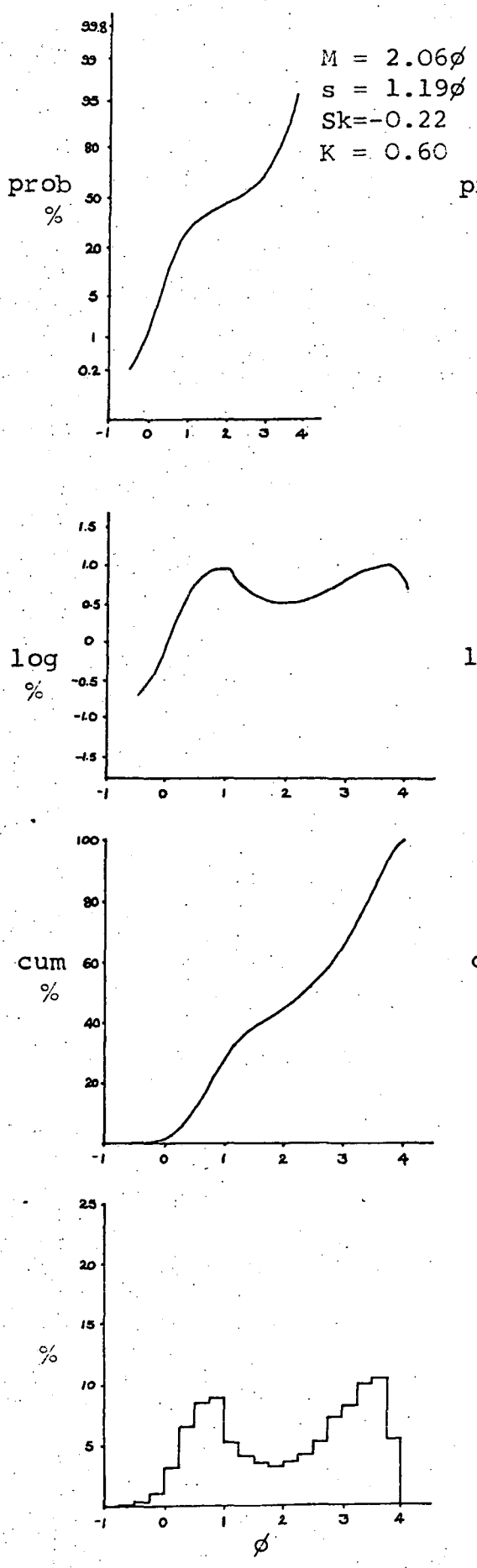

Lamination: Sand-sheet

Locality: Sherburn Hill W Face (08,05)

FIG.7.10b

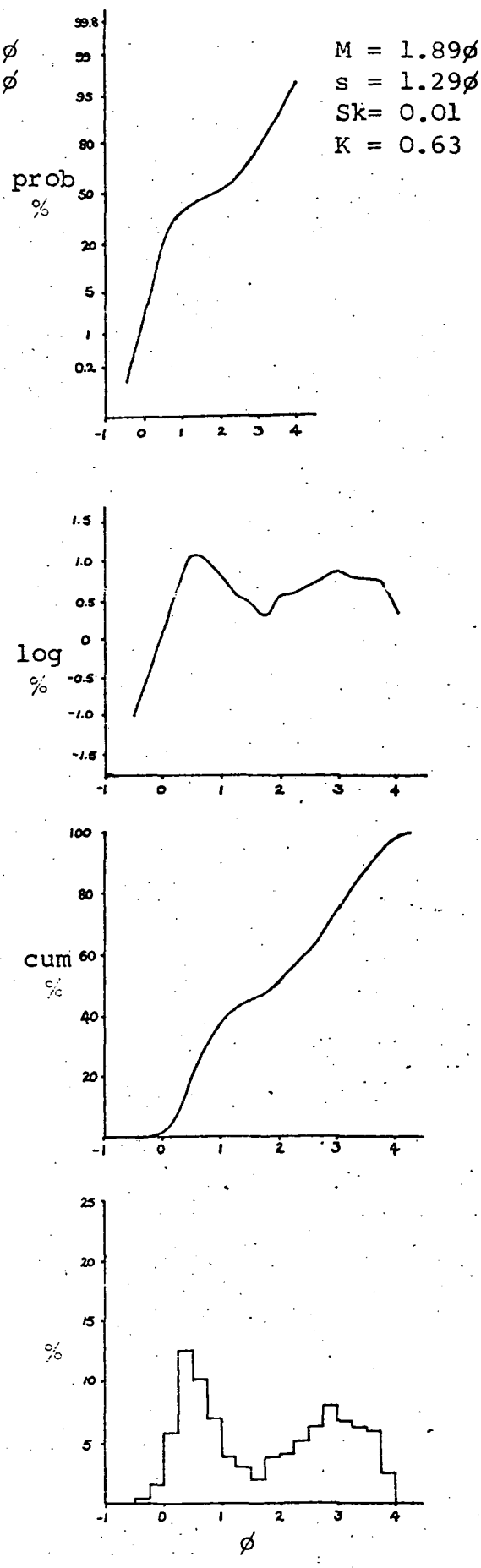

Sand-sheet

Sherburn Hill N Face

FIG. 7.11a

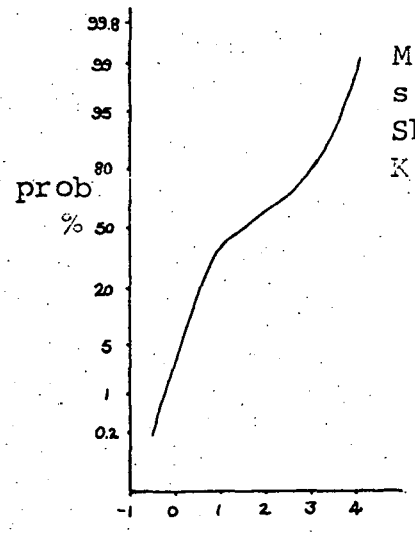

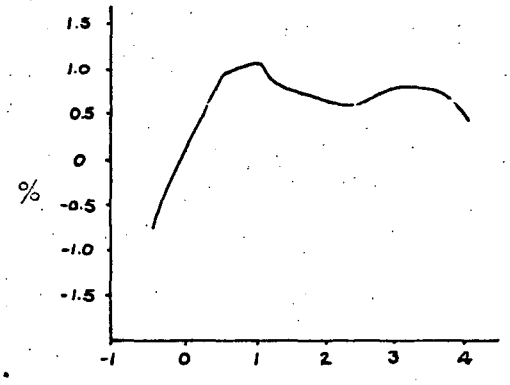

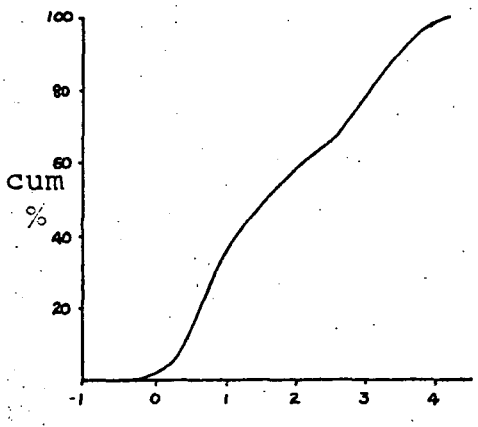

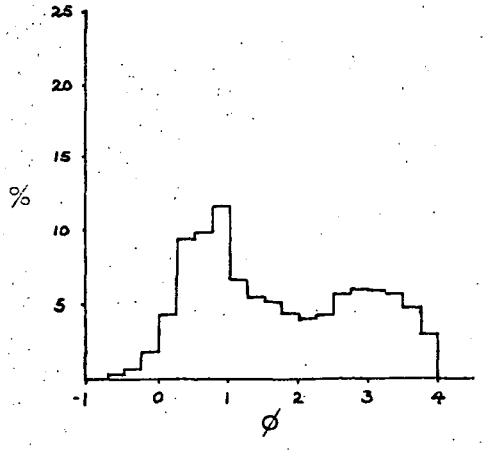

FIG.7.11b

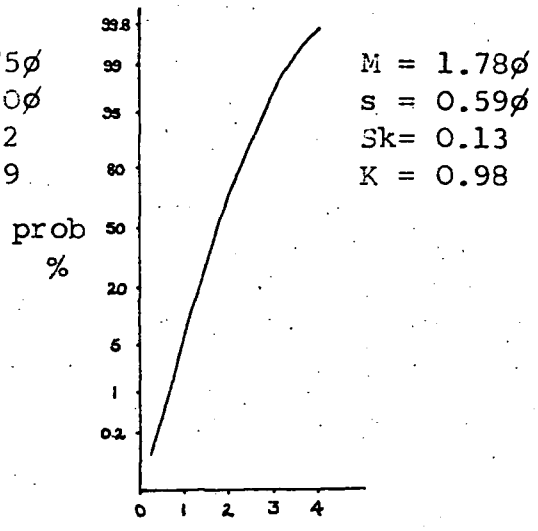

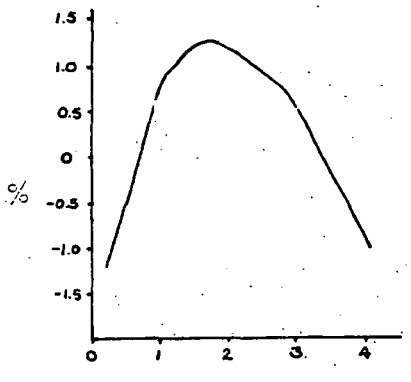

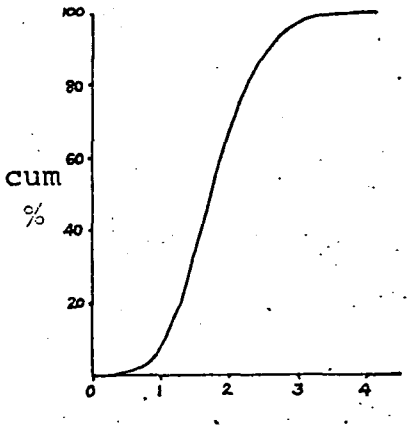

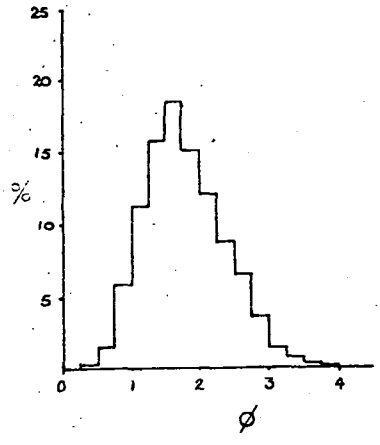

Lamination: Wind-ripple Wind-ripple

Locality: Quarrington Hill face D Hetton Downs

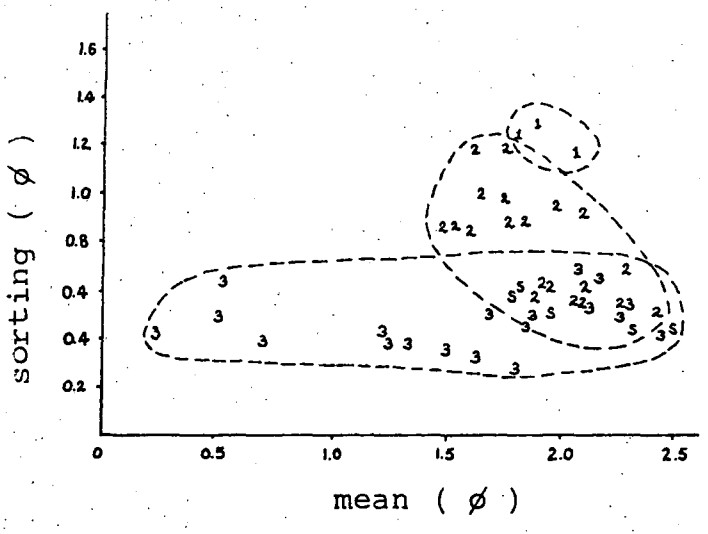

FIG. 7.12 Graphic mean v. sorting (graphic standard deviation) by lamination for the Yellow Sands.

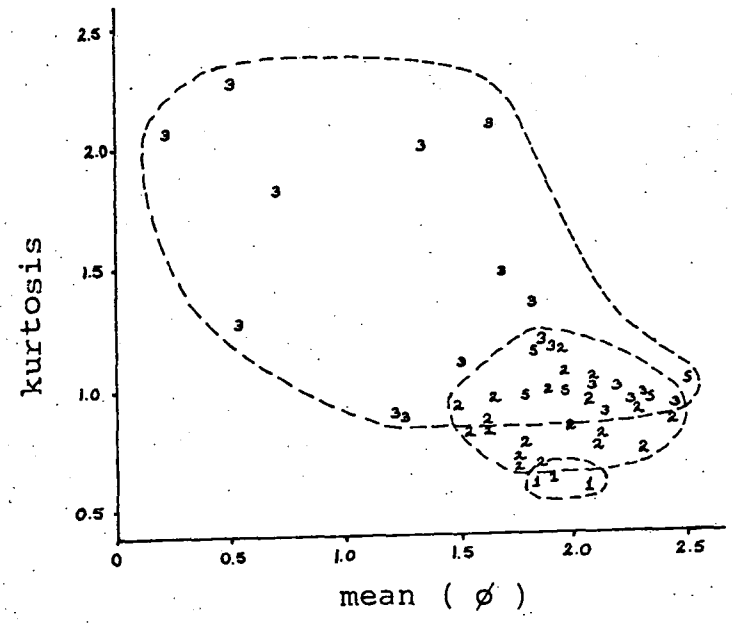

FIG. 7.13 Graphic mean v. graphic kurtosis by lamination for the Yellow Sands.

Key to lamination types:

1 = sand-sheet

2 = wind-ripple

3 = sandflow

S = apparently structureless

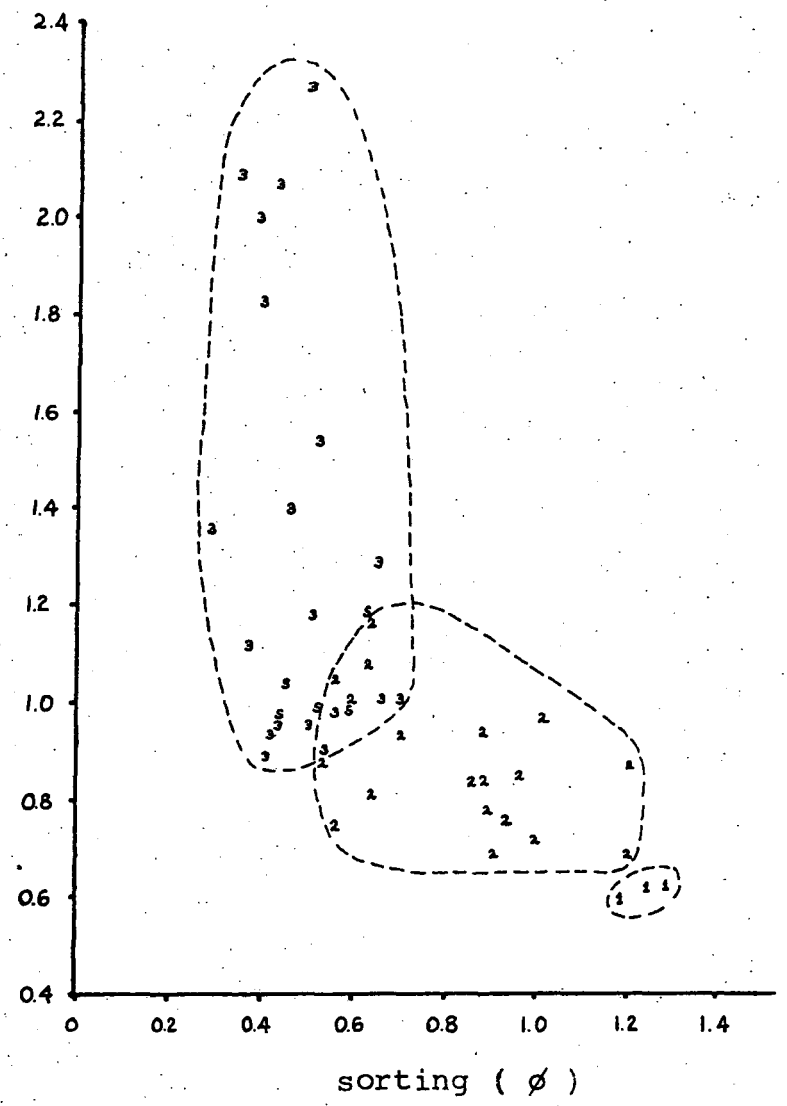

FIG.7.14 Sorting (inclusive graphic standard deviation) v. graphic kurtosis by lamination for the Yellow Sands.

Key to lamination types:

1 = sand-sheet

2 = wind-ripple

3 = sandflow

S = apparently structureless

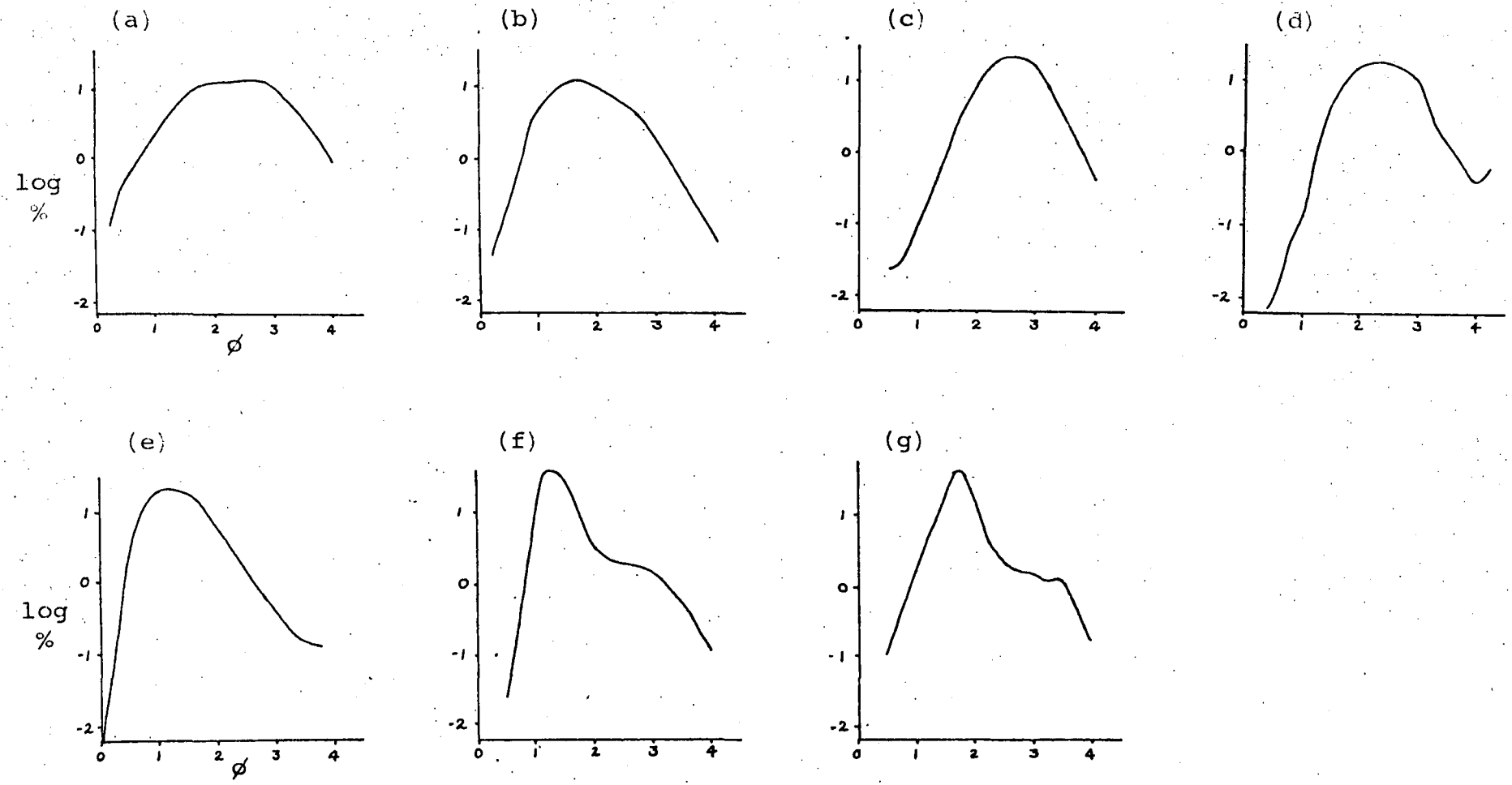

FIG.7.15 Illustrating the continuous variation of grain size distribution shape. (a) & (b) are wind-ripple, (c) & (d) structureless, (e) - (g) sandflow samples. Sorting improves from 0.7ø to 0.35ø from (a) through (g). All graphs are log frequency % v. phi.

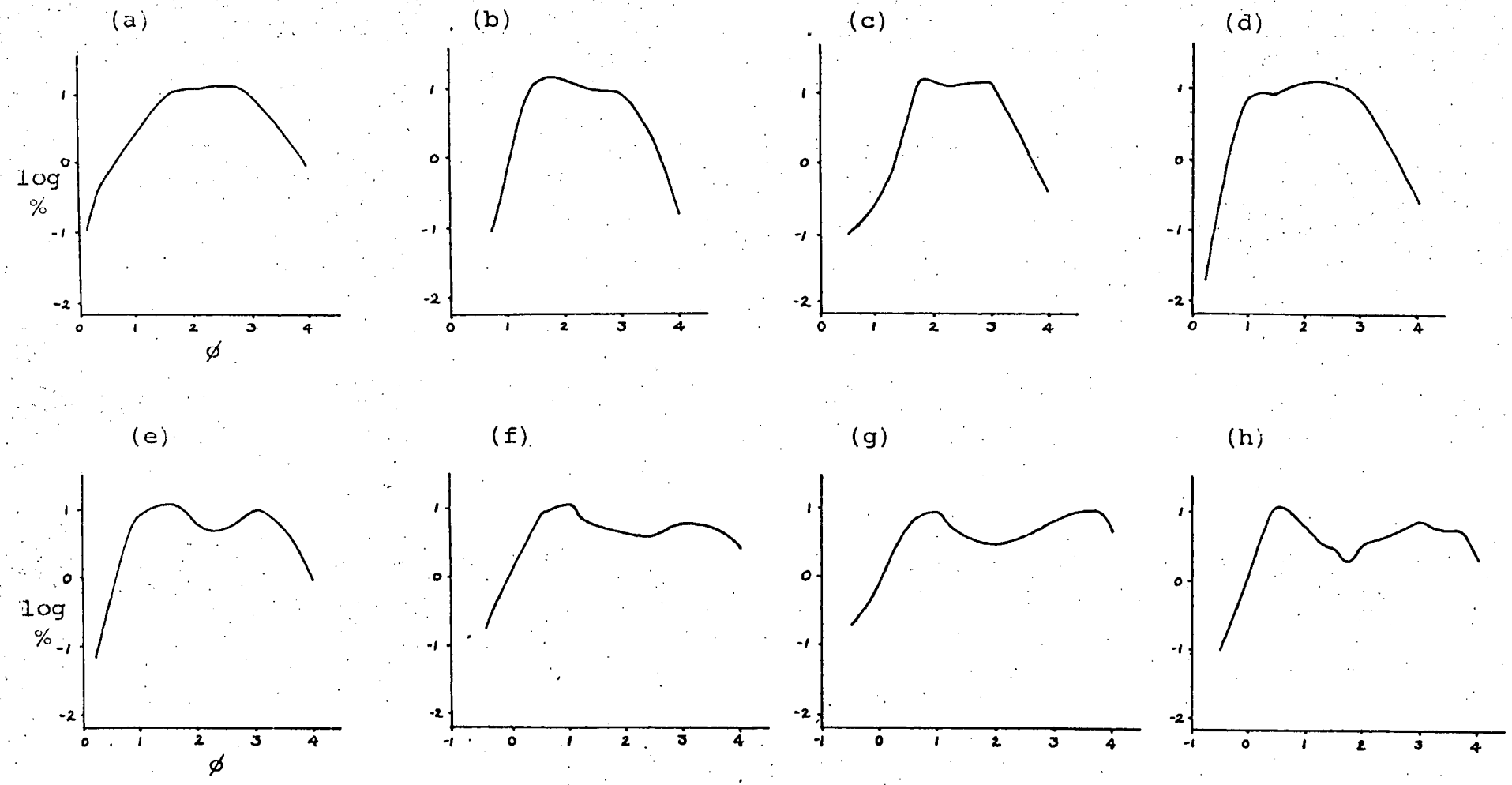

FIG.7.16 Illustrating the continuous variation of grain size distribution shape. (a) - (e) are wind-ripple samples, (f) - (h) sand-sheet. Sorting worsens from 0.7ø to 1.29ø from (a) through (h). Curve (a) here & (a) on fig. are identical. All graphs are log frequency % v. phi.

FIG. 7.17 Split cores of the Yellow Sands - Carboniferous unconformity (dotted) in N.C.B. boreholes D8B, D1 and D2 (L to R). The Carboniferous rocks are broken and fissured, and those in D2 consist of fractured Carboniferous siltstone with Yellow Sands filling a fissure. Note the grey colour of the Yellow Sands. Core D1 is stained red. Scale is 0.15m long.

HUE	VALUE	CHROMA /4	CHROMA /6	CHROMA /8
2.5YR	7	-	4	-
	6	-	1	-
	5	-	1	-
10YR	7	5	6	2
	6	-	3	1
2.5Y	8	1	-	-
	7	7	7	-

TABLE 7.2 Yellow Sands Munsell colour determinations.
(n = 38)

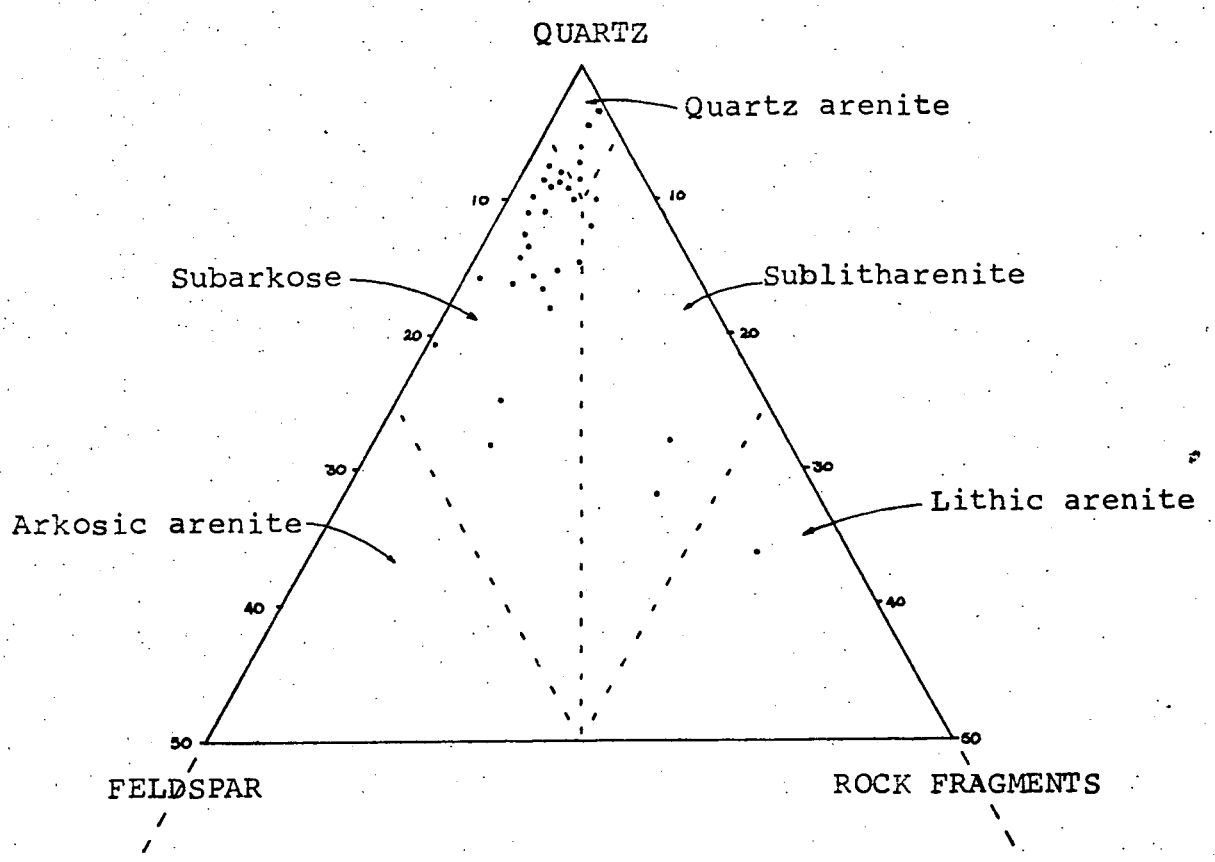

FIG.7.18 Petrographic classification of the Yellow Sands. Scheme of Pettijohn (1975, p.211).

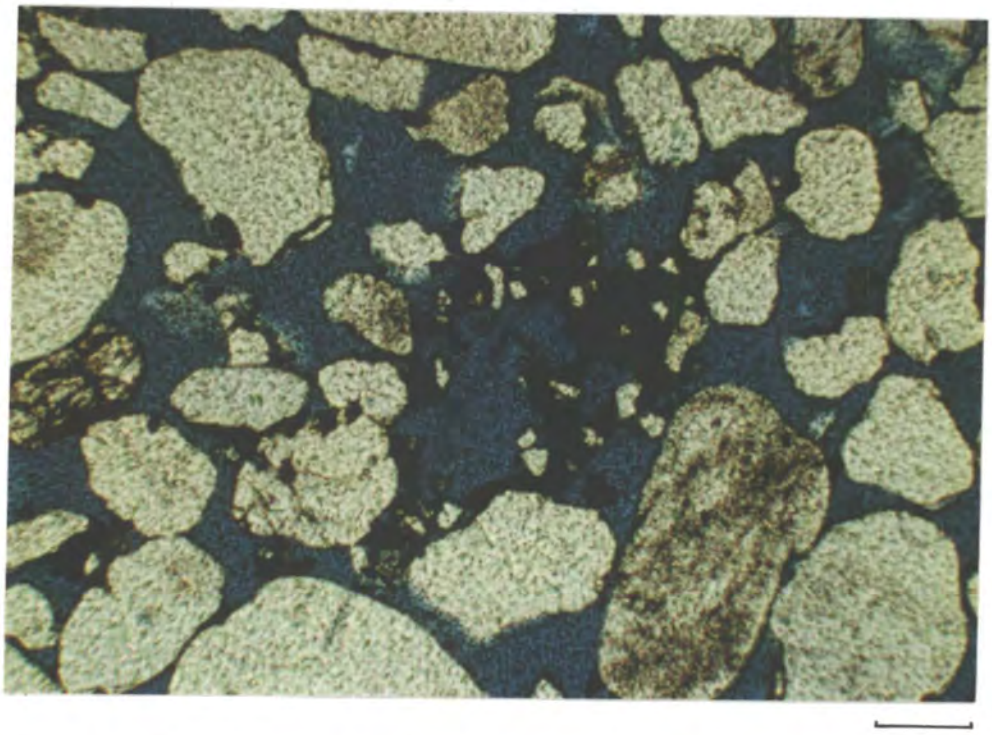

FIG. 7.19 Sandstone rock fragment breaking down, generating pigment. Note the concentration of pigment in hollows on other grains, the lack of cement and loose packing. Pore spaces filled with resin. Plane polarised light, scale bar = 100μ. Specimen from 105,16 (Encl. 3), McCall's Quarry.

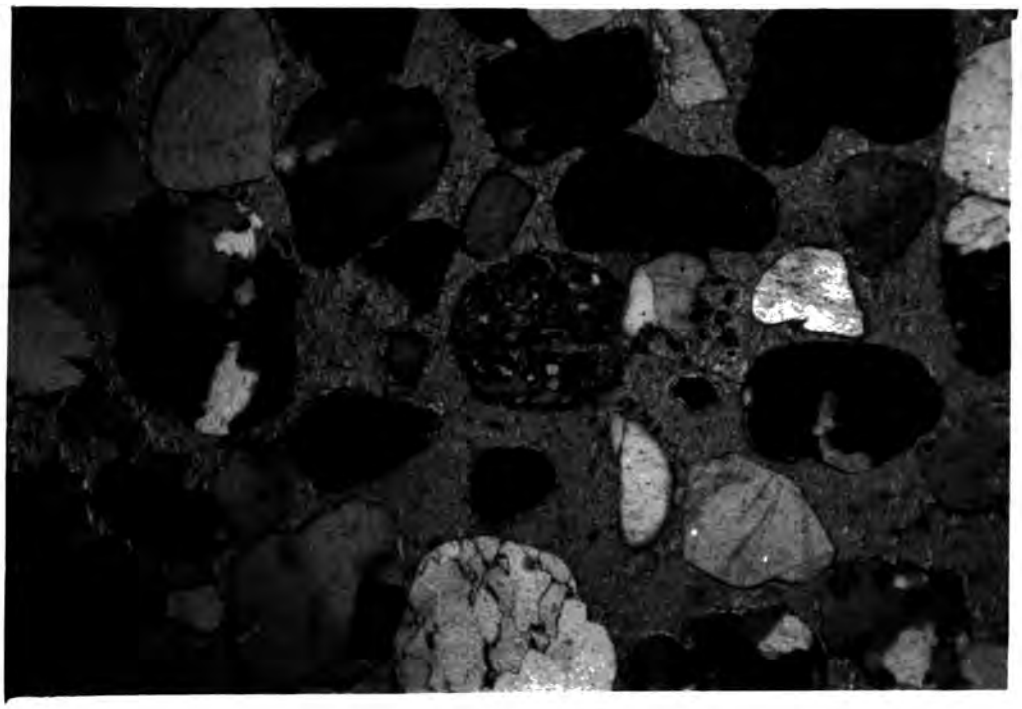

FIG. 7.20 Degrading sandstone rock fragment with a rim of dolomite, in calcite- cemented sand. Note how the rock fragment has preferentially attracted the dolomite. Dept of Geological Sciences, University of Durham, specimen no. 22236, locality unknown. Crossed polars, scale bar = 1000μ.

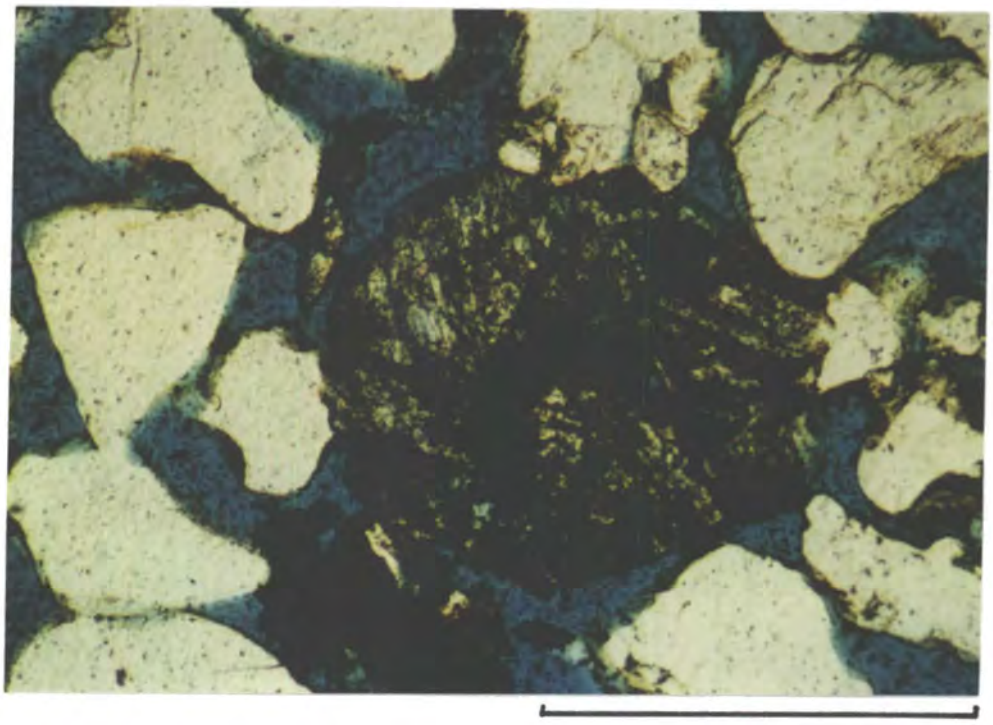

FIG. 7.21 Possible basic igneous rock fragment in Yellow Sands from 76,16 Sherburn Hill, west face. Consists of a network of partially dissolved feldspar (type indeterminate), with interstitial rust-coloured opaques. Pore space filled with blue resin. Scale bar = 100μ.

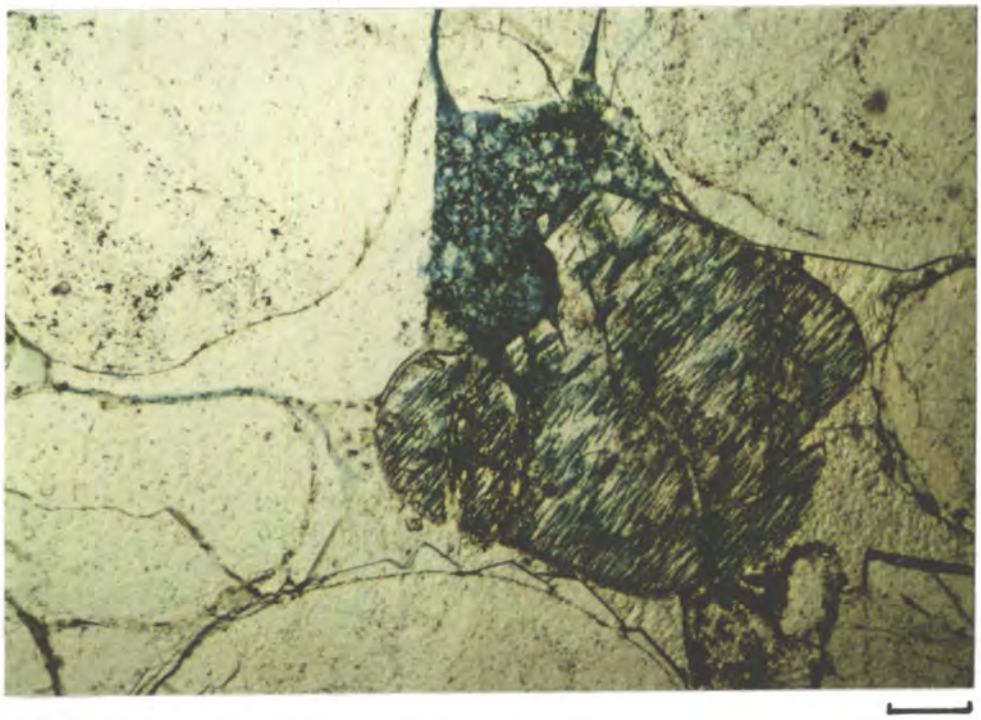

FIG. 7.22 Specimen from Ferryhill railway cutting showing a partially dissolved K-feldspar grain with associated authigenic kaolinite. Also note quartz overgrowths and poikilotopic calcite cement. Plane polarised light. Pore space impregnated with blue resin. Specimen taken from 120,02 (Encl. 2), Ferryhill railway cutting. Scale bar = 100μ.

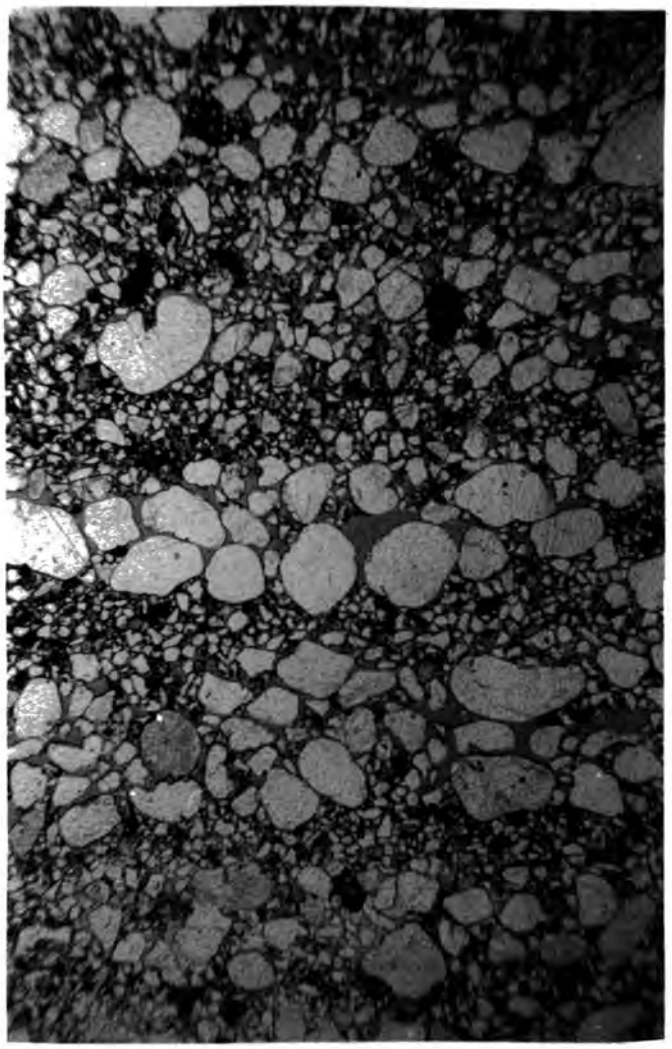

FIG. 7.23 Wind-ripple lamination. Note the bimodality and good packing (cf FIG. 7.24). Fine laminae partially cemented by calcite. From a loose block, McCall's Quarry. Pore space impregnated with resin. Plane polarised light. Scale bar = 1000μ.

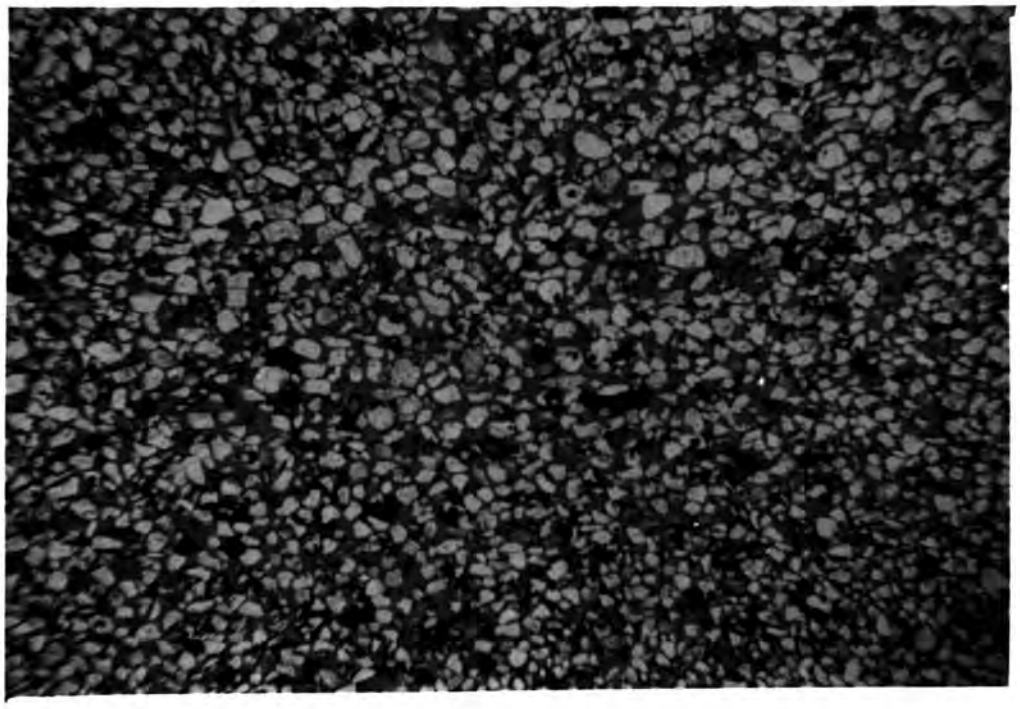

FIG. 7.24 Thin section view of sandflow lamination, specimen from Sherburn Hill Sand Pit. Note the contrast in packing and sorting with FIG.7.23. Pore space impregnated with resin. Plane polarised light. Scale bar = 1000μ.

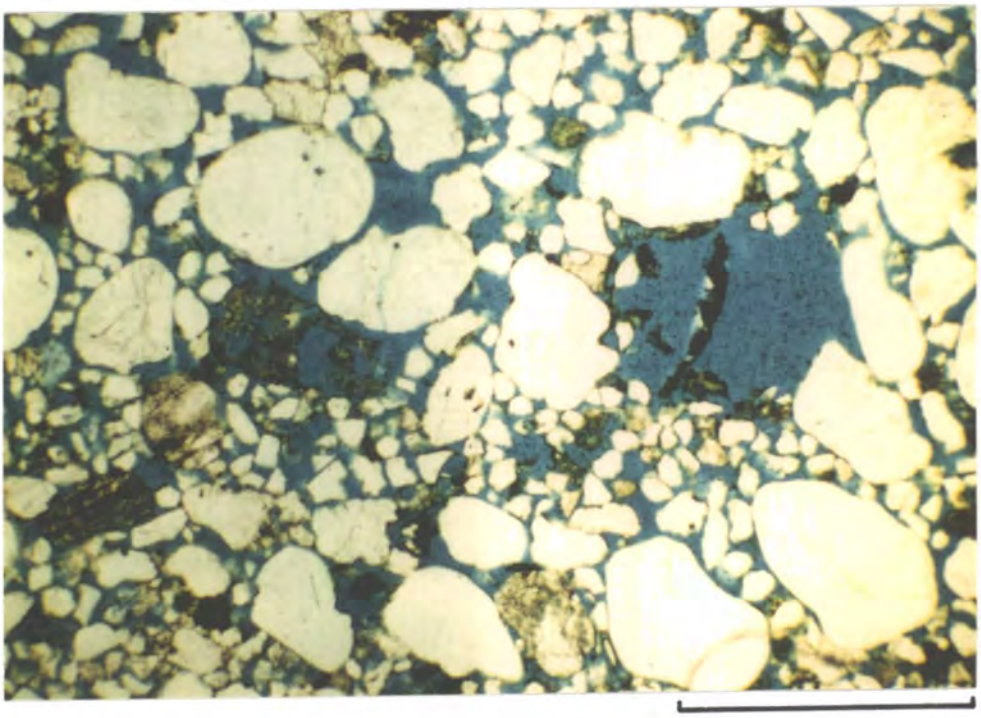

FIG. 7.25 Secondary porosity from grain dissolution. Pore space filled with blue resin. Plane polarised light. Scale bar = 1000μ. Specimen from Sherburn Hill Sand Pit.

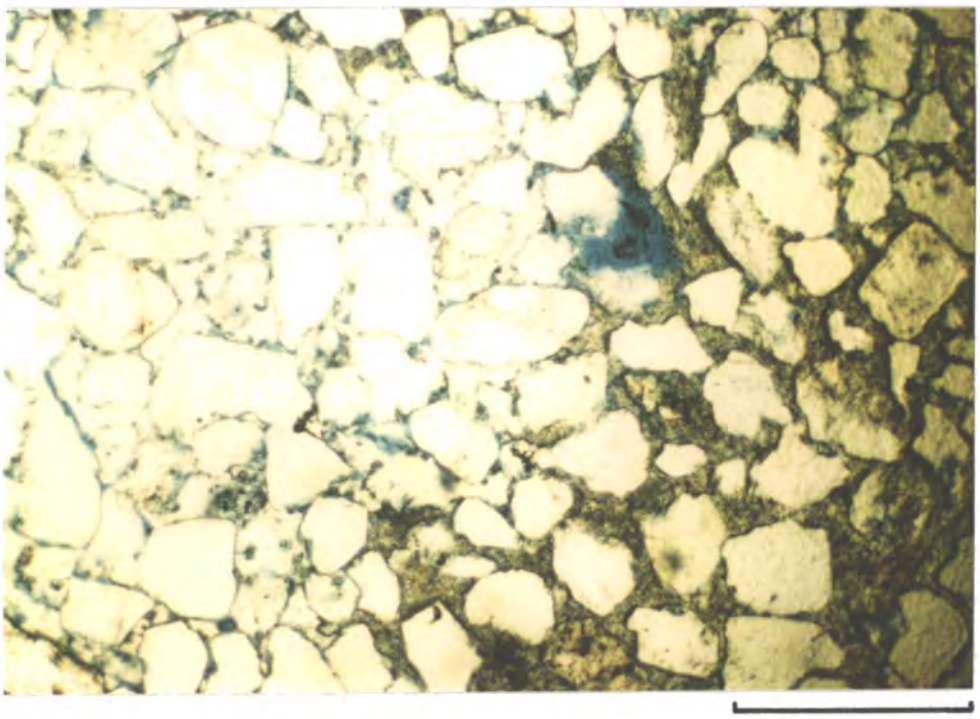

FIG. 7.26 Specimen from Hetton Downs Quarry, showing lamellar pores between calcite cement and clastic grains, and further secondary porosity from the dissolution of dolomite. Patch of radiating barytes cement visible at right. Plane polarised light. Scale bar = 500μ.

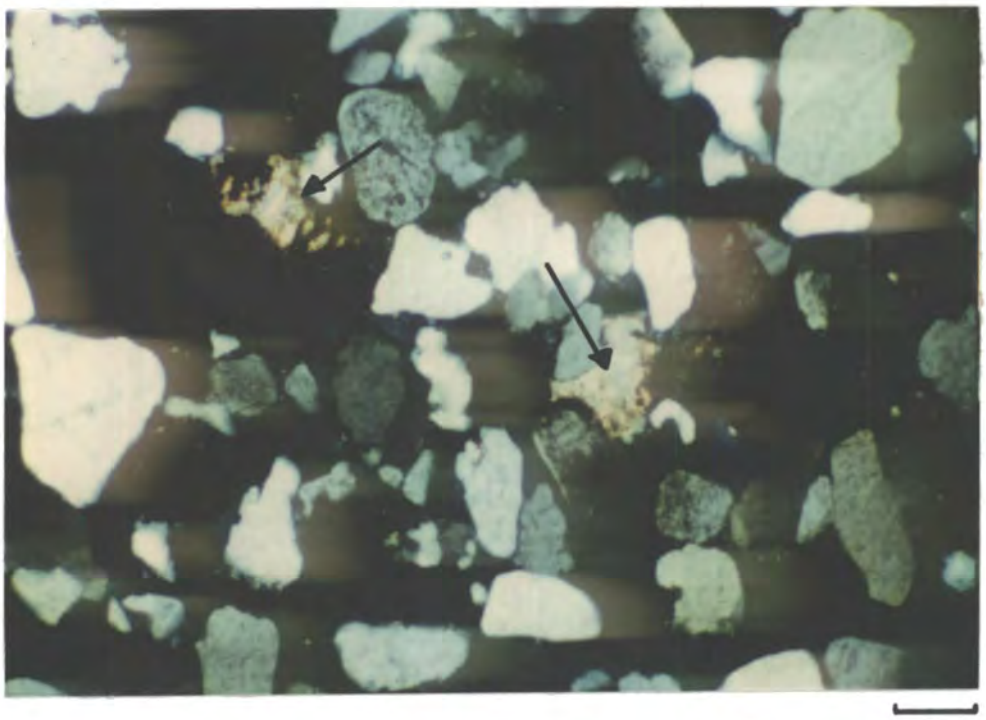

FIG. 7.27 Specimen from face G at Quarrington Hill Quarry, showing the two separate remnant patches of calcite (arrowed) in the same optical orientation, presumably part of a former, much larger crystal. Crossed polars. Scale bar = 100μ.

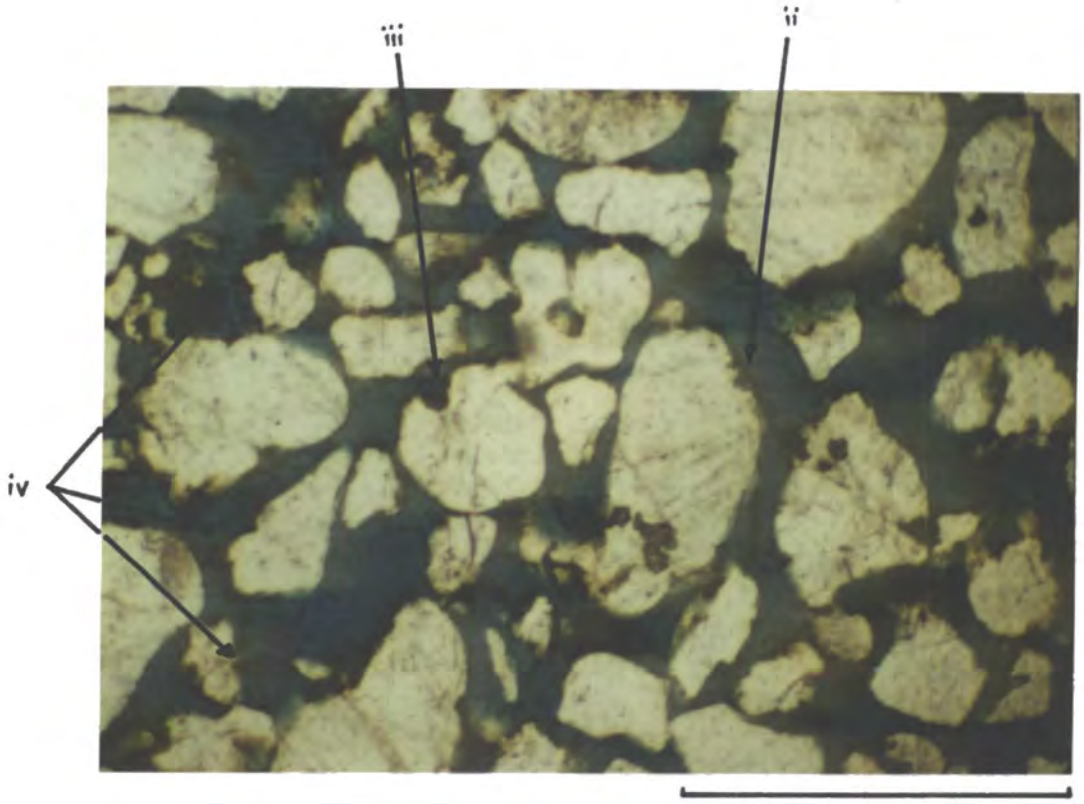

FIG. 7.28 Pigmenting phases in a specimen from the W face of Sherburn Hill Sand Pit. Pigment in hollows (type iii) and some coats on grains (type ii) are readily apparent, granules of ex-pyrite (type iv) less so. Plane polarised light. Scale bar = 500μ.

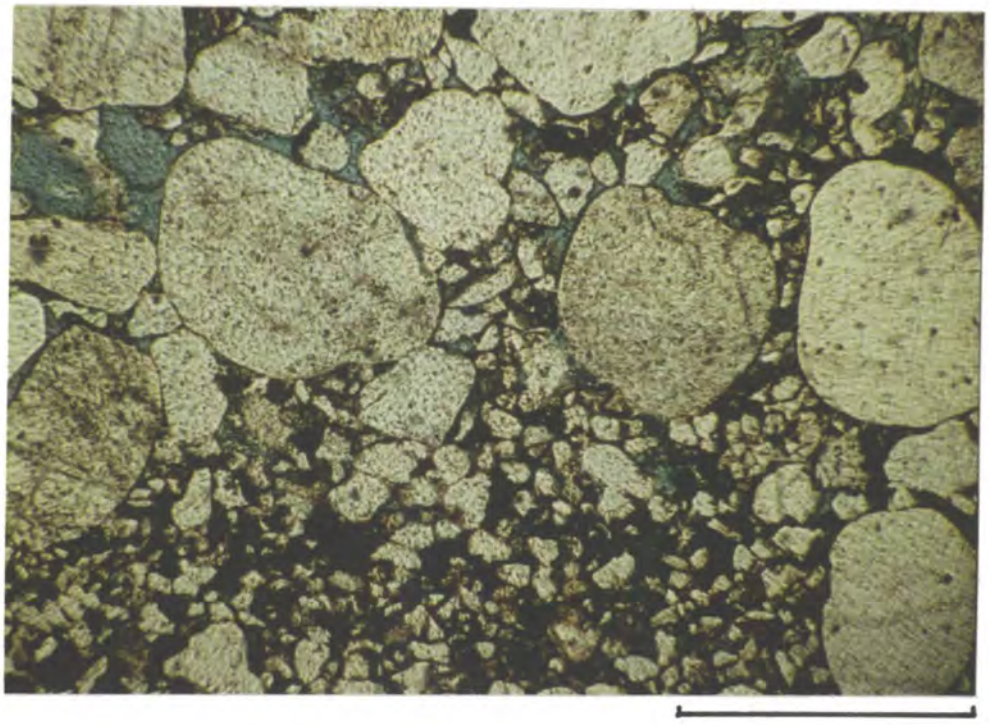

FIG. 7.29 The Yellow Sands in N.C.B. borehole D8B. The rock is wind-ripple laminated, with the fine laminae visible. Cement is calcite and much greyish-brown pigment is present. The coarse grains are coated with a 1-2μ thick layer of radially arranged, colourless kaolinite. Plane polarised light. Scale bar = 1000μ.

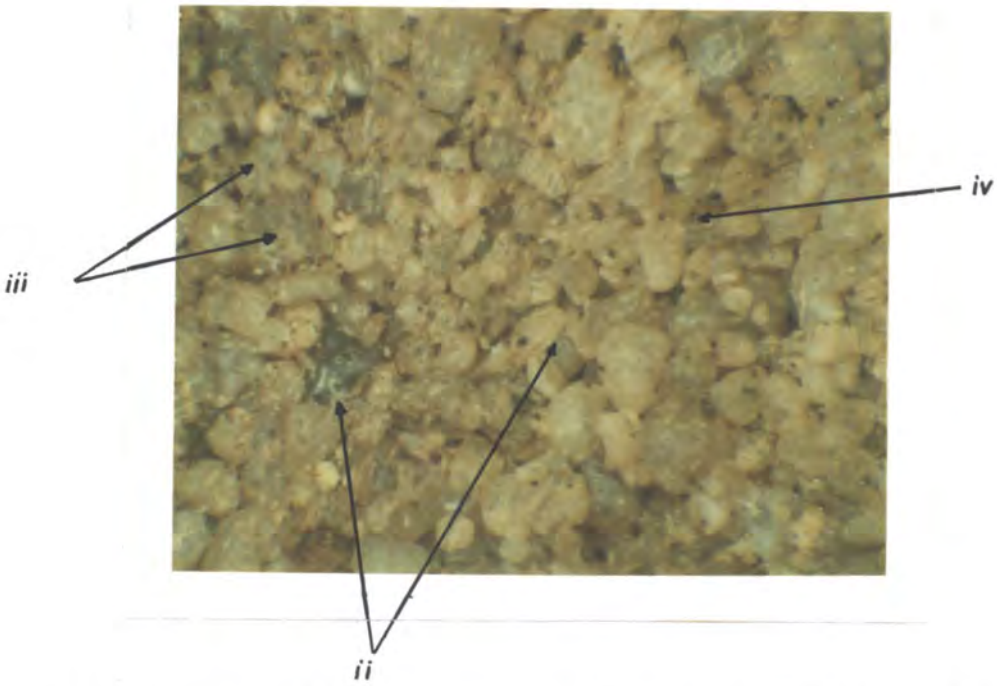

FIG. 7.30 Microscope view of a hand specimen of Yellow Sands from Hetton Downs Quarry. Shows the yellow stain on all grains (pigment type ii), coloured clay coats forming rings around contacts (type ii), concentration of pigment in hollows (type iii), and brown granules of oxidised pyrite (type iv). Field of view 3mm wide. Blurring is unavoidable, due to optics and a 5 minute exposure time.

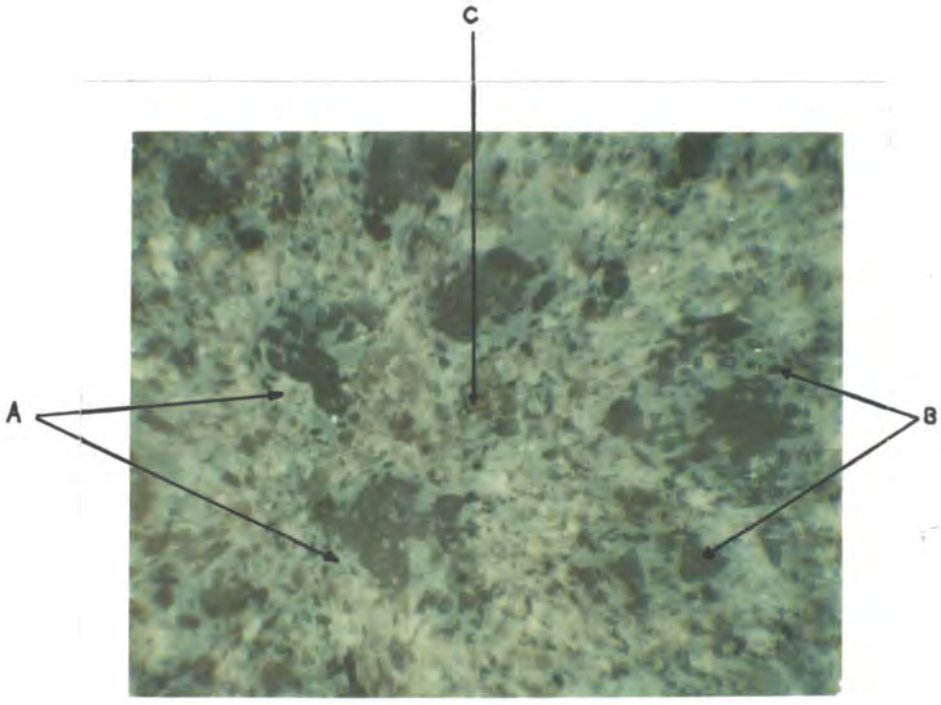

FIG. 7.31 Microscope view of a hand specimen of Yellow Sands from N.C.B. borehole D8B. White areas (A) are grain- coating authigenic kaolinite, grey areas (B) are apparently clean quartz surfaces. Authigenic pyrite (C) also visible. The field of view is 3mm wide, and consists of several coarse grains showing large areas of grey quartz surface set in a groundmass of fine sand mostly coated in white kaolinite.

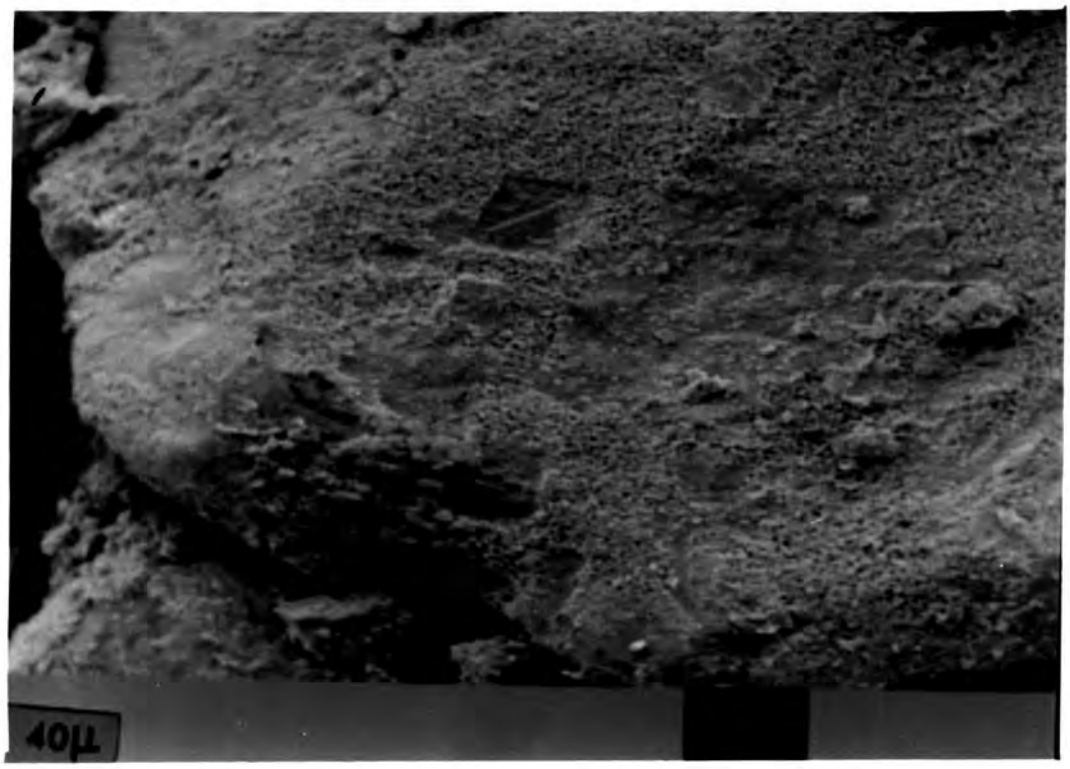

FIG. 7.32 Subsurface specimen from N.C.B. borehole B9A. SEM view showing a grain partially coated in clay, probably kaolinite, with a granular texture.

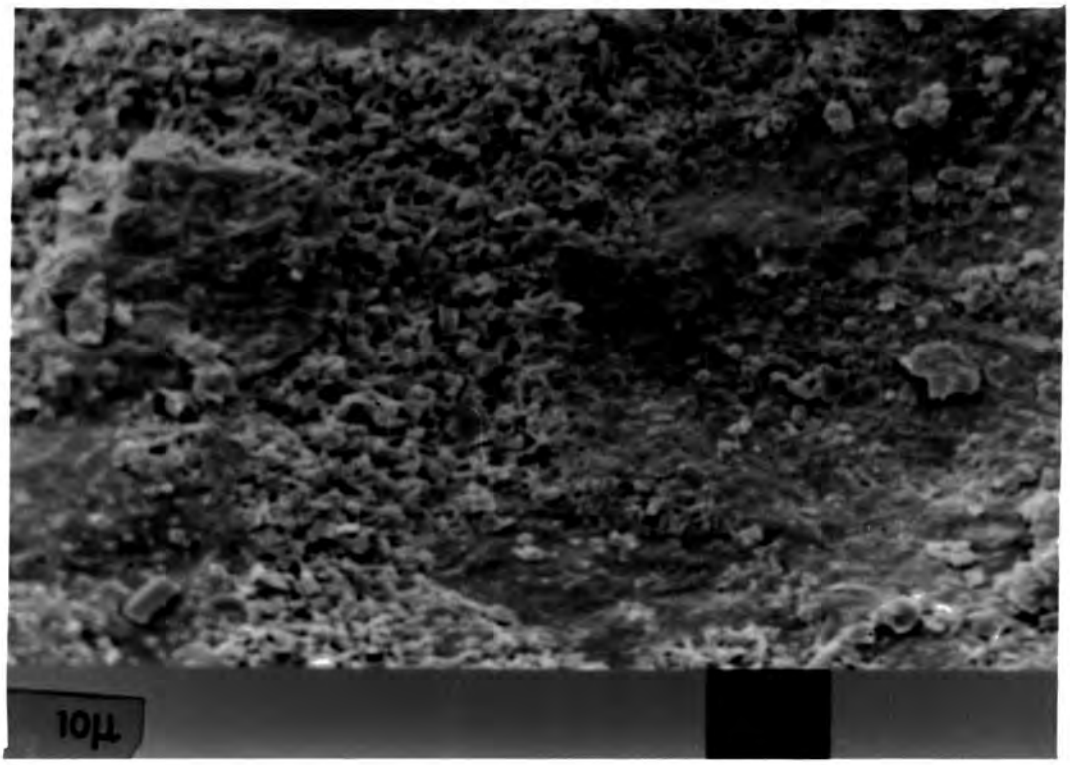

FIG. 7.33 Enlargement of the centre of FIG. 7.32, showing the texture of the clay, and its exclusion from the area of a former grain contact (right).

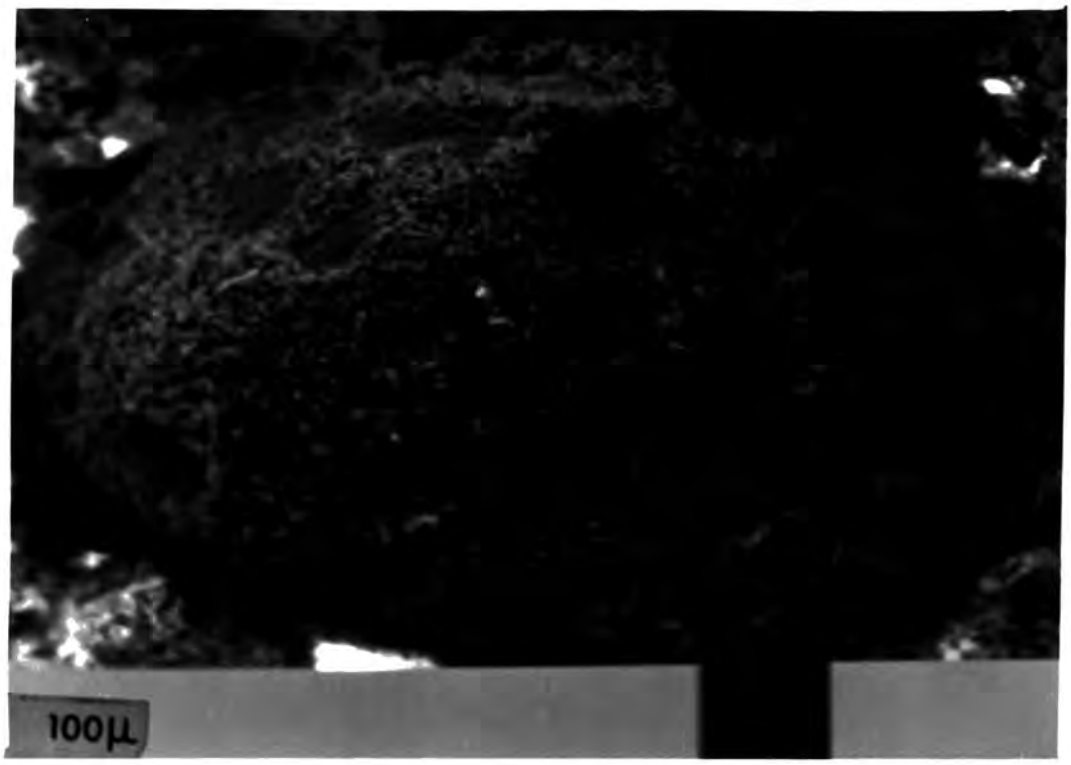

FIG. 7.34 Subsurface specimen from N.C.B. borehole D4. SEM view of a well rounded grain with a coating of authigenic kaolinite, absent from grain contacts.

FIG. 7.35 Clods of rusty brown material on a grain from Sherburn Hill Sand Pit. The clods are made up of 20μ diameter granules which were originally pyrite framboids. Note also the liberal dusting of pigment over the rest of the grain surface. The whole surface of the grain is stained yellow.

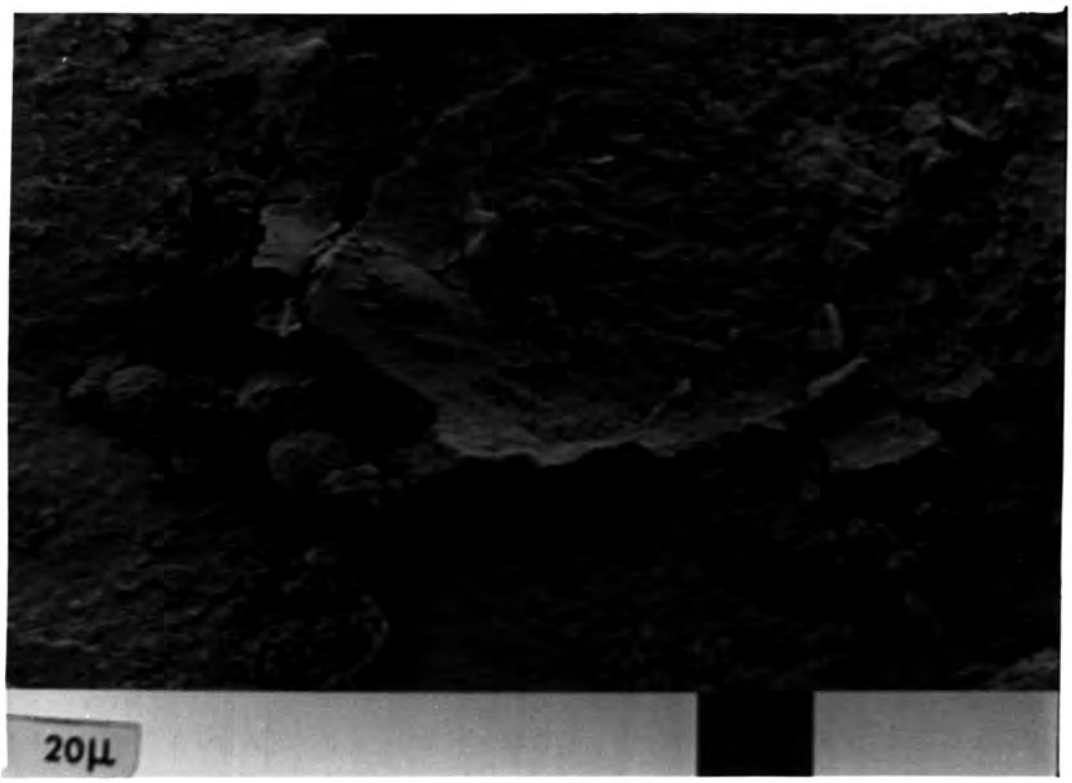

FIG. 7.36 View of a grain from the Sherburn Hill Sand Pit. Shows a collar of ?clay (a meniscus?) around a former grain contact, and oxidised and dissolved remnants of pyrite framboids.

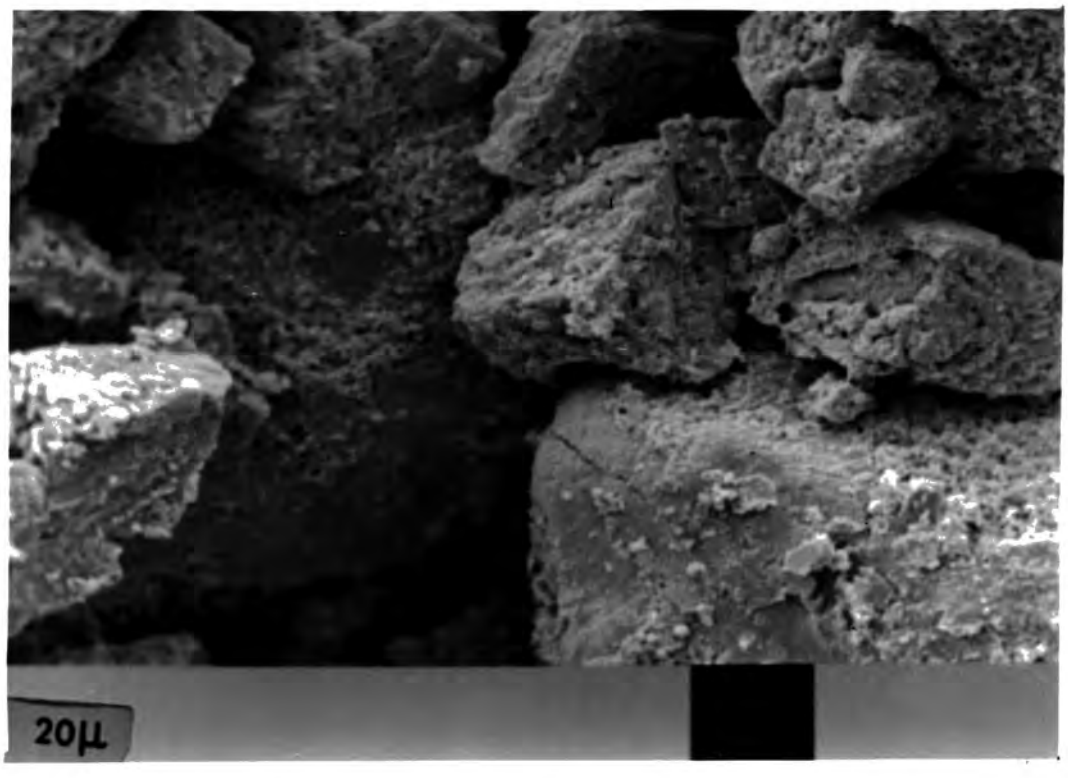

FIG. 7.37 Specimen from N.C.B. borehole B9A showing rhombs of authigenic dolomite bearing the same clay coats (pigment type ii) as the clastic grains.

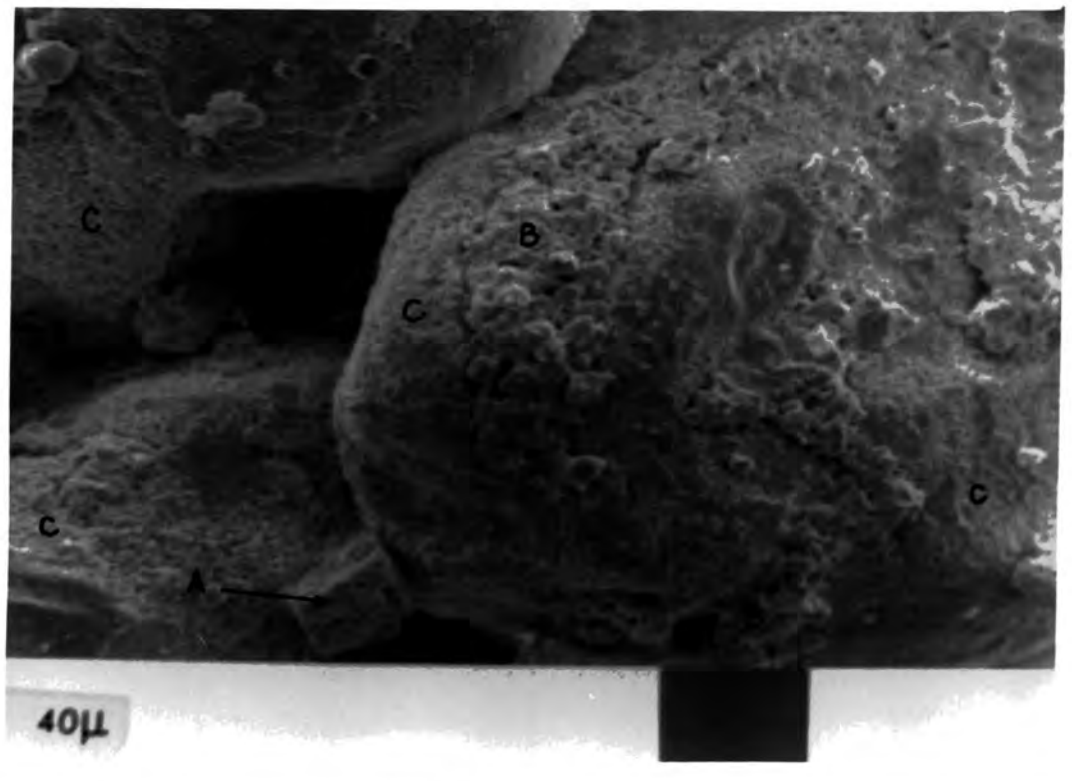

FIG. 7.38 Specimen from N.C.B. borehole B9A. Shows dolomite (A), pyrite as a partial grain coat and in hollows (B), and clay coats (C). Though the resolution and focus are appalling it is just possible to see that the dolomite probably has a clay coat, whereas the pyrite does not.

TABLE 7.3 YELLOW SANDS XRF RESULTS

	Locality	Fe_2O_3	S	Al_2O_3	K_2O	MgO	CaO
1	NCB D1	3.68	1.08	5.03	1.16	9.00	16.15
2	NCB D1	0.71	0.00	4.17	2.14	1.56	2.28
3	NCB D1	1.61	0.72	5.76	2.28	1.02	1.47
4	NCB D8B	0.77	0.00	7.13	1.90	2.07	2.96
5	NCB D8B	0.85	0.00	4.74	1.79	2.40	3.67
6	NCB D4	1.90	0.99	3.44	1.31	0.21	0.30
7	NCB D4	1.75	0.86	7.11	2.67	0.51	0.76
8	NCB B9A	1.76	0.39	4.28	2.05	4.62	7.06
9	NCB B9A	2.40	0.84	4.50	2.18	7.46	12.24
10	ShH yellow	1.33	0.04	4.87	2.16	0.22	0.23
11	ShH yellow	0.42	0.15	2.62	1.28	0.05	0.02
12	ShH white	0.47	0.00	5.73	1.90	0.31	1.31
13	ShH white	0.17	0.09	3.33	1.58	0.08	0.02
14	Bbn yellow	2.49	0.03	4.72	2.25	0.12	0.04
15	Bbn yellow	2.87	0.00	4.27	1.93	1.60	18.07
16	Bbn red	1.90	0.01	1.50	0.59	0.16	0.13
17	HD yellow	2.49	0.03	4.72	2.25	0.12	0.04

All figures are percentages, whole rock measurements.

NCB D1 = National Coal Board offshore bore at NZ 530521

NCB D8B = " " " " " " NZ 497526

NCB D4 = " " " " " "

NCB B9A = " " " " " "

ShH = Sherburn Hill Sand Pit

Bbn = Bowburn Quarry

HD = Hetton Downs Quarry

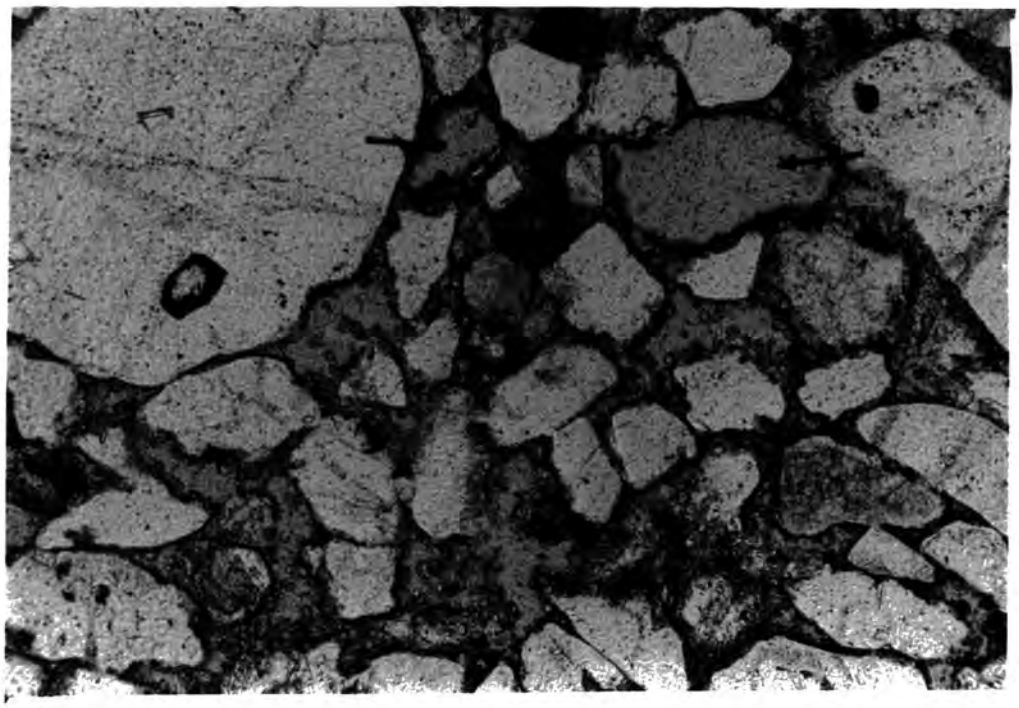

FIG. 7.39 Abundant authigenic dolomite coating grains and filling some spores. Pore space impregnated with resin. A 1μ coating of ?authigenic kaolinite on parts of some grains is just resolvable under high power. Note also secondary porosity (arrowed). Specimen from N.C.B. borehole D1. Plane polarised light. Scale bar = 100μ.

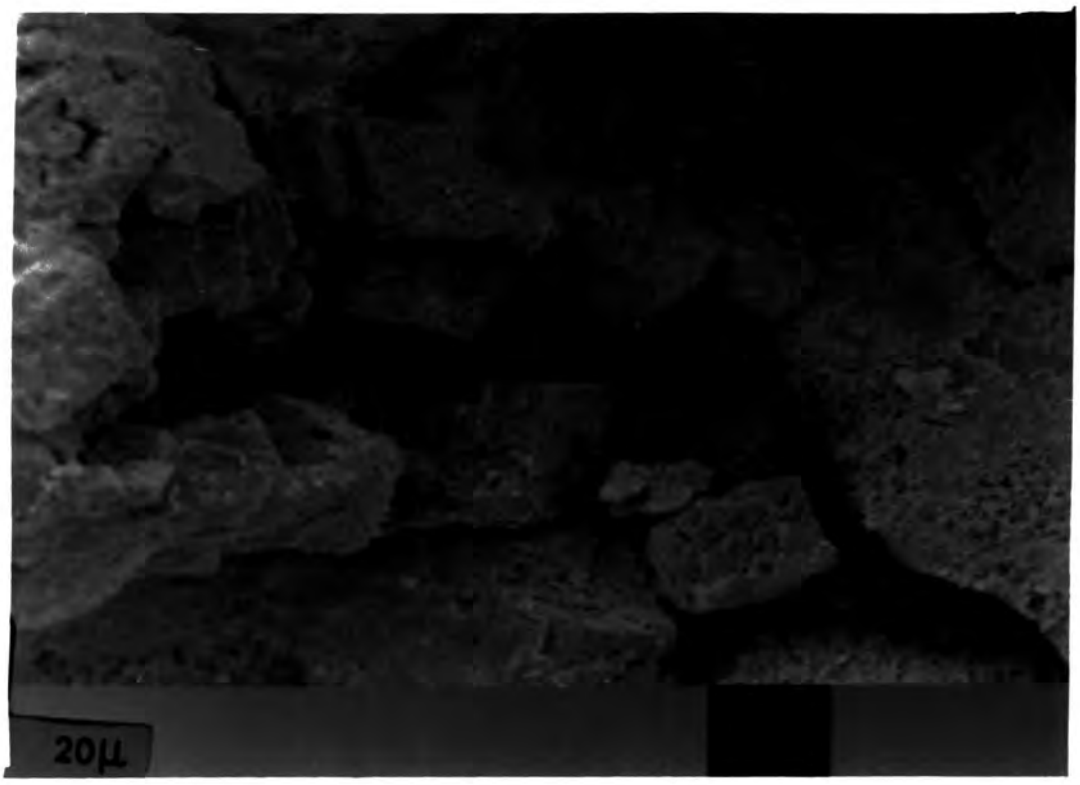

FIG. 7.40 Authigenic dolomite largely free of clay and showing some signs of etching. Specimen from N.C.B. borehole B9A.

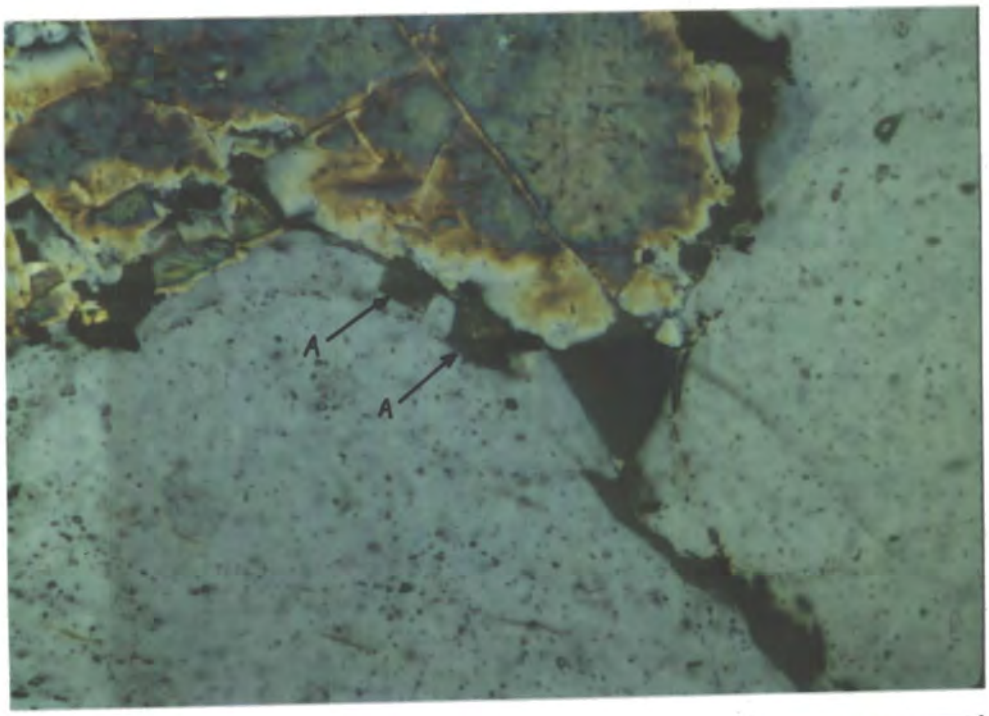

FIG. 7.41 Early dolomite crystal (A) enclosed in a late-formed quartz overgrowth with a subsequent calcite cement. Quarrington Hill Quarry. Crossed polars. Scale bar = 100μ.

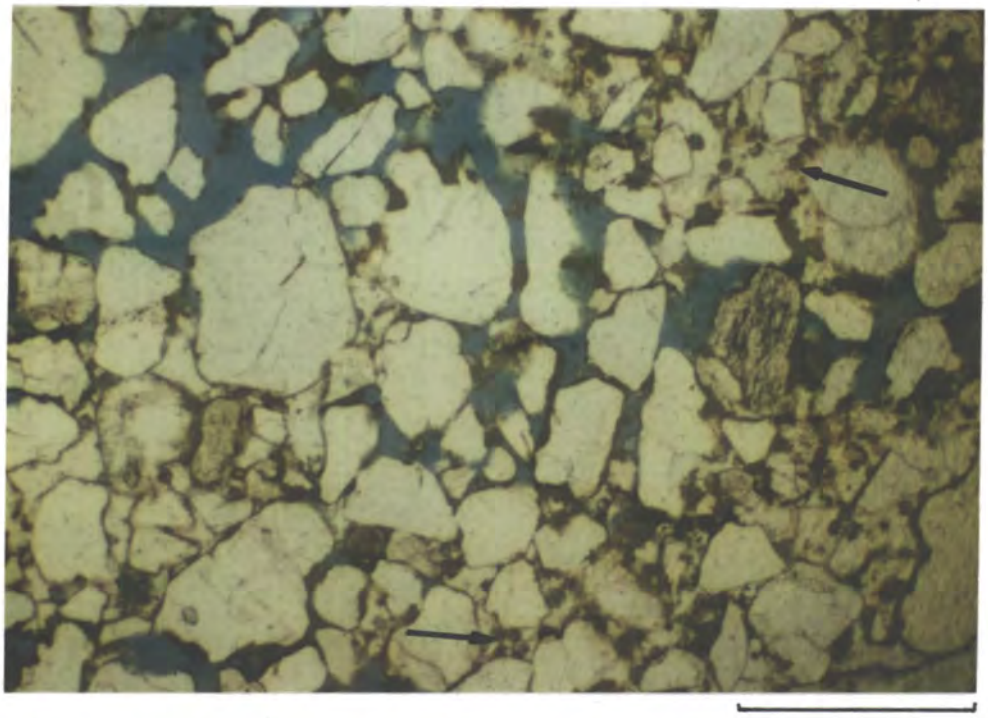

FIG. 7.42 Specimen from McCall's Quarry showing nodular calcite cement (large area free of resin), pigment as grain coats, in hollows and as independent phases, and also colouring some dolomite crystals (arrowed). Scale bar = 500μ.

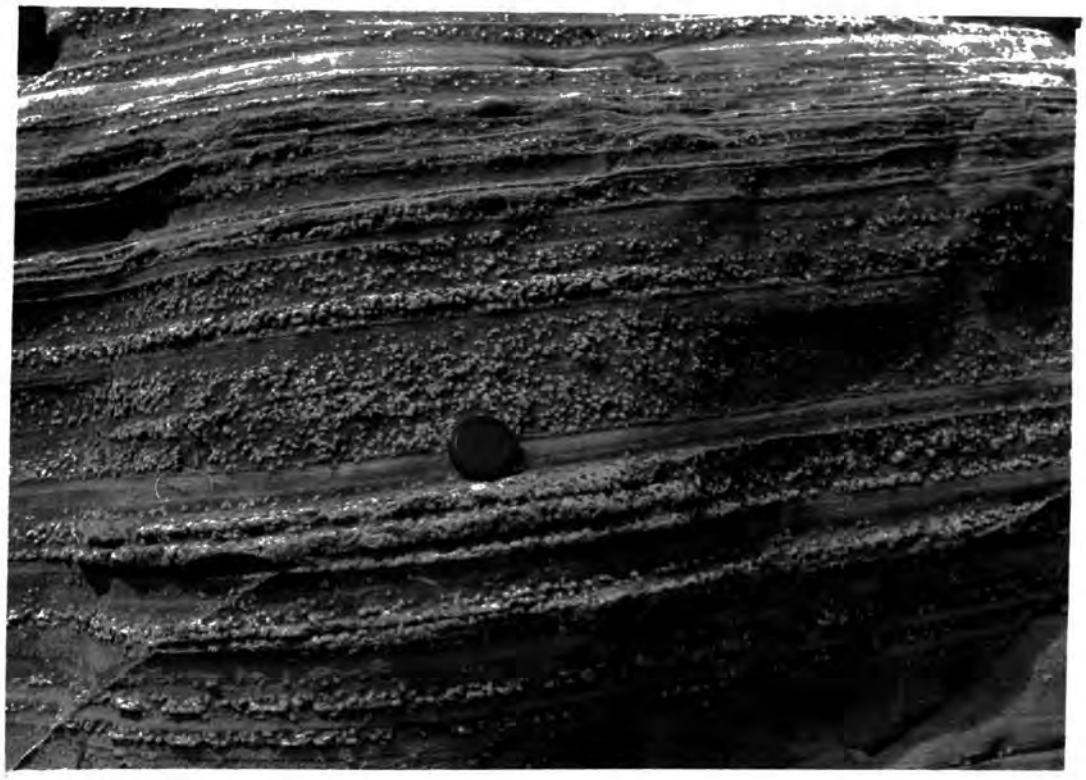

FIG. 7.43 Abundant poikilotopic calcite crystals forming a lamination-controlled nodular cement at Cullercoats. The lamination is a mixture of wind-ripple and sandflow types, the coarser grained laminae are preferentially cemented.

FIG. 7.44 Masses of poikilotopic calcite cementing the upper parts of coarse-grained sandflows. New excavation, N end of Bowburn Quarry. Trowel (arrowed) gives scale.

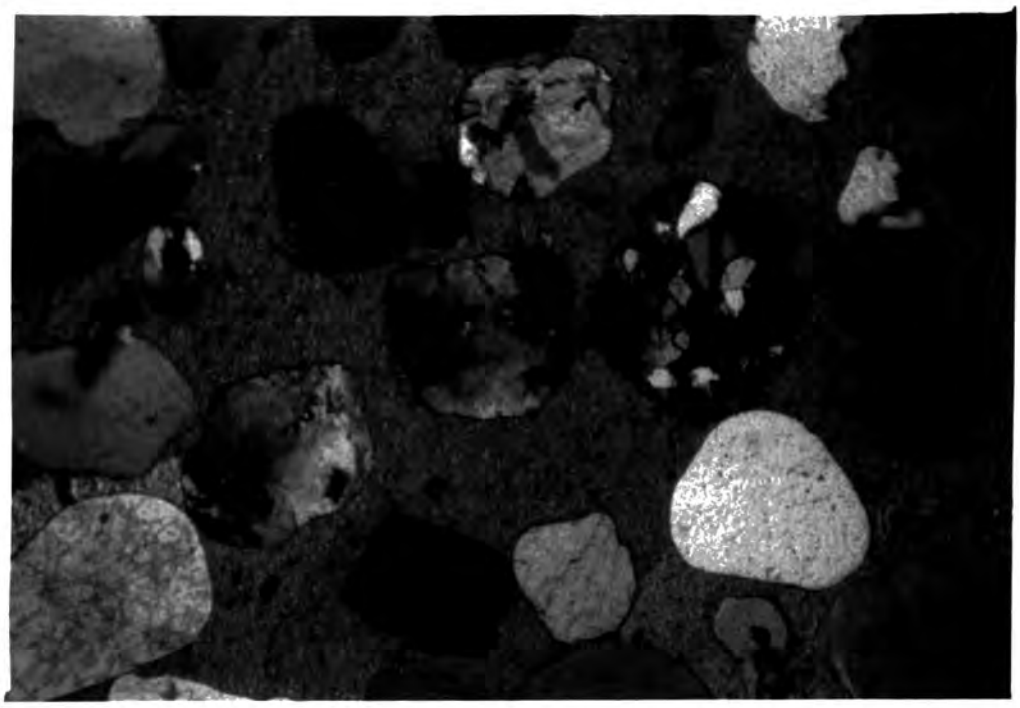

FIG. 7.45 Poikilotopic calcite cement showing a possibly displacive texture. Dept of Geological Sciences, University of Durham, specimen no. 22236. Crossed polars. Scale bar = 500μ.

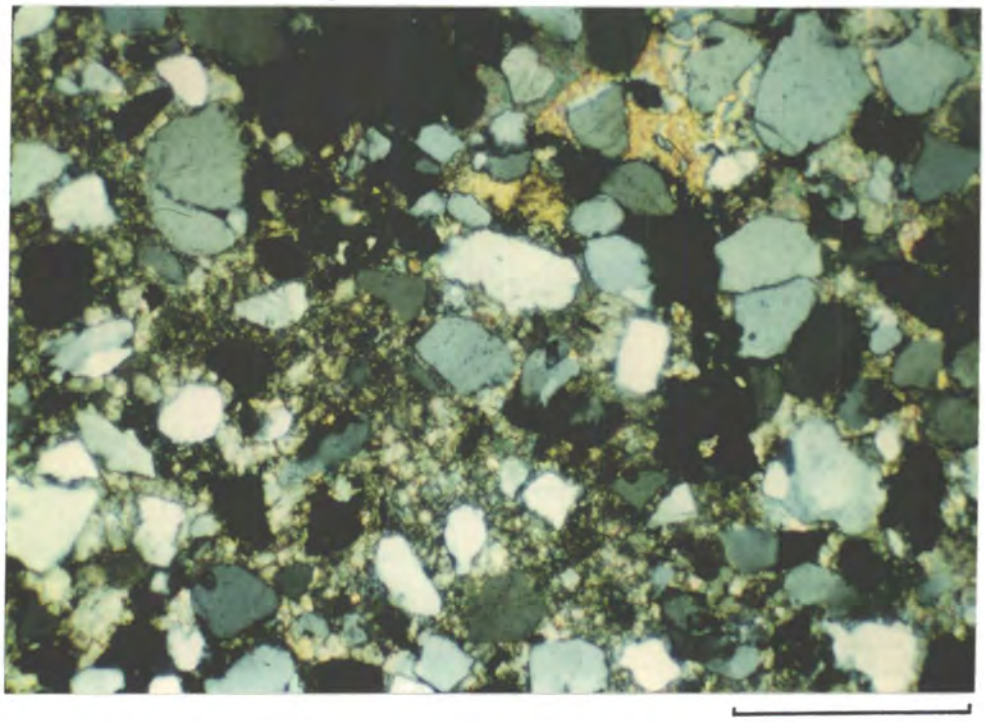

FIG. 7.46 Aggressive and displacive finely crystalline calcite cement in a specimen from Ferryhill railway cutting. Crossed polars. Scale bar = 500μ.

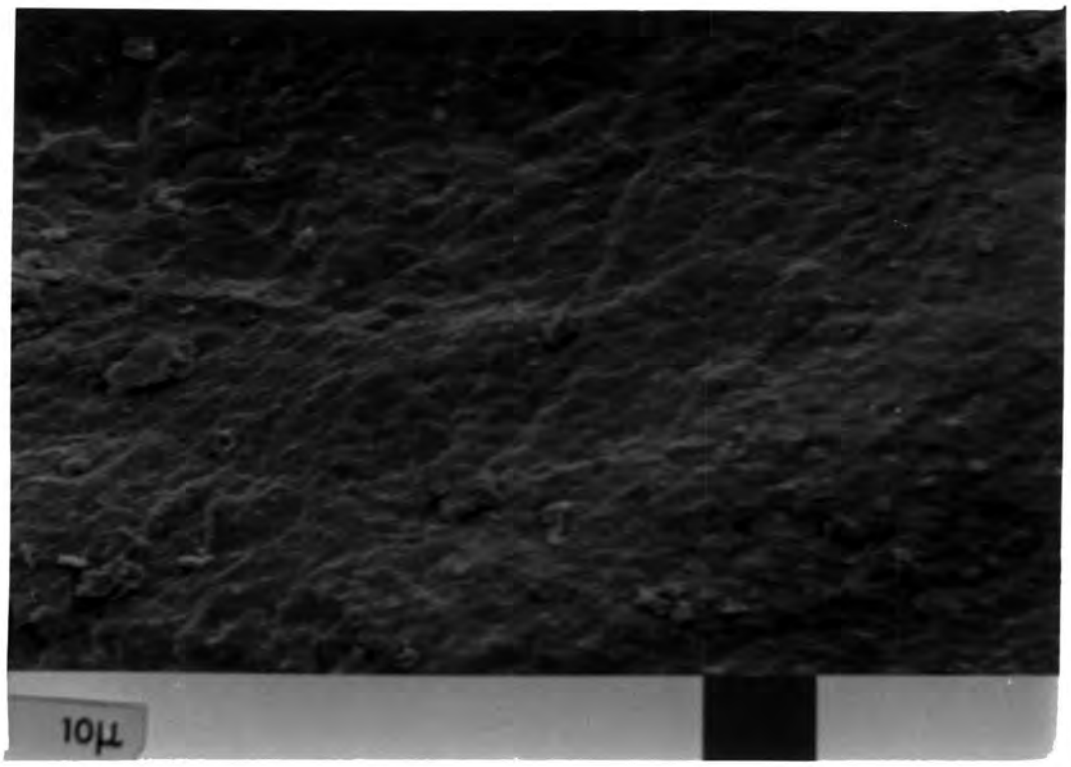

FIG. 7.47 Upturned or cleavage plates, a texture thought to be indicative of aeolian abrasion, on a grain from Sherburn Hill Sand Pit.

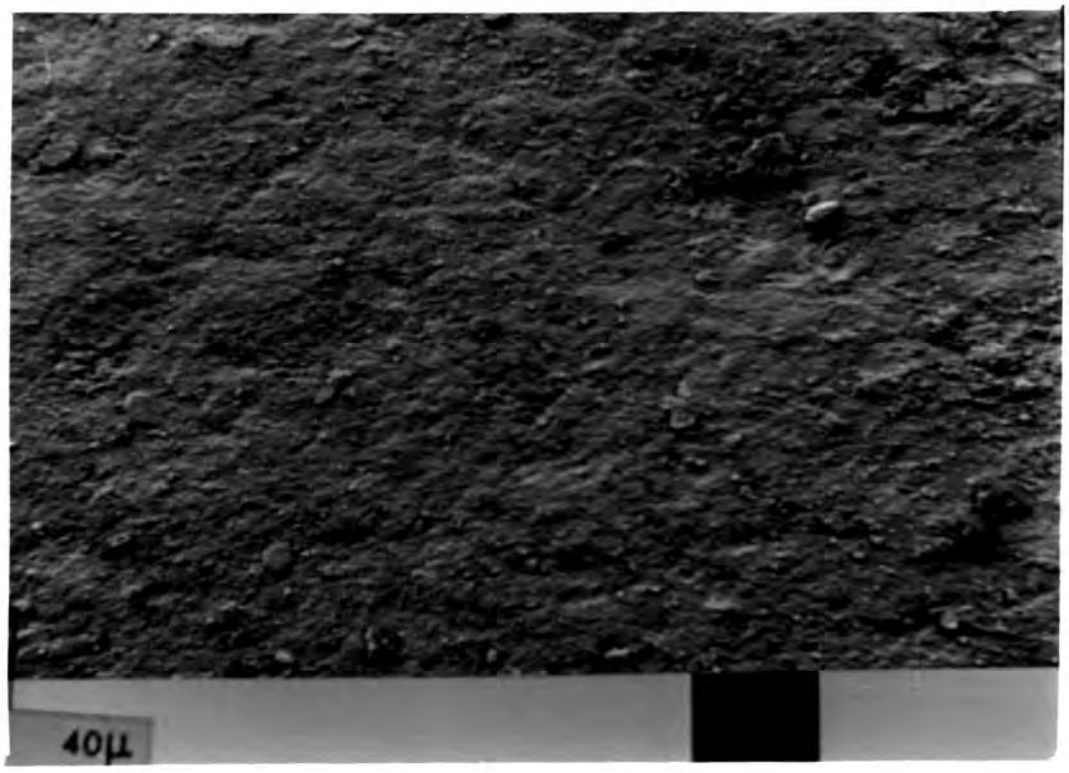

FIG. 7.48 A typical view of a grain surface on an untreated Yellow Sand specimen. Nondescript, hummocky surface with a liberal sprinkling of dust particles of unknown composition. Yellow sand, Sherburn Hill.

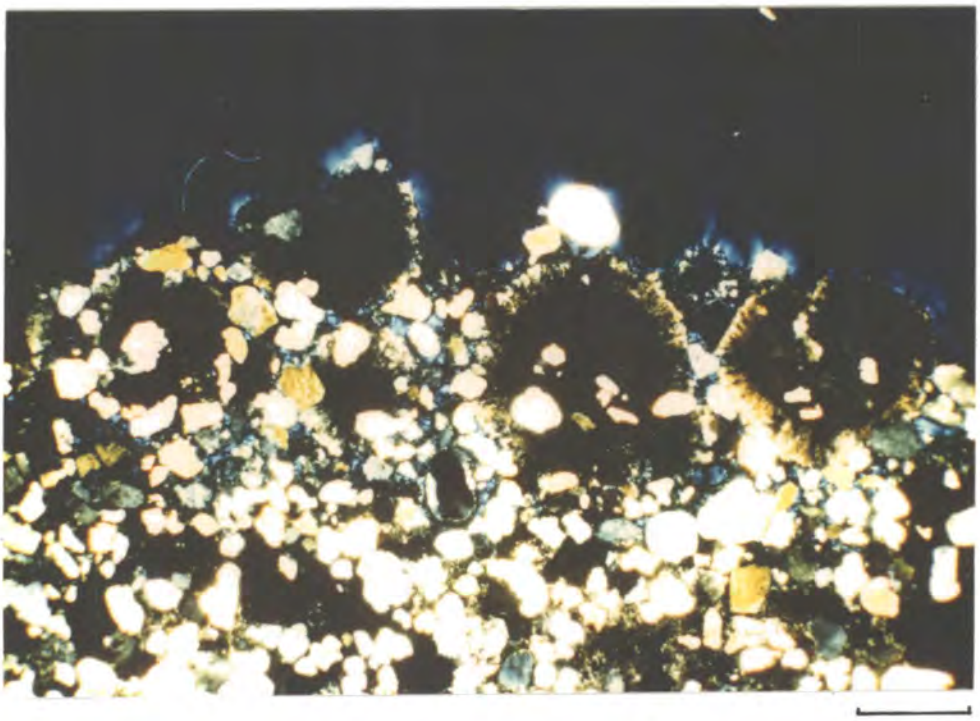

FIG. 7.49 Spherules of barytes on top surface of the Yellow Sands at Sherburn Hill Sand Pit. Spherules appear to be displacive towards the clastic grains, and occur only on the top surface. Remainder of rock is highly dolomitic. Crossed polars. Scale bar = 1000μ.

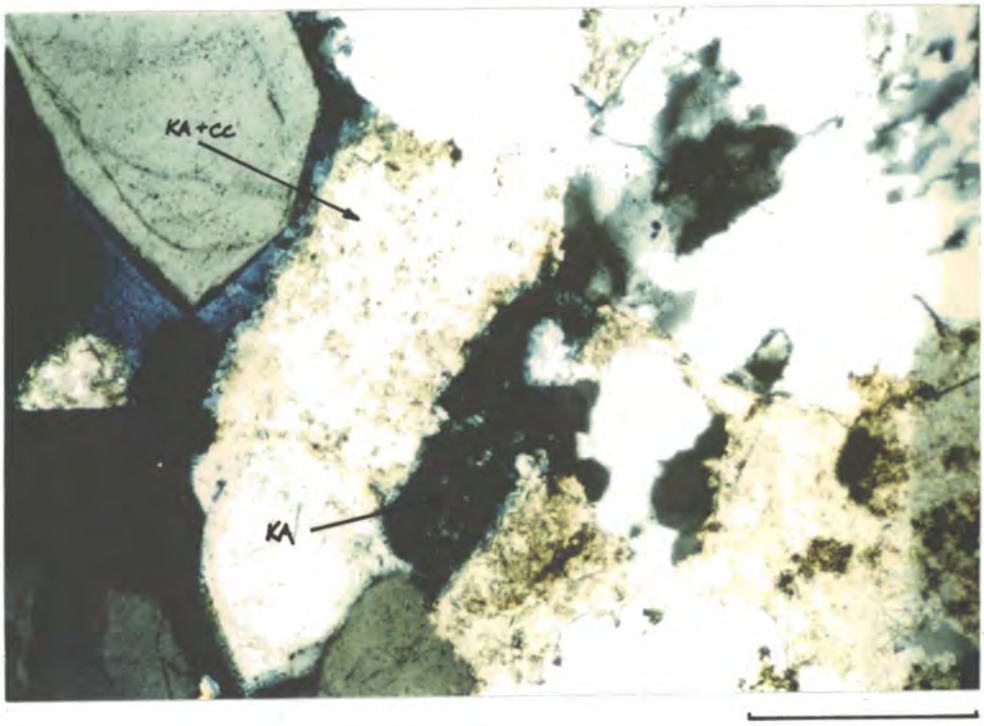

FIG. 7.50 Kaolinite, calcite and quartz overgrowths, 120,02 (Encl. 2), Ferryhill railway cutting. The kaolinite may have originally been pore filling and does not appear to be associated with a feldspar grain. Part of it is porous and impregnated with resin, part has been infused by the later calcite (arrowed). Apologies for the print - it's an appalling reproduction. Crossed polars. Scale bar = 50μ.

CHAPTER EIGHT

THE BRIDGNORTH SANDSTONE

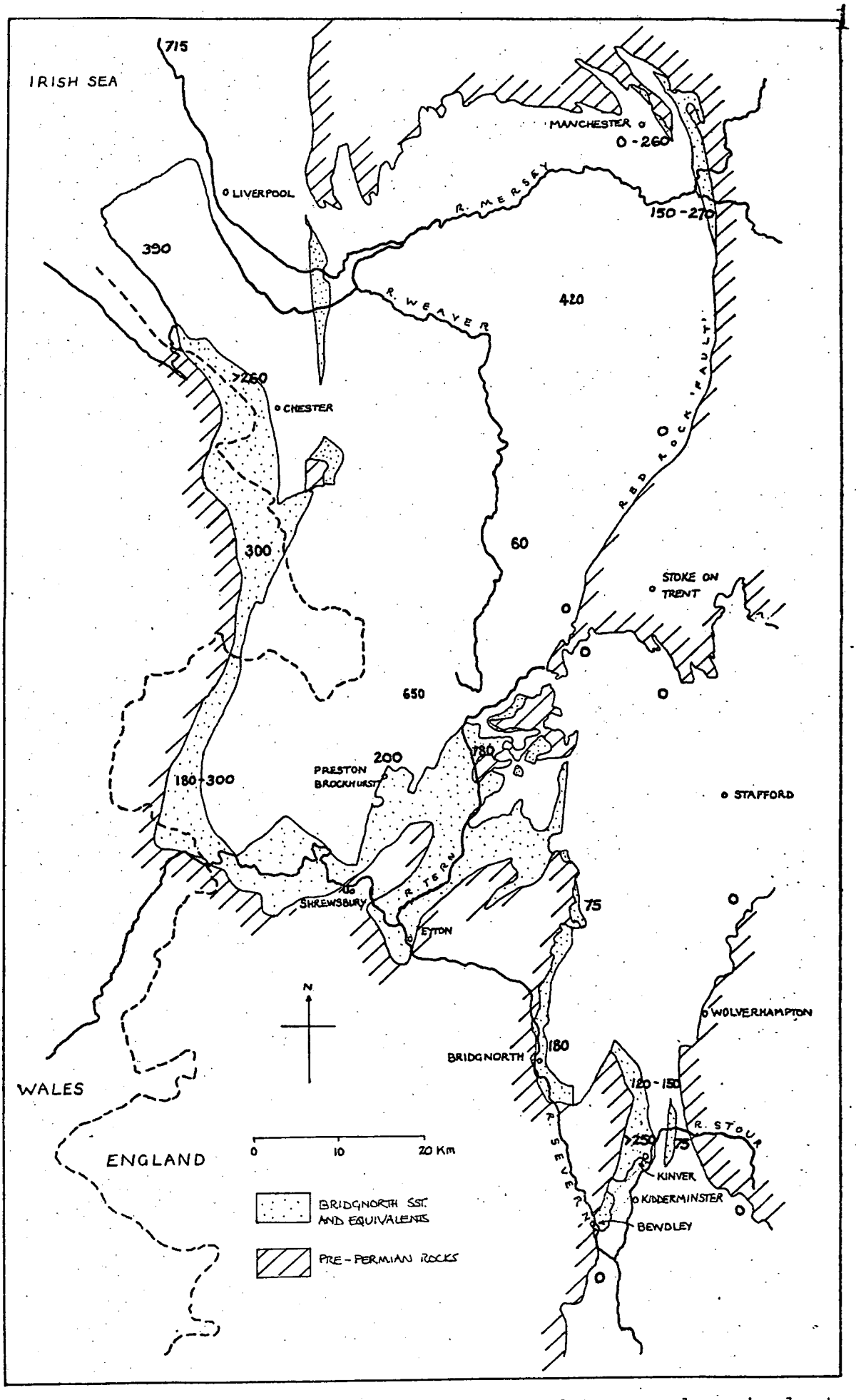

FIG.8.1 Outcrop of the Bridgnorth Sandstone and equivalents with thicknesses in metres marked where information is available.

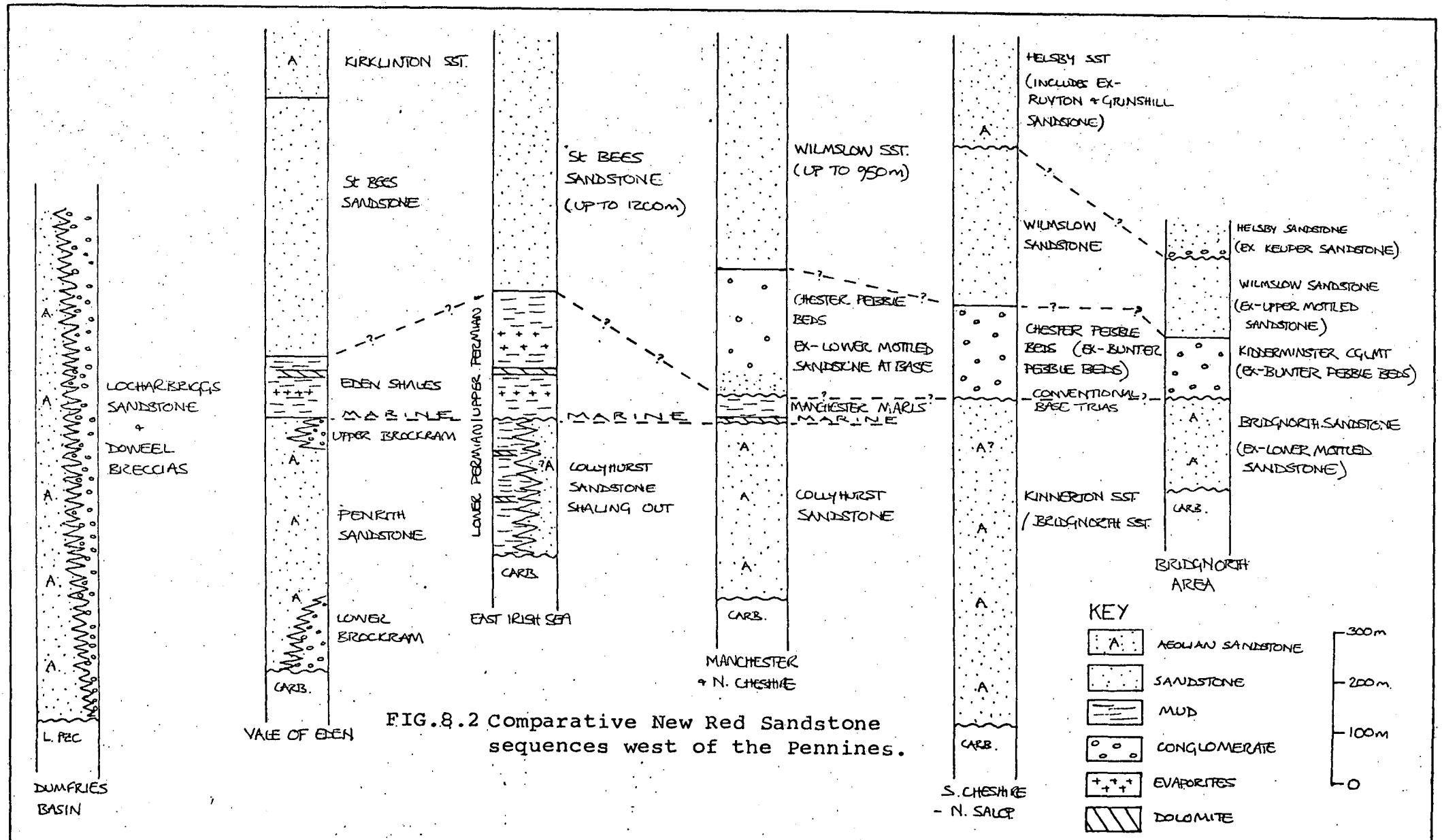

FIG.8.2 Comparative New Red Sandstone sequences west of the Pennines.

FIG. 8.3 Blackstone Rock (SO 793740). The main face of the crag is 25m high. It is entirely made up of sandflows : note their parallellism, thickness and continuity.

FIG. 8.4 Backfilled burrow in Preston Brockhurst road cut (Encl. 14), 0.32m long and 15-20mm wide in sand-sheet deposits. The top of the burrow is level with the top of the tape, and lies at a bounding surface. It may therefore be partially eroded. 0.4m of tape visible.

FIG. 8.5 Other possible burrows (arrowed) in Preston Brockhurst road cut (Encl. 14). These are preferentially cemented and show no back-fill, unlike that in FIG. 8.4. Photograph covers a 2.5m height of face.

HUE		CHROMA /4	CHROMA /6
10R	3	-	2
2.5YR	5	2	8
	4	5	13
	3	-	5
5YR	5	2	1
	4	1	6
10YR	7	1	-

VALUE

TABLE 8.1 Bridgnorth Sandstone Munsell colour determinations.
(n = 46)

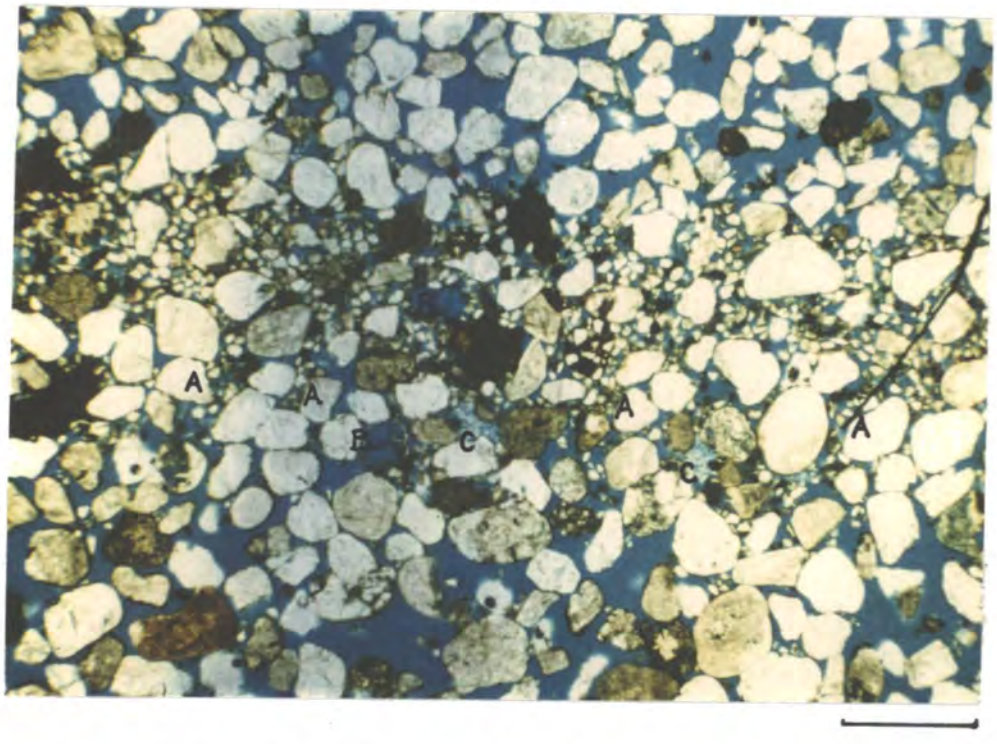

FIG. 8.6 Photomicrograph of the Bridgnorth Sandstone from Wordsley (SO 895871). Way up shown by fine grains in the basal lamina of a sandflow falling through the pores between the coarser grains below (A). Note also secondary porosity (B), and authigenic kaolinite (C). Scale bar = 1000μ.

FIG.8.7a

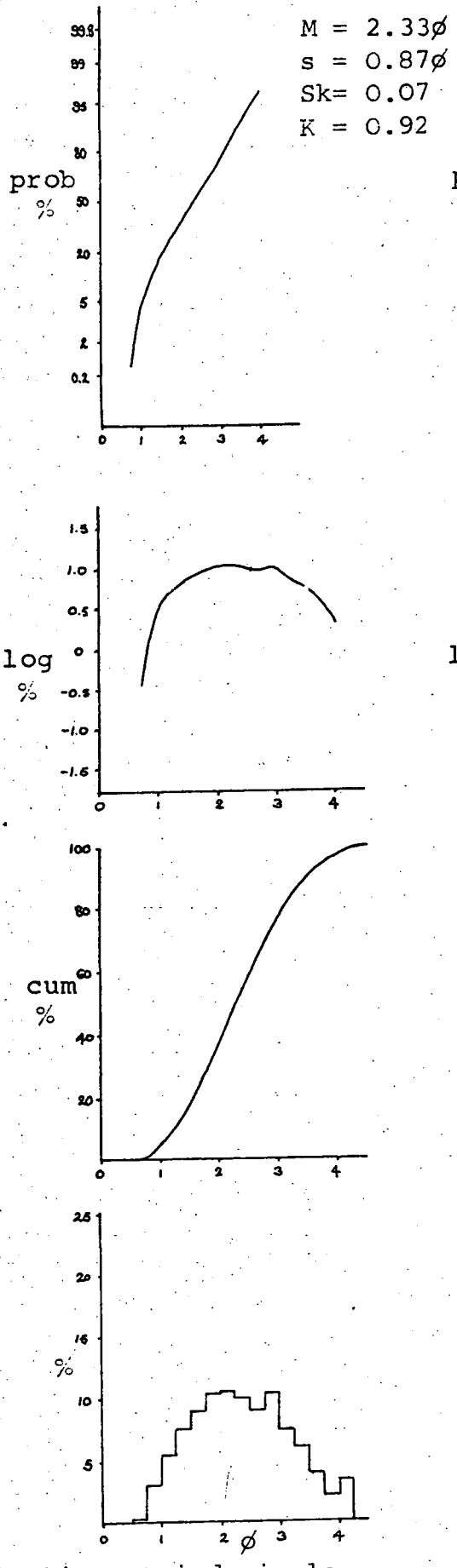

Lamination: wind-ripple

Locality: SO 884859

FIG.8.7b

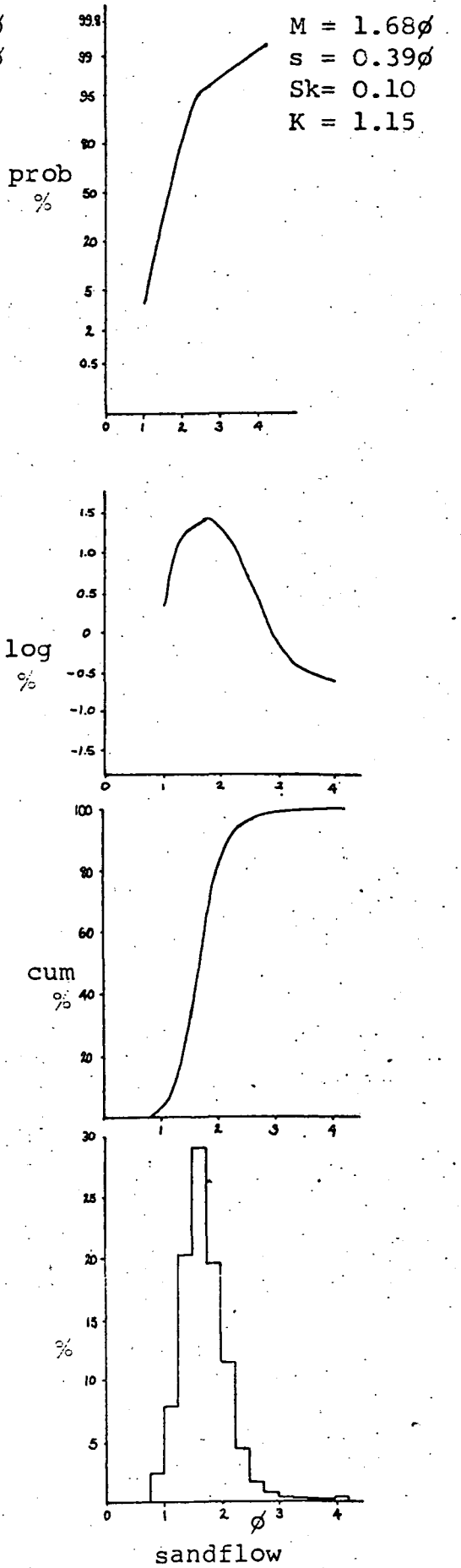

sandflow

Blackstone Rock
(SO 793741)

FIG.8.8a

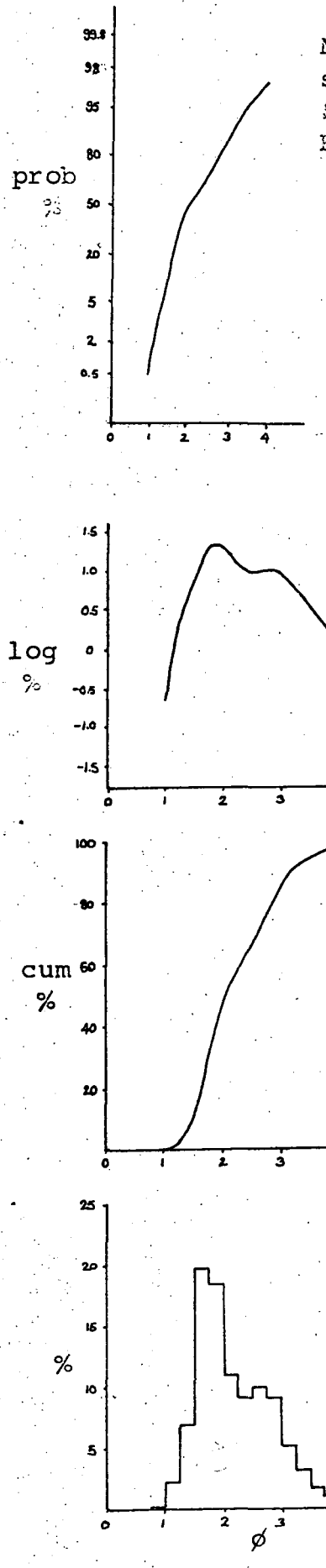

FIG.8.8b

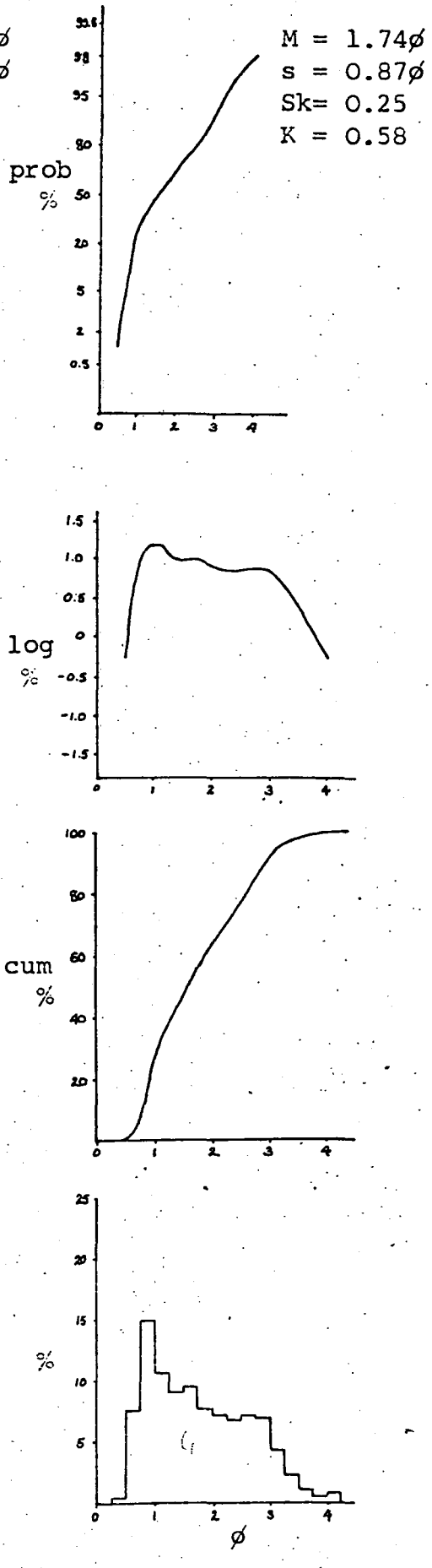

Lamination: wind-ripple

Locality: SO 819806

wind-ripple

Quatford A442 N. cut (SO 738907)

FIG. 8.9a

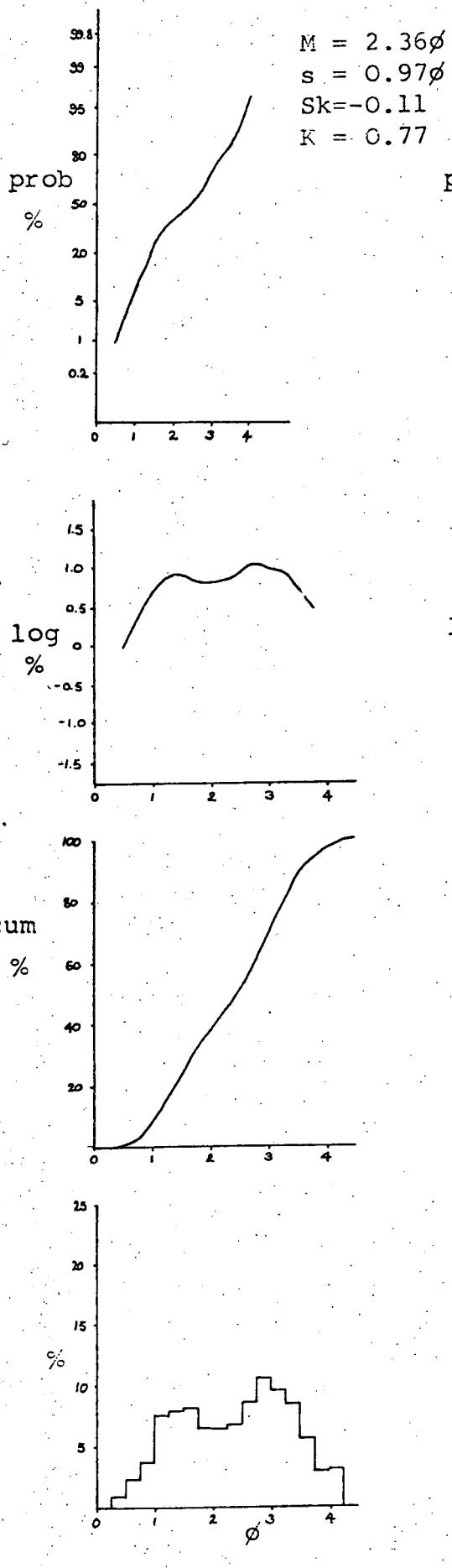

FIG.8.9b

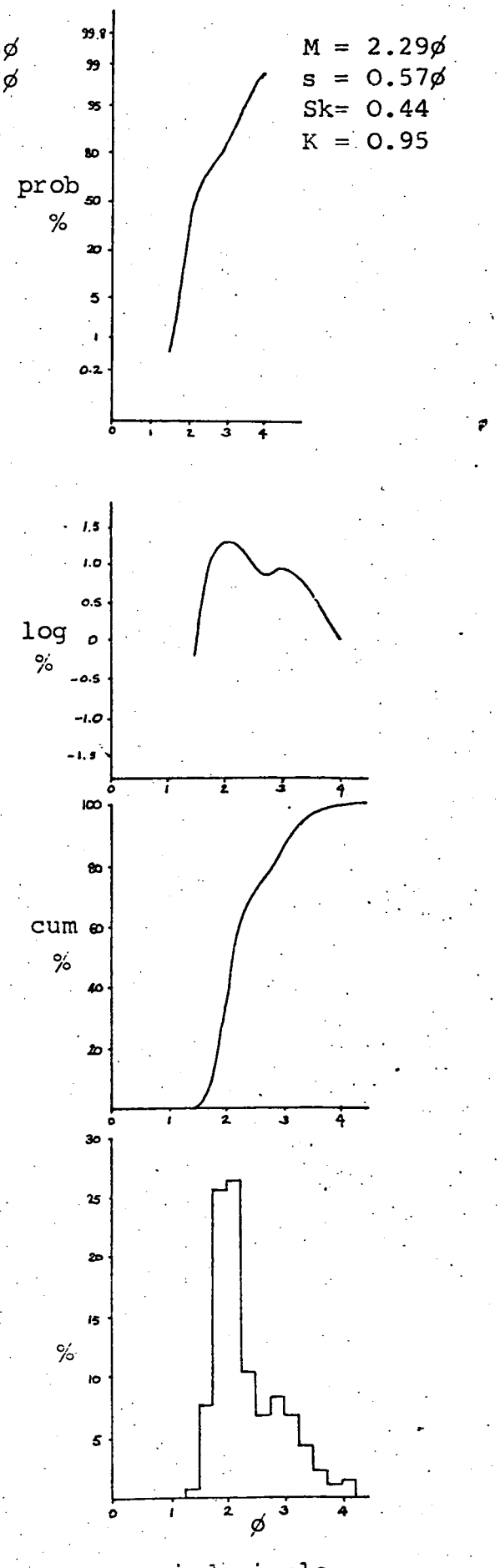

Lamination: sand-sheet

Locality: Preston Brockhurst (SJ 541253)

wind-ripple

Quatford A442 S. Cut (SO 739902)

FIG.8.10a

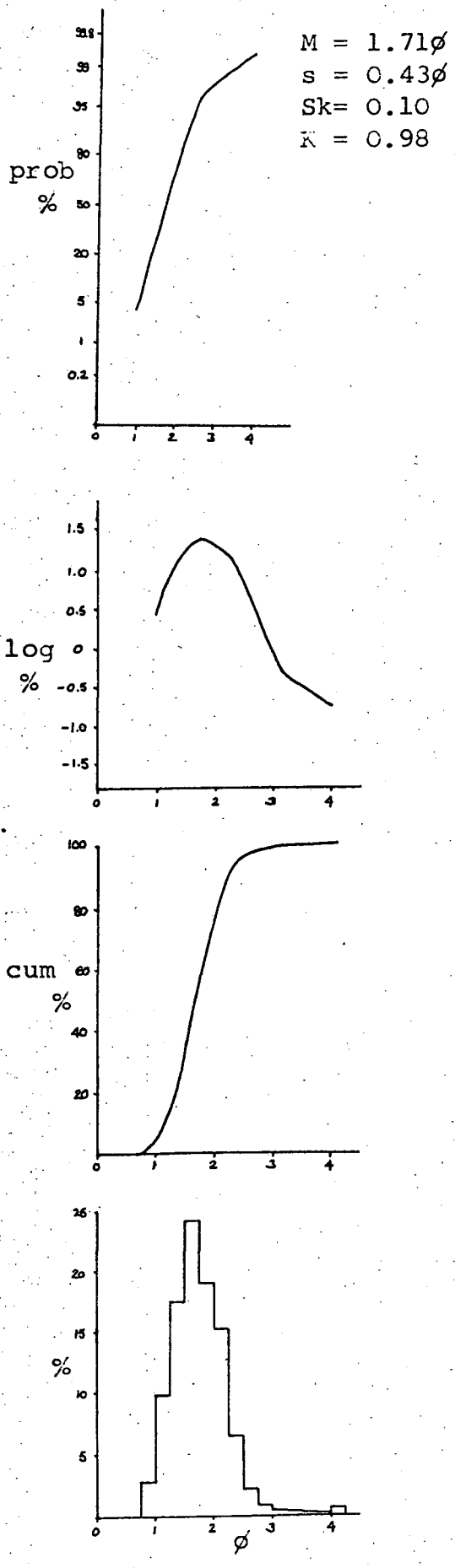

FIG.8.10b

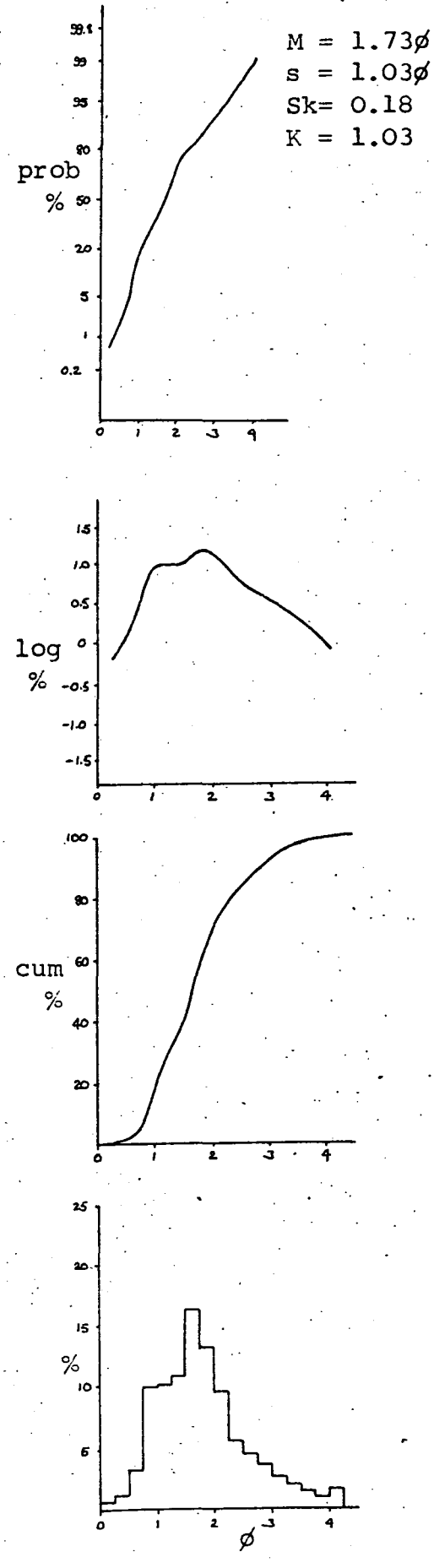

Lamination: sandflow

Locality: SO 850841

sandflow (1 lamina)

SO 895871

FIG.8.11a

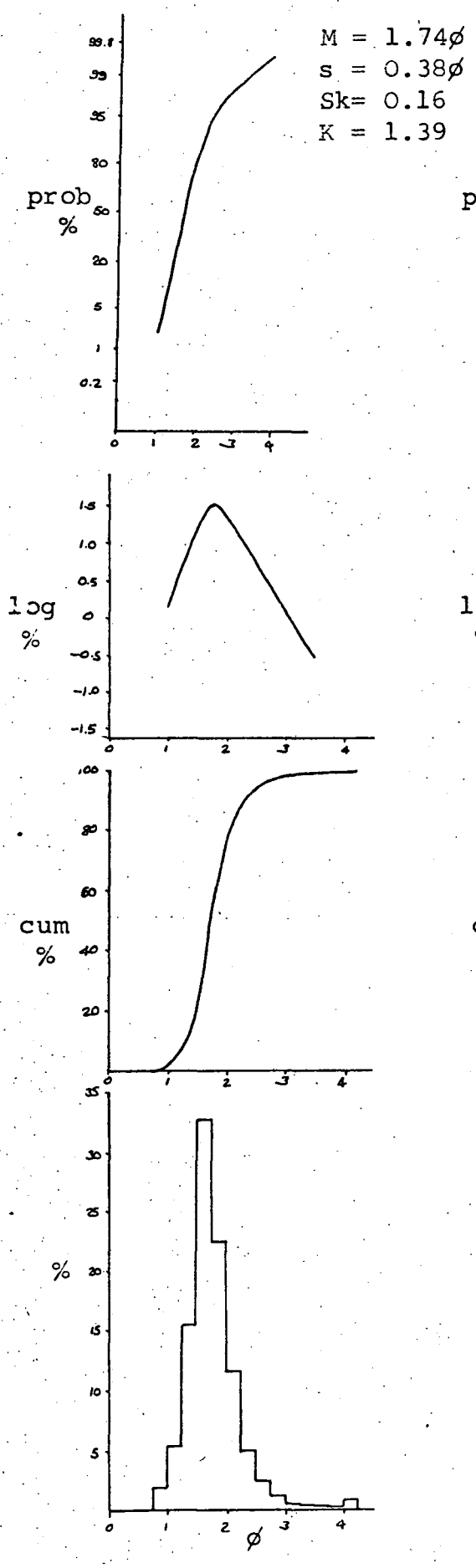

Lamination: sandflow

Locality: SO823837

FIG.8.11b

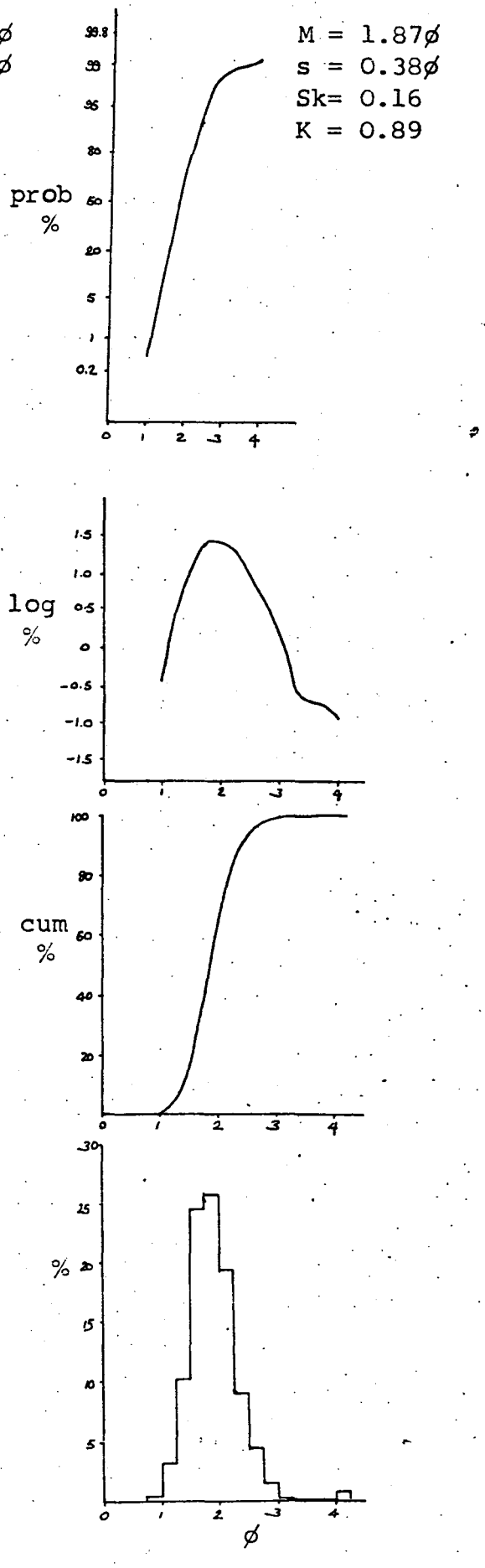

?sandflow

Queen's Parlour, Bridgnorth
(SO 728933)

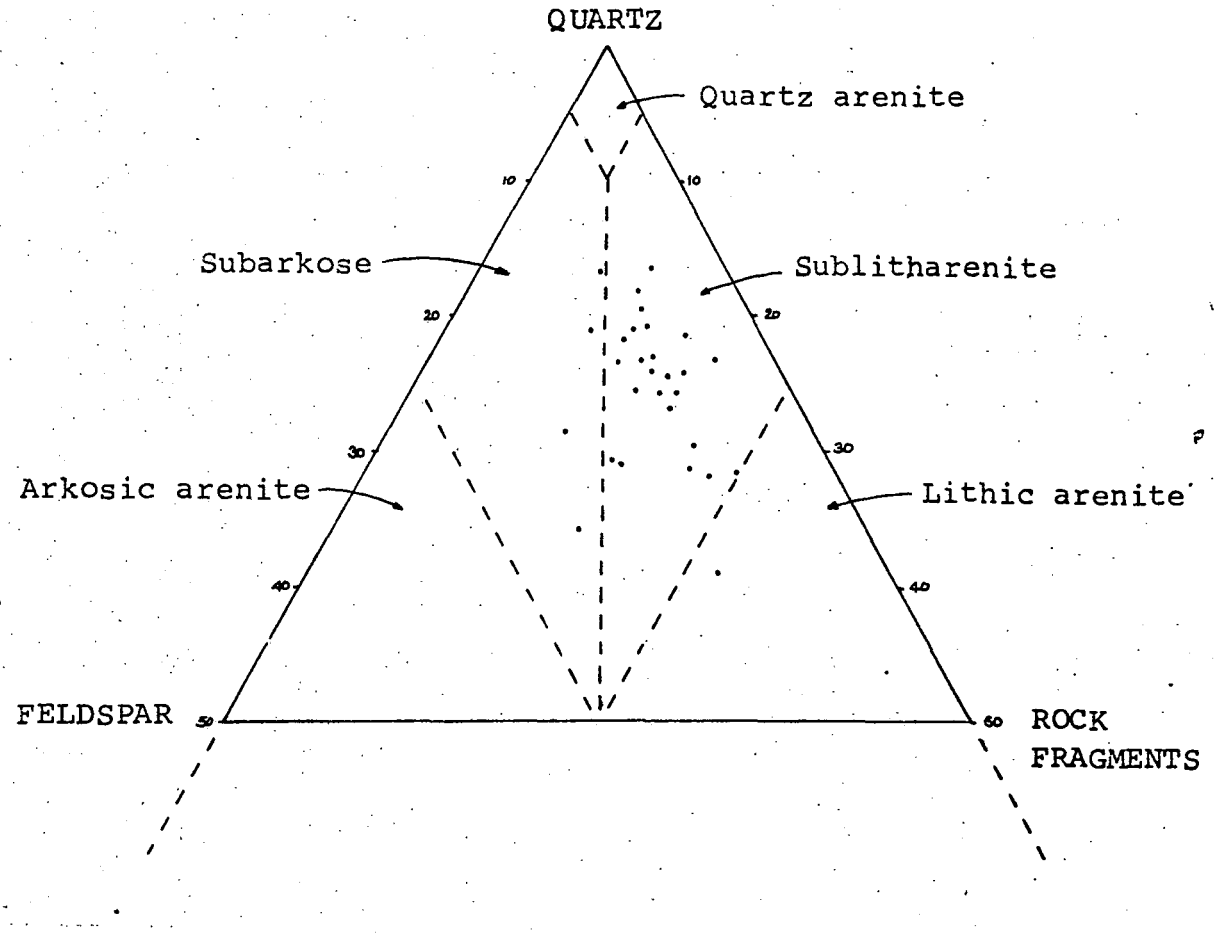

FIG.8.12 Petrographic classification of the Bridgnorth Sandstone. Scheme of Pettijohn (1975, p.211).

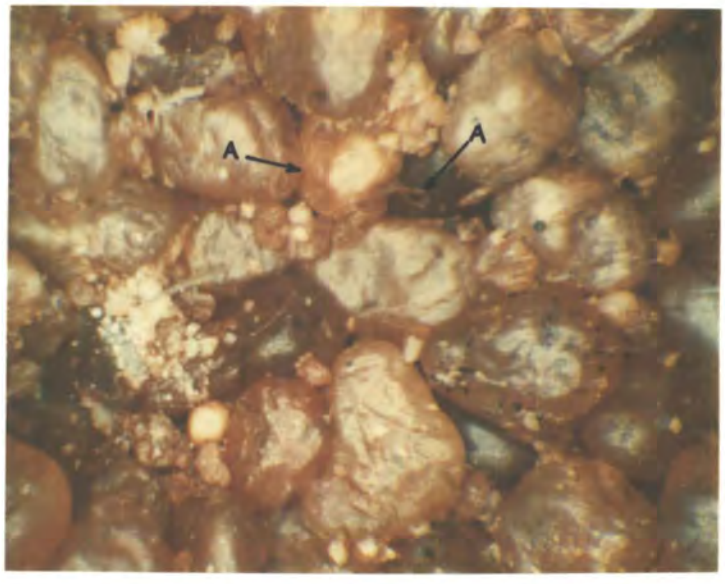

FIG. 8.13 Microscope view of a hand specimen of Bridgnorth Sandstone from Wordsley (SO 895871). Shows rounded and frosted grains, the pervasive red stain and collars of pigment around contacts (A), (?meniscus). Field of view is 3mm wide.

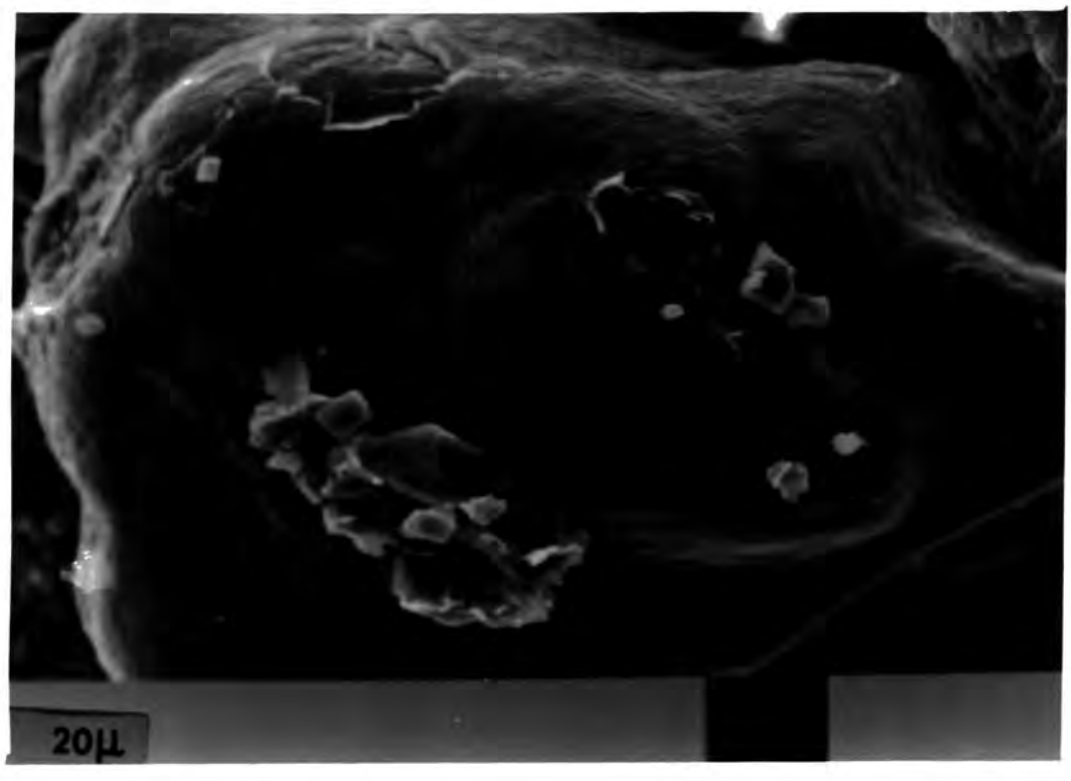

FIG. 8.14 Bridgnorth Sandstone grain showing a suggestion of upturned or cleavage plates over its entire surface. Queen's Parlour, Bridgnorth (Encl. 10).

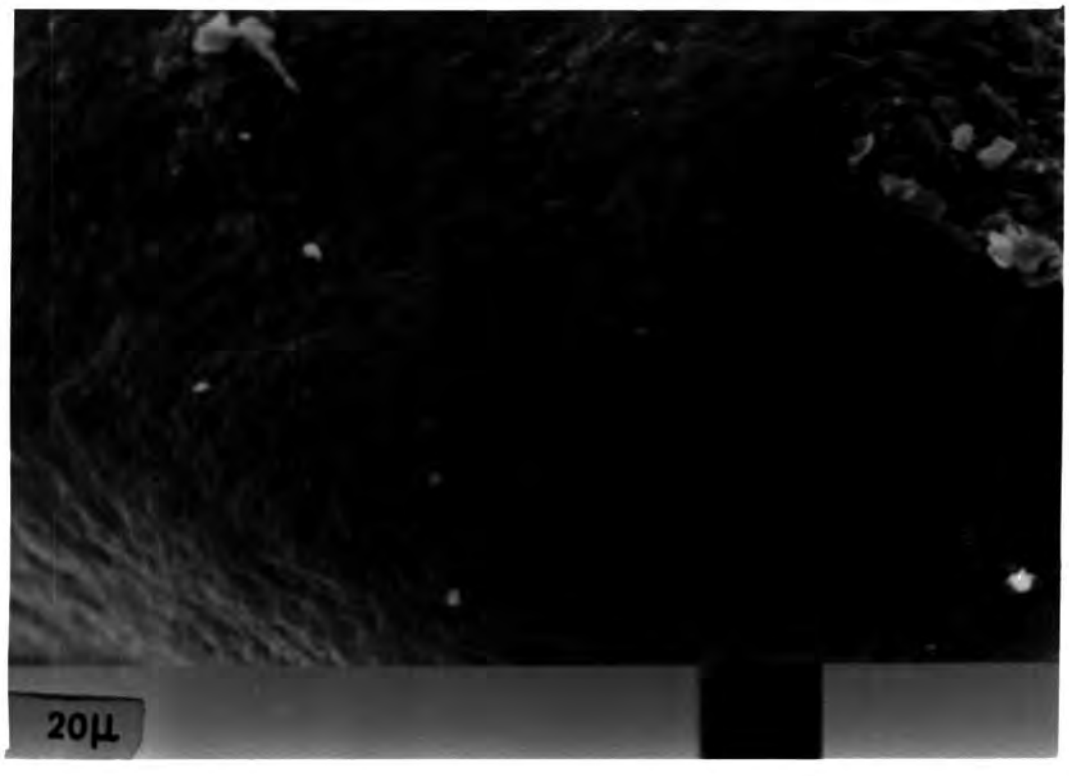

FIG. 8.15 Typical Bridgnorth Sandstone grain surface texture, possibly upturned or cleavage plates. Queen's Parlour, Bridgnorth (Encl. 10).

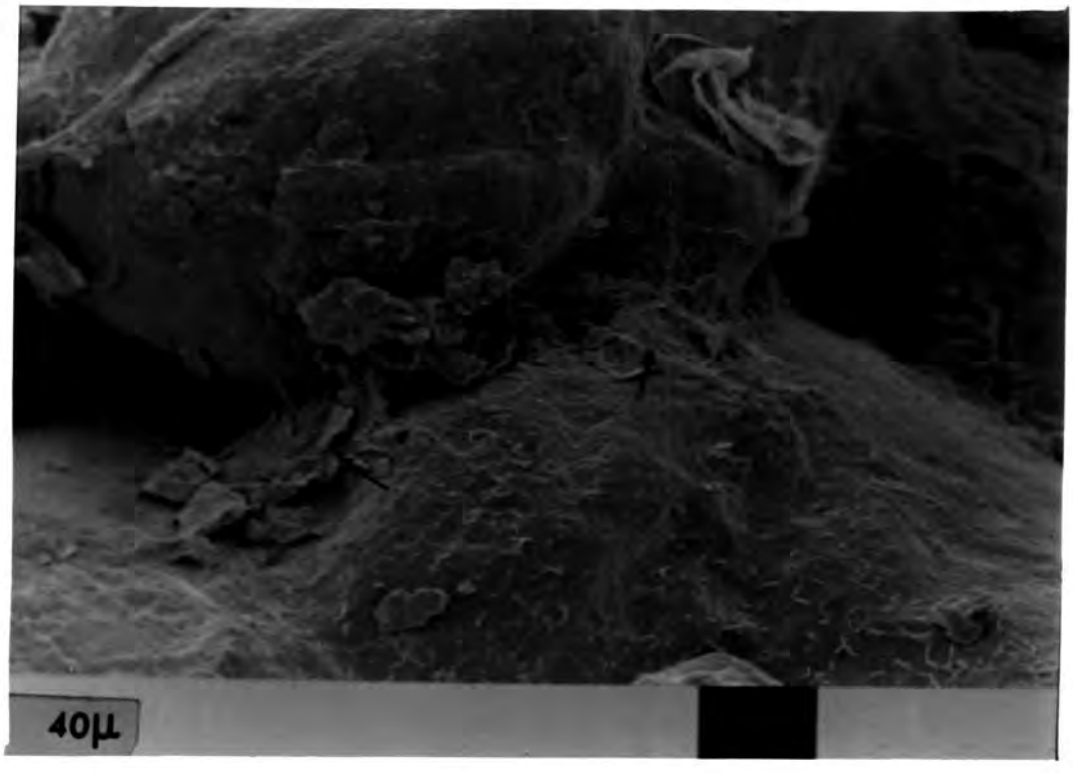

FIG. 8.16 Classic infiltrated meniscus bridging clays (arrowed). Note the ragged, anhedral nature of the material making up the meniscus. The grains also carry a small amount of authigenic boxwork illite. Bridgnorth Sandstone, A442 south cut, Quatford, (Encl. 12).

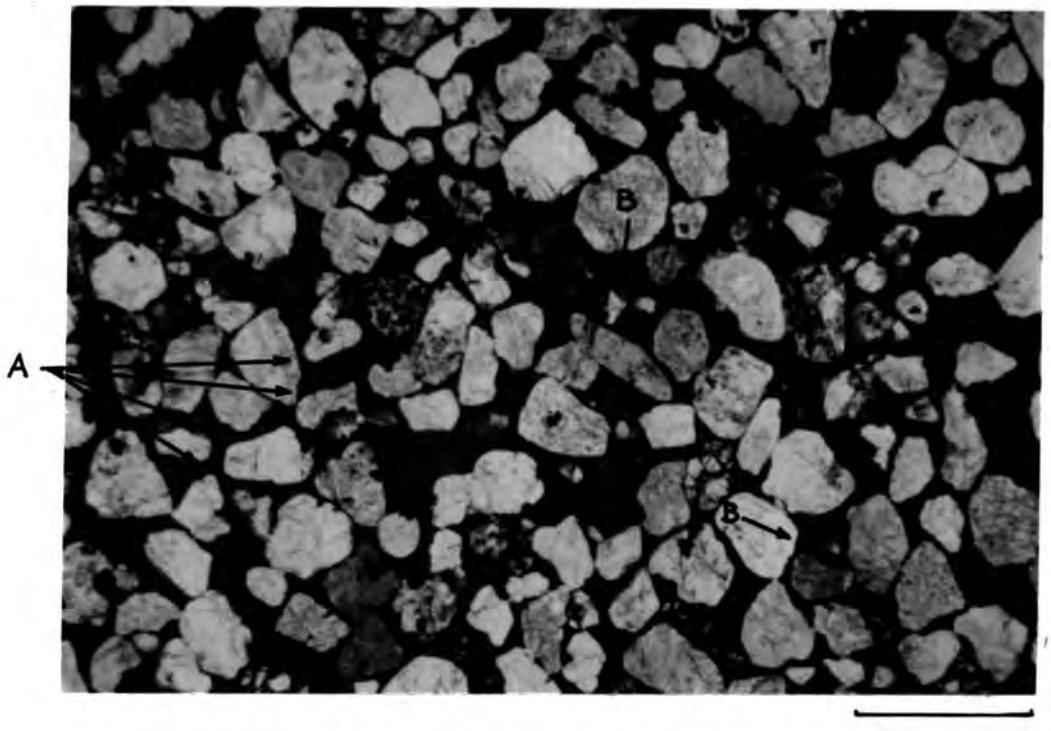

FIG. 8.17 Meniscus bridging clays in thin section, specimen from Eyton (SJ 569060). Menisci (A) and other thick accumulations of pigment (B) arrowed. Scale bar = 1000μ.

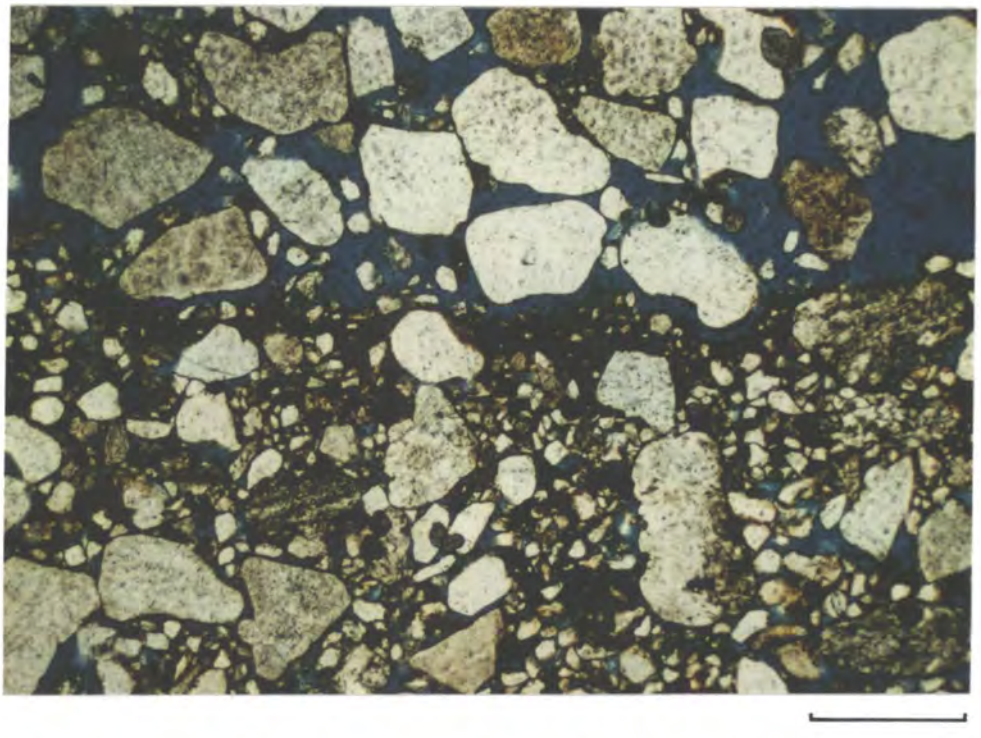

FIG. 8.18 Pigment draping a relatively impermeable fine-grained lamina in wind-ripple laminated sand, thus indicating the way up of the specimen. Bridgnorth Sandstone, near Adeney (SJ 695178). Scale bar = 500μ.

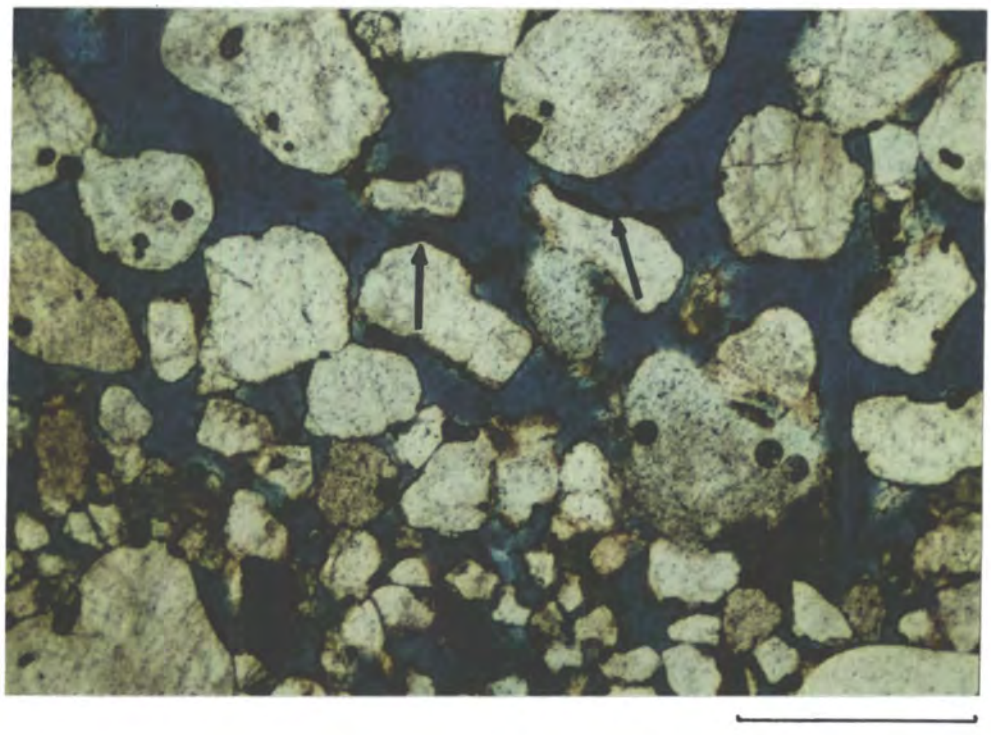

FIG. 8.19 Geopetally arranged pigment (arrowed) concentrated just above the basal lamina of a sandflow. Bridgnorth Sandstone, Holy Austin Rock (Encl. 14). Scale bar = 500μ.

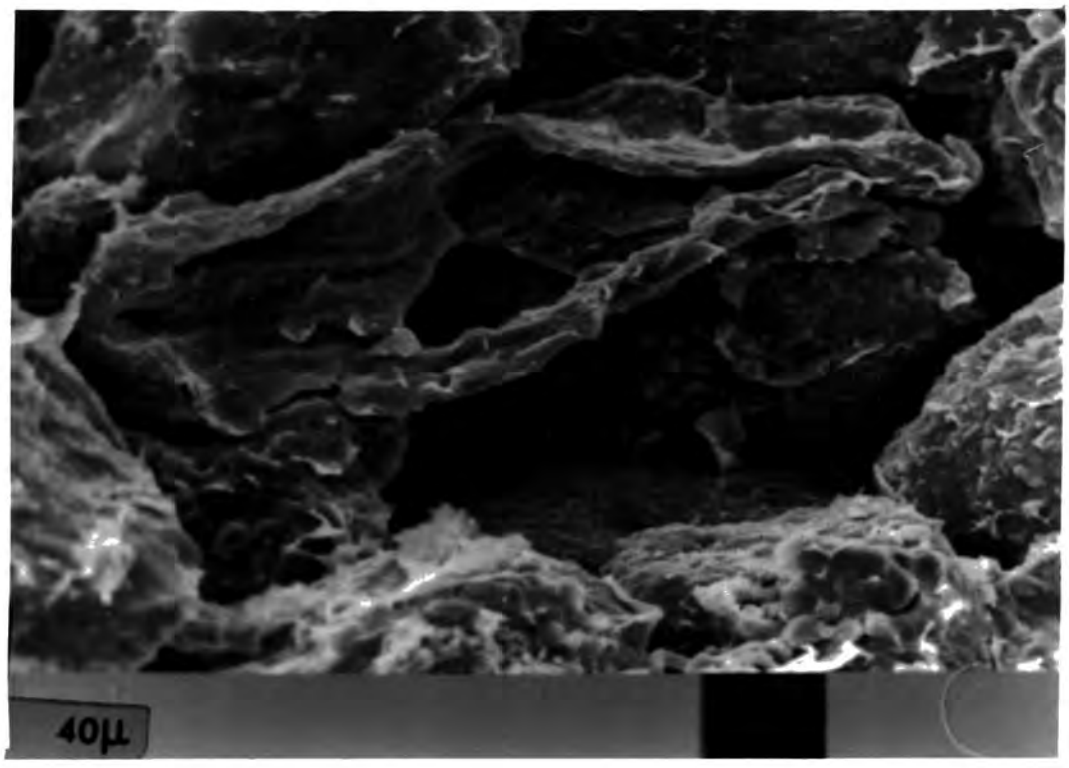

FIG. 8.20 Collapsed pellicle, presumably from a dissolved feldspar or rock fragment. Boxwork illite also visible. Bridgnorth Sandstone, A442, Dudmaston (Encl. 13).

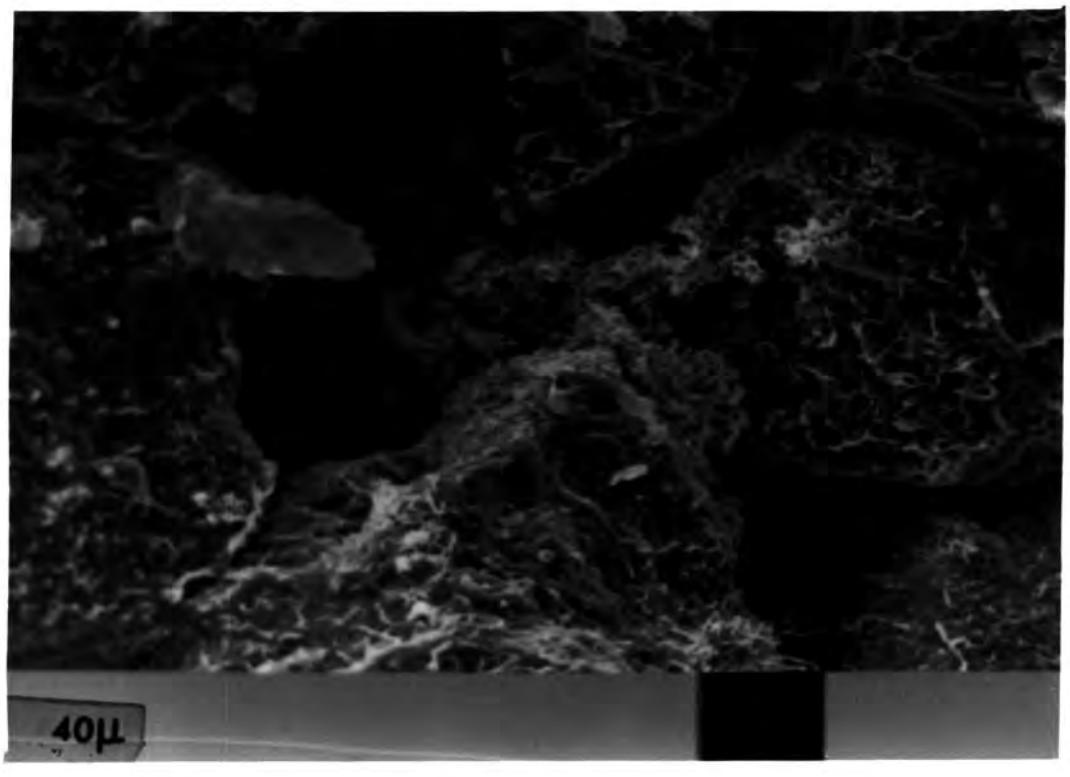

FIG. 8.21 Well developed boxwork illite, branching into a fibrous habit and blocking a pore throat. Bridgnorth Sandstone, A442, Dudmaston.

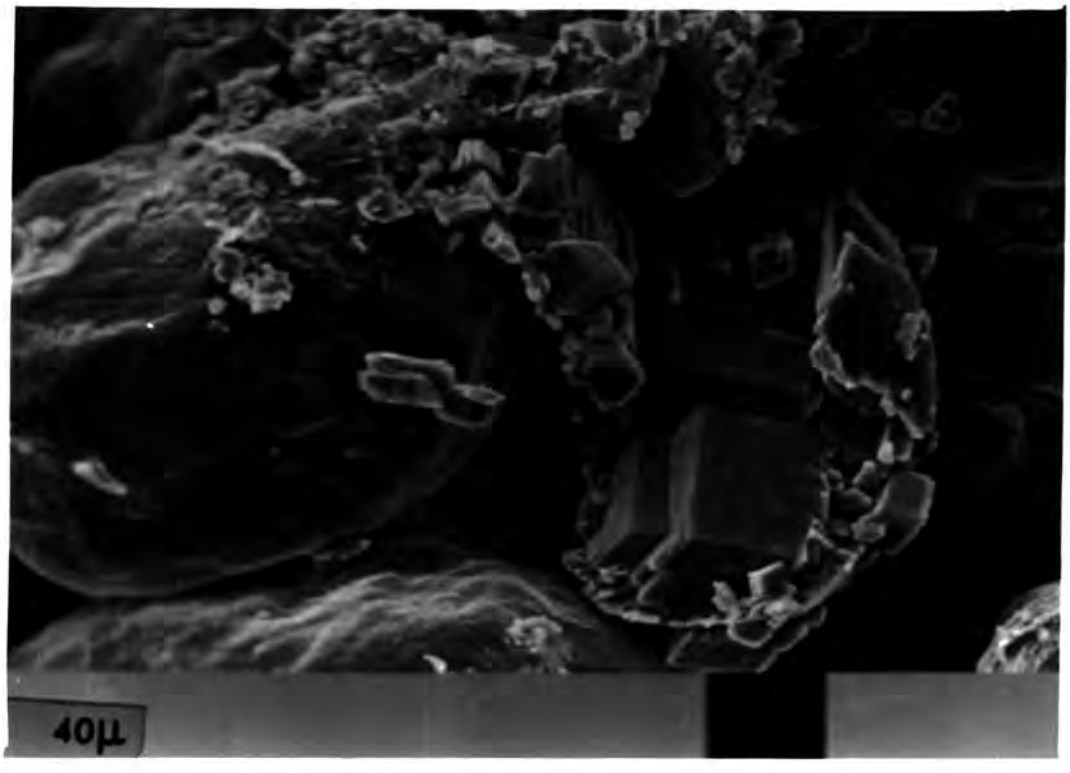

FIG. 8.22 Authigenic feldspar formed on a previously partially dissolved feldspar grain. Small feldspar crystals are also visible on quartz surfaces, apparently independent of any seed crystal. Bridgnorth Sandstone, Queen's Parlour, Bridgnorth (Encl. 10).

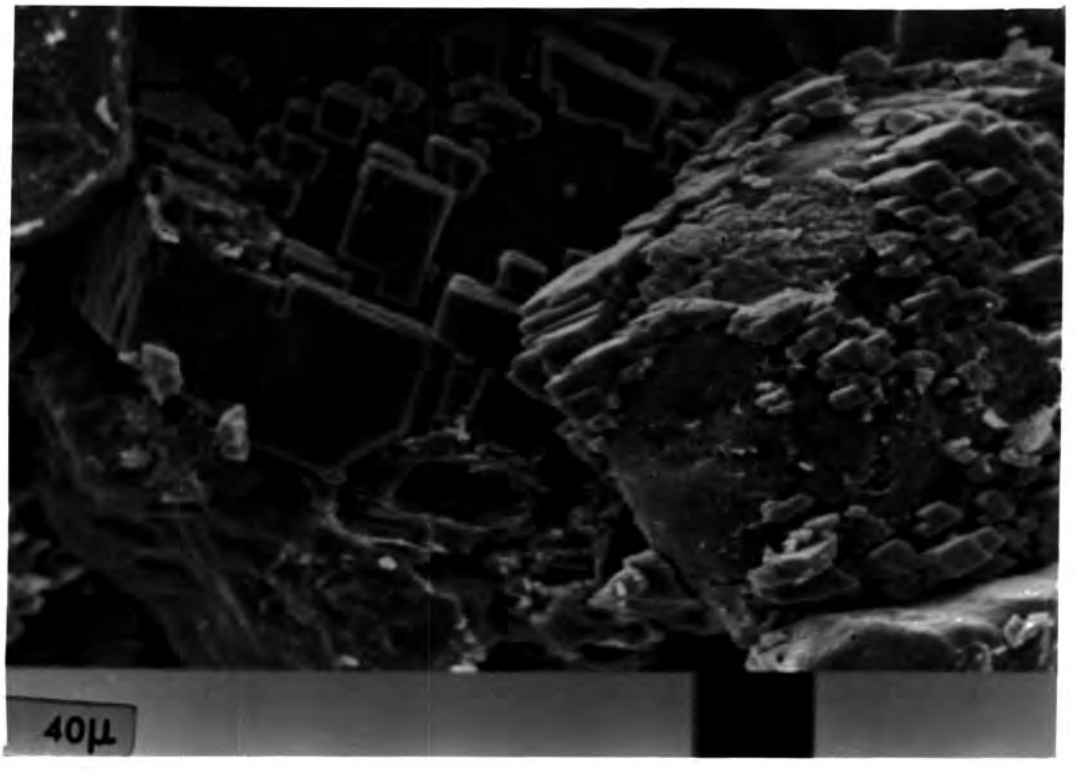

FIG. 8.23 Well developed feldspar overgrowths on apparently fresh grains. Bridgnorth Sandstone, Queen's Parlour, Bridgnorth (Encl. 10).

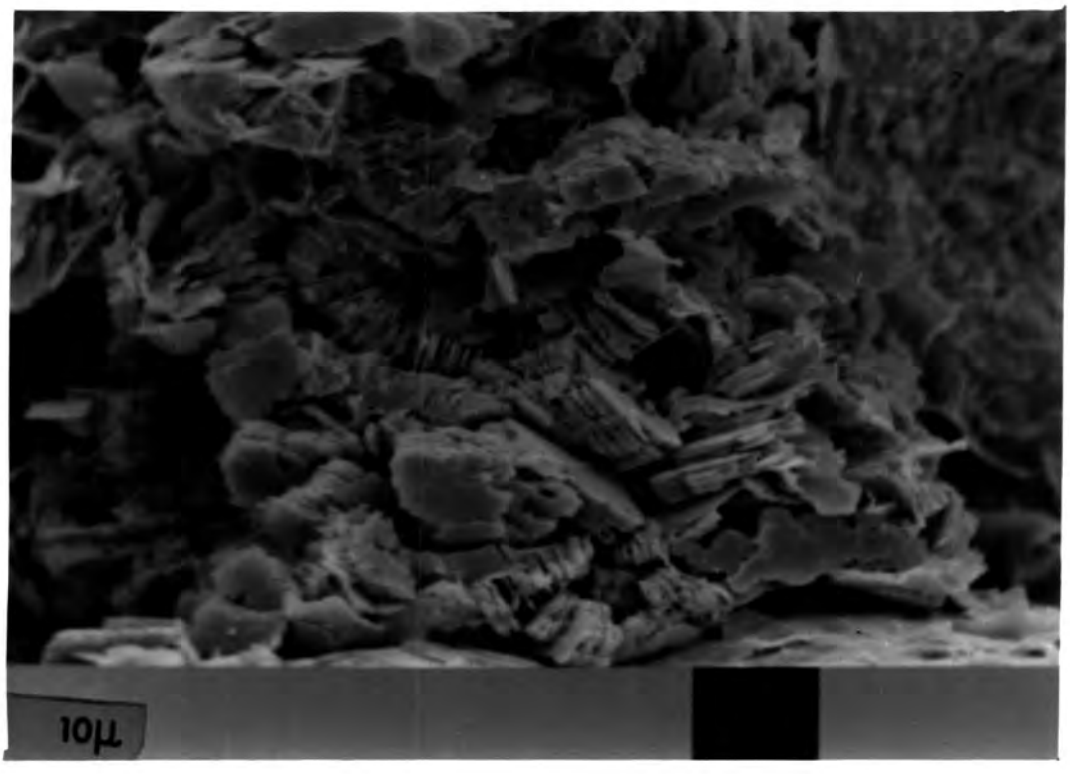

FIG. 8.24 Slightly ragged authigenic pore-filling kaolinite. Bridgnorth Sandstone, A442 south cut, Quatford (Encl. 12).

CHAPTER NINE

THE PENRITH SANDSTONE

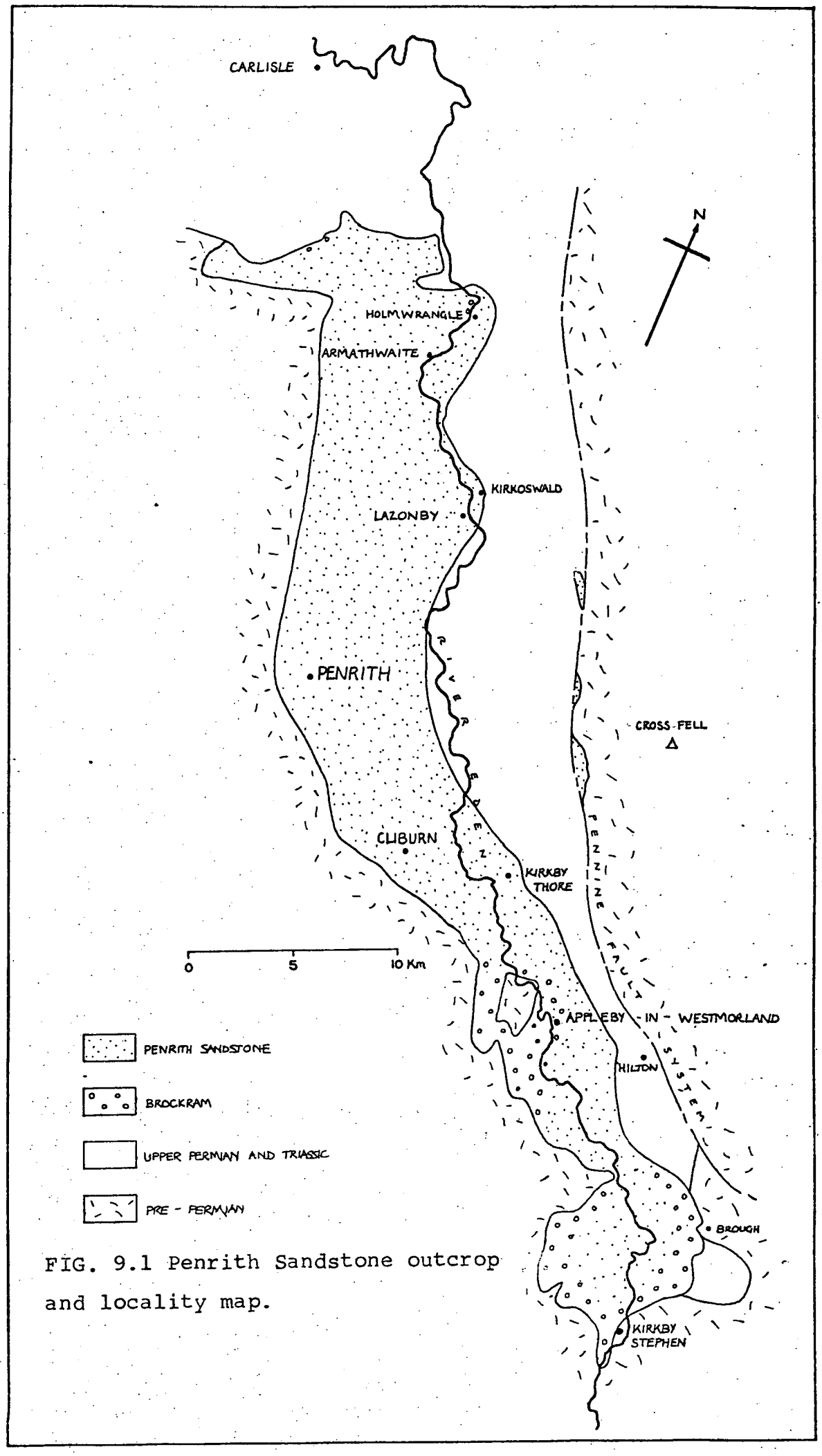

FIG. 9.1 Penrith Sandstone outcrop and locality map.

FIG. 9.2 Halfwaywell Quarry (NY 533352), the only active quarry in the Penrith Sandstone. The quarry is excavated in a single, well-cemented, trough-shaped set directed towards 310°.

FIG. 9.3 Cowraik Quarry (NY542310) near Penrith. The main face of silicified sandstone is ~10m high and here consists of a single set.

FIG. 9.4 One-sided parting lineation in wind-ripple laminae at Locharbriggs North Quarry (NX 990810). The similarity of form to wind ripples is striking (cf. FIG. 2.2) and it is possible that the stair-step fracturing mimics at least the orientation of the original ripples, if not their wavelength. Trowel is 0.29m long.

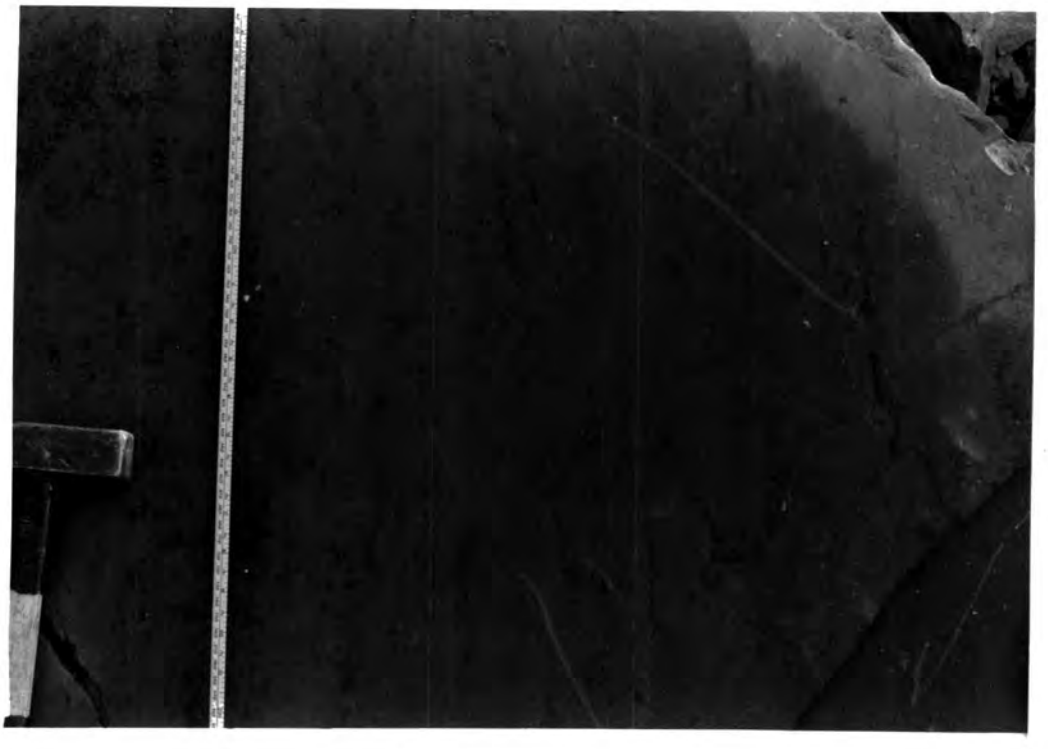

FIG. 9.5 Two-sided parting lineation, in wind-ripple laminae, on a loose block at Halfwaywell Quarry. The feature consists of a preferential orientation of step-like fractures across a single lamina.

HUE		CHROMA /4	/6	/8
10R	5	-	1	-
	4	-	3	-
	3	-	1	1
2.5YR	6	3	2	-
	5	3	9	-
	4	3	7	-
	3	-	6	-
5YR	7	-	1	-
	6	-	-	-
	5	4	7	-
	4	-	4	-
	3	1	1	-

VALUE

TABLE 9.1 Penrith Sandstone Munsell Soil Colour determinations, made on hand specimens in the laboratory. n = 57.

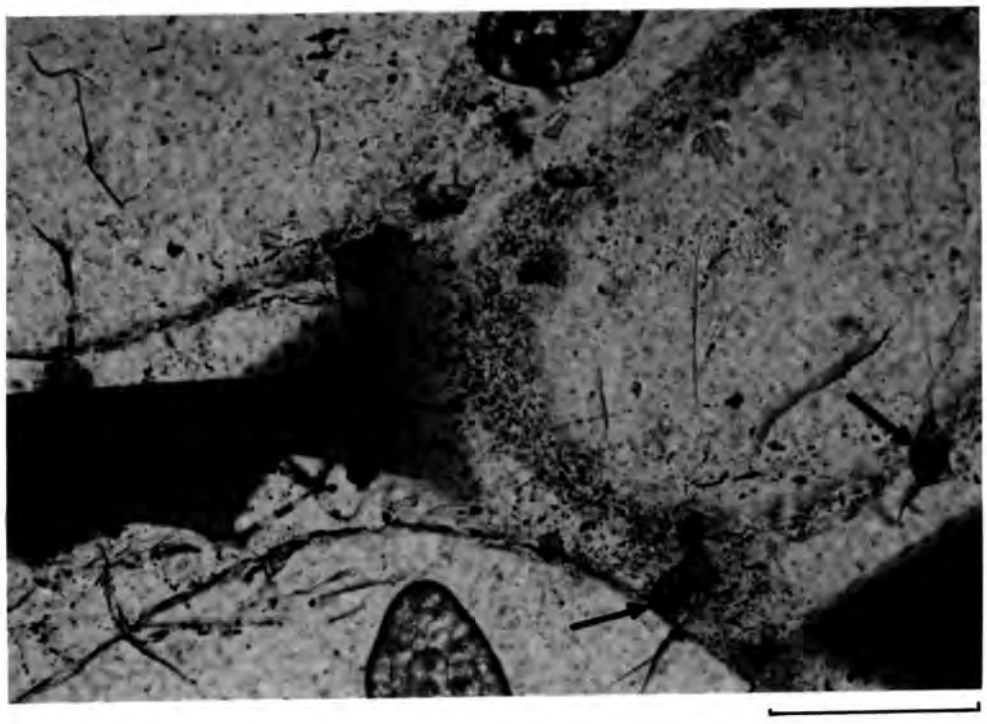

FIG. 9.6 View of part of a grain surface lying within the plane of the thin section. Shows the thin red stain which covers most grains and is common to other red aeolian sandstones in the U.K. No positive clues to its identity can be gained in thin section. Note also dolomoulds (arrowed) and quartz overgrowths. Penrith Sandstone, Bowscar Quarry. Scale bar = 100μ.

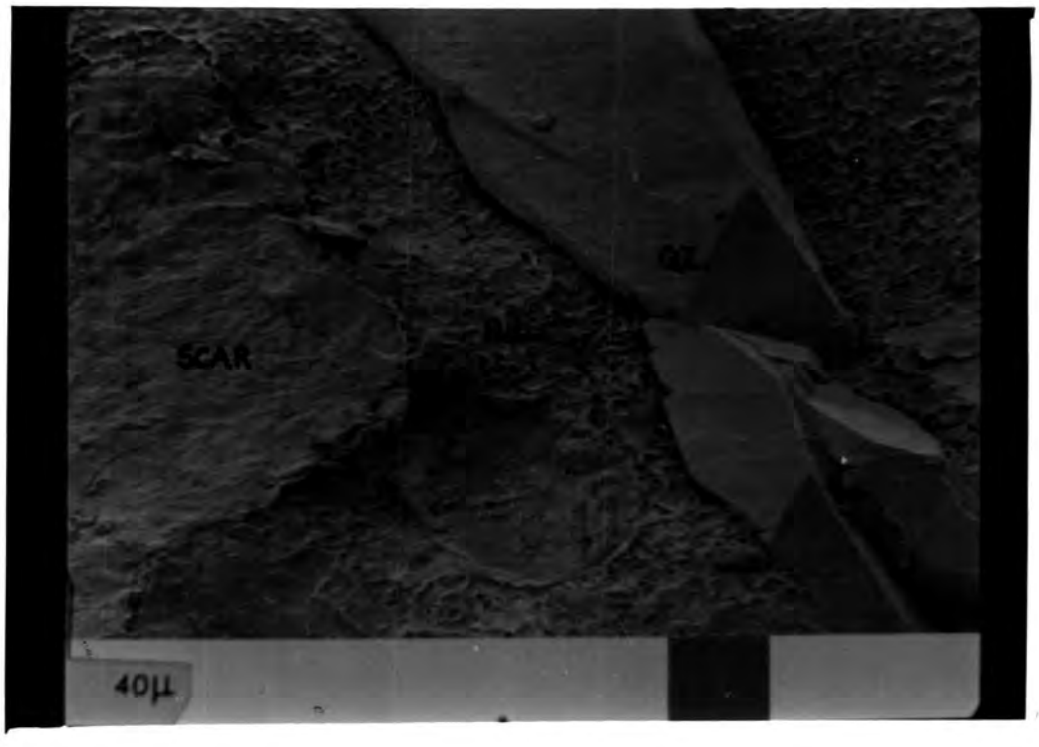

FIG. 9.7 Boxwork illite, absent from the scars of grain contacts and apparently lying under quartz overgrowths. Penrith Sandstone, Hilton Beck.

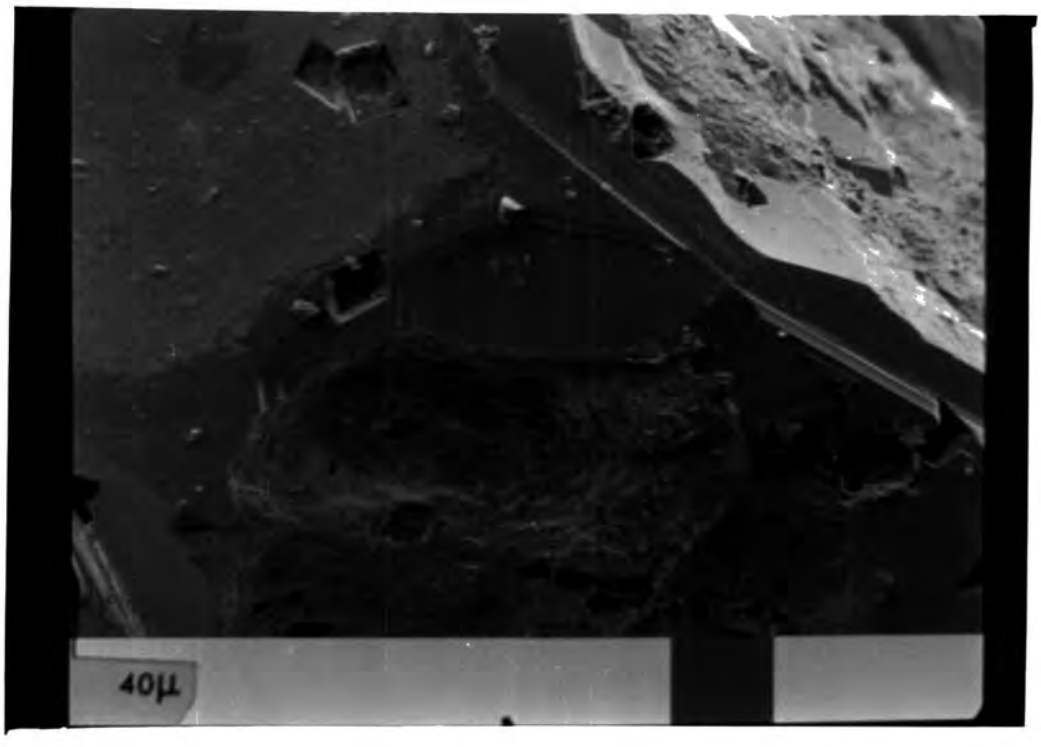

FIG. 9.8 Quartz overgrowths showing dolomoulds as rhomb and parallelepiped cavities 10-15μ across. Penrith Sandstone, Bowscar Quarry.

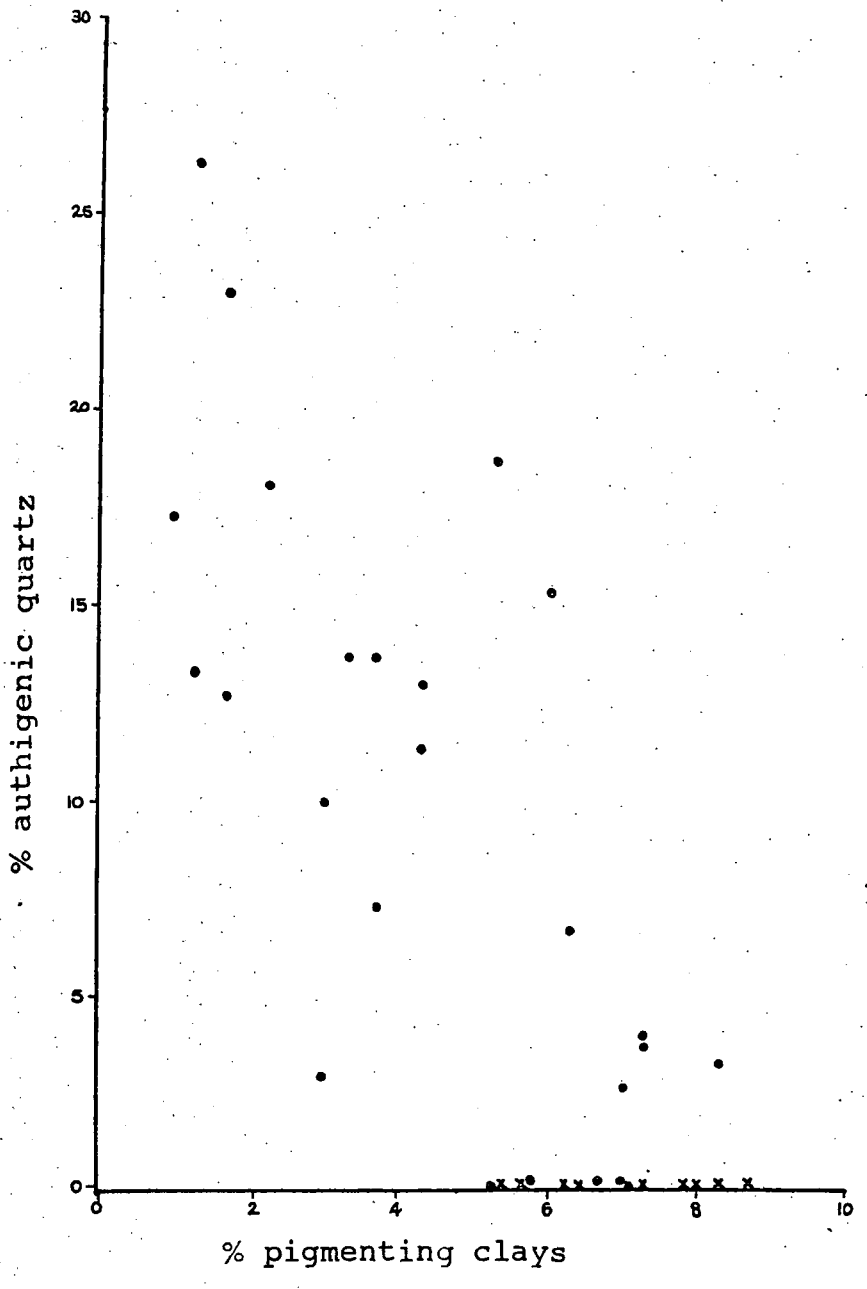

FIG. 9.9 Per cent pigmenting clays v. per cent authigenic quartz in the Penrith Sandstone, measured by point counting of thin sections. The inverse relationship of the two quantities is well displayed. n = 34

• = specimens from north of Cliburn (i.e. silicified)

× = specimens from south of Cliburn (i.e. non-silicified)

CHAPTER TEN

THE SIGNIFICANCE, CHARACTERISTICS AND IDENTIFICATION OF AEOLIAN SANDS

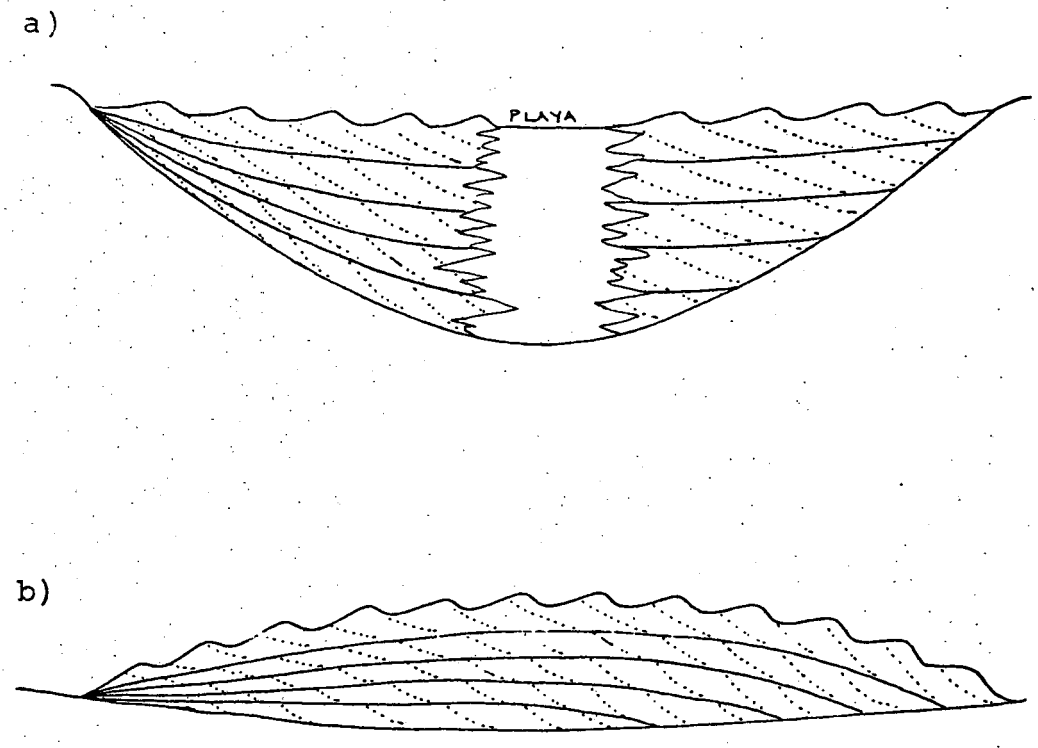

FIG. 10.1 The relationship between erg and first order set thickness for different patterns of erg growth. Left-hand sides of diagrams show ergs aggrading with fixed margins, right-hand sides show ergs expanding laterally with aggradation. Patterns drawn rest on the assumption that all parts of the ergs are traversed by the same number of draa. Further explanation in text.

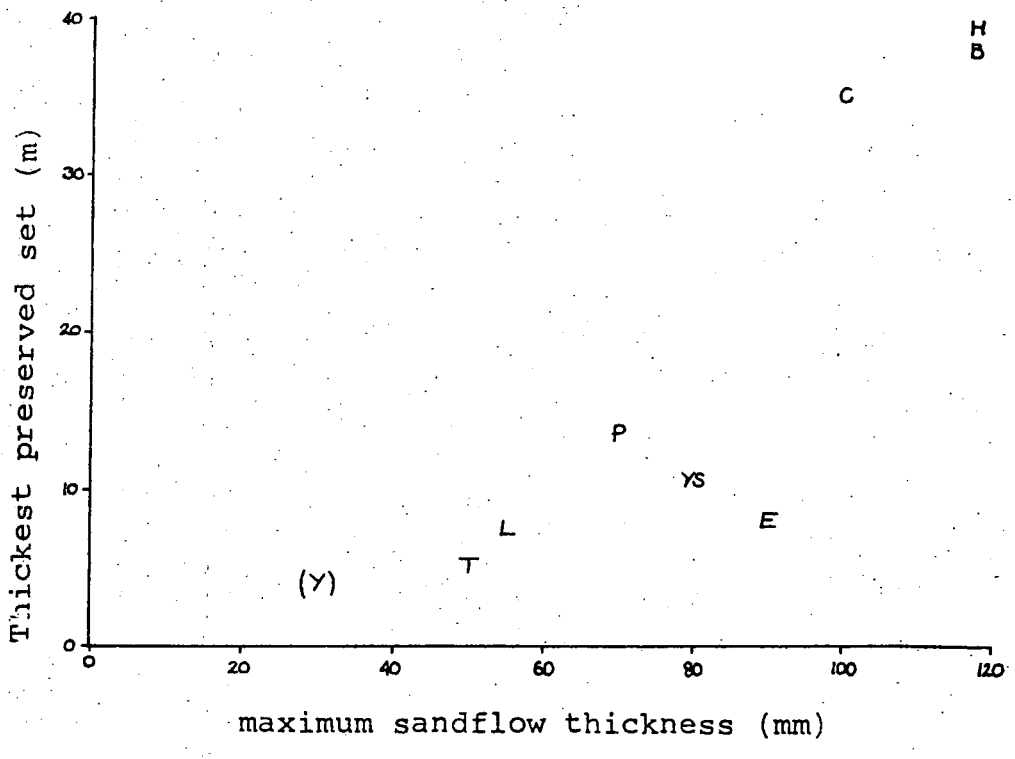

FIG. 10.2 Maximum sandflow thickness v. thickest exposed set in 9 aeolian formations. Those believed to represent only dunes (on slipfaceless draa) are;

(Y) = Yesnaby Sandstone (bracketed because figures are dubious; see Section A.1)

T = Thornhill Sandstone

L = Locharbriggs Sandstone

P = Penrith Sandstone

YS = Yellow Sands.

Those believed to represent slipfaced draa are;

E = Entrada Sandstone (data from Kocurek & Dott, 1981)

C = Corncockle Sandstone

B = Bridgnorth Sandstone

H = Hopeman Sandstone.

FIG. 10.3 The Woburn Sands in Arnold's Quarry at SP 930242. The lamination is much disturbed by bioturbation. Dark grains are either phosphate or phosphate-coated.

FIG. 10.4 The Woburn Sands at 9 Acre Quarry (SP 938277) near Leighton Buzzard. Shows a thick avalanche-laminated set resting on medium scale cross-bedded sand and overlain by flat-bedded sand. Top of face to floor of quarry is ~9m.

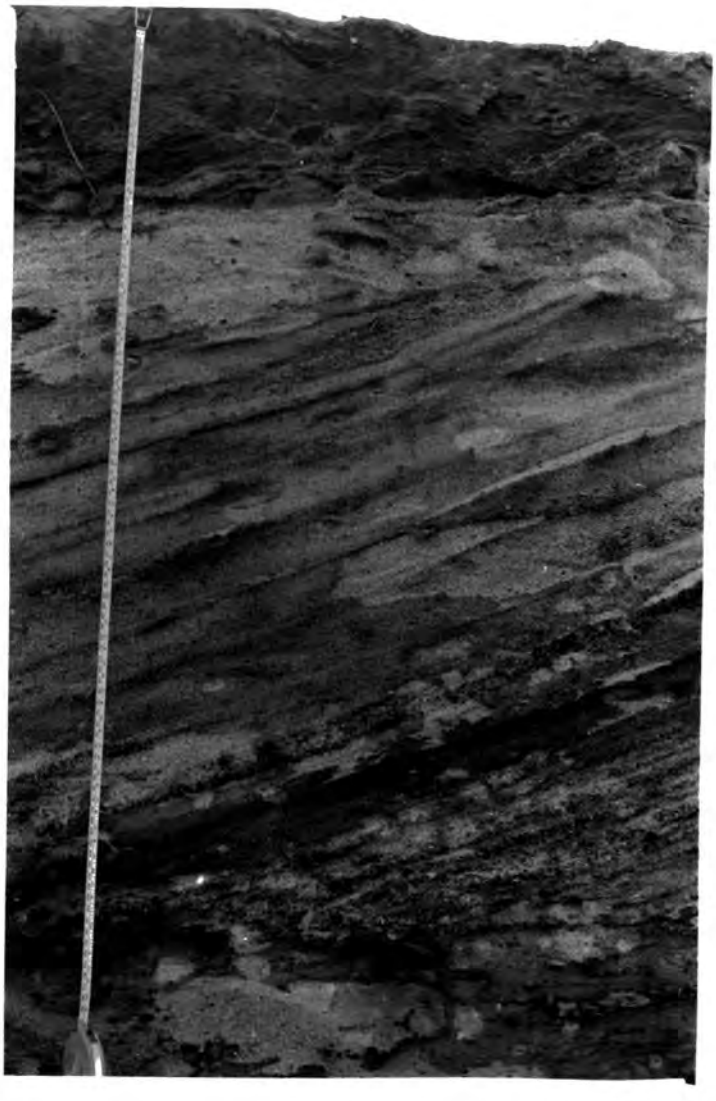

FIG. 10.5 Woburn Sands in Arnold's Quarry (SP 939288) near Leighton Buzzard. Set is of avalanche laminae, showing poorer distinction than many aeolian samples. Note the abundant fine and very fine pebbles at the base of the set. 1m length of tape visible.

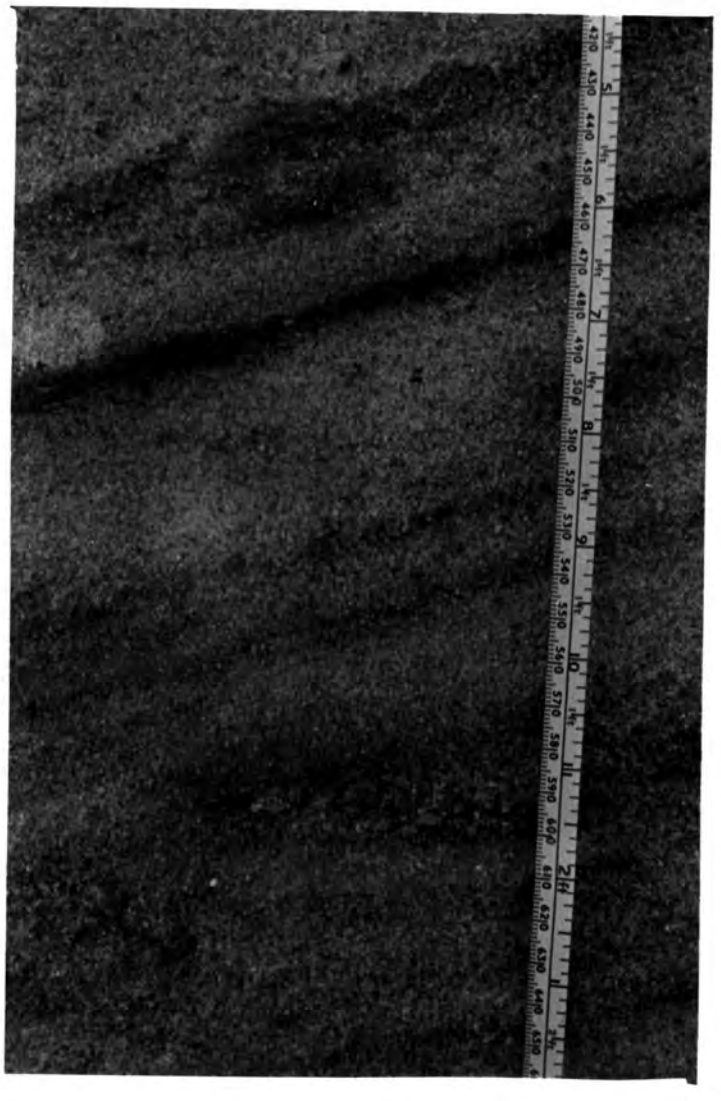

FIG.10.6 Close-up of FIG. 10.5 (mid-left) showing details of the lamination. Compare with FIG. 3.2.

APPENDIX

OTHER AEOLIAN SANDSTONES IN THE U.K.

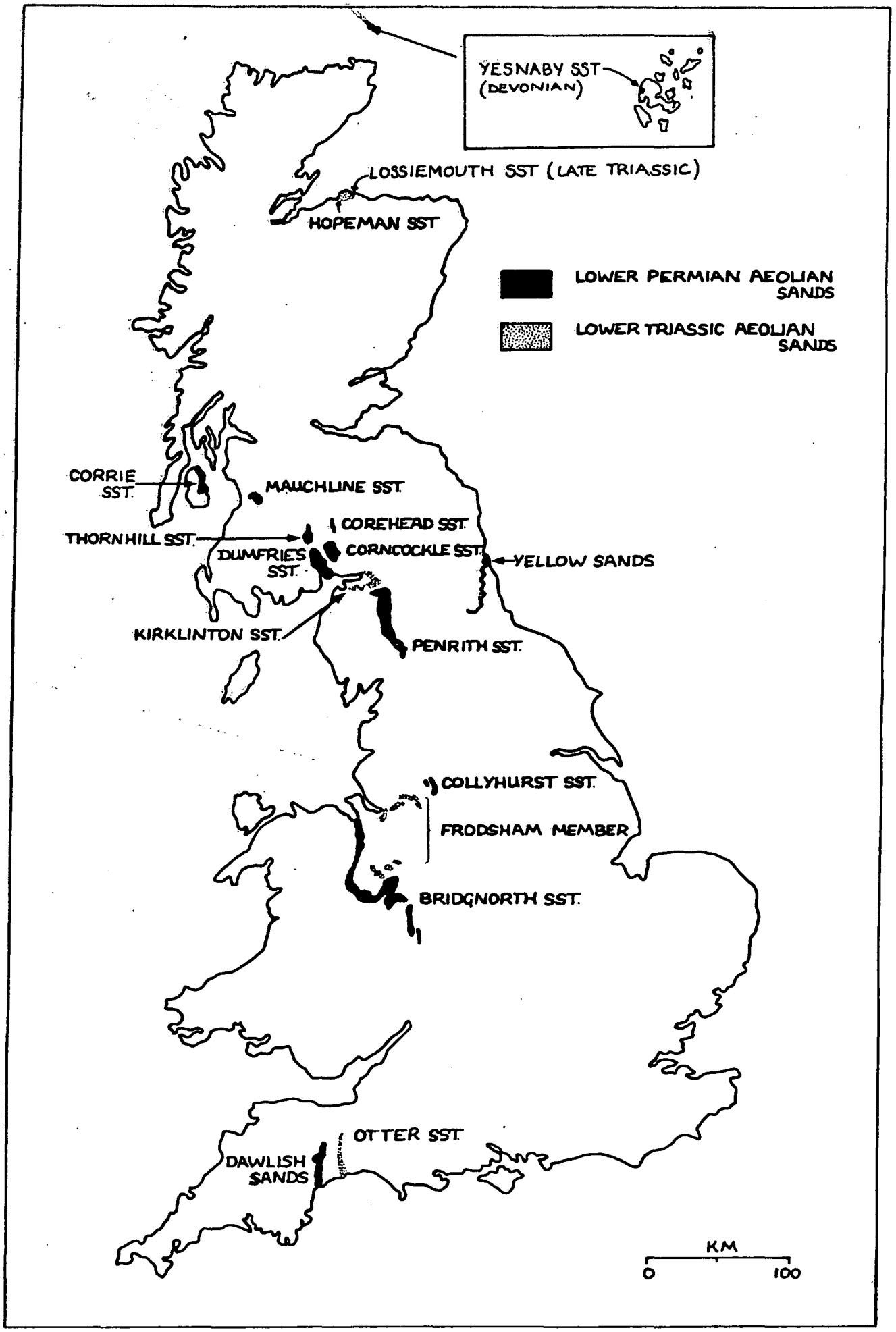

FIG. A.1 Map showing the outcrop of the rocks listed in the Appendix.

FIG. A.2 The Yesnaby Sandstone in a sea cliff at Yesnaby, on the west coast of Orkney Mainland. ~20m of cliff visible showing a succession of 2-4m sets stacked apparently horizontally. Part of author at extreme top left for scale.

FIG. A.3 Sea cliffs at Yesnaby (view to the left of FIG. A.2). Cliffs are ~20m high, of Yesnaby Sandstone. The headland in the distance at top centre is Qui Ayre, the upper part of which contains the non-aeolian, highest beds of the formation.

FIG. A .4 The Hopeman Sandstone at NJ 168704. The whole cliff, some 35m high, is occupied by a single set, with neither top nor base visible. Large-scale contortion of the bedding is visible towards the top of the cliff. The set probably records a slip-faced draa.

FIG. A.5 Different view of the same cliff as shown in FIG. A.4. The wave-cut platform (250-300m from the camera) reveals the broad, sweeping curvature of the draa leeside which the set records. The rocks in the immediate foreground belong to the same set which is directed westwards.

FIG. A.6 Zig-zag folding of sandflow laminae in the Hopeman Sandstone at NJ 180708. Hammer is 0.36 metres long.

FIG. A.7 Laminated blocks of aeolian sand within a structureless matrix. Believed to be the result of liquefaction of incoherent and partially coherent sand. Hopeman Sandstone at NJ 157703. Hammer is 0.36m long.

FIG. A.8 Possible trace fossils in the Hopeman Sandstone. Photograph is of the underside of in situ bedding planes at the foot of the cliff in FIG. A.4. Circular protruberances are a cementation feature, the linear markings (arrowed) may be biogenic. Slab bearing traces is ~1m across.

FIG. A.9 Inclined ?burrows in wind-ripple laminated Hopeman Sandstone at NJ 174707. The features show a broad consistency in size and an unerring consistency in inclination.

FIG. A.10 The south face of Corncockle Quarry (NY 086870). Note the inaccessibility of the rocks and that the visible area of the face is made up of a single SW directed set. Face is 25m high.

FIG. A .11 The Frodsham Member at the foot of Grinshill Hill (SJ 523327). The rock here has a colour of 2.5YR4/6 (red), and shows large-scale cross-bedding directed westwards. The set is visible to a thickness of 9m. Left hand face is ~8m high.

KEY TO ENCLOSURES

Sections

Bounding surfaces, coded by colour

Lamination

Reworked sand at the top of the formation

Pebbly layer (Cullercoats only)

Deformed cross laminae

250 → Orientation of exposure (degrees clockwise from true north)

16/320 Selected cross-bedding dip and dip direction data

Laminae dip into face

Laminae dip out of face

Lamination assessed according to the following scheme:

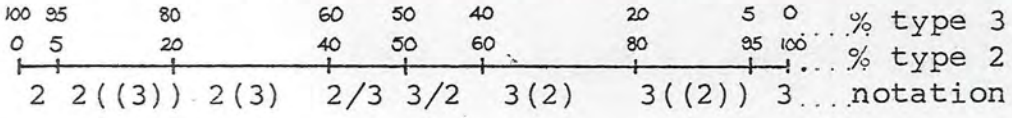

where 1 = sand sheet lamination

2 = wind ripple lamination

3 = sandflow lamination

Maps

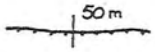

Line of face (hachure indicates facing direction). Distance marks correspond to those on sections.

Obscured or inaccessible face

Currently active areas in working quarries

Resultant (large arrow) and modes (smaller arrows) of the composite cross-bedding azimuth rose diagram of the formation (fig. 5.33).

BOUNDING SURFACES

1st order

2nd order

3rd order

4th order

migration surfaces (i.e. 1st or 3rd)

modification surfaces (i,e. 2nd or 4th)

Surfaces left uncoloured are uncertain

ENCLOSURE 1

CULLERCOATS SHORE SECTION

NZ 364713

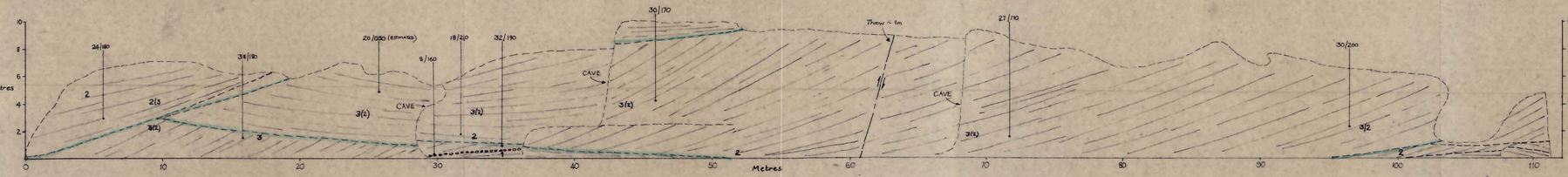

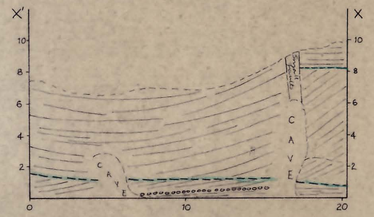

NOTES The section is demarked by the S-directed limit of a single trough-shaped set 9 m thick. The pebbly layer at 35,01 might suggest that the Carboniferous lies not far below. The whole section probably has a tectonic dip of a few degrees to the south. Measurement of long axis orientation of pebbles in the coarse layer are shown below right.

CULLERCOATS SHORE SECTION: SKETCH MAP

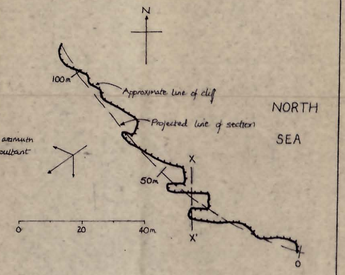

TYNEMOUTH PRIORY SHORE SECTION

NZ 385634

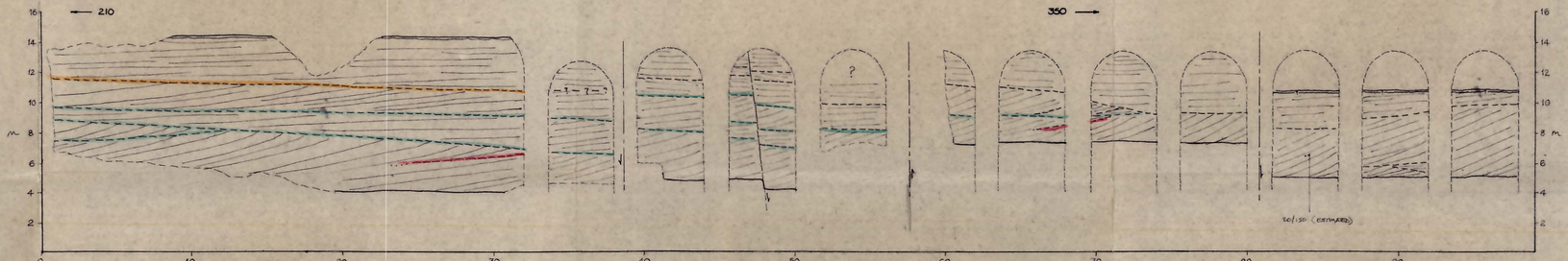

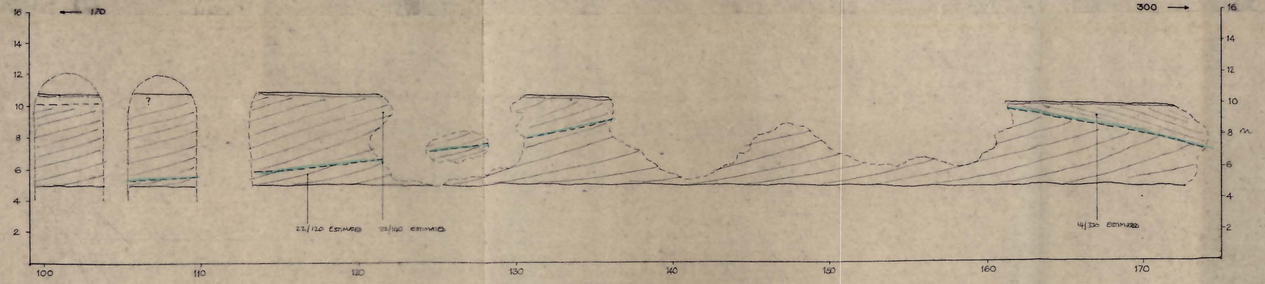

NOTES The formation thins from 11m to 5m northwards along the section suggesting that the exposure reveals an area close to the northern margin of a dune. There is no record of the dune developing instability as a sand sheet. From 0-60m the evidence indicates dune aggradation by the climbing of south-migrating dunes at angles of 2-5°, if the given interpretation of the bounding surfaces is correct and the diagram accurate.

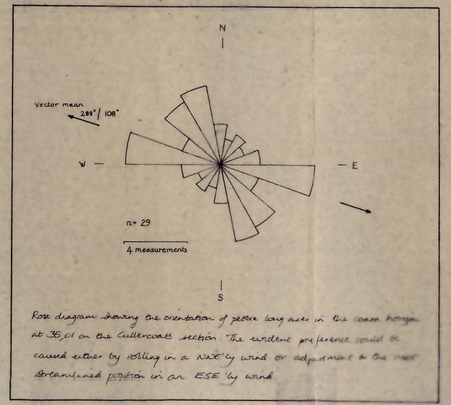

Rose diagram showing the orientation of pebble long axes in the coarse horizon at 35,01 on the Cullercoats section. The evident preference could be caused either by rolling in a NNE'ly wind or adjustment to the most fortuitous position in an ESE'ly wind.

TYNEMOUTH PRIORY SHORE SECTION SKETCH MAP

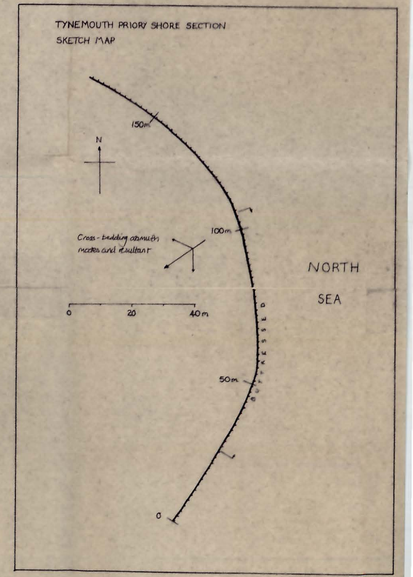

ENCLOSURE 2

FERRYHILL RAILWAY CUTTING NZ 303323

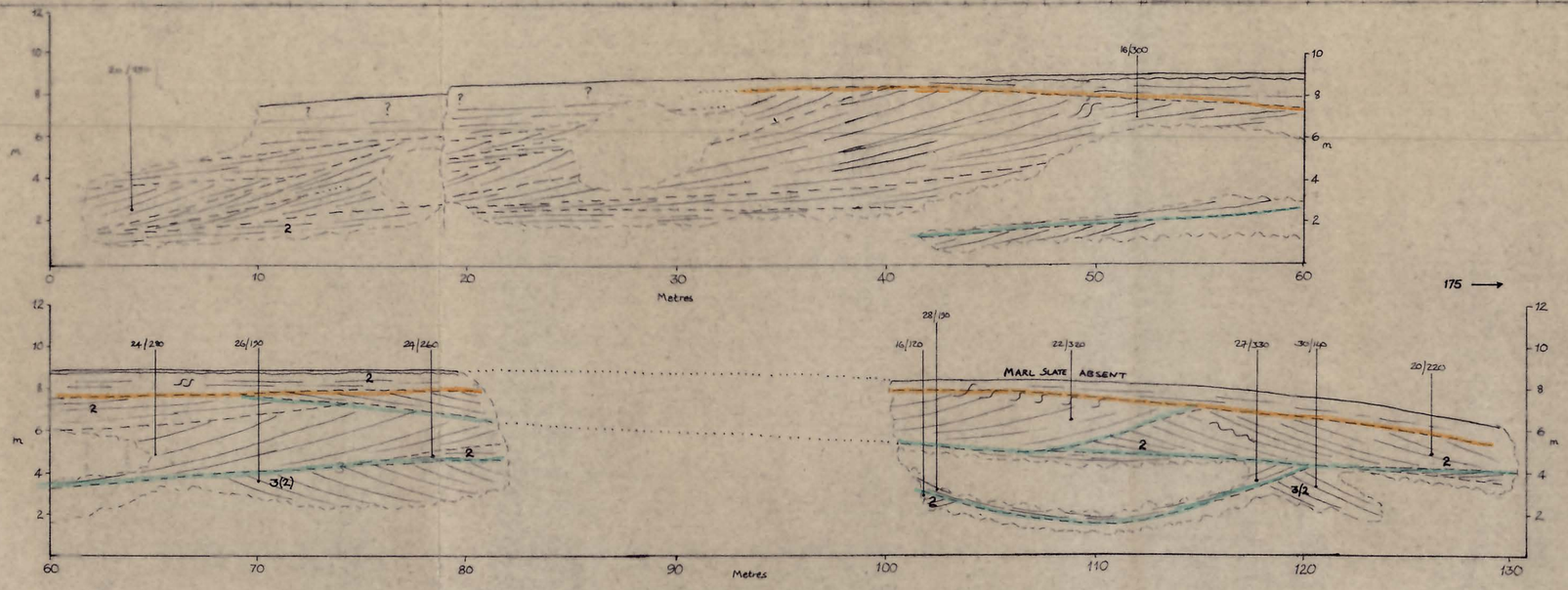

N S The exposure is in the centre of a 1.6 Km wide ridge. Note the relief on the top surface of the formation in the cutting and the occurence of concretions within the planar-bedded zone.

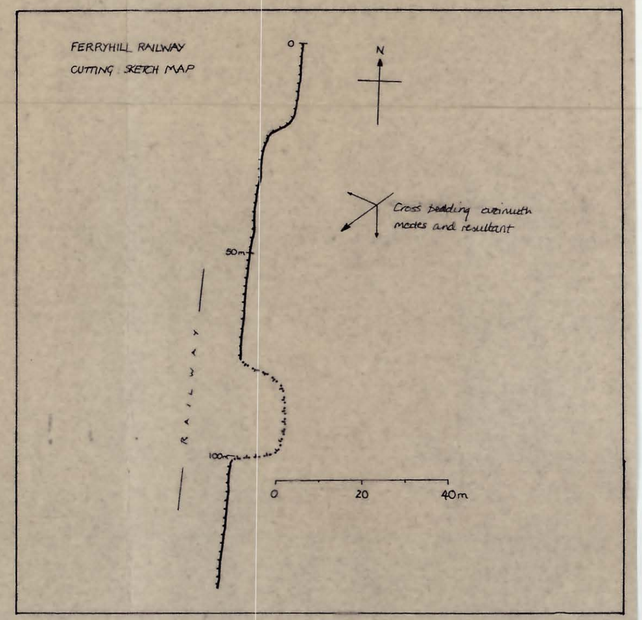

NORTH HYLTON NZ 355574

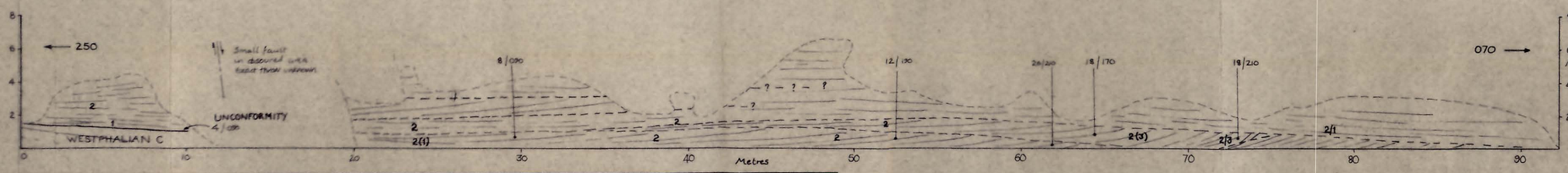

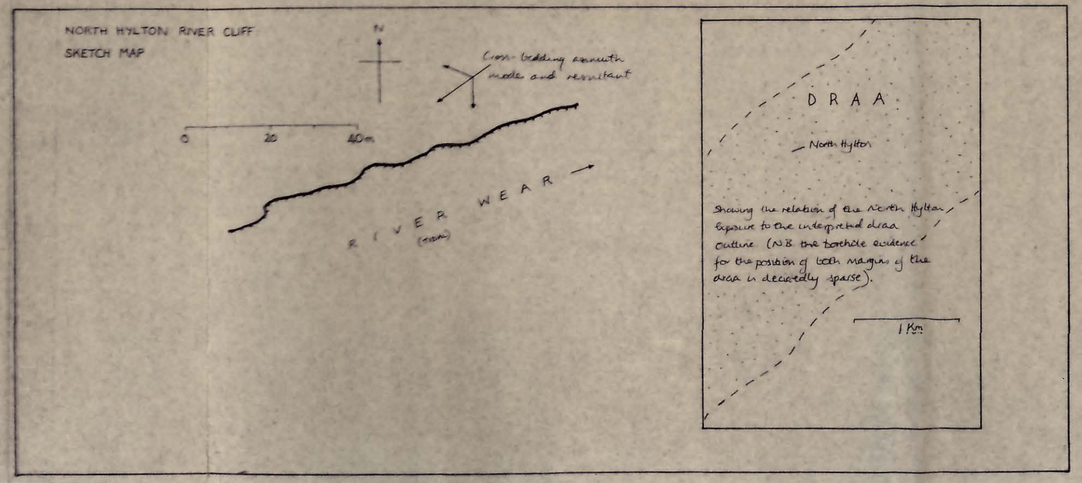

NOTES The exposure records initial development of the draa as a sand sheet. If the throw on the fault at 12m is not great a propensity for reversion to a sand sheet appears to have persisted for some time, allowing the accumulation of several metres of such sediment.

ENCLOSURE 3

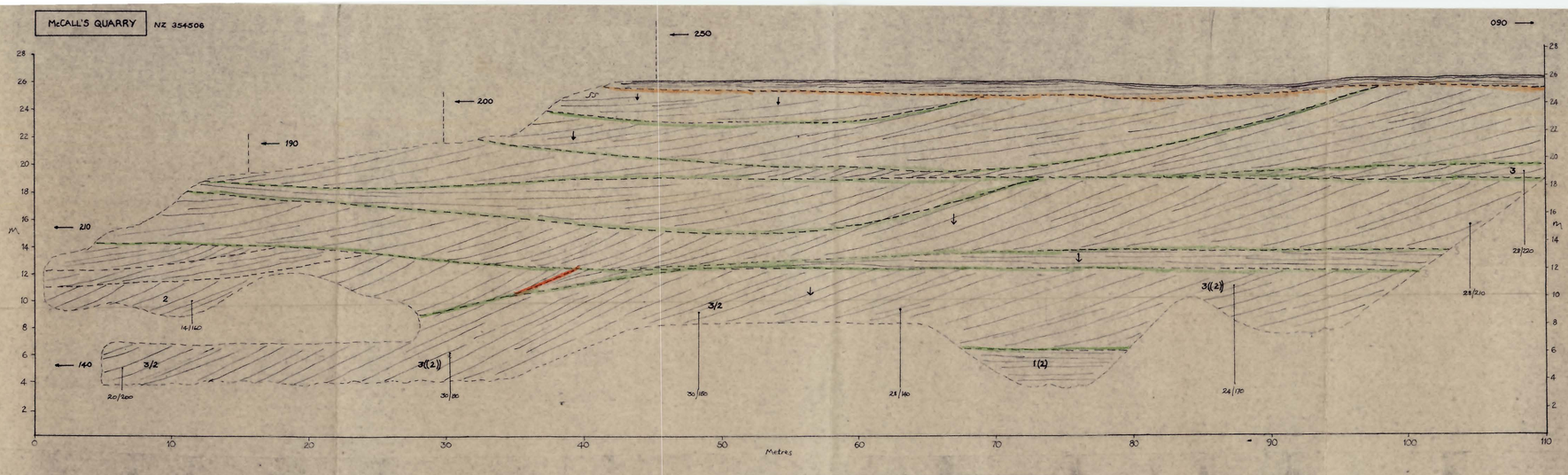

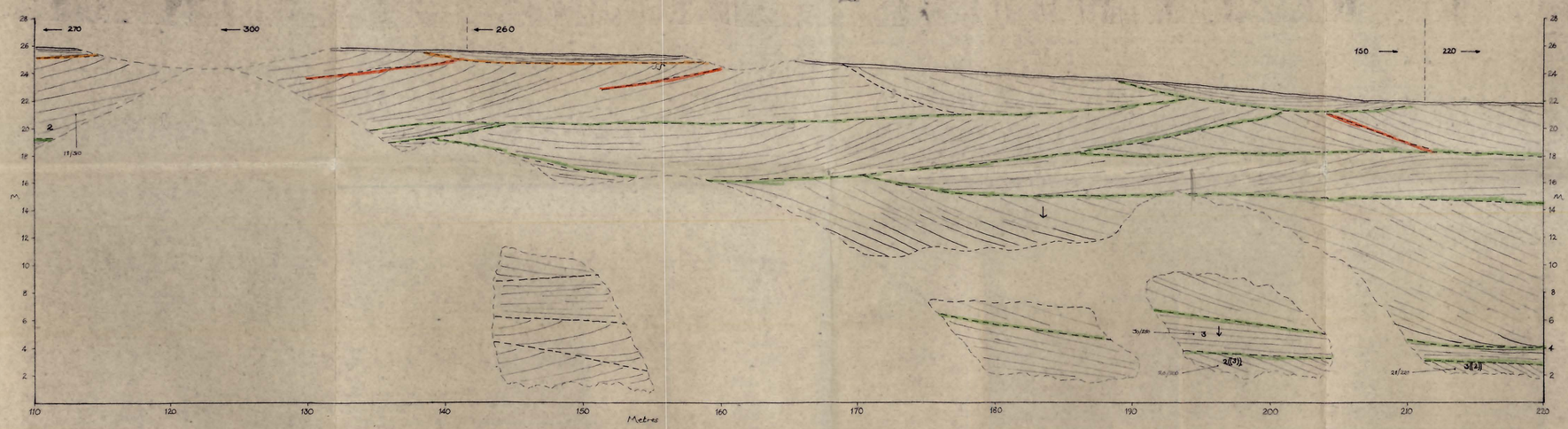

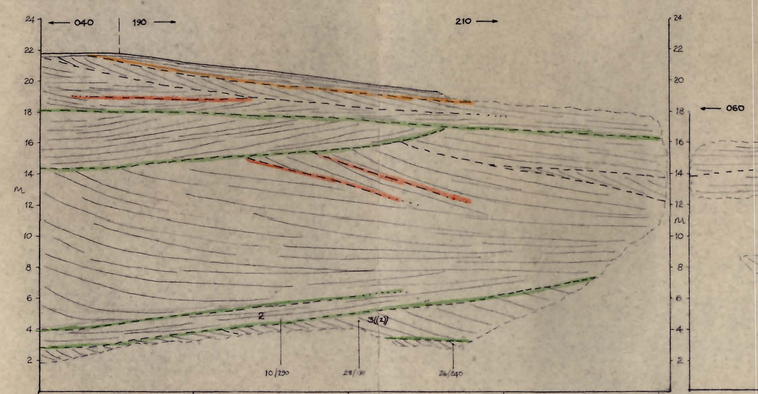

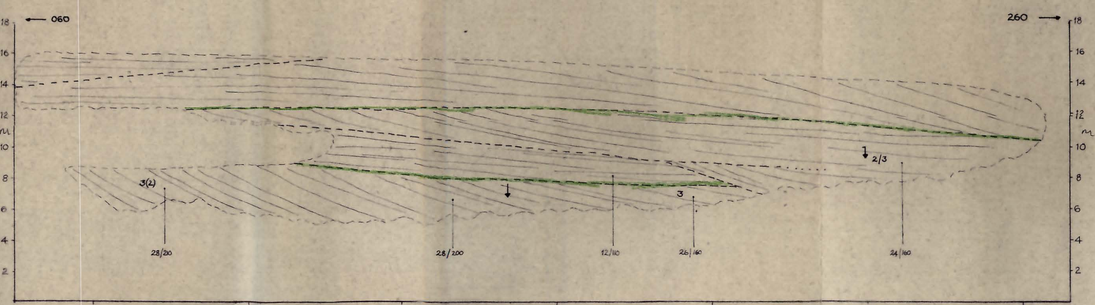

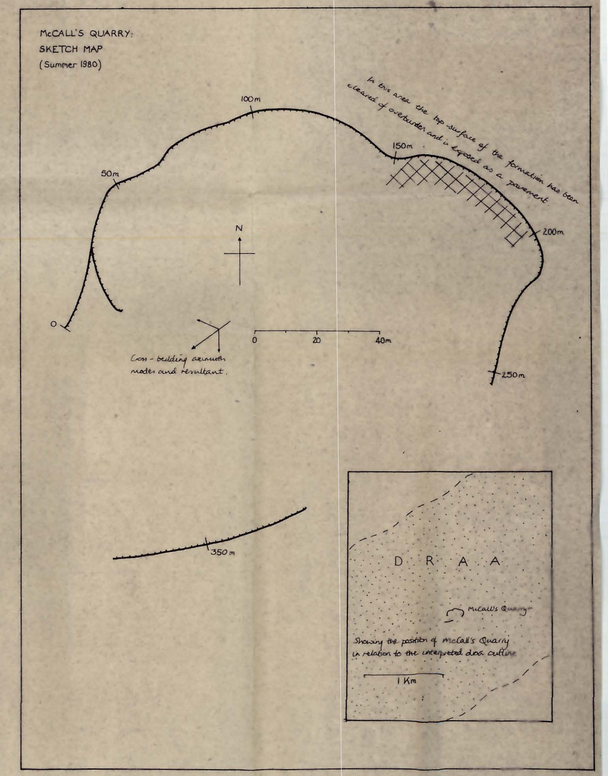

NOTES The quarry primarily displays an almost complete section through the formation. Thick, simple sets lacking internal bounding surfaces are more common here than elsewhere. This may be due partly to the order bounding surfaces being poorly defined in the weathered higher parts of the faces and partly to the natural variation of cross-bedding style within the formation. It could have some specific systematic cause such as some special feature of grain size, sand supply or dune type but there are no other reasons to suppose that this particular area should have been so favoured.

HETTON DOWNS QUARRY

NZ 3584 83

ENCLOSURE 4

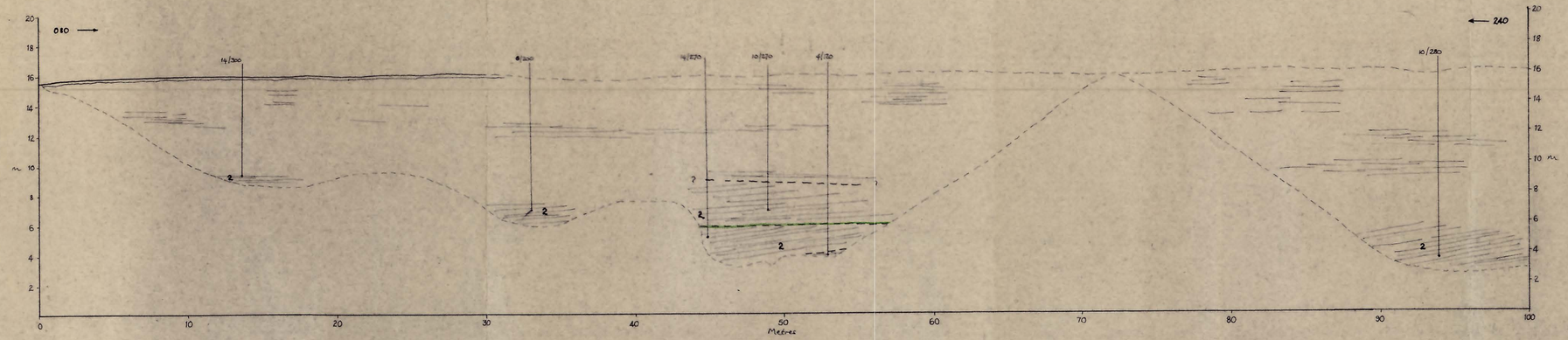

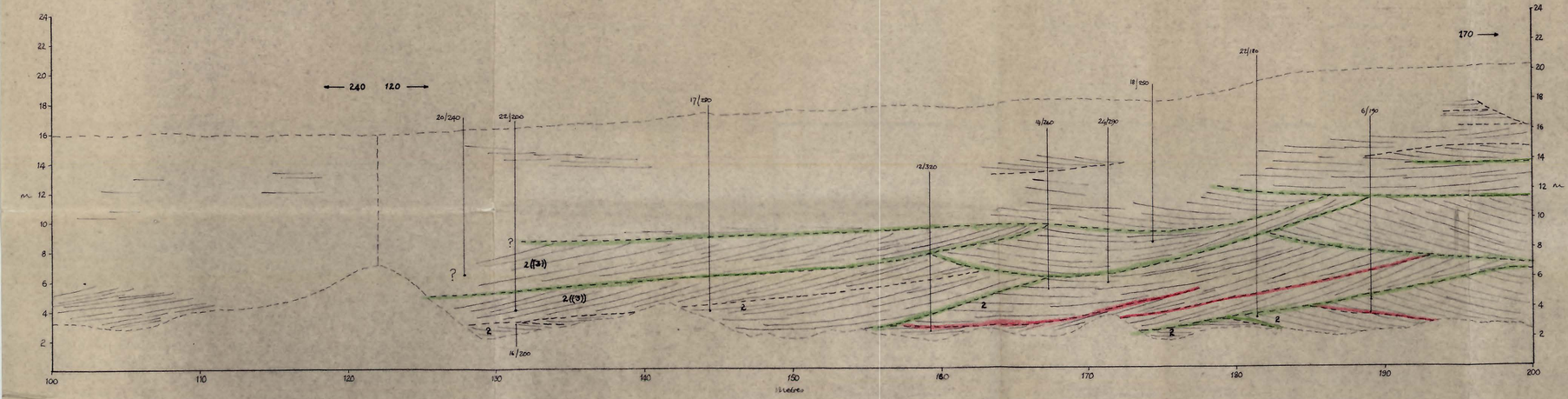

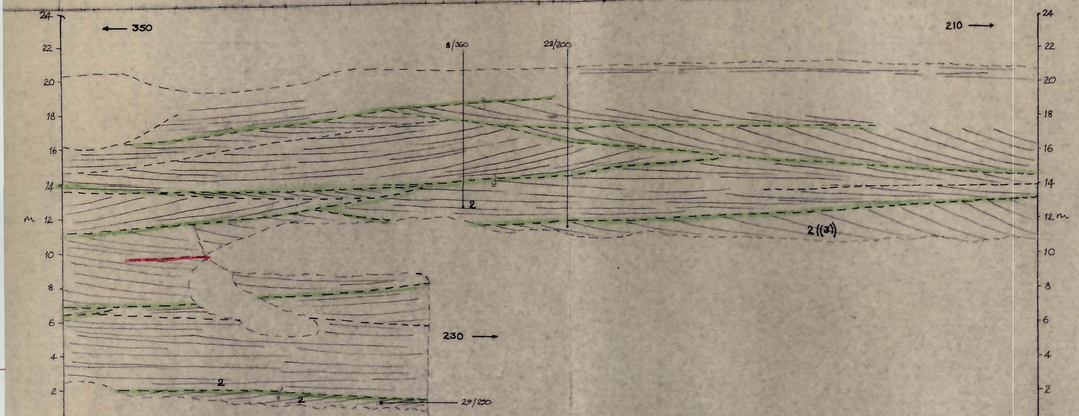

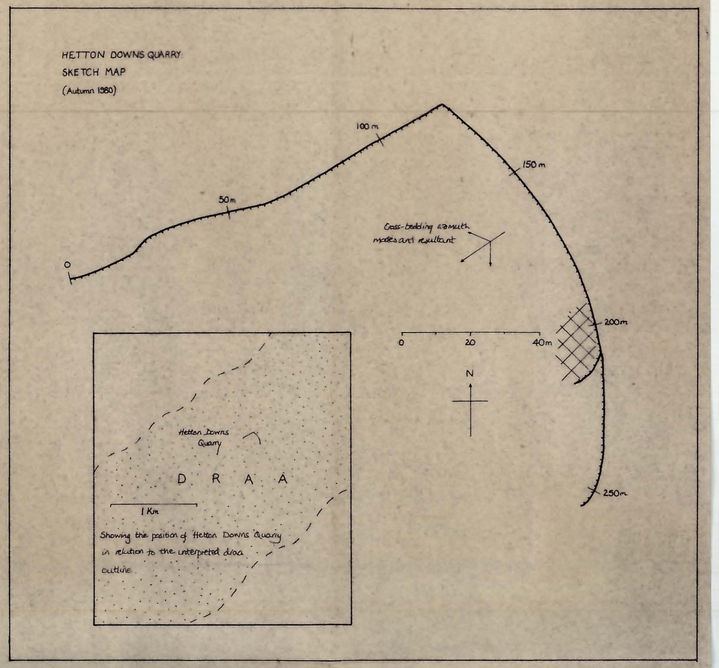

NOTES The lack of discernible structures over much of the exposure is thought to be due to adverse weathering. The east face, from 150–200m clearly shows a pattern of stacked, overlapping trough-shaped sets, each set being ~4m thick and 30–40m wide.

ENCLOSURE 5

SHERBURN HILL SAND PIT – WEST FACE NZ 344417

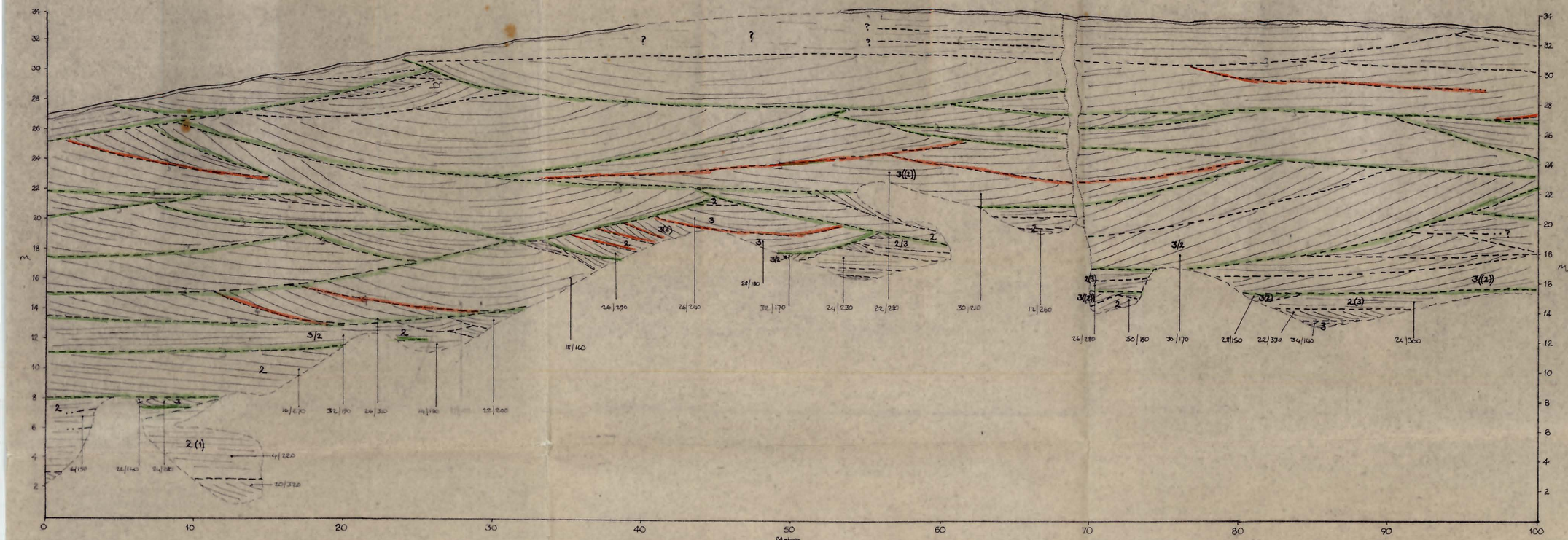

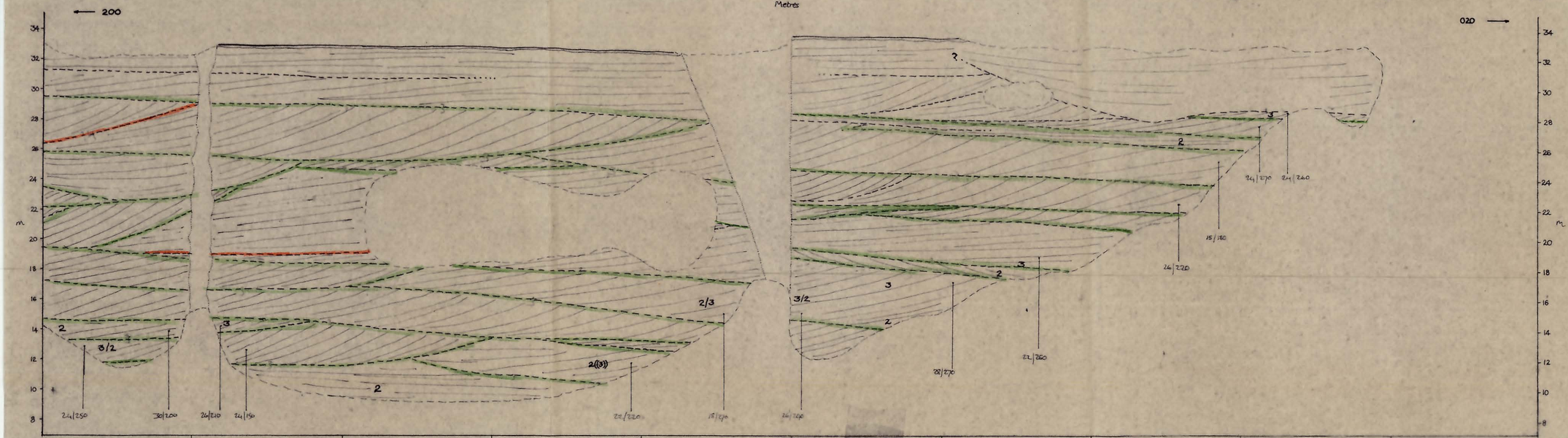

NOTES Transverse sections of trough-shaped sets are inwise from 10-60m, more longitudinal sections from 60-130m. The longitudinal sections indicate that the dunes migrated along subhorizontal paths bearing generally parallel bounding surfaces. The lateral containment of each set shows that each dune deposited preservable cross-bedding for only a limited period, though this does not necessarily correspond to the lifetime of the dune. It is likely that the base of the formation lies only a short distance below the floor of the quarry.

ENCLOSURE 6

SHEABURN HILL SAND PIT – NORTH FACE

NZ 344417

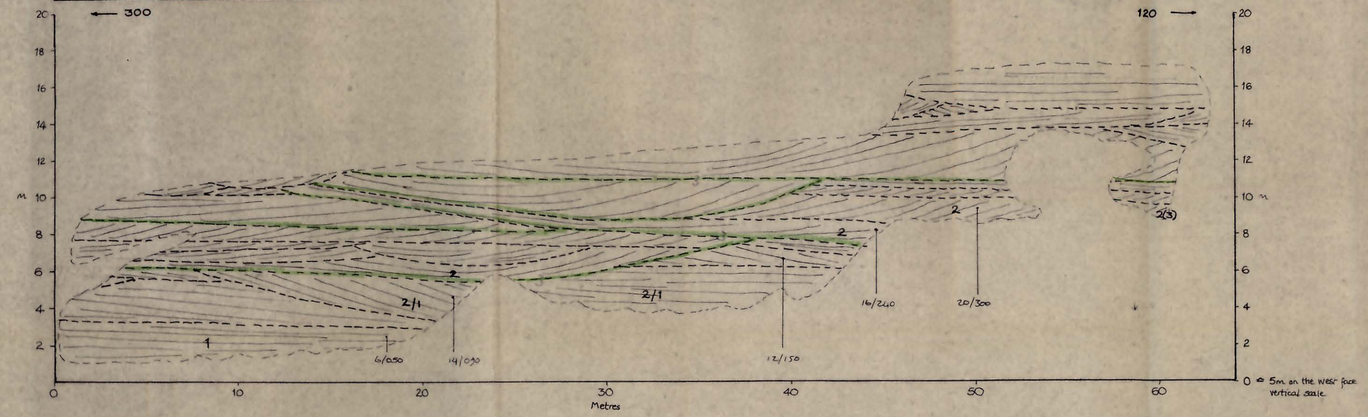

SHERBURN HILL SAND PIT – EAST FACE

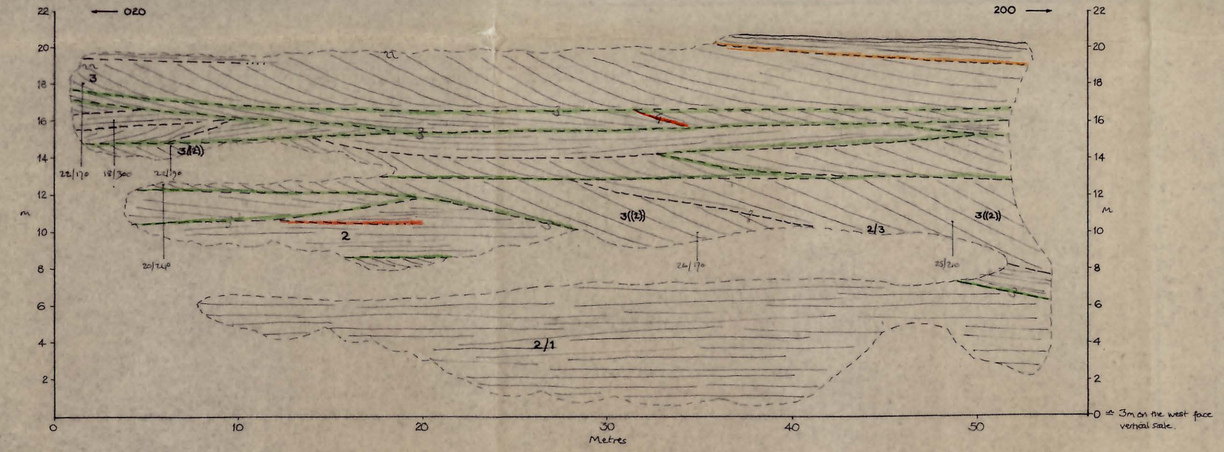

NOTES If, as is likely, the base of the formation lies only a few metres below the floor of the quarry both these faces record an early development of the area as sand sheets. The elucidation of bounding surface type is difficult in both faces.

SHERBURN HILL SAND PIT:
SKETCH MAP
(Spring 1981)

AREA OF

CRIME RIGG QUARRY

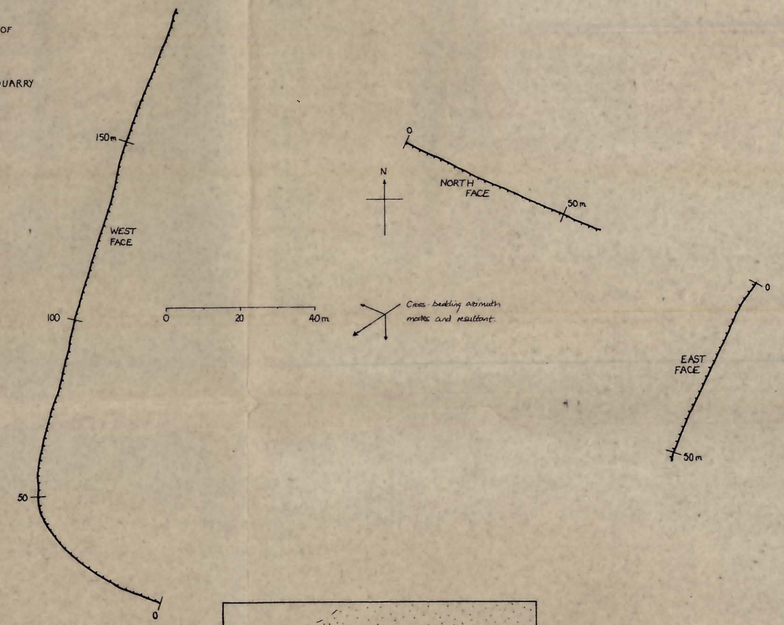

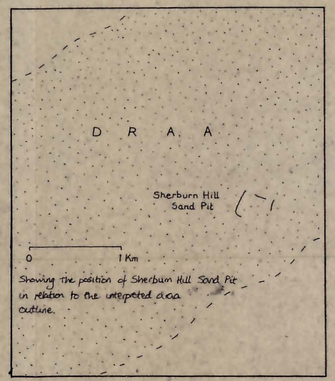

Showing the position of Sherburn Hill Sand Pit in relation to the interpreted drift outline.

ENCLOSURE 7

BOWBURN QUARRY

NZ 327382

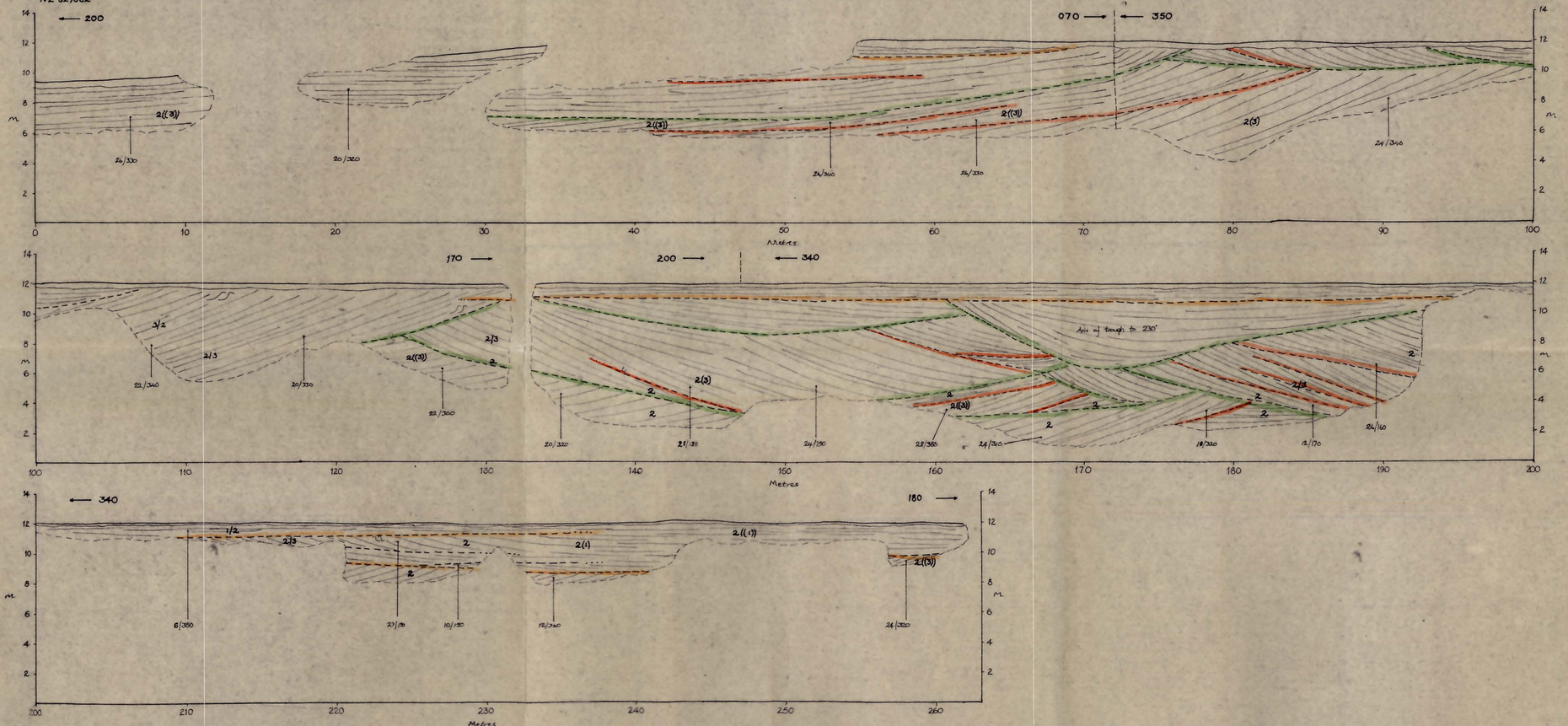

NOTES At the northern end of the quarry (0-120m on the section) the cross-bedding dips consistently towards the margin of the draa. Also note the complex arrangement of sets and bounding surfaces between 150 and 200m. In this area, with exposure limited both laterally and vertically it is extremely difficult to be confident in labelling the bounding surfaces.

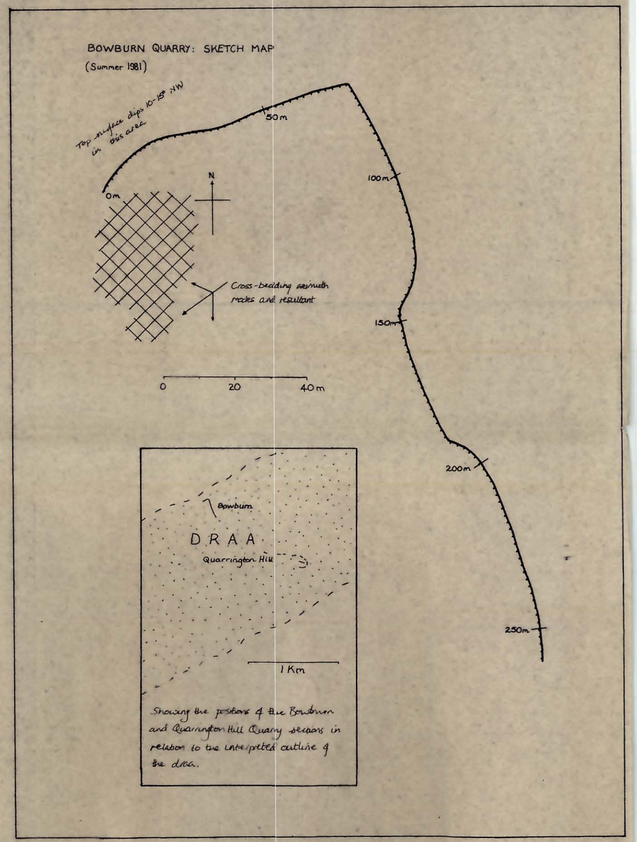

Showing the position of the Bowburn and Quarrington Hill Quarry sections in relation to the interpreted outline of the draa.

ENCLOSURE 8

QUARRINGTON HILL QUARRY

NZ 334377

FACE A

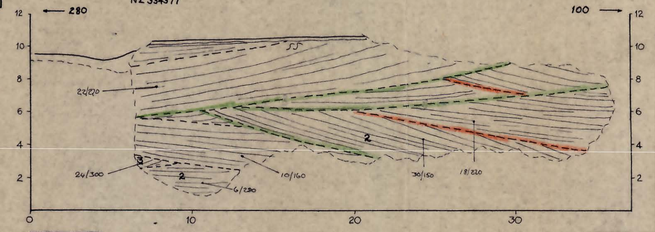

FACE B

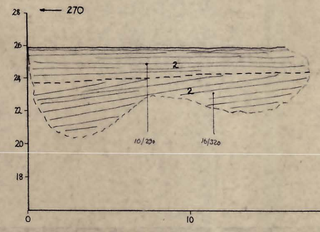

FACE C

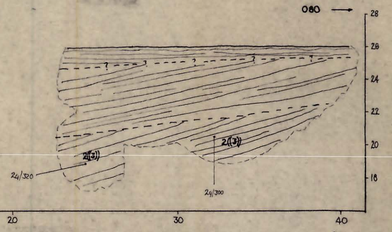

FACE D

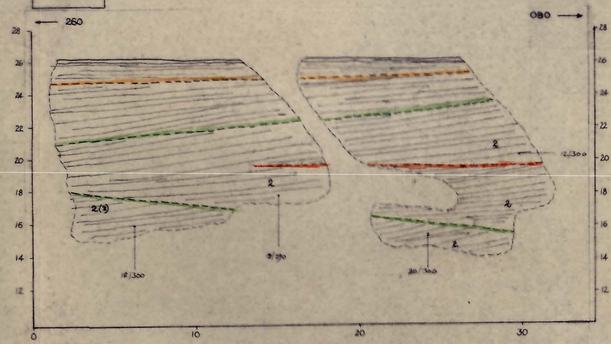

FACE E

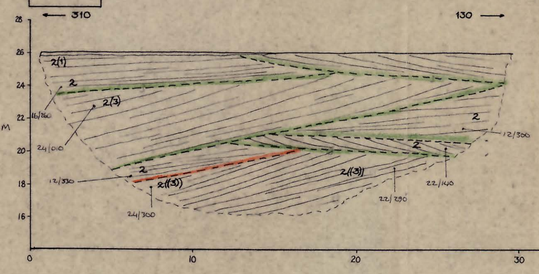

FACE F

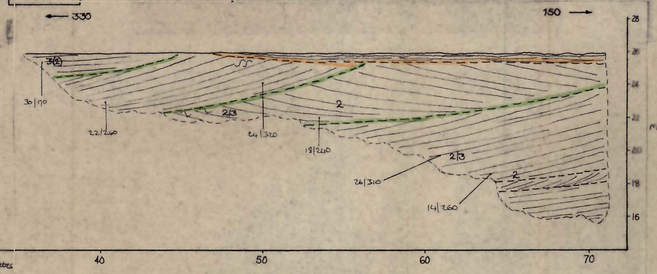

FACE H

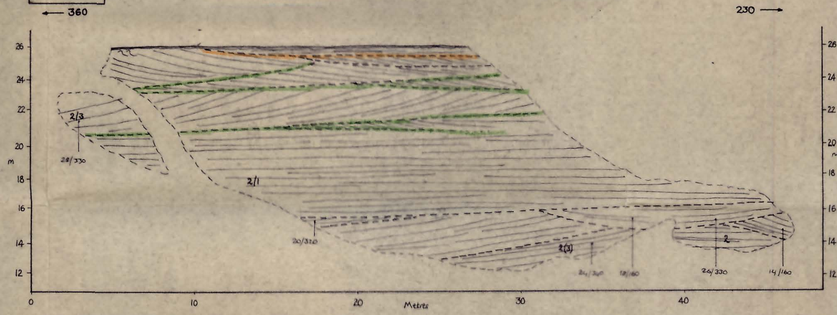

NOTES Faces A - I inclusive are approximately coordinated to the same vertical scale. The quarry probably shows a near complete section through the formation. The limited size of the individual exposures makes bounding surface identification difficult. Note the examples of deformation at C1, D and H6 in face I which may be 15m or more below the top of the formation. Faces E, F and G show the most explicit examples of trough cross-bedding, being oriented transverse to the palaeocurrent resultant.

FACE G

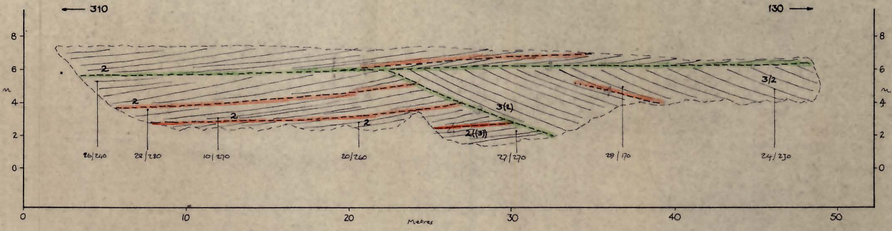

FACE I

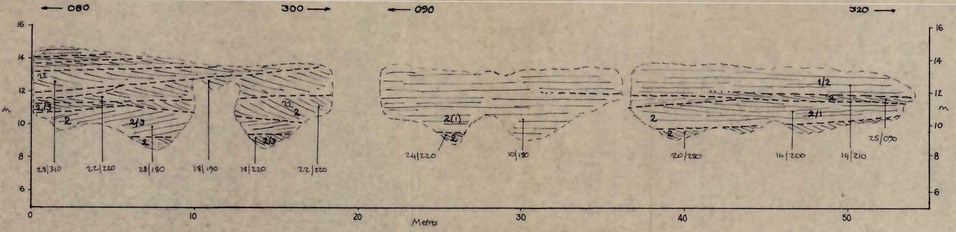

QUARRINGTON HILL QUARRY SKETCH MAP

N.B. Scale is HALF that of all other maps.

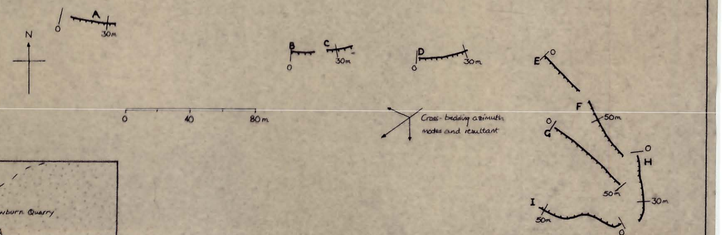

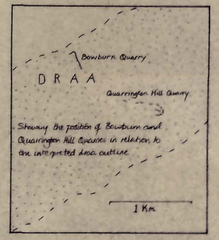

ENCLOSURE 9

A442 WORFE BRIDGE (SO 732957)

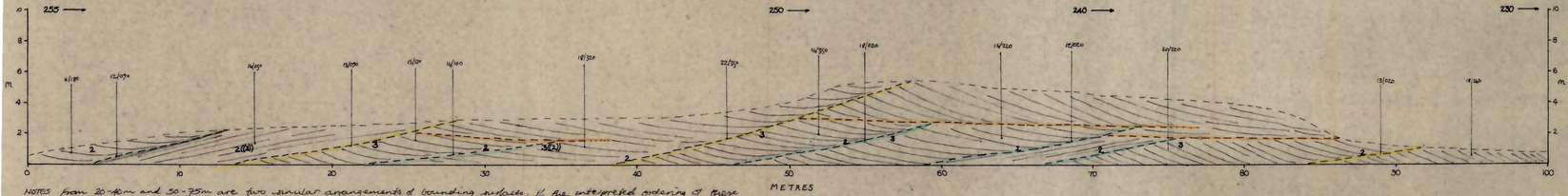

NOTES From 20-40m and 50-75m are two similar arrangements of bounding surfaces. If the interpreted ordering of these surfaces is correct these may represent the transformation of a slipfaceless dune into a dispersed dune as the lateral interfingering of two such parts of the same dune. An alternative interpretation would be that the two surfaces labelled 1st order are in fact 3rd, with all the others involved 4th.

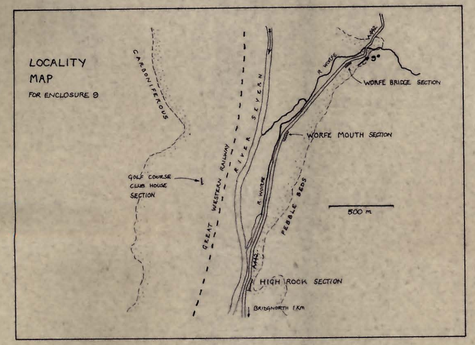

A442 WORFE MOUTH (SO 727952)

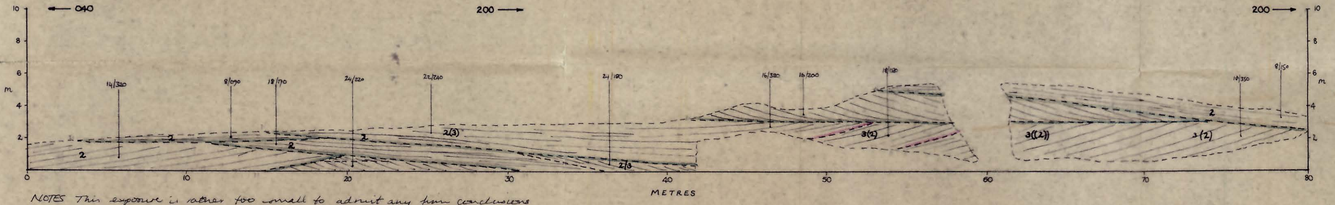

NOTES This exposure is rather too small to admit any firm conclusions but it looks like a section normal to palaeocurrent through dune-sized trough cross-bedding.

BRIDGNORTH GOLF CLUB CAR PARK (SO 720948)

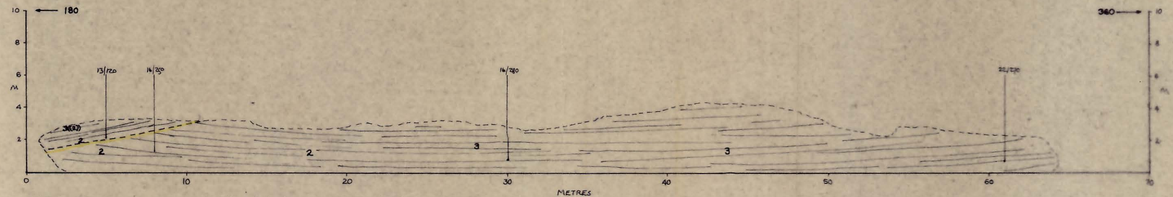

NOTES The main set here is believed to be part of a slipfaced dune on the grounds of its size (compare with the sets in the Worfe Mouth section). Note that the slip direction measurements show this part of the dune to be slightly leeward.

HIGH ROCK, BRIDGNORTH (SO 725941)

NOTE CHANGE OF SCALE

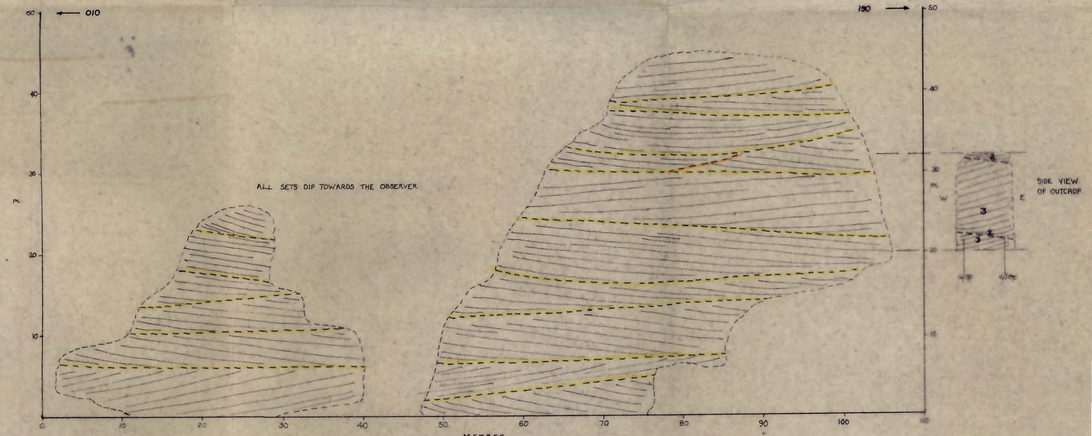

NOTES The huge size of all the sets here is counted as a strong argument in favours of them representing slipfaced dunes. Dune sets might individually reach this size but the consistently large thickness and lateral extent of these sets compared with those at Quatford Rock must militate against them being the deposits of dunes. This diagram covers only that part of High Rock which faces a distance. Exposure is in fact much more extensive but obscured by trees and not amenable to survey.

ENCLOSURE 10

CASTLE HILL, BRIDGNORTH (SO 717927)

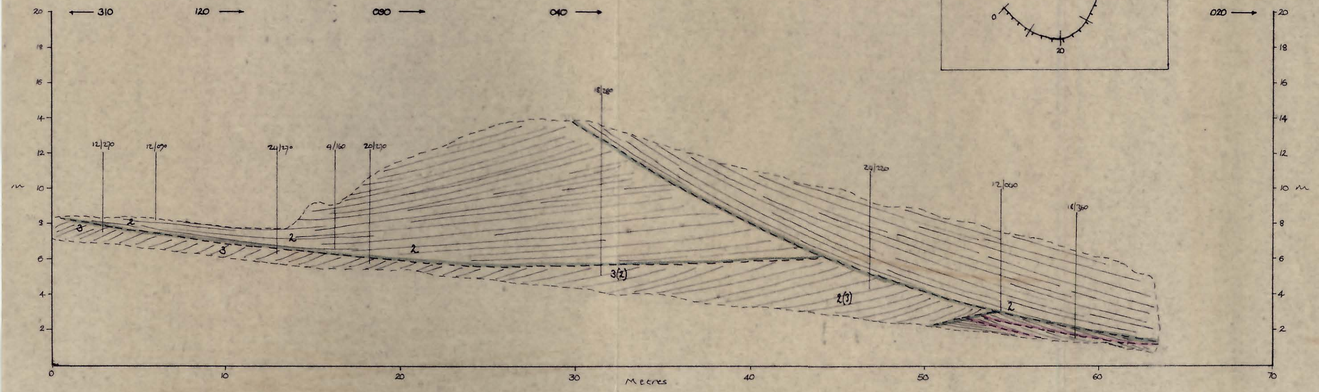

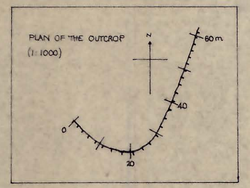

NOTES Faces C+D at the Hermitage probably record dunes. The remaining exposures on this chart are too small to show several complete sets of cross-bedding and consequently little can be said of the generating bedforms.

QUEEN'S PARLOUR, BRIDGNORTH (SO 728933)

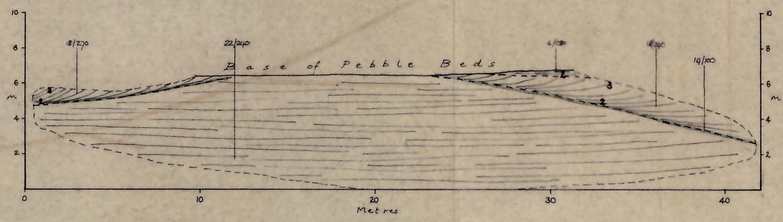

THE HERMITAGE & ASSOCIATED EXPOSURES, BRIDGNORTH (SO 728935)

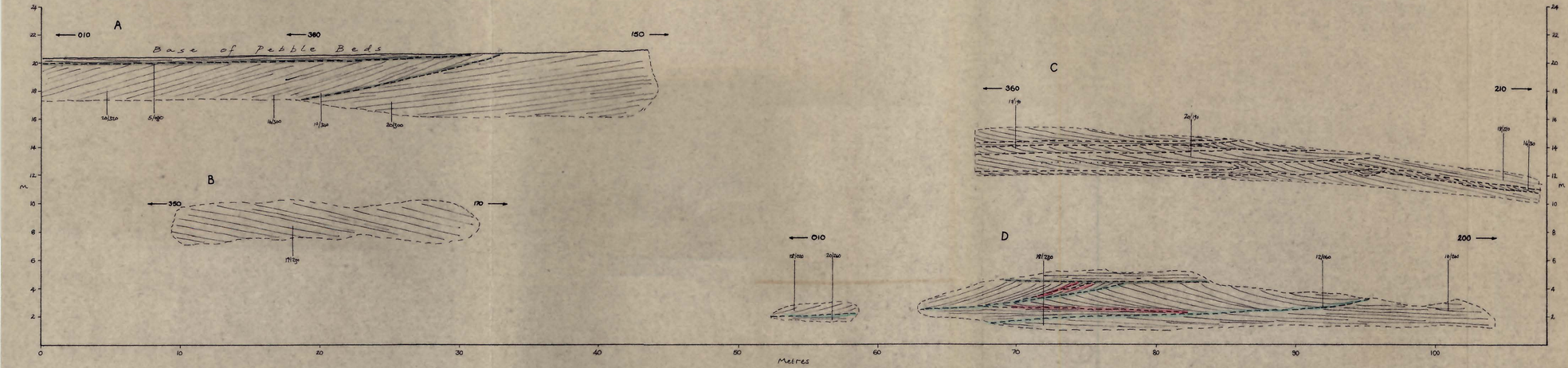

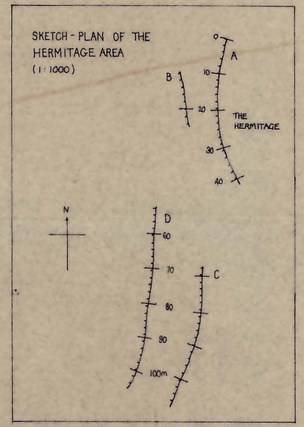

ENCLOSURE 11

QUATFORD ROCK (SO 738907)

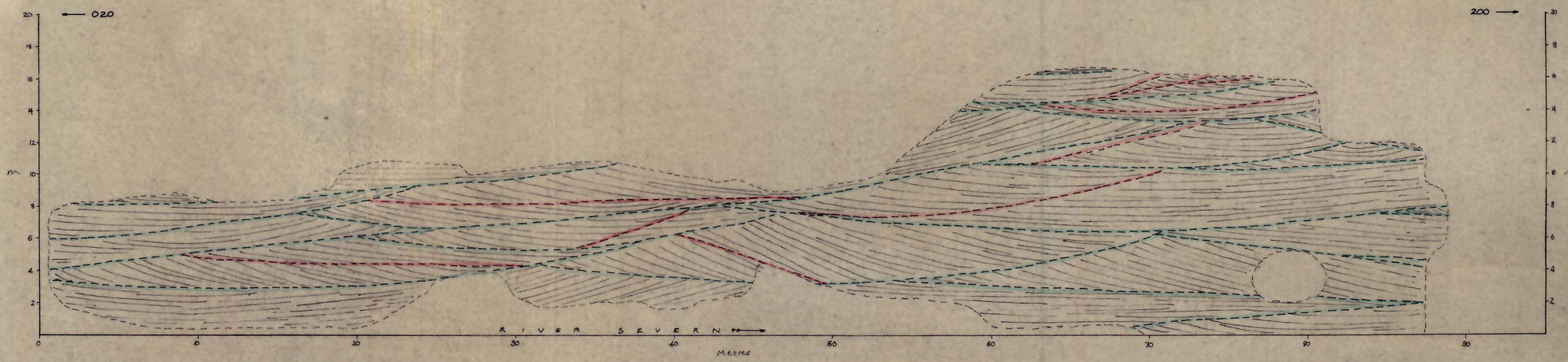

NOTES This exposure is taken as the 'type' example of dune cross-bedding (i.e. dunes on slip-faceless dsaa). The section is a transverse cut through trough cross-bedding, troughs being 2-4 m thick and 20-40 m wide. Most laminae dip out of the face. No dip and lamination data is available because the exposure was abruptly cut off by the River Severn.

A454 LOWER SECTION, SOUTH SIDE (SO 724932)

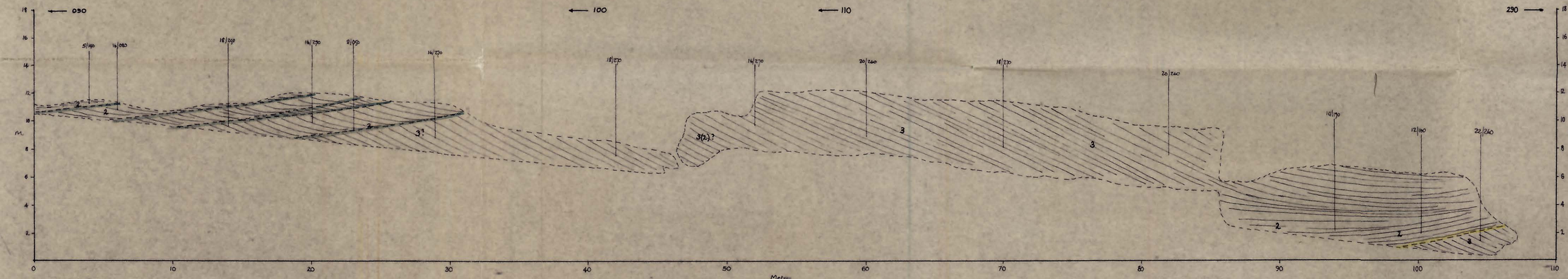

NOTES These sections are cut parallel to palaeocurrent. The main set is 20m thick and most probably records the passage of a slipfaced dsaa. It is interesting that on the south side of the cutting this set is uninterrupted by internal surfaces whereas on the north side several are present at the western end. These may be 2nd order (dsaa modification) surfaces or possibly 3rd order, recording the development of dunes on the dsaa slipface. The relatively small scale cross-bedding in the sediments above the main set tempts interpretation as dunes. If so it is interesting that the bounding surfaces between them are parallel to the 1st order surface below. This would not be expected of dunes on a slipfaceless dsaa. Exposure is too limited to justify further comment.

NORTH SIDE

N.B. THIS SECTION HAS BEEN TRANSPOSED AND IS DRAWN AS IF VIEWED FROM THE NORTH

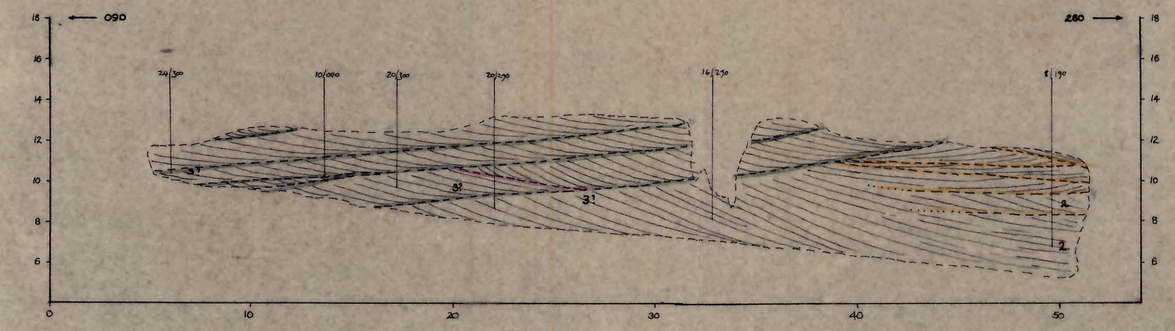

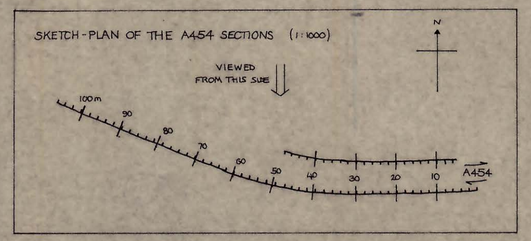

ENCLOSURE 12

A442 QUATFORD, NORTH CUT, WEST SIDE (SO 738907)

N.B. THIS SECTION HAS BEEN TRANSPOSED AND IS DRAWN AS IF VIEWED FROM THE WEST.

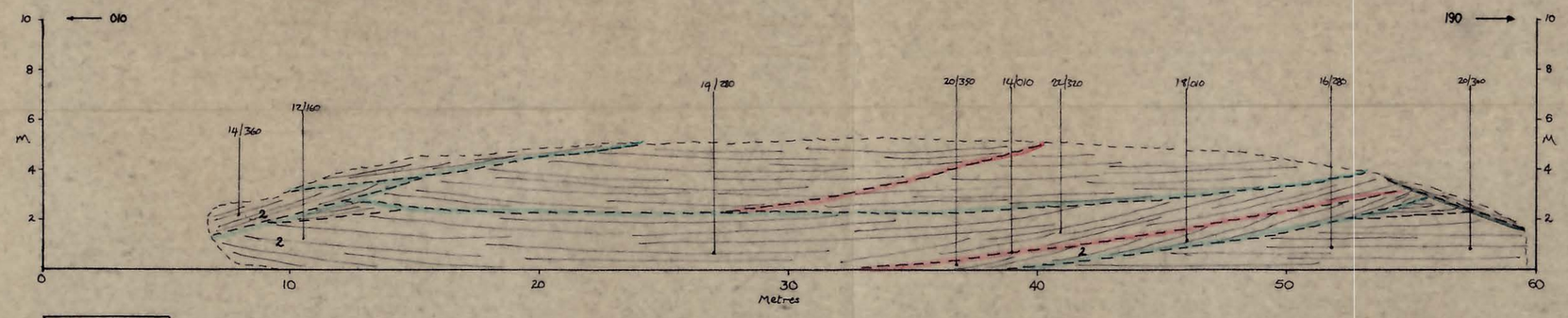

EAST SIDE

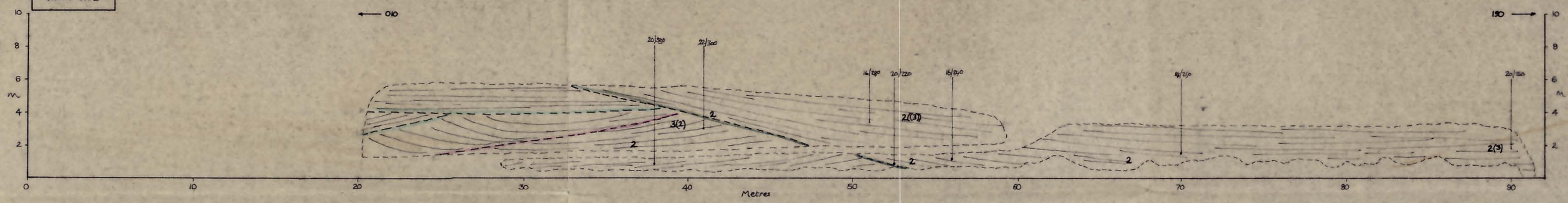

A442 QUATFORD, SOUTH CUT (SO 739902)

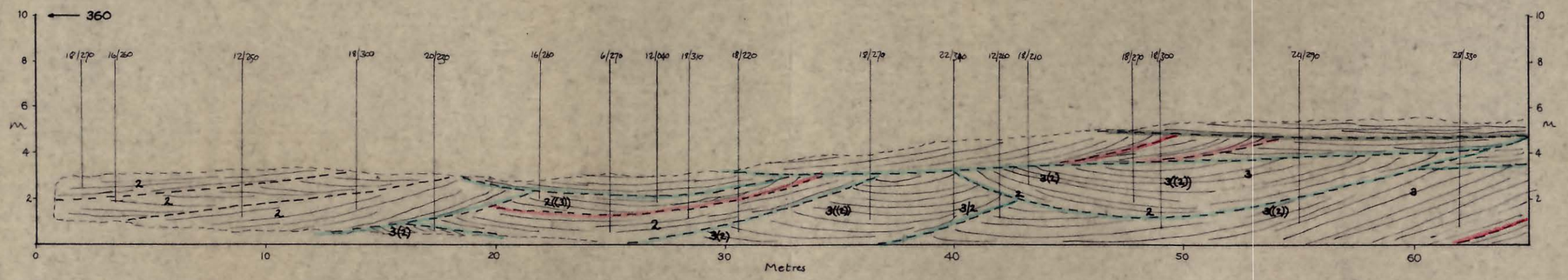

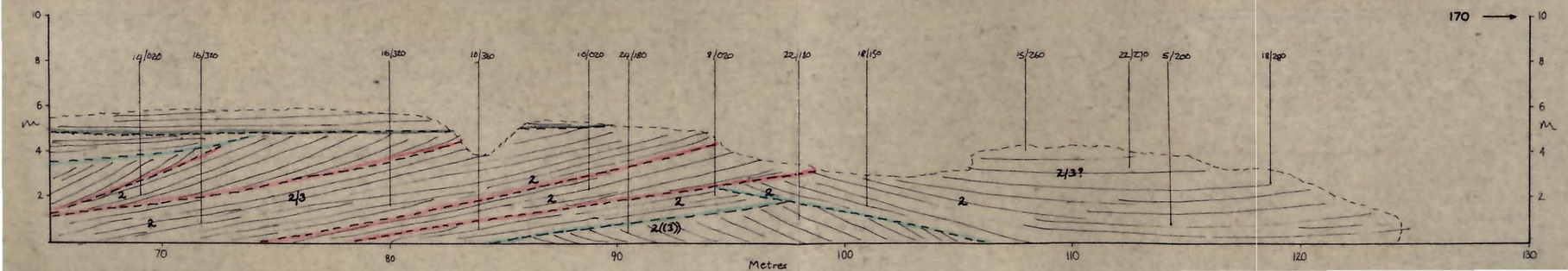

NOTES All the sections on this sheet are explicable as transverse cuts through trough cross-bedding deposited by dunes. Note the variation in thickness and lateral extent of the preserved parts of the troughs – factors determined as much by the erosive capabilities of the succeeding bedforms as the size of the depositing bedform.

ENCLOSURE 13

A442 DUDMASTON (SO 743854)

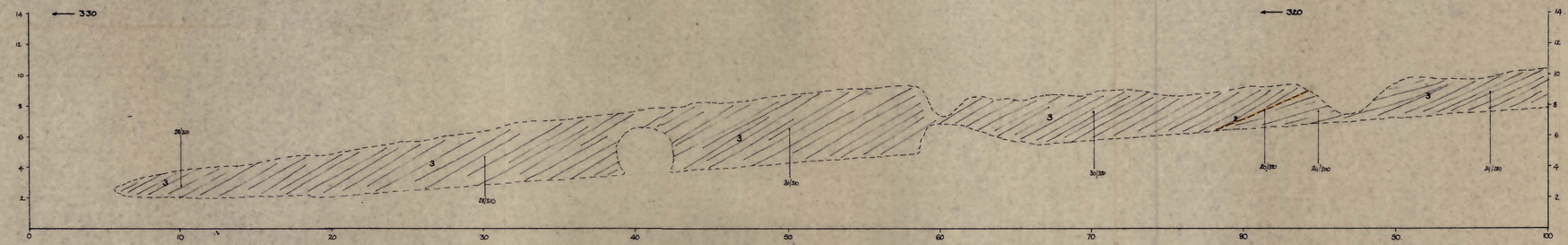

NOTES Interpretation of the bounding surfaces in this section is difficult because so few intersections are exposed. One possible interpretation of the section is that it is the deposit of a single dune with the inclusets from 160 - 180 m representing the temporary establishment of dunes on the dune lee side. In this case the thickness of the whole set is at least 20 m.

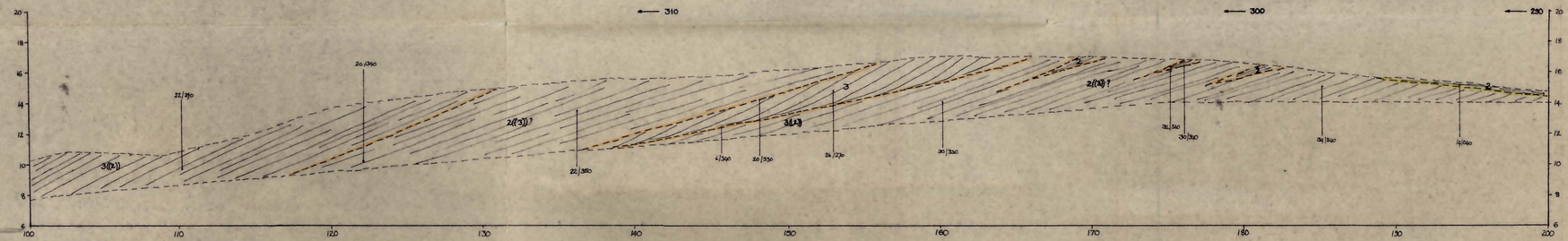

KNOWLESANDS (SO 713913)

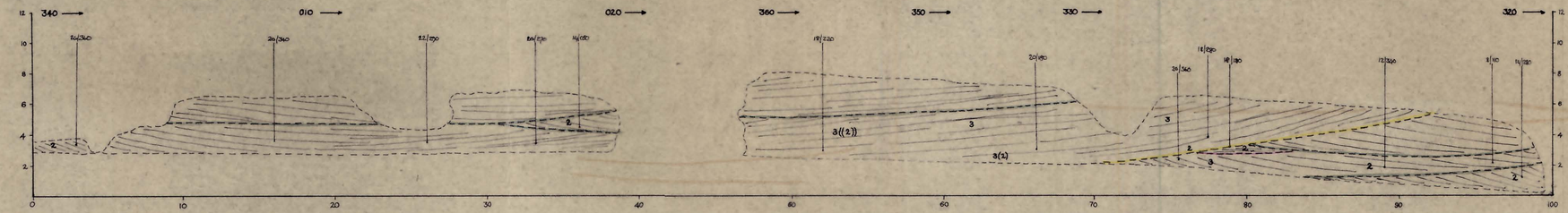

NOTES This exposure is too small to interpret the cross-bedding solely on the basis of scale however the presence of sandflows 100mm thick around 75, 09 would suggest a displaced dune origin for that set at least. The mismatch in bounding surfaces between 39 + 47m suggests the presence of a fault. The exposure lies only a few metres above the base of the formation.

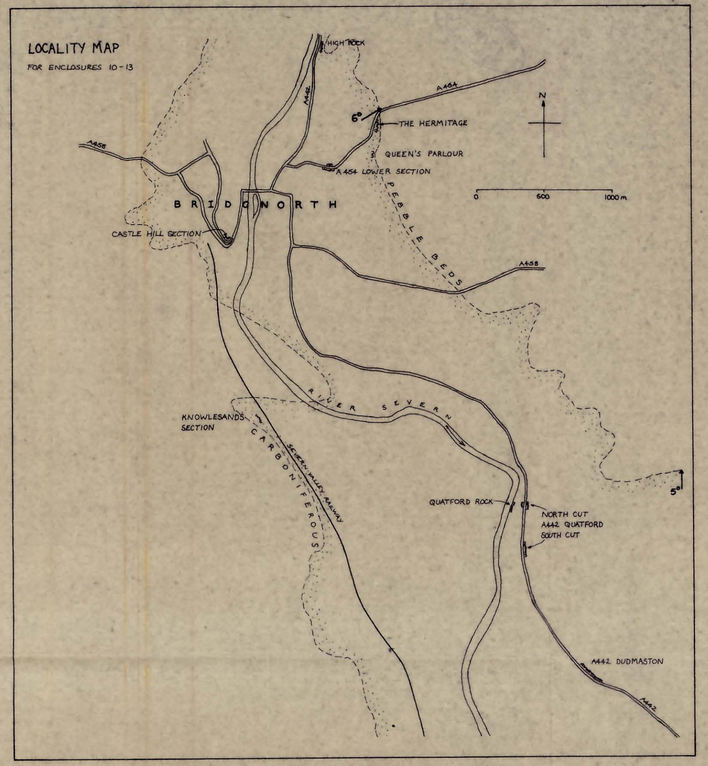

ENCLOSURE 14

LWAY CUTTING (SO 798748)

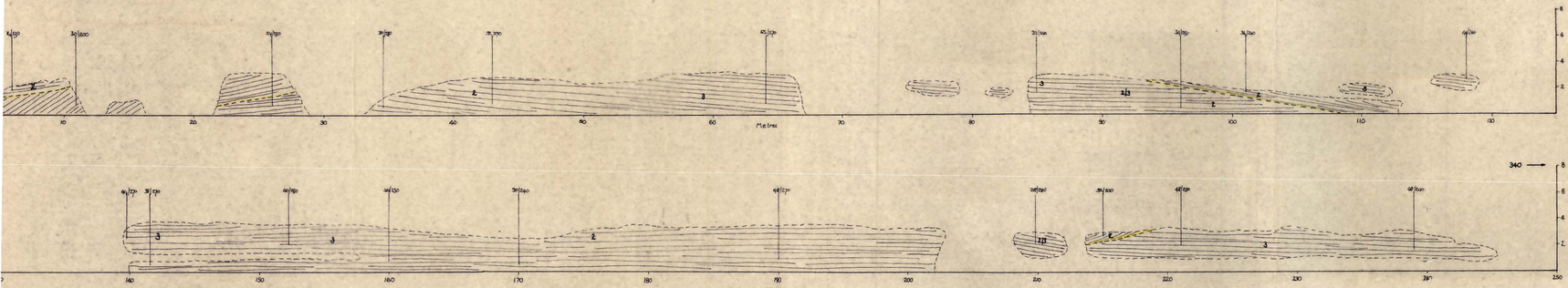

NOTES: The great lateral extent of individual sets suggests an origin as slipfaced dunes. The sections transverse to palaeocurrent mostly are probably present at 20m and 215m

N ROCK, KINVER (SO 837836)

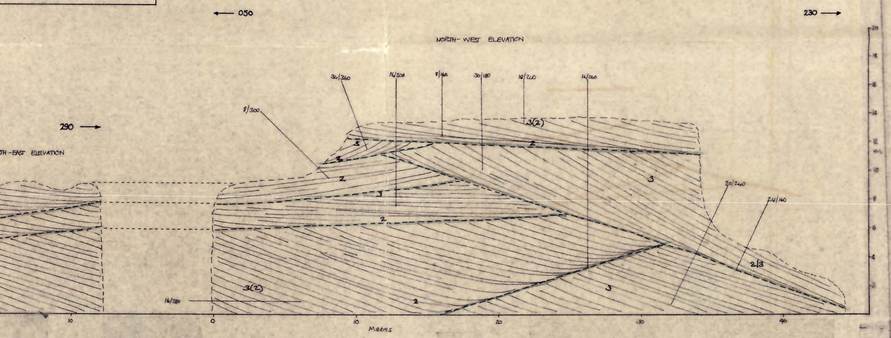

of this exposure in hollow - there used to be a cafeteria in it. et at 17.5 contains sandstones 100mm thick, suggestive of a ed dune, for the remainder too little in view of their lateral to offer an interpretation.

DRAKELOW DEPOT (SO 820808)

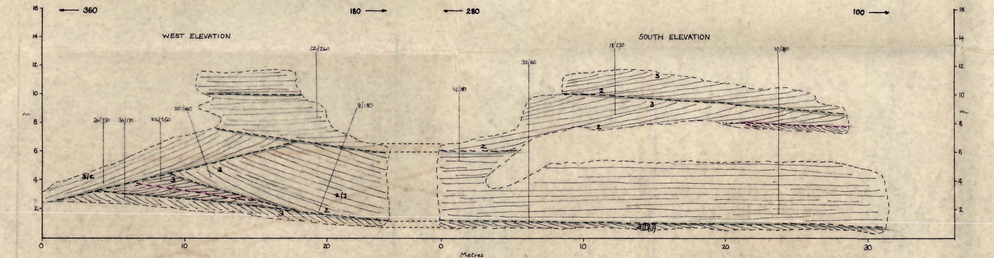

B5063, NEAR PRESTON BROCKHURST (SJ 541253)

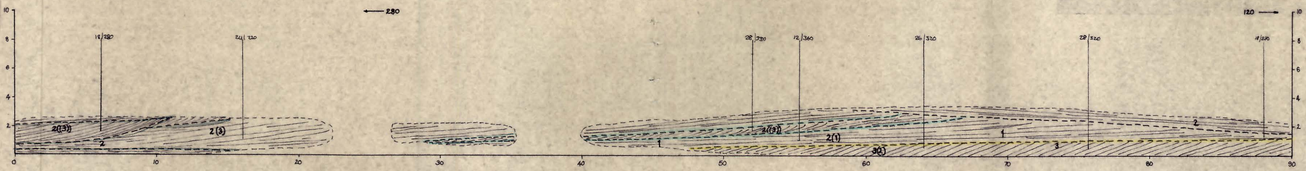

NOTES: 30mm sandflows in the set at the foot of this exposure suggest that it records the passage of a slipfaced dune. The sand sheet set represents an interdune area with the set passing through 80,02 possibly showing the development of a dune on this area. The backfilled burrow is truncated by this dune at the 50m mark.